

Three ways to decipher the nature of exotic hadrons: multiplets, three-body hadronic molecules, and correlation functions

Ming-Zhu Liu,^{1,2} Ya-Wen Pan,³ Zhi-Wei Liu,³ Tian-Wei Wu,⁴ Jun-Xu Lu,⁵ and Li-Sheng Geng^{3,6,7,8,*}

¹*Frontiers Science Center for Rare Isotopes, Lanzhou University, Lanzhou 730000, China*

²*School of Nuclear Science and Technology, Lanzhou University, Lanzhou 730000, China*

³*School of Physics, Beihang University, Beijing 102206, China*

⁴*School of Science, Shenzhen Campus of Sun Yat-sen University, Shenzhen 518107, China*

⁵*School of Physics, Beihang University, Beijing 100191, China*

⁶*Beijing Key Laboratory of Advanced Nuclear Materials and Physics, Beihang University, Beijing 102206, China*

⁷*Peng Huanwu Collaborative Center for Research and Education, Beihang University, Beijing 100191, China*

⁸*Southern Center for Nuclear-Science Theory (SCNT), Institute of Modern Physics,
Chinese Academy of Sciences, Huizhou 516000, China*

(■Dated: April 10, 2024)

In the past two decades, a plethora of hadronic states beyond the conventional quark model of $q\bar{q}$ mesons and qqq baryons have been observed experimentally, which motivated extensive studies to understand their nature and the non-perturbative strong interaction. Since most of these exotic states are located near the mass thresholds of a pair of conventional hadrons, the prevailing picture is that they are primarily hadronic molecules. In principle, one can verify the molecular nature of these states by thoroughly comparing their masses, decay widths, and production rates in a particular picture with experimental data. However, this is difficult or impossible. First, quantum mechanics allows for the mixing of configurations allowed by symmetries and quantum numbers. Second, data are relatively scarce because of their small production rates and the many difficulties in the experimental measurements. As a result, other alternatives need to be explored. This review summarizes three such approaches that can help disentangle the nature of the many exotic hadrons discovered.

In the first approach, based on the molecular interpretations for some exotic states, we study the likely existence of multiplets of hadronic molecules related by various symmetries, such as isospin symmetry, SU(3)-flavor symmetry, heavy quark spin/flavor symmetry, and heavy antiquark diquark symmetry, which are known to be approximately satisfied and can be employed to relate the underlying hadron-hadron interactions responsible for the formation of hadronic molecules. The masses of these multiplets of hadronic molecules can then be obtained by solving the Lippmann-Schwinger equation. Their decay and production patterns are also related. As a result, experimental discoveries of such multiplets and confirmations of the predicted patterns will be invaluable to understanding the nature of these hadronic molecular states.

In the second approach, starting from some hadronic molecular candidates, one can derive the underlying hadron-hadron interactions. With these interactions, one can study related three-body

systems and check whether three-body bound states/resonances exist. The existence of such three-body molecules can directly verify the molecular nature of exotic hadrons of interest.

In the third approach, one can turn to the femtoscopy technique to derive the hadron-hadron interactions, hence inaccessible. This technique provided an unprecedented opportunity to understand the interactions between unstable hadrons. Although the past focus was mainly on the light quark sector, we have seen increasing theoretical activities in the heavy quark sector in recent years. We review relevant studies and point out future directions where more effort is needed.

Finally, to provide valuable information for present and future experiments, the decay widths and production rates of these multiplets and three-body hadronic molecules are estimated using the effective Lagrangian approaches and discussed.

* lisheng.geng@buaa.edu.cn

CONTENTS

I. Introduction	5
II. Experimental and theoretical progress on selected exotic hadrons	11
A. $D_{s0}^*(2317)$ and $D_{s1}(2460)$	11
B. $X(3872)$ and some X states	14
C. $Y(4230)$, $Y(4360)$, and some Y states	17
D. $Z_c(3900)$, $Z_c(4020)$, and $Z_{cs}(3985)$	19
E. $P_c(4380)$, $P_c(4312)$, $P_c(4440)$, and $P_c(4457)$	20
F. $T_{cc}(3875)$	22
III. Multiplets of hadronic molecules	23
A. Symmetries	23
B. Mass spectra	26
1. $D^{(*)}K$ molecules	27
2. $\bar{D}^{(*)}\Sigma_c^{(*)}$ molecules	28
3. $\bar{D}^{(*)}D^{(*)}$ molecules	39
4. $\bar{D}^{(*)}D_{1,2}$ and $B_c\bar{B}_c$ molecules	46
C. Strong and radiative decays	50
1. Three-body decays	50
2. Two-body decays	53
D. Production mechanisms	60
1. Production rates of DK and D^*K molecules	61
2. Production rates of \bar{D}^*D and \bar{D}^*D^* molecules	64
3. Production rates of the pentaquark states	69
IV. Three-body hadronic molecules	73
A. $DD(\bar{D})K$ molecules	74
B. $\bar{D}\bar{D}^*\Sigma_c$ molecules	77
C. $D^{(*)}D^{(*)}D^{(*)}$ molecules	80
D. Other heavy-flavor three-body molecules	81
V. Femtoscopic correlation functions for exotic hadrons	85
A. Experimental and theoretical basics of Femtoscopy	86

B. Some general features of correlation functions	89
C. Correlation functions for $D_{s0}^*(2317)$, $D_0^*(2300)$, $D_1(2420)$, and $D_1(2430)$	90
D. Correlation functions for $T_{cc}(3875)$ and $X(3872)$	94
E. Correlation functions for $P_c(4312)$, $P_c(4440)$, and $P_c(4457)$	95
F. Correlation functions for T_{bb}	96
VI. Summary and Outlook	97
VII. Acknowledgments	101
A. Contact-range potentials	101
1. $\bar{D}^{(*)}\Sigma_c^{(*)}$ heavy anti-meson and heavy baryon systems	101
2. $\bar{D}^{(*)}D^{(*)}$ heavy anti-meson and heavy meson systems	104
3. $\Sigma_Q\bar{\Sigma}_Q$ heavy baryon and heavy anti-baryon systems	106
B. Light-meson saturation approach	107
C. Effective Lagrangians	110
D. Lippmann-Schwinger equation	111
E. The Gaussian-Expansion Method	115
References	117

I. INTRODUCTION

Quantum Chromodynamics (QCD), the underlying theory of the strong interaction, dictates that quarks can only exist in color singlet states, i.e., hadrons. Theoretically, they can contain very complex structures [1–3]. In the simplest form, hadrons are classified into mesons composed of a pair of quarks and antiquarks and baryons of three quarks, which is the somehow surprisingly successful conventional or naive quark model, where quarks are the so-called constituent quarks [4]. The naive quark model can well describe the static properties of most ground-state hadrons [5, 6], e.g., the ground states of heavy quarkonia [7–9]. However, for excited charmonium states, the conventional quark model encounters many difficulties reproducing their masses, decay widths, and other properties. Such hadrons beyond the conventional quark model are often called exotic hadrons. Among them, the $X(3872)$ state discovered by the Belle Collaboration [10] may be the most well-known one, which has motivated extensive experimental and theoretical studies. Some of these states carry exotic quantum numbers that the conventional quark model forbids, for instance, the $\eta_1(1855)$ with the exotic quantum number $J^{PC} = 1^{-+}$ [11] observed very recently by the BESIII Collaboration. The multiquark states with a minimum quark number of more than three are another kind of exotic states, such as the tetraquark states $Z_c(3900)$ [12], $T_{cc}(3985)$ [13], and the pentaquark states $P_c(4312)$, $P_c(4440)$, $P_c(4457)$ [14]. It is worth noticing that QCD does not exclude the existence of gluons in the form of glueballs or the mixture with quarks in the form of hybrids [15–21], though no experimental confirmation for these two kinds of exotic states exists so far. Such types of exotic states have attracted the interest of theorists and experimentalists. There have been many excellent reviews on studies of exotic hadrons in the past years; see, e.g., Refs. [22–40].

To investigate the nature of these exotic states, one often calculates their mass, (partial) decay widths, and production rates in a given picture and a particular model. The potential model and quark pair creation model (often referred to as the 3P_0 model) have been successfully applied to explain the masses and strong decay widths of conventional hadrons [5, 6, 41, 42]. Most exotic states are located near the mass thresholds of hadron pairs, yet such coupled-channel effects are not considered in the conventional quark model. In the language of string theory, the string between the quarks will break if the distance between a pair of quarks reaches a certain length, creating a pair of light quarks from the vacuum. Such quark rearrangements generate a pair of new hadrons, which can be estimated in the unquenched quark model [43–46]. The exotic hadrons are often explained in this picture as mixtures of hadronic molecules and conventional $q\bar{q}$ mesons or qqq baryons. In particular, the effect of coupled-channel hadron-hadron interactions can be considered by revising the confining potential as a screening potential in the conventional quark model [47–49]. As indicated in Ref. [50], the excitation modes of the same energy scale, e.g., quark radial excitation, quark

pair creation, and meson creations, may compete in forming a hadron.

The exotic states can also be explained as compact multiquark states. A simple model with only the color-magnetic interaction assigns exotic hadrons as compact multiquark states, where the basic structure contains diquarks [51–58]. The diquarks composed of a pair of quarks are decomposed into $3 \otimes 3 = \bar{3} \oplus 6$ in terms of the SU(3)-color symmetry, where the representation $\bar{3}$ is equivalent to an anti-quark. Based on this symmetry, the parameters in the diquark model can be estimated. For instance, one can relate the masses of $\Sigma_c^{(*)}$ baryons or $\Xi_{cc}^{(*)}$ baryons with that of the doubly charmed tetraquark state T_{cc} [59–64]. In this sense, the diquark model can simplify the calculations of multiquark systems, which otherwise are achieved by numerically solving the few-body schrödinger equation [65–67]. The MIT bag model embedding the asymptotic freedom at short distances and confinement at long distances has been applied to investigate the properties of conventional hadrons and multiquark states [68–74]. The QCD sum rule approach is another efficient method to handle the non-perturbative strong interaction, which has been widely applied to study the masses and decay widths of exotic states [75–81]. Last, a brute-force method exists at the quark level, lattice QCD, where space-time is discretized. The QCD Lagrangian is reformulated in Euclidean space to computer correlation functions defined in the Feynman path integral formalism via numerical Monte Carlo Methods. Lattice QCD simulations have made remarkable progress in studies of hadron spectroscopy [82–86], hadron-hadron interactions [87–96], electromagnetic form factors [97–102], meson decay constants [103–108], and hadron transition matrix elements [109–113]. This approach is quite promising in revealing the internal structure of exotic states. For instance, several lattice QCD studies [89, 114–117] supported that the DK interaction plays an important role in forming the exotic state $D_{s0}^*(2317)$, which is helpful to reveal its nature. A recent lattice QCD study [118] provided support to the two-pole structure of the $\Lambda(1405)$ at unphysical light quark masses consistent with the theoretical expectation [119].

A large number of theoretical studies have concluded that hadron-hadron interactions can affect the behavior of the corresponding conventional $q\bar{q}$ or qqq bare states [43–46, 120]. Therefore, an outstanding issue is whether molecules mainly composed of a pair of conventional hadrons exist. One famous example is $\Lambda(1405)$, whose mass is difficult to understand in the constitute quark model as an $sud\ 1^-/2\ p$ -wave excited state [121]. However, it can be generated by the $\bar{K}N$ coupled-channel interaction in the unitary chiral approach [122–124]. The existence of a $\bar{K}N$ molecule has attracted long and heated discussions both experimentally and theoretically [125–134], which triggered a lot of research on other likely hadronic molecules related by SU(3)-flavor symmetry [125–129]. Hadronic molecules containing heavy quarks can be traced to the proposal of $\psi(4040)$ as a \bar{D}^*D^* hadronic molecule [135, 136]. Although nowadays $\psi(4040)$ is widely viewed as a conventional charmonium state, the idea has inspired early theoretical studies on the possible existence of heavy hadronic molecules [137, 138]. Such studies were revived after the discovery

of $X(3872)$ [10]. The lower mass (compared to the conventional quark model prediction) and the isospin violation of the strong decays of $X(3872)$ can be easily understood, assuming that $X(3872)$ is a $D\bar{D}^*$ bound state or contains a sizeable molecular component [139–141].

The molecular picture, where hadronic molecules are composed of conventional hadrons held together by the residual strong interaction, is analogous to the picture where the nuclear force binds the deuteron (and atomic nuclei). The one-pion exchange mechanism was firstly applied to study deuteron-like loosely bound states by Törnqvist [142], while it alone is not attractive enough to form molecules [23, 143]. Inspired by the extensive studies of the nuclear force, the one-meson exchange theory has been applied to construct hadron-hadron potentials [144–149], where the π , σ , and $\rho(\omega)$ are responsible for the long, middle, and short-range interactions. In the OBE model, the S -wave potential is strongly related to the coupling constants of each exchanged meson and its spin-isospin quantum numbers [150]. However, the lattice QCD simulation of the strong interactions of the $N\Omega$ [151] and $\Omega_{ccc}\Omega_{ccc}$ systems [152] obtained bound states below their respective mass thresholds, which is difficult to understand in the OBE mechanism. The potentials responsible for transitions between open-charm channels and hidden-charm channels, such as $\bar{D}D^* \rightarrow J/\psi\pi$ [153] and $\bar{D}^*\Sigma_c \rightarrow J/\psi p$ [154–156] via one-charm-meson exchange may not be valid for short-range interactions since the one-gluon exchange at this energy scale may play a more critical role [157]. Recently, many studies argued that the vector meson exchange alone is enough to generate hadron-hadron potentials, which can explain several exotic states as hadronic molecules in a unified picture [158–164].

Effective field theories (EFTs) are another widely adopted approach in exotic hadrons studies, which allow a systematic estimate of theoretical uncertainties. The downside is that it sometimes contains many unknown couplings, which need to be determined in one way or another, e.g., by fitting experimental or lattice QCD data. Chiral effective field theory (ChEFT) is one of QCD's most successful low-energy effective field theories. It is formulated in hadronic degrees of freedom and organized in chiral expansion, e.g., an expansion in powers of external momenta and light quark masses. ChEFT has been successfully applied to describe the $\pi\pi$ [165, 166] and πN [167] scattering, and then the nucleon-nucleon interaction [168, 169], which has become the de-facto standard approach to constructing high precision nuclear forces [170–172]. ChEFT has been extended to study exotic states in heavy quark sectors [40, 173–175] as well. Due to the many LECs that appear at higher chiral orders and the scarce experimental data for exotic states, one is often restricted to the lowest order, e.g., contact and one-pion-exchange terms [176–178]. For heavy hadronic molecules, the one-pion exchange can often be treated as a perturbative correction [160]. Nevertheless, there still exist unknown parameters, which can be estimated via relevant symmetries [179–181] or the light meson saturation mechanism [164, 182]. Both approaches can reduce the number of unknown parameters. It is worth noticing that in the chiral unitary approach, which simplifies the scattering equation to an al-

gebraic equation via the on-shell approximation, one can systematically study the dynamical generation of exotic hadronic molecules and the relevant invariant mass distributions [27, 123, 156, 159, 183–186].

In general, by fitting the experimental invariant mass distributions with a Breit-Wigner parameterization, one can obtain the mass and width of a state. However, some peaks or dips in the invariant mass distributions are difficult to understand as genuine states [187]. Instead, they can be better described as kinetic effects, such as triangle singularities or cusp effects [188–192]. A genuine state that interferes with coupled channels can generate a dip structure in the invariant mass distribution. A relevant example is the dip in the $J/\psi J/\psi$ invariant mass distribution around 6.8 GeV that can be reproduced by considering coupled-channel effects [187, 193]. In Ref. [191], Dong et al. discussed the dependence of the cusp effect on the reduced mass and the potential strength of a pair of hadrons, which helps discriminate the cusp effect from a genuine state. On the other hand, triangle singularities always proceed via three on-shell intermediate particles in a loop diagram [194–197]. They are located in the physical region and may produce some observable effects in the invariant mass distributions [36]. Recently, after early claims by the COMPASS Collaboration of the “ $a_1(1420)$ ” discovery [198], it was explained as the consequence of a triangle singularity in which the $a_1(1260)$ resonance decays into $K^* \bar{K}$, $K^* \rightarrow \pi K$ and then $K \bar{K}$ fuses to give the $f_0(980)$ resonance, the $\pi f_0(980)$ being the observed decay mode [189, 190, 192]. Therefore, it is necessary to consider kinetic effects in analyzing peaks in the experimental invariant mass distributions. Every enhancement in the invariant mass distribution contains crucial information on the interactions, which can be employed to reveal further the inner structures or properties of related genuine states. In Ref. [199], Guo argued that the enhancement in the mass distribution of $X(3872)\gamma$ induced by the triangle diagram mechanism is helpful to determine whether $X(3872)$ is above or below the $D\bar{D}^{*0}$ mass threshold. The cusp for $\pi^0\pi^0$ scattering is expected to be at the $\pi^+\pi^-$ threshold [200], which is used to extract their scattering length difference with high precision [201–206].

Once the hadron-hadron interactions are determined, one can obtain the pole positions (mass and width) in the vicinity of the mass threshold of a pair of hadrons, and then within the molecular picture, analyze other physical observables, such as the invariant mass distributions and production rates. In Refs. [27, 156, 177, 185, 207, 208], assuming that the weak interaction vertex can be parameterized with one single unknown parameter, the invariant mass distributions in the exclusive weak decays are used to identify the molecular nature of exotic states, where the final-state interactions dynamically generate the hadronic molecules. However, the internal mechanism of three-body weak decays is unknown, which is often parameterized assuming SU(3)-flavor symmetry [209–212], in the generalized factorization approach [213–219], the pole model [220–223], and the perturbative QCD approach [224–227]. These three-body decays accompanied by the productions of exotic states can also be described in the triangle mechanism [228–232],

which usually proceed via the Cabibbo-favored two-body weak decays that can be well described through the naive factorization approach [233, 234]. Some exotic states can be produced in the inclusive process in pp , e^+e^- , $p\bar{p}$, and heavy ion collisions, which have been studied in the molecular picture with the statistical model [235–237], the coalescence model [238–242], the multiphase transport model (AMPT) model [243], and the PACIAE model [244, 245]. Moreover, the pentaquark states can be produced in the J/ψ photoproduction off protons [246–249], which can distinguish whether they are genuine states or anomalous triangle singularities.

In the past two decades, many new hadrons have been discovered [250–252]. Due to their proximity to the thresholds of pairs of conventional hadrons and unique properties, many can only be understood as hadronic molecules or considering final-state interactions. The rapidly evolving experimental situation has inspired a large number of theoretical works. It is impossible to cover all of them in the present review. In addition, there are already many excellent reviews in this regard. See, e.g., Refs. [22–40]. As a result, we only focus on three relatively new but less-discussed approaches, which can shed light on the nature of exotic states, particularly whether they fit into the molecular picture and how to verify or refute such a picture.

The first approach relies on symmetry considerations. Historically, the discovery of the Ω baryon helped verify the quark model, where the SU(3)-flavor symmetry plays an important role. Such an approach has been extended to study hadronic molecules. For instance, assuming $X(3872)$ is a $J^{PC} = 1^{++} \bar{D}D^*$ bound state, it is natural to expect the existence of a $J^{PC} = 2^{++} \bar{D}^*D^*$ bound state and a $J^{PC} = 1^{++} \bar{B}B^*$ bound state (denoted as X_b) according to heavy quark spin symmetry (HQSS) and heavy quark flavor symmetry (HQFS) [159, 253–258]. The CMS Collaboration has searched for the X_b in the decay channel of $\Upsilon(1S)\pi\pi$ in pp collisions without success [259]. Later, the Belle Collaboration also obtained negative results in the decay channel of $\Upsilon(1S)\omega$ in e^+e^- collisions [260]. As a result, based on the molecular nature of exotic states, various symmetries, such as SU(3)-flavor symmetry, HQSS, HQFS, and heavy antiquark diquark symmetry (HADS) predicted the existence of their partners [179–181]. We can see that the existence of these partners is tied to the molecular nature of these states and the underlying hadron-hadron interactions. Thus, experimental searches for these partners can help verify or refute their molecular nature. We review the studies of several good molecular candidates and their partners related by various symmetries, including their masses, decay widths, and production mechanisms.

Along with this idea, we proposed a second approach to verify the molecular nature of exotic states. Nowadays, it is well-accepted that atomic nuclei are made of nucleons. For instance, the deuteron comprises a neutron and a proton, the triton consists of two neutrons and a proton, and the alpha particle contains two neutrons and two protons. In practice, using the precise two-body NN potential, one can reproduce most

properties of the ground-state and low-lying excited states of light nuclei, where the residual three-body potential NNN is also considered [261–265].¹ Such a picture has been successfully extended to studies of hypernuclei, i.e., adding one or more hyperons to the nuclear system [268, 269]. We can replace the deuteron bound by the NN interaction with other molecular candidates generated by certain hadron-hadron interactions. Then, we can predict the existence of three-body or even four-body hadronic molecules [270–272]. One example is that assuming $D_{s0}^*(2317)$ is a DK bound state, three-body DDK and four-body $DDDK$ hadronic molecules exist. These multi-hadron states rely on the underlying DK interaction [273]. In other words, the DDK and $DDDK$ molecules, if discovered experimentally or on the lattice, will verify the molecular nature of $D_{s0}^*(2317)$. This review discusses the studies on the masses, decay widths, and production rates of possible three-body hadronic molecules associated with some chosen two-body molecular candidates of an exotic nature.

Due to the low production rates of hadrons containing heavy quarks, direct experimental studies of hadron-hadron interactions are challenging. In recent years, it has been shown that the femtoscopic technique is a promising method for such purposes [274–278], accessible in high energy pp , pA , and AA collisions [239, 279]. Such approaches have recently been utilized in studying exotic hadronic molecular candidates [280–289], which show great potential in deriving the relevant hadron-hadron interactions and deciphering the nature of the many exotic hadrons discovered. We will review recent theoretical and experimental femptoscopic studies of the hadron-hadron interactions related to understanding the nature of exotic hadrons.

This review is organized as follows. In Sec. II, we briefly introduce the experimental progress on the exotic states covered in the present review. In Sec. III, we adopt the contact-range effective field theory approach to assign several exotic states as hadronic molecules and predict the existence of multiplets employing various symmetries, including $SU(3)$ flavor symmetry, HQSS, HQFS, and HADS. In Sec. IV, based on specific good candidates of hadronic molecules and the underlying hadron-hadron interactions, we predict the corresponding three-body hadronic molecules by solving the three-body Schrödinger equation. In Sec. V, we review recent efforts in decoding the nature of specific candidates of hadronic molecules using Femptoscopic techniques. Finally, this review ends with a summary and outlook in Sec. VI. We relegate some of the theoretical tools, which are helpful to understanding the studies covered in this review, to the Appendices.

¹ We note that none of the existing studies can simultaneously describe medium-mass nuclei and nuclear matter in a truly ab initio way yet [266, 267].

II. EXPERIMENTAL AND THEORETICAL PROGRESS ON SELECTED EXOTIC HADRONS

In recent years, with ever-increasing energy and statistics and rapid developments in detection and analysis techniques, a large number of new hadrons containing heavy quarks have been discovered experimentally [37, 250–252, 290, 291]. In the following, we briefly introduce some selected exotic states that are deemed as robust hadron molecular candidates. These hadrons are mainly discovered in two modes, i.e., inclusive and exclusive processes, and the latter usually proceeds via b -hadron decays. In Table I and Table III, we summarise the productions of the heavy hadronic molecular candidates covered in this review. In addition, we also briefly review related theoretical studies, particularly those in the hadronic molecular picture, to put things into perspective.

A. $D_{s0}^*(2317)$ and $D_{s1}(2460)$

In 2003, the BaBar Collaboration discovered a narrow state near 2.32 GeV in the $D_s^+\pi^0$ invariant mass distribution [292], named $D_{s0}^*(2317)$. It was subsequently confirmed by the CLEO [293] and Belle Collaboration [296]. In addition, a new state near 2.46 GeV, named $D_{s1}(2460)$, was also discovered [293, 296]. The BESIII Collaboration observed $D_{s0}^*(2317)$ in the process of $e^+e^- \rightarrow D_s^{*+}D_{s0}^*(2317)$ with a statistical significance more than 5σ [295]. Assuming $D_{s0}^*(2317)$ and $D_{s1}(2460)$ as the $c\bar{s}$ charmed strange mesons of $J^P = 0^+$ and $J^P = 1^+$, their masses are lower by 160 and 100 MeV than the prediction of the Godfrey-Isgur (GI) model [5]. Therefore, $D_{s0}^*(2317)$ and $D_{s1}(2460)$ are often considered exotic states. In addition to its dominant decay mode $D_s^+\pi^0$ [297, 301], the upper limit of the branching fraction of the $D_{s0}^*(2317)$ decaying into $D_s^+\gamma$, $D_s^{*+}\gamma$, and $D_s^{*+}\pi^0$ were obtained by the Belle [294, 296] and BaBar [351] collaborations. The decays of $D_{s1}(2460)$ into $D_s^+\gamma$, $D_s^+\pi^0\gamma^2$, and $D_s^+\pi^+\pi^-$ were observed by the BaBar collaboration [299, 301, 351]. The upper limit of the branching fraction of the decay $D_{s1}(2460) \rightarrow D_s^+\pi^0$ was obtained by the Belle collaboration [294]. Moreover, the Belle Collaboration observed $D_{s0}^*(2317)$ in the decay process $\bar{B}^0 \rightarrow [D_{s0}^{*+}(2317) \rightarrow D_s^+\pi^0]K^-$ [352]. In Table I, we summarise the production and decay modes of $D_{s0}^*(2317)$ and $D_{s1}(2460)$. We note that the $D_{s0}^*(2317)$ and $D_{s1}(2460)$ are only discovered in e^+e^- collisions, while they have not been observed in pp , pA , and AA collisions.

Because of their unique properties, the $D_{s0}^*(2317)$ and $D_{s1}(2460)$ have attracted intensive discussions on their nature. In Ref. [49], the authors found that the masses of $D_{s0}^*(2317)$ and $D_{s1}(2460)$ do not agree with the experimental data, even adding the screening potential to the conventional quark model, where the Coulomb potential and linear potential are modified because in the energy region near the mass thresh-

² The significant decay mode of $D_s^+\pi^0\gamma$ is from $D_s^{*+}\pi^0$ [300]

TABLE I. Production and decay modes of $D_{s0}^*(2317)$, $D_{s1}(2460)$, $X(3872)$, $X(4014)$, $Y(4220)$, and $Y(4360)$.

State	J^P	Inclusive process	Decay modes	Exclusive process	Decay modes
$D_{s0}^*(2317)$	0^+	e^+e^- [292–295]	$D_s^+\pi^0$	$B \rightarrow \bar{D}^{(*)}D_{s0}^*$ [296–298]	$D_s^+\pi^0$
		e^+e^- [293, 294]	$D_s^{*+}\pi^0$		
$D_{s1}(2460)$	1^+	e^+e^- [294]	$D_s^+\gamma/D_s^+\pi^+\pi^-$	$B \rightarrow \bar{D}^{(*)}D_{s1}$ [296, 297, 299]	$D_s^{*+}\pi^0/D_s^+\gamma$
		e^+e^- [300, 301]	$D_s^+\gamma\pi^0$		
		$p\bar{p}$ [302–306]	$J/\psi\pi^+\pi^-$	$B^+ \rightarrow X(3872)K^+$ [10, 307–311]	$J/\psi\pi^+\pi^-$
		pp [312, 313]	$J/\psi\pi^+\pi^-$	$B^+ \rightarrow X(3872)K^+$ [314–317]	$J/\psi\gamma/\psi(2S)\gamma$
		e^+e^- [318]	$\pi^0\chi_{c1}$	$\Lambda_b^0 \rightarrow X(3872)pK^-$ [319]	$J/\psi\pi^+\pi^-$
		e^+e^- [320]	$J/\psi\omega$	$B^+ \rightarrow X(3872)K^+$ [321]	$J/\psi\rho^0$
		e^+e^- [322]	$\bar{D}^{*0}D^0$	$B_s^0 \rightarrow X(3872)\phi$ [323, 324]	$J/\psi\pi^+\pi^-$
$X(3872)$	1^+			$Y(4260) \rightarrow X(3872)\gamma$ [325]	$J/\psi\pi^+\pi^-$
				$B^+ \rightarrow X(3872)K^+$ [326]	$J/\psi\eta$
				$B^+ \rightarrow X(3872)K^+$ [314]	$J/\psi\gamma$
				$B^+ \rightarrow X(3872)K^+$ [327, 328]	$\bar{D}^{*0}D^0$
				$B^+ \rightarrow X(3872)K^+$ [329]	$J/\psi\omega$
				$B^+ \rightarrow X(3872)K^+$ [330]	$D^0\bar{D}^0\pi^0$
				$B^+ \rightarrow X(3872)\pi^+\pi^-$ [331]	$J/\psi\pi^+\pi^-$
$X(4014)$	$??$	$\gamma\gamma$ [332]	$\psi(2S)\gamma$		
		e^+e^-	$J/\psi\pi^+\pi^-$ [333], $h_c\pi^+\pi^-$ [334]		
		e^+e^-	$\psi(2S)\pi^+\pi^-$ [335, 336]		
$Y(4220)$	1^-	e^+e^-	$\omega\chi_{c0}$ [337, 338], $J/\psi K^+K^-$ [339]		
		e^+e^-	$\pi^+D^0D^{*-}$ [340], $\pi^+D^{*0}D^{*-}$ [341]		
		e^+e^-	$J/\psi K_s^0 K_s^0$ [342], $J/\psi\eta$ [343, 344]		
		e^+e^-	$\psi(2S)\pi^+\pi^-$ [335, 345–348]		
		e^+e^-	$J/\psi\pi^+\pi^-$ [333], $h_c\pi^+\pi^-$ [334]		
$Y(4360)$	1^-	e^+e^-	$J/\psi\eta$ [343, 344]		
		e^+e^-	$\pi^+\pi^-D^+D^-$ [349]		
		e^+e^-	$\gamma\chi_{c2}$ [350]		

old of a pair of hadrons, the linear potential is screened by the vacuum polarization effects of dynamical fermions [8, 47]. The effect of vacuum polarisation can also be described by hadron loops, which have been considered on top of the conventional quark model [353–359]. Therefore, if the DK and D^*K components were embodied into the conventional quark model, the mass puzzle of $D_{s0}^*(2317)$ and $D_{s1}(2460)$ can be resolved [46, 360–364], which indicates that the $D^{(*)}K$ components play an important role in forming $D_{s0}^*(2317)$ and $D_{s1}(2460)$. The molecular picture of $D_{s0}^*(2317)$ and $D_{s1}(2460)$ can not only explain their mass puzzle but also reconcile their mass splitting [273, 365–371]. A bound state below the DK mass threshold has been identified by lattice QCD simulations [89, 114, 116, 372, 373]. The couplings between a single channel and the relevant bare state are included in the potential of single-channel scattering [120, 374–377]. Consequently, with the $D^{(*)}K$ potentials supplemented by the $c\bar{s}$ core couplings to the $D^{(*)}K$ components, $D_{s0}^*(2317)$ and $D_{s1}(2460)$ can be dynamically generated [115, 378–380], indicating that the $D^{(*)}K$ molecular components account for a large proportion of their wave functions in terms of the Weinberg compositeness rule [378].

In addition to the studies on their masses, the decay and production rates of $D_{s0}^*(2317)$ and $D_{s1}(2460)$ have been extensively discussed. The dominant decays of $D_{s0}^*(2317)^+$ and $D_{s1}(2460)^+$ to $D_s^+\pi^0$ and $D_s^{*+}\pi^0$ imply that $D_{s0}^*(2317)^+$ and $D_{s1}(2460)^+$ are quite narrow states since the decays of $D_{s0}^*(2317)^+ \rightarrow D_s^+\pi^0$ and $D_{s1}(2460)^+ \rightarrow D_s^{*+}\pi^0$ break isospin. The partial decay widths of $D_{s0}^*(2317) \rightarrow D_s\pi$ and $D_{s1}(2460) \rightarrow D_s^*\pi$ are estimated to be tens of keV assuming $D_{s0}^*(2317)$ and $D_{s1}(2460)$ as $c\bar{s}$ excited states [49, 381–384], while hundreds of keV assuming them as hadronic molecules [385–387], which can not discriminate the nature of $D_{s0}^*(2317)$ and $D_{s1}(2460)$. In Ref. [388], Faessler et al. calculated the decays $B \rightarrow D_{s0}^*(2317)\bar{D}^{(*)}$ and $B \rightarrow D_{s1}(2460)\bar{D}^{(*)}$ assuming $D_{s0}^*(2317)$ and $D_{s1}(2460)$ as $D^{(*)}K$ molecules [388]. The results are consistent but a bit smaller than the experimental data. Assuming $D_{s0}^*(2317)$ and $D_{s1}(2460)$ as $c\bar{s}$ excited states, the decays $B \rightarrow D_{s0}^*(2317)\bar{D}^{(*)}$ and $B \rightarrow D_{s1}(2460)\bar{D}^{(*)}$ were investigated as well. However, the results suffer from large uncertainties [389–394]. Moreover, the production rates of $D_{s0}^*(2317)$ and $D_{s1}(2460)$ in the Λ_b decays are found to be larger than those in the corresponding B decays [395, 396].

The yield of a hadron in electron-positron and heavy ion collisions reflects its internal structure. It is an important observable for discriminating the different interpretations of exotic states. The productions of $D_{s0}^*(2317)$ and $D_{s1}(2460)$ in e^+e^- and AA collisions have been investigated. Using the coalescence model [238], the yields of $D_{s0}^*(2317)$ as an excited $c\bar{s}$ state, a compact multiquark state $c\bar{s}q\bar{q}$, and a DK hadronic molecule in heavy ion collisions are estimated. Ref. [379] argued that the enhancement in the DK invariant mass distribution of the weak decay $B \rightarrow DDK$ implies the existence of $D_{s0}^*(2317)$ as a DK bound state and claimed that using the mass distribution can probe the molecular nature of an exotic

state. Identifying $D_{s0}^*(2317)$ and $D_{s1}(2460)$ as $D^{(*)}K$ hadronic molecules and $c\bar{s}$ excited states, Wu et al. estimated their production rates in e^+e^- collisions [245]. The hadronic molecular picture is more consistent with the experimental data [301].

B. $X(3872)$ and some X states

In 2003, the Belle Collaboration discovered a charmonium-like state named $X(3872)$ in the $J/\psi\pi^+\pi^-$ mass distribution of the decay $B \rightarrow KJ/\psi\pi^+\pi^-$ [10], later confirmed by many collaborations, e.g., BaBar [326], CDF [302], D0 [303], CMS [313], LHCb [312], and BESIII [325]. Moreover, it was measured in many other decay modes, including $J/\psi\eta$ [326], $\bar{D}^0 D^0 \pi^0$ [330], $\bar{D}^{*0} D^0$ [322, 327, 328], $J/\psi\gamma$ [314, 315, 322, 397], $J/\psi\omega$ [320], $J/\psi\rho^0$ [321], $\chi_{c1}\pi^0$ [318, 398], and $\psi(2S)\gamma$ [315, 317]. The BaBar Collaboration reported the absolute branching fraction $\mathcal{B}(X(3872) \rightarrow J/\psi\pi^+\pi^-) = 4.1 \pm 1.3\%$ [399]. It is worth noting that the $X(3872)$ is observed not only in e^+e^- collisions, but also in pp collisions [312], $p\bar{p}$ collisions [302], and heavy ion collision(Pb-Pb) [400]. Interestingly, $X(3872)$ is also produced in both the Λ_b decay [319] and B_s decay [324, 331]. The average mass and width of $X(3872)$ are $m = 3871.65 \pm 0.06$ MeV and $\Gamma = 1.19 \pm 0.21$ MeV [401]. The mass is lower than the GI model prediction by 90 MeV [5].

The branching ratios of the $X(3872)$ decay play an important role in revealing its nature. The branching ratio of $Br(X(3872) \rightarrow J/\psi\pi\pi\pi)/Br(X(3872) \rightarrow J/\psi\pi\pi)$ is measured to be around 1 [320, 329, 397, 402]. Such a branching ratio is difficult to understand regarding the $X(3872)$ as a pure $c\bar{c}$ charmonium state. The branching fraction ratios $\mathcal{B}(B^+ \rightarrow K^+ X(3872))/\mathcal{B}(B^0 \rightarrow K^0 X(3872))$ [403, 404], $\mathcal{B}(X(3872) \rightarrow \chi_{c2}\gamma)/\mathcal{B}(X(3872) \rightarrow \chi_{c1}\gamma)$ [405], and $\mathcal{B}(X(3872) \rightarrow \psi(2S)\gamma)/\mathcal{B}(X(3872) \rightarrow \psi\gamma)$ [315–317] play an important role in clarifying the nature of $X(3872)$ because different models can yield distinct predictions. Moreover, the ratios of the production of $X(3872)$ to the production of $\psi(2S)$ measured experimentally, i.e., $\mathcal{B}(B_s^0 \rightarrow X(3872)\pi^+\pi^-) \times \mathcal{B}(X(3872) \rightarrow J/\psi\pi^+\pi^-)/\mathcal{B}(B_s^0 \rightarrow \psi(2S)\pi^+\pi^-) \times \mathcal{B}(\psi(2S) \rightarrow J/\psi\pi^+\pi^-) = (6.8 \pm 1.1 \pm 0.2) \times 10^{-2}$ [331], $\mathcal{B}(B^+ \rightarrow X(3872)K^+) \times \mathcal{B}(X(3872) \rightarrow J/\psi\pi^+\pi^-)/\mathcal{B}(B^+ \rightarrow \psi(2S)K^+) \times \mathcal{B}(\psi(2S) \rightarrow J/\psi\pi^+\pi^-) = (3.69 \pm 0.07 \pm 0.06) \times 10^{-2}$ [311], and $\mathcal{B}(\Lambda_b^0 \rightarrow X(3872)pK^-) \times \mathcal{B}(X(3872) \rightarrow J/\psi\pi^+\pi^-)/\mathcal{B}(\Lambda_b^0 \rightarrow \psi(2S)pK^-) \times \mathcal{B}(\psi(2S) \rightarrow J/\psi\pi^+\pi^-) = (5.4 \pm 1.1 \pm 0.2) \times 10^{-2}$ [319], are likely to tell us more information on the nature of $X(3872)$. The line-shape of $X(3872)$ is precisely analyzed by the BESIII [406], LHCb [407], and Belle [408] collaborations, which are very helpful in constraining various theoretical interpretations of its nature.

In 2004, the Belle Collaboration observed a state around 3940 MeV in the $J/\psi\omega$ invariant mass distribution of the $B \rightarrow J/\psi\omega K$ decay [409], which was later confirmed by the BaBar Collaboration in the same

process but with the mass determined to be 3915 MeV [410]. In 2009, the Belle Collaboration observed a state near 3915 MeV in the $\gamma\gamma \rightarrow J/\psi\omega$ reaction [411]. Later, the BaBar Collaboration determined its quantum numbers to be $J^{PC} = 0^{++}$ [412]. In 2020, the LHCb Collaboration observed a similar state $\chi_{c0}(3930)$ in the D^+D^- mass distribution of the $B^+ \rightarrow D^+D^-K^+$ decay [413, 414]. In the Review of Particle Physics (RPP) [401], all these states are referred to as $\chi_{c0}(3915)$ and viewed as a candidate for the $\chi_{c0}(2P)$ charmonium [415, 416]. The LHCb Collaboration recently reported a charmonium state named $X(3960)$ with $J^{PC} = 0^{++}$ in the $D_s^+D_s^-$ mass distribution of the $B^+ \rightarrow D_s^+D_s^-K^+$ decay. Its mass and width are determined to be $m = 3955 \pm 6 \pm 11$ MeV and $\Gamma = 48 \pm 17 \pm 10$ MeV [417, 418]. In the same energy region, a charmonium $\chi_{c2}(3930)$ with $J^{PC} = 2^{++}$ was discovered by the Belle [419], BaBar [420], and LHCb [413, 421] collaborations, which indicate that the mass splitting between $\chi_{c2}(2P)$ and $\chi_{c0}(1P)$ is only around 10 MeV, inconsistent with the predictions of the GI model [5].

In 2008, the CDF Collaboration observed a resonance $X(4140)$ in the $J/\psi\phi$ mass distribution in the decay of $B \rightarrow J/\psi\phi K$ with the mass and width being $m = 4143.0 \pm 2.9 \pm 1.2$ MeV and $\Gamma = 11.7_{-5.0}^{+8.3} \pm 3.7$ MeV [422]. Later, the CDF Collaboration updated their analysis of $B \rightarrow J/\psi\phi K$ and confirmed the existence of $X(4140)$ [423], which was also confirmed by the CMS [424] and $D0$ [425, 426] collaborations. Moreover, another new state with a mass of $4274.4_{-6.7}^{+8.4} \pm 1.9$ MeV and a width of $32.3_{-15.3}^{+21.9} \pm 7.6$ MeV is observed by the CDF Collaboration [423]. All of them were later confirmed, and a new state $X(4685)$ was discovered by the LHCb Collaboration [427, 428].

The discovery of $X(3872)$ motivated intensive discussions on its nature and other X states. According to recent studies [120, 356, 376, 429–431], $X(3872)$ contains two components, e.g., a \bar{D}^*D molecular component and a $\chi_{c1}(2P)$ charmonium component. The former one accounts for more than 80% of the $X(3872)$ wave function according to the recent analysis of the BESIII Collaboration [406], which indicates that $X(3872)$ couples strongly to the \bar{D}^*D channel. A recent work concluded that the non-molecular component of $X(3872)$ is not dominant judging from the scattering length a and effective range r [431]. Therefore, identifying $X(3872)$ as a pure \bar{D}^*D hadronic molecule, several puzzles associated with $X(3872)$ are resolved. The mass deviation from the conventional quark state can be easily understood in the \bar{D}^*D molecular picture [139, 144, 146, 179, 254, 255, 257, 432–434]. Studying the \bar{D}^*D interaction, lattice QCD simulations found a bound state below the \bar{D}^*D mass threshold, which can be identified as $X(3872)$ [91]. One should note that whether the $X(3872)$ is located above or below the $\bar{D}^{*0}D^0$ mass threshold has not been determined experimentally, which is key to clarifying its nature.

Many decay modes of the $X(3872)$ have been measured. In addition to its total decay width, $\Gamma = 1.19 \pm 0.21$ MeV, obtained from a global analysis of the Belle, BaBar, BESII, and LHCb measurements [435], the absolute branching fractions of the $X(3872)$ decays are given in Table II. The remaining branching fractions

TABLE II. Absolute branching fractions of the $X(3872)$ decays obtained in Ref. [435].

decay modes	Branching fractions(10^{-2})
$X(3872) \rightarrow J/\psi \pi^+ \pi^-$	$4.1^{+1.9}_{-1.1}$
$X(3872) \rightarrow D^{*0} \bar{D}^0 + c.c$	$52.4^{+25.3}_{-14.3}$
$X(3872) \rightarrow J/\psi \gamma$	$1.1^{+0.6}_{-0.3}$
$X(3872) \rightarrow \psi(2S) \gamma$	$2.4^{+1.3}_{-0.8}$
$X(3872) \rightarrow \chi_{c1} \pi^0$	$3.6^{+2.2}_{-1.6}$
$X(3872) \rightarrow J/\psi \omega$	$4.4^{+2.3}_{-1.3}$
$X(3872) \rightarrow \text{Unknown}$	$31.9^{+18.1}_{-31.5}$

of $X(3872)$ is 31.9%, which implies that other partial decays of $X(3872)$ have not been detected. The ratios of the branching fractions of the $X(3872)$ decays are of great value in revealing its nature because, in the ratios, both experimental and theoretical uncertainties are reduced. Assuming $X(3872)$ as a pure excited charmonium state, the ratio of $\Gamma[X(3872) \rightarrow J/\psi \rho]/\Gamma[X(3872) \rightarrow J/\psi \omega]$ is heavily suppressed in the isospin limit, quite different from the experimental data [320, 329, 397], which can, however, be naturally described in the molecular picture [139–141, 356, 436–439]. In Ref. [141], with the molecular interpretation of $X(3872)$ the ratio of $\Gamma[X(3872) \rightarrow \pi^0 \chi_{cJ}]/\Gamma[X \rightarrow \pi^+ \pi^- J/\psi]$ with $J = 0, 1, 2$ measured by the BESIII Collaboration [318] is well described. For the radiative decays, Dong et al. argued that including the $c\bar{c}$ component into the $\bar{D}^* D$ hadronic molecule is necessary to explain the ratio $\Gamma[X(3872) \rightarrow \gamma \psi]/\Gamma[X \rightarrow \gamma \psi(2S)]$ [440], which agrees with the expectation for a pure charmonium [7, 8, 441–443] but inconsistent with that for a pure molecule [444]. From the theoretical analyses of these ratios, one can obtain conclusions on the structure of $X(3872)$ similar to those obtained by analyzing its mass.

The $X(3872)$ has been observed in many modes. First, we examine the productions of $X(3872)$ in b -flavored hadron decays. Within the molecular picture of $X(3872)$, the absolute branching fractions of the decays $B^+ \rightarrow X(3872) K^+$ and $B^0 \rightarrow X(3872) K^0$ and their ratio can be explained [445]. At the same time, they are difficult to understand in the case of a pure charmonium state [446]. In particular, the branching fractions of the decays $B \rightarrow X(3872) K^*$ and $B_s \rightarrow X(3872) \phi$ are explained in the molecular picture of $X(3872)$ in a unified framework [445, 447]. The productions of $X(3872)$ in Y states can also help probe its nature. In Ref. [448], Guo et al. proposed to produce $X(3872)$ in the most promising channel $Y(4260) \rightarrow X(3872) \gamma$ in $e^+ e^-$ collisions via the triangle diagram mechanism, where $Y(4260)$ and $X(3872)$ are $\bar{D} D_1$ and $\bar{D} D^*$ molecules, which has been verified by the BESIII Collaboration [325]. Recently, $X(3872)$ is observed in the process of $e^+ e^- \rightarrow \omega X(3872)$ by the BESIII Collaboration [449],

which is proposed to proceed via an intermediate highly excited vector charmonium [450]. The measurements of the differential cross sections for the productions of J/ψ and $X(3872)$ states in the decay channels $J/\psi\pi^+\pi^-$ are performed by the CMS, LHCb, and ATLAS collaborations, which can be well described assuming $X(3872)$ as a hybrid state in the non-relativistic QCD approach [451].

From the studies of the mass, width, and production of $X(3872)$, one can conclude that it contains a large $\bar{D}D^*$ component. Similarly, other X states are also expected to couple strongly to a pair of charmed mesons. In Refs. [415, 430, 452], it was argued that the couplings of the excited charmonia $\chi_{c0}(2P)$ and $\chi_{c2}(2P)$ to a pair of charmed mesons lead to two physical states around 3.9 GeV, i.e., $X(3915)$ and $Z(3930)$. The invariant mass distributions of these two states were well described in the pionless EFT, indicating that these two states are hadronic molecules generated by the coupled-channel potentials [453]. $X(3915)$ and $Z(3940)$ are assigned as the charmonia $\chi_{c0}(2P)$ [454] and $\chi_{c2}(2P)$ [455] in the conventional quark model. On the other hand, studying the coupled-channel potentials of $D\bar{D}$ and $D_s\bar{D}_s$, lattice QCD simulations found two bound states near these two thresholds [456]. The mixing of hadronic molecules and excited charmonium states makes the energy region 3.9 GeV complex. The newly discovered charmonium state $X(3960)$ is a candidate neither for $\chi_{c0}(2P)$ nor for $\chi_{c0}(3P)$, but is explained as an enhancement in the $D_s\bar{D}_s$ invariant mass distribution due to the existence of a $D_s\bar{D}_s$ bound state [457], a mixture of $c\bar{c}$ and $D_s^+D_s^-$ [458] or a compact tetraquark state [459]. As for the $\chi_{cJ}(3P)$ states with $J = 0, 1, 2$, the predicted masses are around 4.2 GeV in the conventional quark model [8]. Therefore, $X(4140)$ is regarded as a candidate for $\chi_{c1}(3P)$ [429, 460, 461], and $X(4274)$ is regarded as a candidate for $\chi_{c1}(3P)$ [430, 462, 463]. However, there are no good candidates for $\chi_{c0}(3P)$ and $\chi_{c2}(3P)$ experimentally.

C. $Y(4230)$, $Y(4360)$, and some Y states

Immediately after the observation of J/ψ in 1974 [464, 465], several vector charmonia (denoted by Y or ψ) were discovered in e^+e^- annihilations, which, because of the allowed quantum numbers, is ideal for searching for Y states. The most famous vector charmonium state $Y(4260)$ is firstly discovered by the BaBar Collaboration in the $J/\psi\pi\pi$ mass distribution of the $e^+e^- \rightarrow \gamma_{ISR}\pi^+\pi^-J/\psi$ process [466], which was later confirmed by the CLEO [467] and Belle [468] collaboration. On the other hand, the Belle Collaboration found another state near 4.008 GeV, in addition to $Y(4260)$ [468]. The BESIII Collaboration reported a more precise measurement of the $e^+e^- \rightarrow \pi^+\pi^-J/\psi$ process, concluding that there exist two states, i.e., $Y(4220)$ and $Y(4360)$. The former is consistent with the $Y(4260)$ reported by the previous experiment [333]. In the process of $e^+e^- \rightarrow \omega\chi_{c0}$, the BESIII Collaboration observed a resonant state near 4.22 GeV [337, 338], in agreement with the $Y(4220)$, which was also confirmed in the processes $e^+e^- \rightarrow$

$D^0 D^{*-} \pi^+$ [340], $e^+ e^- \rightarrow h_c \pi^- \pi^+$ [334], $e^+ e^- \rightarrow \pi^+ D^{*0} D^{*-}$ [341], $e^+ e^- \rightarrow J/\psi K^+ K^-$ [339], $e^+ e^- \rightarrow \psi(2S) \pi^- \pi^+$ [335], and $e^+ e^- \rightarrow J/\psi \eta$ [343, 344] by the BESIII Collaboration as shown in Table I. Moreover, BaBar and Belle have tried to search for $Y(4220)$ in the decay of $B^+ \rightarrow K^+ \pi^+ \pi^- J/\psi$, but without success [469, 470].

In addition to $Y(4220)$ and $Y(4260)$, other excited vector charmonium states were also needed to explain the experimental data. The BaBar Collaboration observed a resonant state $Y(4320)$ in the process $e^+ e^- \rightarrow \pi^+ \pi^- \psi(2S)$ [345]. This process has been reanalyzed by the Belle Collaboration later, finding that there exist two structures at 4.36 and 4.66 GeV, denoted as $Y(4360)$ and $Y(4660)$ [346], which were later confirmed by the BaBar Collaboration [347]. However, the BESIII Collaboration only confirmed the $Y(4360)$ and the $Y(4220)$ in the process $e^+ e^- \rightarrow \pi^+ \pi^- \psi(2S)$ [335]. In particular, the Belle Collaboration observed a state at 4.63 GeV, named $Y(4630)$, in the $\Lambda_c^+ \Lambda_c^-$ mass distribution [471], consistent with the $Y(4660)$ observed in the process $e^+ e^- \rightarrow \psi(2S) \pi^- \pi^+$. Recently, some highly excited charmonium states, such as $Y(4500)$ [339, 341, 472] and $Y(4700)$ [342, 472], were discovered by the BESIII Collaboration. In the measured R value by the BES Collaboration, the peaks around the energies of $\psi(3770)$, $\psi(4040)$, $\psi(4160)$, and $\psi(4415)$ are pronounced [473], which indicates that these states are pure $c\bar{c}$ charmonia. The studies show that the Y states have strong couplings to hidden-charm final states, while the Y states decaying into open-charm mesons have also been observed recently.

For vector charmonium states, the orbital angular momentum between the charmed quark and antiquark can be $L = 0$ or $L = 2$, mixing S -wave and D -wave. Ref. [474] claimed that the $4S - 3D$ mixing results in two vector charmonium states, $Y(4220)$ and $Y(4380)$. The latter one is a prediction. In the same scheme, the $5S - 4D$ mixing results in two states, $Y(4415)$ and $Y(4500)$. Regarding the quark constituents, the Y states strongly couple to a pair of S -wave charmed meson and P -wave charmed meson. Therefore, $Y(4260)$ is assigned as a $\bar{D}D_1$ bound state [145, 475–480].³ The $Y(4260)$ splits into $Y(4220)$ and $Y(4360)$, which can be nicely arranged into the bound states of $\bar{D}D_1$ and \bar{D}^*D_1 [483–485]. These two states can not be accommodated in the $c\bar{c}$ spectrum [430]. Moreover, the unquenched quark model shows that $\psi(3770)$, $\psi(4040)$, $\psi(4160)$, and $\psi(4415)$ dominantly couple to $\bar{D}D$, \bar{D}^*D^* , \bar{D}^*D^* , and \bar{D}^*D_1 [430]. As the masses of excited vector charmonia reach 4.6 GeV, other configurations, such as charmed baryon and antibaryon pairs or three-body charmed mesons, should be considered on top of the $c\bar{c}$ configurations.

³ We note that, however, Ref. [481] explained $Y(4260)$ as a $J/\psi K \bar{K}$ three-body molecule, similar to the picture where the $X(2175)$ state is a $\phi K \bar{K}$ three-body molecule [482].

D. $Z_c(3900)$, $Z_c(4020)$, and $Z_{cs}(3985)$

Next, we turn to the Z_c states. In 2013, the BESIII Collaboration reported a hidden-charm tetraquark state $Z_c(3900)$ in the $\psi\pi^\pm$ mass distribution of $e^+e^- \rightarrow J/\psi\pi^+\pi^-$ [12], which was reported by the Belle Collaboration several days later [486]. The $Z_c(3900)$ was also observed in the $(D\bar{D}^*)^\pm$ invariant mass distribution [487]. Its neutral partner $Z_c(3900)^0$ was also observed [488]. We note that the $Z_c(3900)$ is an isovector state and located close to the $D\bar{D}^*$ mass threshold. Another state $Z_c(4020)$ near the mass threshold of $D^*\bar{D}^*$ was discovered in the $\pi^\pm h_c$ mass distribution of $e^+e^- \rightarrow h_c\pi^+\pi^-$ [489] and the $(D^*\bar{D}^*)^\pm$ mass distribution of $e^+e^- \rightarrow (D^*\bar{D}^*)^\pm\pi^\pm$ [490] by the BESIII Collaboration. The Belle Collaboration reported a charged charmonium-like structure at $M_{\pi^\pm\psi(2S)} = 4.05$ GeV in the $Y(4360)$ decays with 3.5σ [348]. We note that the $Z_c(3900)$ has not been seen in b hadron decays such as $\bar{B}^0 \rightarrow (J/\psi\pi^+)K^-$ by the Belle collaboration [491] and $B^0 \rightarrow (J/\psi\pi^+)\pi^-$ by the LHCb collaboration [492]. The Belle Collaboration has reported the upper limit of $Z_c^0(3900)$ and $Z_c^0(4020)$ in B decays, i.e., $\mathcal{B}(B^\pm \rightarrow K^\pm Z_c^0(3900))\mathcal{B}(Z_c^0(3900) \rightarrow \eta_c\pi^+\pi^-) = 4.7 \times 10^{-5}$ and $\mathcal{B}(B^\pm \rightarrow K^\pm Z_c^0(4020))\mathcal{B}(Z_c^0(4020) \rightarrow \eta_c\pi^+\pi^-) = 1.6 \times 10^{-5}$ [493]. In the semi-inclusive weak decays of b -favored hadrons, the D0 Collaboration first observed $Z_c(3900)$ in the $J/\psi\pi^\pm$ mass distribution in $p\bar{p}$ collisions [494], which is correlated to the $J/\psi\pi^+\pi^-$ system in the invariant mass spectrum including $Y(4230)$ and $Y(4360)$. Recently, the BESIII Collaboration observed a state $Z_{cs}(3985)$ near the $D_s^- D^{*0}/D_s^{*-} D^0$ mass threshold in the K^+ recoil mass distribution of the $e^+e^- \rightarrow D_s^- D^{*0} K^+ / D_s^{*-} D^0 K^+$ process [495], which is generally viewed as the SU(3)-flavor partner of $Z_c(3900)$. Very recently, the $Z_{cs}(4000)$ is observed in the $J/\psi\phi$ mass distribution in the decay of $B^+ \rightarrow J/\psi\phi K^+$ by the LHCb Collaboration [428]. The masses of $Z_{cs}(4000)$ and $Z_{cs}(3985)$ are consistent with each other, but the width of the former is much larger than that of the latter. There are heated discussion on whether they are the same states [496–500].

Another charged hidden-charm tetraquark state is the $Z_c(4430)$ discovered by the Belle Collaboration in the $\pi\psi(2S)$ mass distribution of the decay $B \rightarrow \pi^\pm K\psi(2S)$ [501]. Although this state was not confirmed by the BaBar Collaboration [502], it was confirmed in the same process by the LHCb collaboration seven years later [503]. One should note that much progress has been made in searching for the Z_c states in exclusive b decays. The Belle Collaboration observed two states $Z_{c1}(4050)$ and $Z_{c2}(4250)$ in the $\pi^-\chi_{c1}$ mass distribution of the $B^0 \rightarrow K^+\pi^-\chi_{c1}$ decay [504]. These two states are not confirmed by the BaBar Collaboration [505]. In the decay of $B^0 \rightarrow \eta_c(1S)\pi^- K^+$, the LHCb Collaboration observed a state $Z_c(4100)$ in the $\eta_c(1S)\pi^-$ mass distribution [506]. Due to the low significance of $Z_c(4100)$ in the LHCb data, more data are required to confirm this state. The Belle Collaboration observed two charged bottomonium-like resonant states, $Z_b(10610)$ and $Z_b(10650)$, in five different decay channels, $\pi^\pm\epsilon(nS)$ ($n = 1, 2, 3$), and

$h_b(mP)\pi^\pm$ ($m = 1, 2$) [507], which are close to the \bar{B}^*B and \bar{B}^*B^* mass thresholds, similar to the $Z_c(3900)$ and $Z_c(4020)$.

Given that $Z_c(3900)$ and $Z_c(4020)$ are located in the vicinity of the \bar{D}^*D and \bar{D}^*D^* mass thresholds, they are expected to be the \bar{D}^*D and \bar{D}^*D^* resonant states [508–511]. The isovector $\bar{D}^*D^{(*)}$ potentials are less attractive than the isoscalar $\bar{D}^*D^{(*)}$ potentials, and therefore there are no bound states in the isovector sector [254, 512]. However, if the next-to-leading order potentials are taken into account, one can obtain the molecules above the \bar{D}^*D and \bar{D}^*D^* mass thresholds [513, 514]. Considering SU(3)-flavor symmetry, the molecules above the $D_s^*\bar{D}$ and $D_s^*\bar{D}^*$ mass thresholds are expected [496, 514–516], the former of which corresponds to $Z_{cs}(3985)$ discovered by the BESIII Collaboration. Similarly, with heavy quark flavor symmetry, two hadronic molecules above the \bar{B}^*B and \bar{B}^*B^* mass thresholds may correspond to $Z_b(10610)$ and $Z_b(10650)$ [513, 517–519]. In the QCD sum rule approach, $Z_c(3900)$, $Z_c(4020)$, and $Z_{cs}(3985)$ are assigned as compact tetraquark states [500], in agreement with Refs. [77, 520–524]. Since the isovector $\bar{D}^*D^{(*)}$ potentials are not strong enough to form bound states, they may manifest themselves as cusp structures in the vicinity of the $\bar{D}^*D^{(*)}$ mass thresholds [475, 477, 525–529].

E. $P_c(4380)$, $P_c(4312)$, $P_c(4440)$, and $P_c(4457)$

In 2015, the LHCb Collaboration observed two hidden-charm pentaquark states, $P_c(4380)$ and $P_c(4450)$, in the $J/\psi p$ mass distribution of the decay of $\Lambda_b \rightarrow J/\psi p K$ [538], which are also analyzed in the full amplitude fit to the decay of $\Lambda_b \rightarrow J/\psi p \pi$ with a low significance [541]. In the updated analysis of a large data sample in 2019, the $P_c(4450)$ splits into two states $P_c(4440)$ and $P_c(4457)$, and in addition a new state $P_c(4312)$ was observed in the same process [14]. The quest for the $P_c(4312)$ in the $\eta_c p$ mass distribution of the $\Lambda_b \rightarrow \eta_c p K$ decays is performed by the LHCb Collaboration, while no evidence is found [542]. In 2020, the LHCb Collaboration observed a hidden-charm strange pentaquark $P_{cs}(4459)$ in the $J/\psi \Lambda$ mass distribution in the decay of $\Xi_b \rightarrow J/\psi \Lambda K$ [540]. Such a state can also be viewed as a mixture of two pentaquark states near the mass of $P_{cs}(4459)$. The hidden-charm pentaquark state $P_c(4337)$ was observed in the $J/\psi p$ and $J/\psi \bar{p}$ mass distribution of the decay $B_s \rightarrow J/\psi p \bar{p}$ [543]. Very recently, the LHCb Collaboration reported a hidden-charm strange pentaquark $P_{cs}(4338)$ in the $J/\psi \Lambda$ mass distribution of the decay $B \rightarrow J/\psi \Lambda \bar{p}$ [544].

Recent studies [177, 186, 232, 545, 546] show that the $\bar{D}^{(*)}\Sigma_c^{(*)}$, $\bar{D}^{(*)}\Lambda_c$, $J/\psi p$, and $\eta_c p$ channels all contribute to the formation of the hidden-charm pentaquark molecules, where the $\bar{D}^{(*)}\Sigma_c^{(*)}$ channels play the dominant role. From the perspective of the one-meson exchange theory, the potentials of $\bar{D}^{(*)}\Sigma_c^{(*)} \rightarrow \bar{D}^{(*)}\Sigma_c^{(*)}$, $\bar{D}^{(*)}\Sigma_c^{(*)} \rightarrow \bar{D}^{(*)}\Lambda_c$, and $\bar{D}^{(*)}\Lambda_c \rightarrow \bar{D}^{(*)}\Lambda_c$ are induced by light meson exchanges, while

TABLE III. Production and decay modes of $Z_c(3900)$, $Z_c(4020)$, $P_c(4312)$, $P_c(4440)$, $P_c(4457)$, $P_c(4380)$, $P_{cs}(4338)$, $P_{cs}(4459)$, and $T_{cc}^+(3875)$.

State	J^P	Inclusive process	Decay modes	Exclusive process	Decay modes
$Z_c(3900)$	1^+	$e^+e^- \rightarrow J/\psi\pi^0\pi^0$	$J/\psi\pi^0$ [530]	$Y(4260) \rightarrow J/\psi\pi^+\pi^-$	$J/\psi\pi^\pm$ [12, 486]
		$e^+e^- \rightarrow \pi^\pm(\bar{D}D^*)^\mp$	$(\bar{D}D^*)^\mp$ [487, 531]	$Y(4160) \rightarrow J/\psi\pi^+\pi^-$	$J/\psi\pi^\pm$ [488]
		$e^+e^- \rightarrow \pi^0(\bar{D}D^*)^0$	$(\bar{D}D^*)^0$ [532]	$Y(4220) \rightarrow J/\psi\pi^0\pi^0$	$J/\psi\pi^0$ [533]
		e^+e^-	$\pi^+\pi^-D^+D^-$ [349]		
		e^+e^-	$\gamma\chi_{c2}$ [350]		
		$e^+e^- \rightarrow \pi^\pm Z_c^\mp(3900)$	$\rho^\mp\eta_c$ [534]		
$Z_c(4020)$	1^+	$e^+e^- \rightarrow h_c\pi^+\pi^-$	$h_c\pi^\pm$ [489]		
		$e^+e^- \rightarrow h_c\pi^0\pi^0$	$h_c\pi^0$ [535]		
		$e^+e^- \rightarrow \pi^0(\bar{D}^*D^*)^0$	$(\bar{D}^*D^*)^0$ [536]		
		$e^+e^- \rightarrow \pi^\pm(\bar{D}^*D^*)^\mp$	$(\bar{D}^*D^*)^\mp$ [490]		
$Z_{cs}(3985)$	1^+	$e^+e^- \rightarrow K^+(D_s^-D^{*0} + D_s^{*-}D^0)$	$RM(K^+)$ [495]		
		$e^+e^- \rightarrow K_S^0(D_s^+D^{*-} + D_s^{*+}D^-)$	$RM(K_S^0)$ [537]		
$P_c(4312)$	$1/2^+$			$\Lambda_b \rightarrow J/\psi p\bar{K}$	$J/\psi p$ [14]
$P_c(4380)$	$3/2^+$			$\Lambda_b \rightarrow J/\psi p\bar{K}$	$J/\psi p$ [538]
$P_c(4440)$??			$\Lambda_b \rightarrow J/\psi p\bar{K}$	$J/\psi p$ [14]
$P_c(4457)$??			$\Lambda_b \rightarrow J/\psi p\bar{K}$	$J/\psi p$ [14]
$P_{cs}(4338)$	$1/2^+$			$B \rightarrow J/\psi\Lambda\bar{p}$	$J/\psi\Lambda$ [539]
$P_{cs}(4459)$	$1/2^+$			$\Xi_b \rightarrow J/\psi\Lambda\bar{K}$	$J/\psi\Lambda$ [540]
$T_{cc}^+(3875)$	1^+	pp	$D^0D^0\pi^+$ [13]		

those of $\bar{D}^{(*)}\Sigma_c^{(*)} \rightarrow J/\psi p$ and $\bar{D}^{(*)}\Sigma_c^{(*)} \rightarrow \eta_c p$ are from the exchanges of charmed mesons, which are difficult to be accommodated in a unified model since the charmed meson exchange may not work at short distances [157]. Due to the uncertainties in the off-diagonal potentials, the partial decays of hidden-charm pentaquark molecules have large uncertainties. As shown in Ref. [232], once the coupled-channel potentials are considered, Scenario A is more favored than Scenario B, which is quite different from the single-channel case [547]. In the heavy quark limit, the contact potentials of the $\bar{D}^{(*)}\Sigma_c^{(*)}$ system can be parameterized by two parameters C_a and C_b , corresponding to the spin-spin independent term and spin-spin dependent term. The ratio of C_b to C_a in the single-channel case is determined as -0.176 in scenario A and 0.158 in

scenario B [149], consistent with that in the couple-channel case [232]. Ref. [231] argued that the visible structure of $P_c(4457)$ is due to the effect of triangle singularity, while the ratio C_b/C_a is around 0.5, which violates the spirit of EFTs. The two-body decays of pentaquark molecules are investigated in the contact EFT approach, which can also be studied via the triangle mechanism [545, 548]. The three-body decays of pentaquark molecules have also been estimated, and the decays of pentaquark molecules with Σ_c^* baryons account for a large proportion of their total widths [549]. In addition to the molecular interpretations, there exist other explanations for these pentaquark states, e.g., hadro-charmonia [550], compact pentaquark states [551–557], virtual states [558], triangle singularities [559], and cusp effects [231]. With SU(3)-flavor symmetry, the $\bar{D}^{(*)}\Sigma_c^{(*)}$ molecules indicate the existence of the $\bar{D}^{(*)}\Xi_c^{\prime(*)}$ molecules [560–563], but no bound states near the $\bar{D}^{(*)}\Xi_c$ mass thresholds [561]. However, $P_{cs}(4338)$ and $P_{cs}(4459)$ discovered by the LHCb Collaboration are in the vicinity of mass thresholds of $\bar{D}\Xi_c$ and $\bar{D}^*\Xi_c$. There may exist some mechanism to increase the strength of the $\bar{D}^{(*)}\Xi_c$ potentials, such as coupled-channel effects and SU(3)-flavor symmetry breaking effects [564].

F. $T_{cc}(3875)$

In 2017, the LHCb Collaboration observed a doubly charmed baryon Ξ_{cc}^{++} in the $\Lambda_c^+ K^- \pi^+ \pi^+$ mass distribution in pp collisions [565]. In 2020, the LHCb Collaboration observed a narrow doubly charmed tetraquark state T_{cc} in the $DD\pi$ mass distribution in pp collisions [13]. Its mass and width are of the order of hundreds of keV [566], which is the most precisely measured exotic state. Such states containing a pair of charm quarks are explicitly exotic and have attracted much attention.

Since the doubly charmed tetraquark state lies close to the DD^* mass threshold, the discussions on the DD^* potential motivated several lattice QCD groups [567–569], indicating that there exists a virtual state at the DD^* mass threshold. According to Refs. [257, 570], the isoscalar DD^* potential is less attractive than the isoscalar $\bar{D}D^*$ potential, which is likely to generate a weakly bound state below the DD^* mass threshold. Identifying the doubly charmed tetraquark state T_{cc} as a DD^* molecule, the decay widths of T_{cc} can be reasonably explained as well [571–574]. It is worth noting that the precise mass of T_{cc} inspired studies of high order contributions to the DD^* potentials in effective field theories [575–577], as well as the impact of the left-hand cut in the DD^* scattering [578–580]. The compositeness analysis indicates that the newly discovered T_{cc} is dominantly a DD^* molecule [178, 376, 581–584], which implies the existence of a small compact tetraquark component. In Refs. [64, 585–588], the compact tetraquark picture for the T_{cc} was investigated.

III. MULTIPLTS OF HADRONIC MOLECULES

A. Symmetries

This review only focuses on the hadronic molecular interpretation of the exotic states introduced in the previous section. If these states are dominantly hadronic molecules, one can deduce the underlying hadron-hadron interactions from their masses and related properties. Using symmetry arguments, these interactions can then be extended to those between pairs of other hadrons.

It is well known that symmetries play a crucial role in particle and nuclear physics. Considering SU(3)-flavor symmetry, Gellmann classified the ground-state light mesons and baryons and predicted the existence of the 10th particle Ω in the ground-state decuplet [4], which was later verified experimentally [589]. Symmetries can also help relate hadronic molecules; thus, they play a vital role in understanding them. The SU(3)-flavor symmetry, HQSS, HQFS, and HADS have been widely applied to study hadronic molecules. Symmetries also manifest themselves in the potentials between pairs of hadrons. This can be best demonstrated in the contact-range effective field theory. As a result, in this review, we take the contact-range potentials to discuss hadronic molecules and the symmetry implications for the existence of multiplets of hadronic molecules.

Effective field theories (EFTs) are low-energy theories that apply to specific systems within a specified energy range, where the underlying high-energy theory for these systems is unknown or unsolvable. The interactions of a given system are expressed by the Lagrangian, which contains all the terms satisfying the relevant symmetry requirements. The terms are ordered by a small quantity M_s/M_h , where M_s and M_h represent the soft scale and hard scale. The advantage of EFTs is that they can systematically improve the results according to an appropriate power counting rule, and one can estimate the uncertainties of any given order. In the following, we briefly introduce the kinds of EFTs relevant to the present reviews. For details on these EFTs, one can refer to the comprehensive reviews [32, 170, 171, 263, 590].

QCD is part of the Standard Model of particle physics that deals with quarks, gluons, and their strong interactions. The strong interaction is weak at short distances or high momentum transfer, referred to as the asymptotic freedom. At the same time, it is strong at long distances or low energies, leading to the confinement of quarks into colorless objects, i.e., hadrons, which dictates that the strong interaction is non-perturbative at low energies. ChEFT is one of the most successful theories for the non-perturbative strong interaction. It is based on chiral symmetry and its breaking pattern, which strongly constrains the interactions between hadrons consisting of light quarks (u , d , and to a lesser extent s). In recent years, it has been extended to the heavy quark sector. A recent review on this topic is Ref. [40]. Chiral symmetry

is explicitly broken due to the non-vanishing quark masses. In addition, a spontaneously broken global symmetry implies the existence of (massless) Nambu-Goldstone bosons with the quantum numbers of the broken generators. The pion masses are not exactly zero because the up and down quark masses are not exactly zero, i.e., explicit chiral symmetry breaking. ChEFT has traditionally been widely applied to understand hadron-hadron interactions in the light-quark sector, where the relevant degrees of freedom are hadrons and pions. Because the interactions with the Nambu-Goldstone bosons must vanish in the chiral limit, the low-energy expansion of the chiral Lagrangian is arranged in powers of derivatives and the pion mass. The hard scale of ChEFT is the chiral symmetry breaking scale, $\Lambda_\chi \approx 1$ GeV, and the soft scale Q is a small external momentum or the pion mass. As the nucleon is embodied into ChEFT, the above power counting rule is destroyed due to the non-vanishing nucleon mass in the chiral limit, which can be solved by treating baryons as heavy static sources (i.e., HBChPT) [591, 592] or adopting the so-called extended on-mass-shell scheme [593, 594].

The effective field theory dealing with heavy hadrons is the heavy quark effective field theory (HQFT) [595, 596], where the hard scale and soft scale are the masses of heavy quarks m_Q ($Q=c,b$) and QCD scale Λ_{QCD} , leading to a new expansion parameter Λ_{QCD}/m_Q . Since m_Q is larger than Λ_{QCD} , i.e., $\Lambda_{QCD}/m_Q \ll 1$, the heavy quark acts like a static color source, similar to the HBChPT. A heavy quark inside a hadron shares the velocity v as the hadron. Thus, its momentum can be written as $p = mv + k$, where k is a small residual momentum of the order of Λ_{QCD} . In this picture, the heavy quark field Ψ is decomposed into

$$\Psi(x) = e^{-imv \cdot x} (h_v(x) + H_v(x)), \quad (1)$$

where $h_v(x)$ and $H_v(x)$ are defined as

$$\begin{aligned} h_v(x) &= e^{-imv \cdot x} \frac{1 + \not{v}}{2} \Psi(x), \\ H_v(x) &= e^{-imv \cdot x} \frac{1 - \not{v}}{2} \Psi(x). \end{aligned} \quad (2)$$

In the rest frame of the heavy quark, h_v and H_v correspond to the upper and lower components of Ψ , also called the large and small components of Ψ . The QCD Lagrangian $\mathcal{L}_{QCD} = \bar{\Psi} i \not{D} \Psi - m \bar{\Psi} \Psi$ with $D_\mu = \partial_\mu - ig T^a A_\mu^a$ is simplified as

$$\mathcal{L}_{eff} = \bar{h}_v i v \cdot D h_v + \bar{h}_v i \not{D}_\perp \frac{1}{i v \cdot D + 2m - i\varepsilon} i \not{D}_\perp h_v. \quad (3)$$

The lowest order of the above effective Lagrangian in $1/m_Q$ is written as

$$\mathcal{L}_{eff}^0 = \bar{h}_v (i v^\mu \partial_\mu + g v^\mu T^a A_\mu^a) h_v, \quad (4)$$

which exhibits the crucial features of HQET: the quark-gluon coupling is independent of the quark's spin, and the Lagrangian is independent of the heavy quark flavor, showing the heavy quark spin-flavor symmetry,

i.e., HQSS and HQFS, which are broken by the $1/m_Q$ -contributions. The heavy quark symmetry dictates that the strong interaction is independent of the heavy quark spin, which provides a natural explanation for the mass difference of (D, D^*) and (B, B^*) and those of their baryon counterparts. It is important to note that the effective Lagrangian describing the interactions between heavy mesons and Nambu-Goldstone bosons should satisfy heavy quark symmetry, Lorentz invariance, and chiral symmetry [597]. The fields of a pair of (D, D^*) mesons are written as a superfield, i.e., $H = \frac{1+\not{v}}{2}(D^{*\mu}\gamma_\mu - D\gamma_5)$ and $\bar{H} = (D^{*\mu\dagger}\gamma_\mu + D^\dagger\gamma_5)\frac{1+\not{v}}{2}$ [598]. Thus, the effective Lagrangians are written as

$$\mathcal{L} = \frac{i}{2} \text{Tr} \bar{H}_a v^\mu (\xi^\dagger \partial_\mu \xi + \xi \partial_\mu \xi^\dagger)_{ba} H_b, \quad (5)$$

where ξ is the pseudoscalar octet meson field. To include the effect of HQSS breaking, the color magnetic moment term is included

$$\delta\mathcal{L} = \frac{\lambda_2}{m_Q} \text{Tr} \bar{H}_a \sigma^{\mu\nu} \sigma_{\mu\nu} H_b. \quad (6)$$

The heavy quark symmetry has been applied to analyze the exclusive semileptonic decays of $B \rightarrow D l \nu_l$ and $B \rightarrow D^* l \nu_l$. The B mesons transiting into D mesons are parameterised as [599, 600]

$$\begin{aligned} \langle D(v') | \bar{c} \gamma^\mu b | B(v) \rangle &= \sqrt{m_D m_B} \xi(v \cdot v') (v + v')_\mu \\ \langle D^*(v', \varepsilon) | \bar{c} \gamma^\mu b | B(v) \rangle &= \sqrt{m_D m_B} i \xi(v \cdot v') \varepsilon_{\mu\nu\alpha\beta} \varepsilon^{*\nu} v'^\alpha v^\beta \\ \langle D^*(v', \varepsilon) | \bar{c} \gamma^\mu b | B(v) \rangle &= \sqrt{m_D m_B} \xi(v \cdot v') \varepsilon_{\mu\nu\alpha\beta} [(1 + v \cdot v') \varepsilon_\mu^* - (\varepsilon^* \cdot v) v_\mu], \end{aligned} \quad (7)$$

where $\xi(v \cdot v')$ is the Isgur-Wise function, which indicates that the heavy quark symmetry constrains the form factors [601, 602].

HQET only separates the scales Λ_{QCD} and m_Q . In contrast, the scale of the doubly heavy baryon is characterized by $m_Q v$ and $m_Q v^2$ as the diquark taken as elementary degrees of freedom is embodied into HQFT, where v is the typical velocity of heavy quarks in the bound states [603, 604]. On the other hand, the energy scale that governs the interaction between the heavy diquark and light one is Λ_{QCD} . For $m_Q v \gg \Lambda_{QCD}$, a pair of heavy quarks behaves like a point-like particle referred to as a diquark in an antitriplet or sextet color configuration. The interaction of the antitriplet field with the light quark is similar to that of the heavy antiquark with a light quark in the D and B mesons. Consequently, the behavior of a pair of heavy quarks is similar to a heavy anti-quark regarding the color degree of freedom within the heavy quark limit. This symmetry is often called HADS, first proposed in Ref. [605]. Using the HQET one can derive the relationship of mass splitting between single charmed mesons and doubly charmed baryons, e.g., $m_{D^*} - m_D = \frac{3}{4}(m_{\Xi_{cc}^*} - m_{\Xi_{cc}})$ [604], which has been confirmed by a series of lattice QCD groups. Moreover, one can arrive at the relationship for the single charmed mesons and doubly charmed

baryons couplings to the pion, e.g., $g_{\Xi_{QQ}\Xi_{QQ}\pi} = -\frac{1}{3}g_{H_Q H_Q \pi}$ [606], which is similar to the relationship $g_{\Xi_{QQ}\Xi_{QQ}\pi} = -\frac{5}{12}g_{H_Q H_Q \pi}$ derived in the quark model [607]. However, the HADS has not been explicitly verified experimentally.

At last, we discuss the SU(3)-flavor symmetry. In terms of the recent results of lattice QCD, the ratio of the decay constant of the π meson to that of the K meson is $f_K/f_\pi \approx 1.19$ [608], which indicates that the breaking of SU(3)-flavor symmetry is about 19%. SU(3)-flavor symmetry has also been adopted to study the branching fractions of the nonleptonic decays of charmed baryons and shown to be approximately satisfied [212, 609–615]. Motivated by the exotic states discovered in b -flavored hadron decays, SU(3)-flavor symmetry is employed to discuss their relationships [616–619]. The SU(3)-flavor symmetry is also used in studying hadron-hadron interactions, such as hyperon-nucleon interactions [620–623] and hyperon-hyperon interactions [30, 87, 624–627]. Recently, inspired by the discoveries of the tetraquark state $Z_{cs}(3985)$ as well as the pentaquark states $P_{cs}(4459)$ and $P_{cs}(4338)$, SU(3)-flavor symmetry is employed to predict their symmetry partners [163, 181, 514, 515, 560, 561, 628–633].

Based on the above symmetries, one can find the relationship between hadron-hadron potentials, which can help reduce the number of unknown parameters of the potentials and reduce the uncertainties of theoretical studies. In this review, we mainly focus on the contact potentials of EFTs (see the Appendix for details). Once the hadron-hadron potentials are obtained, one can analyze some physical observables of relevant scattering processes by solving the Schrödinger equation or Lippmann-Schwinger equation. Due to the scarcity of scattering data, one usually employs the masses and widths of exotic states near the mass thresholds of a pair of hadrons as inputs. With the development of lattice QCD simulations in recent years, it has become a reliable approach to extracting information on hadron-hadron scattering.

B. Mass spectra

In this section, we discuss the likely existence of multiplets of hadronic molecules in the $D^{(*)}K$, $\bar{D}^{(*)}\Sigma_c^{(*)}$, $\bar{D}^{(*)}D^{(*)}$, and $\bar{\Sigma}_c^{(*)}\Sigma_c^{(*)}$ systems, where HQSS correlates the states belonging to the same multiplet. Moreover, we discuss the multiplets of hadronic molecules involving the excited charmed mesons or baryons related by HQSS. Based on the established HQSS multiplets of hadronic molecules, we predict other hadronic molecules using the SU(3)-flavor symmetry, HADS, and HQFS.

TABLE IV. Binding energies (B in units of MeV) and mass spectra (M in units of MeV) of isoscalar DK and D^*K molecules.

molecule	I	J^P	B (MeV)	M (MeV)
DK	0	0^+	45	Input
D^*K	0	1^+	48	2456

1. $D^{(*)}K$ molecules

Identifying $D_{s0}^*(2317)$ and $D_{s1}(2460)$ as DK and D^*K molecules, their mass splitting can be naturally explained. Since the D meson and the D^* meson are related to each other by HQSS, $D_{s0}^*(2317)$ and $D_{s1}(2460)$ are viewed as a doublet of hadronic molecules. In terms of the meson exchange theory [634] and chiral perturbation theory [635], the DK and D^*K potentials are the same, which implies that the contact-range potentials of DK and D^*K are the same, denoted by C_a [636]. With the mass of $D_{s0}^*(2317)$, the unknown parameter C_a is determined to be 62.61 GeV^{-2} for a cutoff $\Lambda = 1 \text{ GeV}$, and then the mass of the D^*K molecule is predicted as shown in Table IV, which satisfies HQSS. In the molecular picture [635, 637, 638], $D_{s1}(2460)$ is considered to be the counterpart of $D_{s0}^*(2317)$. Recent studies showed that the compositeness of $D_{s0}^*(2317)$ and $D_{s1}(2460)$ is around 70% and 50% [46, 380], where the impact of other components on the $D^{(*)}K$ scattering can come from the CDD pole or the form factors. Replacing the K meson by the K^* meson, one would naturally expect other multiplets of hadronic molecules of DK^* [367] and D^*K^* [184].

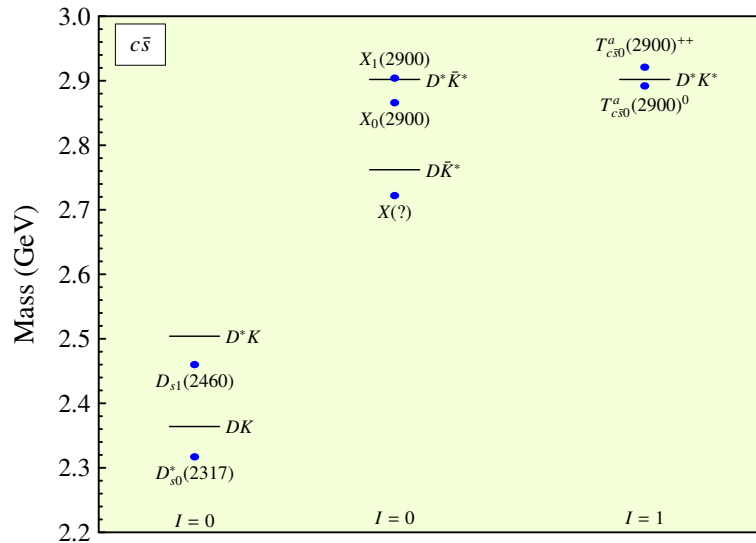


FIG. 1. Locations of charmed-strange hadronic molecular candidates with respect to the $D^{(*)}K$, $D^{(*)}\bar{K}^*$, and D^*K^* mass thresholds.

With the G -parity transformation, one can relate the $D^* \bar{K}^*$ system with the $D^* K^*$ system. Several enhancements have been discovered near the $D^* \bar{K}^*$ mass thresholds [414, 639]. The open-charm tetraquark state $X_0(2866)$ is assigned as the isoscalar $D^* \bar{K}^*$ bound state with $J^P = 0^+$ [634, 636, 637, 640–642]. However, it is still controversial for the existence of the two molecules of $J^P = 1^+$ $D^* \bar{K}^*$ and $J^P = 2^+$ $D^* \bar{K}^*$. The OBE model indicates that the $D^* \bar{K}^*$ potential with $J^P = 0^+$ is more attractive than that of $D^* \bar{K}^*$ with $J^P = 2^+$ [634]. However, it is opposite to the results of the local hidden gauge approach [643]. The difference can be traced to the different prescriptions of the spin-spin interactions of the two hadrons. Very recently, assuming that the hadron-hadron interaction at the quark level is only generated by the u and d quarks while the s quark is treated as a heavy spectator, Wang et al. assigned the newly discovered $T_{cs0}(2900)$ and $T_{cs0}^a(2900)$ as the SU(2) partners of T_{cc} and $Z_c(3900)$ in the molecular picture [644]. We show the locations of the above exotic states with respect to the mass thresholds of $D^{(*)}K$, $D^{(*)}\bar{K}^*$, and D^*K^* in Fig. 1.

One can relate a charmed meson to a doubly charmed baryon through HADS in the heavy quark limit. Therefore, motivated by the interpretation of $D_{s0}^*(2317)$ and $D_{s1}(2460)$ as DK and D^*K molecules, several works investigated the $\Xi_{cc}^{(*)}K$ potentials and the likely existence of corresponding hadronic molecules [645–648]. One should note that the $\Xi_{cc}^{(*)}K$ molecules can mix with excited Ω_{cc} baryons. Moreover, in terms of HQFS, one would expect the existence of BK and B^*K molecules [387, 649, 650], the bottom partners of $D_{s0}^*(2317)$ and $D_{s1}(2460)$, i.e., B_{s0}^* and B_{s1} . Currently, there is no experimental sign for the existence of these bottom mesons. Their future discovery will surely help establish the molecular nature of $D_{s0}^*(2317)$ and $D_{s1}(2460)$.

2. $\bar{D}^{(*)}\Sigma_c^{(*)}$ molecules

In the heavy quark limit, the $\bar{D}^{(*)}\Sigma_c^{(*)}$ system develops seven states. Its contact-range potentials are parameterized by two unknown constants, i.e., C_a and C_b . Assuming the three hidden-charm pentaquark states $P_c(4312)$, $P_c(4440)$, and $P_c(4457)$ as $\bar{D}^{(*)}\Sigma_c$ bound states, one can fully determine C_a and C_b , and then predict the masses of the other four states. In Ref. [547] two scenarios are proposed: the $P_c(4440)$ and $P_c(4457)$ as $\frac{1}{2}^-$ and $\frac{3}{2}^-$ $\bar{D}^*\Sigma_c$ molecules (scenario A) or $\frac{3}{2}^-$ and $\frac{1}{2}^-$ $\bar{D}^*\Sigma_c$ molecules (scenario B). The $P_c(4312)$ is used to select the favorable scenario. To show the impact of the cutoff in the form factor on the results, the cutoff is varied from 0.5 GeV to 1 GeV. In addition, a 15% uncertainty originates from HQSS breaking was considered, which is estimated by the expansion $\mathcal{O}(\Lambda_{QCD}/m_c)$ with $\Lambda_{QCD} \sim 200 - 300$ MeV and $m_c = 1.5$ GeV [651].

In Table V, the mass spectra of the $\bar{D}^{(*)}\Sigma_c^{(*)}$ molecules in both scenarios are presented, where the

TABLE V. Binding energies (in units of MeV) for the pentaquarks composed of a charmed baryon and a charmed antimeson, obtained in the contact-range EFT with the two constants fixed by reproducing $P_c(4440)$ and $P_c(4457)$ as $1/2^-$ and $3/2^-$ molecules (scenario A) and $3/2^-$ and $1/2^-$ (scenario B), for cutoffs of 0.5 and 1 GeV. The 15% uncertainty is estimated by the heavy quark spin symmetry breaking for the contact-range potentials.

State	J^P	Threshold	$\Lambda(\text{GeV})$	B.E (Scenario A)	B.E (Scenario B)
$P_c(4312)(\bar{D}\Sigma_c)$	$\frac{1}{2}^-$	4320.8	0.5(1)	$8.8^{+5.0}_{-4.2}$ ($7.6^{+9.2}_{-6.0}$)	$14.4^{+6.5}_{-5.8}$ ($12.8^{+11.8}_{-8.6}$)
$P_c(?) (\bar{D}\Sigma_c^*)$	$\frac{3}{2}^-$	4385.3	0.5(1)	$9.1^{+5.0}_{-4.3}$ ($8.1^{+9.4}_{-6.3}$)	$14.7^{+6.6}_{-5.9}$ ($13.5^{+12.0}_{-8.9}$)
$P_c(4440)(\bar{D}^*\Sigma_c)$?	4462.2	0.5(1)	Input($\frac{1}{2}^-$)	Input($\frac{3}{2}^-$)
$P_c(4457)(\bar{D}^*\Sigma_c)$?	4462.2	0.5(1)	Input($\frac{3}{2}^-$)	Input($\frac{1}{2}^-$)
$P_c(?) (\bar{D}^*\Sigma_c^*)$	$\frac{1}{2}^-$	4526.7	0.5(1)	$25.6^{+9.0}_{-8.4}$ ($26.3^{+16.6}_{-13.7}$)	$3.0^{+2.8}_{-2.0}$ ($3.4^{+6.3}_{-3.2}$)
$P_c(?) (\bar{D}^*\Sigma_c^*)$	$\frac{3}{2}^-$	4526.7	0.5(1)	$15.8^{+6.7}_{-6.1}$ ($15.9^{+12.8}_{-9.8}$)	$10.0^{+5.2}_{-4.5}$ ($10.0^{+10.2}_{-7.2}$)
$P_c(?) (\bar{D}^*\Sigma_c^*)$	$\frac{5}{2}^-$	4526.7	0.5 (1)	$3.0^{+2.8}_{-2.0}$ ($3.4^{+6.3}_{-3.2}$)	$25.6^{+9.0}_{-8.4}$ ($26.3^{+16.6}_{-13.7}$)

values inside and outside the parentheses correspond to the cutoff for $\Lambda = 1 \text{ GeV}$ and $\Lambda = 0.5 \text{ GeV}$. Comparing the results for $\Lambda = 1 \text{ GeV}$ and $\Lambda = 0.5 \text{ GeV}$, one finds that the results only weakly depend on the cutoff. Clearly, one can not discriminate the two scenarios from the $P_c(4312)$ mass. Nevertheless, in addition to $P_c(4312)$, $P_c(4440)$, and $P_c(4457)$, four more molecules are predicted, leading to a complete HQSS multiplet of hadronic molecules [547]. Such a multiplet is later confirmed by many other theoretical studies [177, 186, 375, 546, 549, 652–654]. Given the existence of such a multiplet, searches for the other four molecules are crucial to verify the molecular nature of $P_c(4312)$, $P_c(4440)$, and $P_c(4457)$, which offers a model-independent approach to check the molecular picture of pentaquark states. In addition to the $\bar{D}^{(*)}\Sigma_c$ channels, the $\bar{D}\Lambda_{c1}(2595)$ channel was claimed to play a nonnegligible role in generating the molecular pentaquark states [655]. In Ref. [656], Peng et al. used the contact-range approach to study the impact of the $\bar{D}\Lambda_{c1}(2595)$ channel on the $\bar{D}^{(*)}\Sigma_c$ molecules, suggesting that there may exist two peak structures around $P_c(4457)$ with different parity. However, In the OBE model, the $\bar{D}^{(*)}\Sigma_c$ channel is shown to be less relevant in forming the molecules [654].

It is evident that in the molecular picture, the spins of $P_c(4440)$ and $P_c(4457)$ can not be resolved in the contact-range EFT. As a result, we turn to the phenomenological model, i.e., the OBE model. In our study, after removing the delta term of the spin-spin interaction, we used a unified cutoff to reproduce the masses of $P_c(4312)$, $P_c(4440)$, and $P_c(4457)$ in the $\bar{D}^{(*)}\Sigma_c$ molecular picture, and predict their HQSS partners, in agreement with the results of scenario B of the contact-range EFT approach, which favors the spins of $P_c(4440)$ and $P_c(4457)$ as $1/2$ and $3/2$ [149]. We note that whether to remove the delta term of the spin-

TABLE VI. Binding energies of $D^{(*)}\Sigma_c^{(*)}$ molecules with $I = 1/2$

Molecule	I	J^P	B.E (MeV)	Mass (MeV)
$D\Sigma_c$	$\frac{1}{2}$	$\frac{1}{2}^-$	$31.7^{+16.6}_{-13.9}$	4289.3
$D\Sigma_c^*$	$\frac{1}{2}$	$\frac{3}{2}^-$	$32.5^{+16.8}_{-14.1}$	4352.5
$D^*\Sigma_c$	$\frac{1}{2}$	$\frac{1}{2}^-$	$18.4^{+11.9}_{-9.3}$	4444.6
$D^*\Sigma_c$	$\frac{1}{2}$	$\frac{3}{2}^-$	$57.4^{+24.8}_{-21.9}$	4405.6
$D^*\Sigma_c^*$	$\frac{1}{2}$	$\frac{1}{2}^-$	$19.2^{+12.7}_{-9.8}$	4507.8
$D^*\Sigma_c^*$	$\frac{1}{2}$	$\frac{3}{2}^-$	$32.1^{+17.0}_{-14.2}$	4494.9
$D^*\Sigma_c^*$	$\frac{1}{2}$	$\frac{5}{2}^-$	$61.4^{+25.9}_{-23.7}$	4465.6

spin interaction remains open. In Ref. [654], the authors did not altogether remove the delta term rather than introduced a parameter that controls the delta contribution to calculate the masses of the $\bar{D}^{(*)}\Sigma_c^{(*)}$ molecules in both scenarios. Up to now, the spins of $P_c(4440)$ and $P_c(4457)$ and the nature of the pentaquark states remain still undetermined. Therefore, it is crucial to study these puzzles using other approaches. In addition to searching for the HQSS partners mentioned above, the existence of their SU(3)-flavor partners can also help resolve this issue.

With the G -transformation, one can obtain the $D^{(*)}\Sigma_c^{(*)}$ potentials from the $\bar{D}^{(*)}\Sigma_c^{(*)}$ ones. The only difference in the OBE potentials is the sign of the π and ω exchange potentials. One can straightforwardly obtain the mass spectrum of the $D^{(*)}\Sigma_c^{(*)}$ system in terms of the obtained $\bar{D}^{(*)}\Sigma_c^{(*)}$ mass spectrum as shown in Table VI [634], which has been investigated after the doubly charmed tetraquark state T_{cc} was discovered by the LHCb Collaboration [657–659]. One can see that the $D^{(*)}\Sigma_c^{(*)}$ states bind more than the $\bar{D}^{(*)}\Sigma_c^{(*)}$ ones. Such a feature has been observed in other systems. For instance, the $\bar{D}^{(*)}D^{(*)}$ states bind than the $D^{(*)}D^{(*)}$ ones and the $\bar{\Sigma}_c^{(*)}\Sigma_c^{(*)}$ states more than the $\Sigma_c^{(*)}\Sigma_c^{(*)}$ ones [182]. Refs. [161, 162, 644, 660, 661] have investigated the hadronic molecules near the thresholds of the hidden-charm and open-charm hadron-hadron systems.

With SU(3)-flavor symmetry, one can relate the $\bar{D}^{(*)}\Sigma_c^{(*)}$ system to $\bar{D}^{(*)}\Xi_c^{\prime(*)}$ system. The latter also generates seven states dictated by HQSS [561]. Since the contact-range potentials of the $\bar{D}^{(*)}\Xi_c^{\prime(*)}$ system are the same as those of the $\bar{D}^{(*)}\Sigma_c^{(*)}$ system, one can easily obtain the mass spectrum of the $\bar{D}^{(*)}\Xi_c^{\prime(*)}$ system. In Table VII, we present the masses of the $\bar{D}^{(*)}\Xi_c^{\prime(*)}$ molecules for scenarios A and B, consistent with Refs. [560, 629]. Utilizing the OBE model, Chen et al. arrived at similar conclusions [662]. The experimental searches for $\bar{D}^{(*)}\Xi_c^{\prime(*)}$ molecules are crucial to understand the molecular nature of $P_c(4312)$,

TABLE VII. Bound states of a singly charmed baryon and a singly charmed antimeson, obtained in the contact-range effective field theory with the two constants fixed by reproducing $P_c(4440)$ and $P_c(4457)$ as $1/2^-$ and $3/2^-$ molecules (scenario A) and $3/2^-$ and $1/2^-$ (scenario B), with cutoffs of 0.5 and 1 GeV, and the 25% uncertainty caused by SU(3)-flavor symmetry and heavy quark spin symmetry breaking for the contact-range potentials.

State	J^P	$\Lambda(\text{GeV})$	B. E(A)	Mass(A)	B. E(B)	Mass(B)
$\bar{D}\Xi'_c$	$1/2^-$	1(0.5)	$8.5^{+17.4}_{-8.4}(9.3^{+8.7}_{-6.7})$	4437(4436)	$14.0^{+21.7}_{-12.8}(14.9^{+11.4}_{-9.3})$	4431(4430)
$\bar{D}\Xi_c^*$	$3/2^-$	1(0.5)	$9.0^{+17.7}_{-8.8}(9.5^{+7.8}_{-6.7})$	4504(4504)	$14.7^{+21.9}_{-13.3}(15.2^{+11.4}_{-9.4})$	4499(4498)
$\bar{D}^*\Xi'_c$	$1/2^-$	1(0.5)	$23.4^{+27.0}_{-18.9}(22.5^{+14.2}_{-12.3})$	4563(4564)	$5.6^{+14.3}_{\dagger}(5.2^{+6.4}_{-4.9})$	4581(4581)
$\bar{D}^*\Xi'_c$	$3/2^-$	1(0.5)	$5.6^{+14.3}_{\dagger}(5.2^{+6.4}_{-4.3})$	4581(4581)	$23.4^{+27.0}_{-18.8}(22.5^{+14.2}_{-12.3})$	4563(4564)
$\bar{D}^*\Xi_c^*$	$1/2^-$	1(0.5)	$28.0^{+29.4}_{-21.4}(26.3^{+15.5}_{-13.7})$	4627(4628)	$4.0^{+12.5}_{\dagger}(3.3^{+5.1}_{-3.0})$	4651(4651)
$\bar{D}^*\Xi_c^*$	$3/2^-$	1(0.5)	$17.2^{+23.2}_{-14.9}(16.4^{+11.6}_{-9.8})$	4637(4638)	$11.1^{+18.9}_{-10.5}(10.5^{+9.1}_{-7.2})$	4643(4644)
$\bar{D}^*\Xi_c^*$	$5/2^-$	1(0.5)	$4.0^{+12.5}_{\dagger}(3.3^{+5.1}_{-3.0})$	4651(4651)	$28.0^{+29.4}_{-21.4}(26.3^{+15.5}_{-13.7})$	4627(4628)

$P_c(4440)$, and $P_c(4457)$.

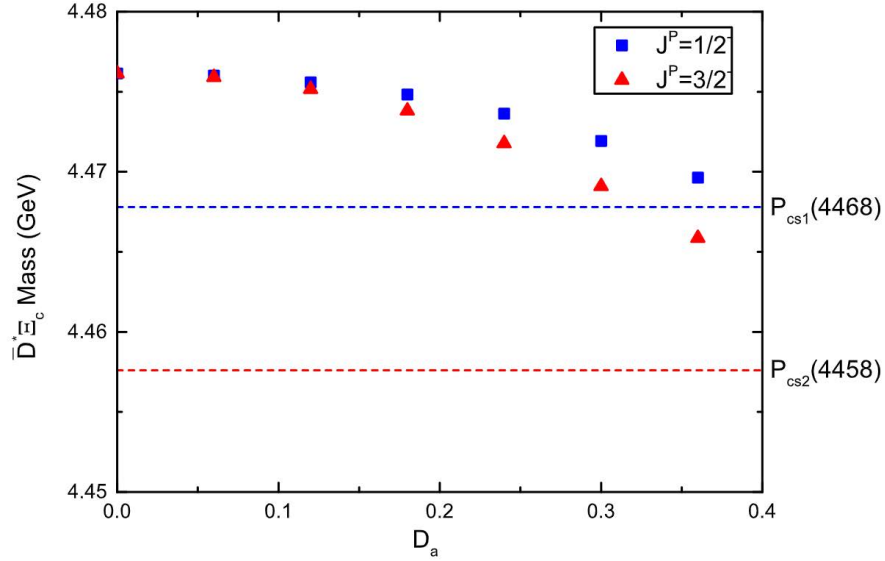


FIG. 2. $J^P = 1/2^-$ $\bar{D}^*\Xi_c$ and $J^P = 3/2^-$ $\bar{D}^*\Xi_c$ mass in scenario A as a function of parameter D_a , where D_a describes the strength of the elastic potentials: $V = D_a \times F'_{1/2}$

We note that the hidden-charm strange pentaquark states $P_{cs}(4459)$ and $P_{cs}(4338)$ discovered by the LHCb Collaboration are near the $\bar{D}^*\Xi_c$ and $\bar{D}\Xi_c$ mass thresholds as shown in Fig. 4. As a result, it is necessary to study the $\bar{D}^{(*)}\Xi_c$ system. In the heavy quark limit, the $\bar{D}^{(*)}\Xi_c$ system develops three states, and the contact-range potentials for all three states are the same. Assuming the $P_{cs}(4459)$ as a $\bar{D}^*\Xi_c$ bound

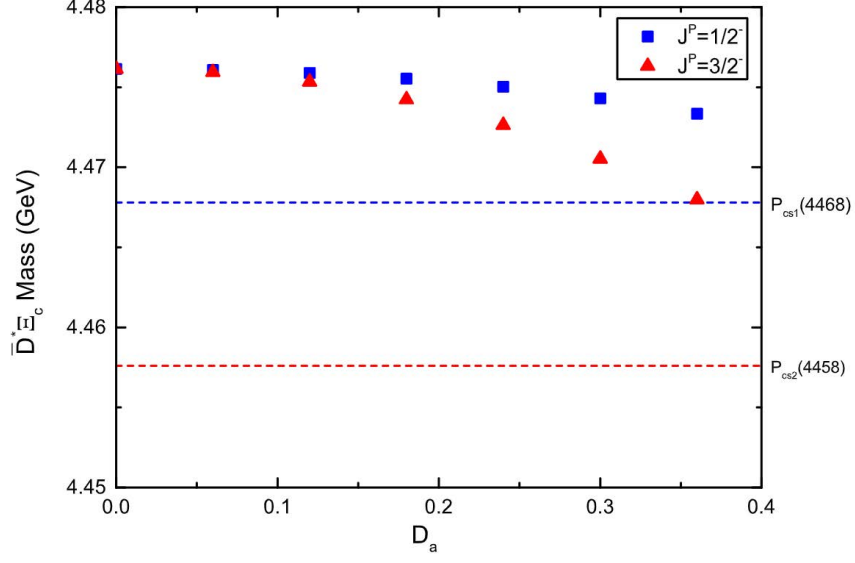


FIG. 3. Masses of $J^P = 1/2^-$ and $J^P = 3/2^-$ $\bar{D}^*\Xi_c$ molecules in scenario B as a function of the parameter D_a , where D_a describes the strength of the elastic potentials: $V = D_a \times F'_{1/2}$

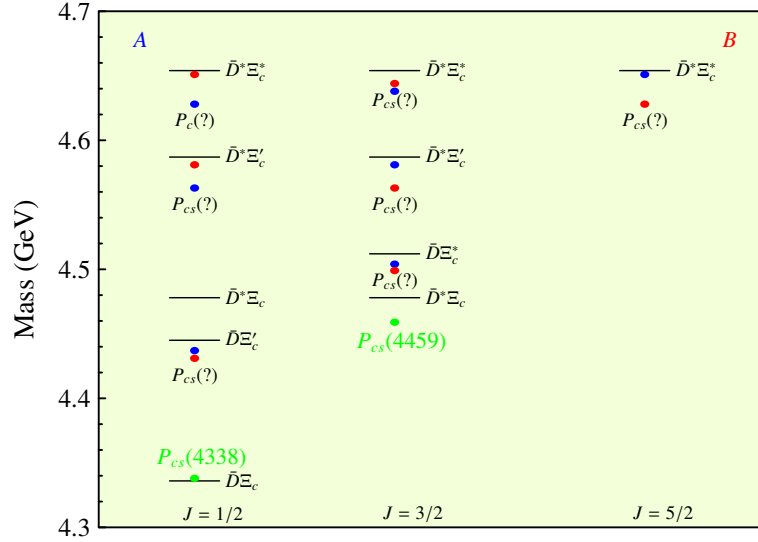


FIG. 4. Spectrum of $\bar{D}^{(*)}\Xi_c'^{(*)}$ hadronic molecules in Scenario A (shown in blue) and Scenario B (shown in red), and the locations of hidden charm strangeness pentaquark hadronic molecular candidates with respect to the $\bar{D}^{(*)}\Xi_c$ mass thresholds. .

state, it is natural to expect a $\bar{D}^*\Xi_c$ bound state and a $\bar{D}\Xi_c$ bound state with the same binding energy, where the $\bar{D}\Xi_c$ molecule corresponds to $P_{cs}(4338)$. Such a naive expectation of a $\bar{D}^{(*)}\Xi_c$ multiplet in the single-channel approximation is not consistent with the current experimental data. One needs to consider coupled-channel effects to understand these pentaquark states better. The meson exchange theory tells that

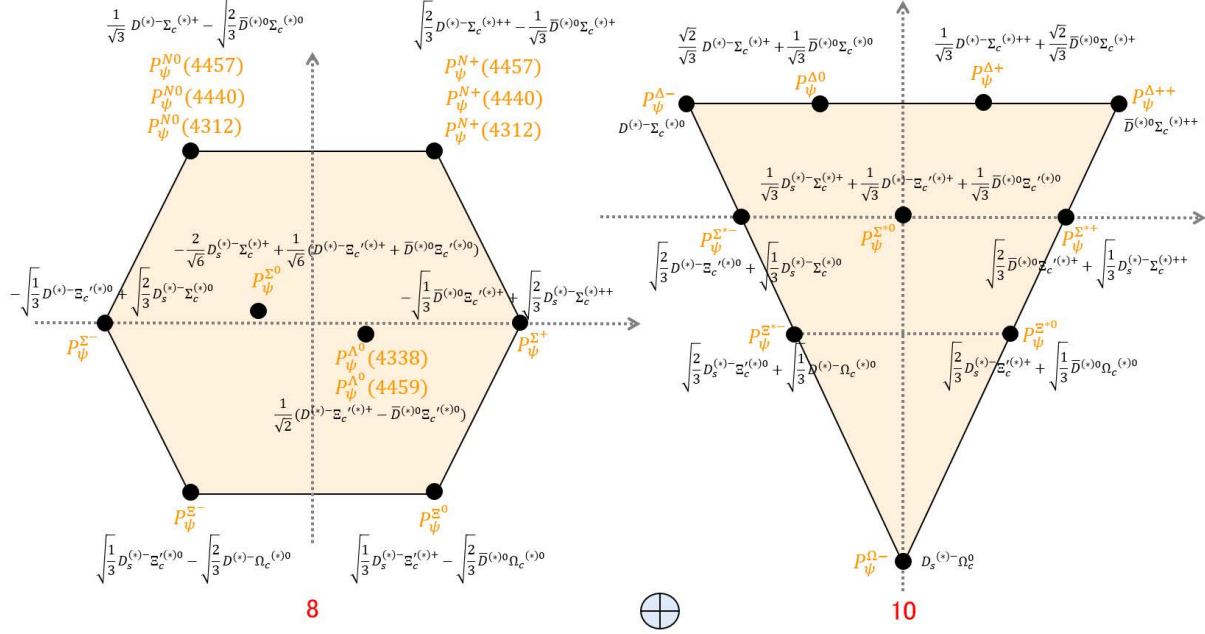


FIG. 5. P_ψ^N and P_ψ^Λ as part of SU(3)-flavor multiplet of hidden charm pentaquark hadronic molecules, and $P_\psi^N(4312)$, $P_\psi^N(4440)$ and $P_\psi^N(4457)$ as part of HQSS multiplet hadronic molecules P_ψ^N as well as $P_\psi^\Lambda(4338)$ and $P_\psi^\Lambda(4459)$ as part of HQSS multiplet hadronic molecules P_ψ^Λ .

the coupled channels are $\bar{D}^*\Xi_c - \bar{D}^*\Xi'_c$ and $\bar{D}^*\Xi_c - \bar{D}\Xi_c^*$ for $J = 1/2$ and $J = 3/2$, but there is no coupling to $\bar{D}\Xi_c$. As depicted in Fig. 4, the $\bar{D}^*\Xi_c$ mass threshold is close to the $\bar{D}^*\Xi'_c$ mass threshold, and the $\bar{D}^*\Xi_c$ mass threshold is close to the $\bar{D}\Xi_c^*$ mass threshold. There are likely strong couplings between these channels. Therefore, we proposed $P_{cs}(4338)$ as a $\bar{D}\Xi_c$ bound state and fixed the contact-range potentials of the $\bar{D}^{(*)}\Xi_c$ system.

The contact-range potentials of the $\bar{D}^*\Xi'_c$ and $\bar{D}\Xi_c^*$ system are determined by the $\bar{D}^{(*)}\Sigma_c^{(*)}$ system for scenarios A and B. The off-diagonal contact potentials parameterized by D_a are difficult to estimate. Facing this situation, we require that the off-diagonal potentials be in a reasonable region. That is to say, the higher pole should always exist, and the imaginary part of the higher pole is smaller than those of $P_c(4440)$ and $P_c(4457)$. One can see that the degeneracy of the two $\bar{D}^*\Xi_c$ states gradually lifts as D_a increases in scenarios A and B as shown in Fig. 2 and Fig. 3. The two states may correspond to the structures around $P_{cs}(4459)$. In both scenarios, we find that the $J^P = 3/2^-$ $\bar{D}^*\Xi_c$ molecule is more bound than the $J^P = 1/2^-$ $\bar{D}^*\Xi_c$ molecule. As a result, we obtain another HQSS multiplet of hadronic molecules composed of $\bar{D}^{(*)}\Xi_c$ and $\bar{D}^{(*)}\Xi_c^{(*)}$ as shown in Fig. 4. Refs. [563, 663] argued for the existence of $\bar{D}^{(*)}\Xi_c$ molecules, while the mechanism for the breaking of two degenerate $\bar{D}^*\Xi_c$ states was not discussed. In Ref. [664], Giachino et al. not only considered the effect of coupled channels but also $S - D$ wave mixing to assign

TABLE VIII. Heavy- and light-flavor symmetry partners of the LHCb pentaquark trio, $P_c(4312)$, $P_c(4440)$, and $P_c(4457)$ (or P_{c1} , P_{c2} , P_{c3} for short). These include the five-flavor pentaquarks with quark contents $\bar{b}csdu$ and $b\bar{c}sdu$. The masses of the P_c s partners are assigned with a 20% uncertainty originating from the SU(3) flavor symmetry breaking.

Molecule	I	S	B_P	M_P	Partner	Molecule	I	S	B_P	M_P	Partner
$\bar{D}\Sigma_c$	$\frac{1}{2}$	0	Input	Input	P_{c1}	$B\Sigma_c$	$\frac{1}{2}$	0	$27.5^{+9.5}_{-8.0}$	$7710.5^{+8.0}_{-9.5}$	P_{c1}
$\bar{D}^*\Sigma_c$	$\frac{1}{2}$	0	Input	Input	P_{c2}	$B^*\Sigma_c$	$\frac{1}{2}$	0	$43.6^{+10.6}_{-9.3}$	$7734.6^{+9.3}_{-10.6}$	P_{c2}
$\bar{D}^*\Sigma_c$	$\frac{1}{2}$	0	Input	Input	P_{c3}	$B^*\Sigma_c$	$\frac{1}{2}$	0	$18.6^{+7.6}_{-6.0}$	$7759.7^{+6.0}_{-7.6}$	P_{c3}
$\bar{D}\Xi'_c$	0	-1	$9.6^{+10.4}_{-7.3}$	$4436.3^{+7.3}_{-10.4}$	P_{c1}	$B\Xi'_c$	0	-1	$29.0^{+18.4}_{-16.1}$	$7829.0^{+16.1}_{-18.4}$	P_{c1}
$\bar{D}^*\Xi'_c$	0	-1	$22.9^{+15.9}_{-13.1}$	$4564.7^{+13.1}_{-15.9}$	P_{c2}	$B^*\Xi'_c$	0	-1	$45.3^{+23.1}_{-21.0}$	$7857.8^{+21.0}_{-23.1}$	P_{c2}
$\bar{D}^*\Xi'_c$	0	-1	$5.4^{+7.7}_{-4.7}$	$4581.8^{+4.7}_{-7.7}$	P_{c3}	$B^*\Xi'_c$	0	-1	$19.8^{+14.5}_{-12.3}$	$7883.3^{+12.3}_{-14.5}$	P_{c3}
$\bar{D}\Sigma_b$	$\frac{1}{2}$	0	$20.2^{+5.3}_{-4.7}$	$7660.1^{+4.7}_{-5.3}$	P_{c1}	$B\Sigma_b$	$\frac{1}{2}$	0	$48.4^{+22.7}_{-18.3}$	$11044.2^{+18.3}_{-22.7}$	P_{c1}
$\bar{D}^*\Sigma_b$	$\frac{1}{2}$	0	$37.5^{+7.3}_{-6.5}$	$7784.2^{+6.5}_{-7.3}$	P_{c2}	$B^*\Sigma_b$	$\frac{1}{2}$	0	$67.5^{+24.9}_{-28.2}$	$11070.3^{+28.2}_{-24.9}$	P_{c2}
$\bar{D}^*\Sigma_b$	$\frac{1}{2}$	0	$14.3^{+4.7}_{-4.0}$	$7807.4^{+4.0}_{-4.7}$	P_{c3}	$B^*\Sigma_b$	$\frac{1}{2}$	0	$37.1^{+19.2}_{-15.2}$	$11100.7^{+15.2}_{-19.2}$	P_{c3}
$\bar{D}\Xi'_b$	0	-1	$20.4^{+14.6}_{-12.3}$	$7782.6^{+12.3}_{-14.6}$	P_{c1}	$B\Xi'_b$	0	-1	$48.8^{+29.0}_{-25.1}$	$11165.7^{+25.1}_{-29.0}$	P_{c1}
$\bar{D}^*\Xi'_b$	0	-1	$37.8^{+20.3}_{-18.2}$	$7907.2^{+18.2}_{-20.3}$	P_{c2}	$B^*\Xi'_b$	0	-1	$68.0^{+33.7}_{-30.1}$	$11191.8^{+33.7}_{-30.1}$	P_{c2}
$\bar{D}^*\Xi'_b$	0	-1	$14.5^{+11.9}_{-9.7}$	$7929.6^{+9.7}_{-11.9}$	P_{c3}	$B^*\Xi'_b$	0	-1	$37.5^{+24.5}_{-20.8}$	$11222.2^{+20.8}_{-24.5}$	P_{c3}

the $P_{cs}(4338)$ and two structures around $P_{cs}(4459)$ as $\bar{D}^{(*)}\Xi_c$ molecules in the meson exchange model, which to some extent explains the binding mechanism of $\bar{D}^{(*)}\Xi_c$ molecules. The $D_s^{(*)}\Lambda_c$ contribution to the $\bar{D}^{(*)}\Xi_c$ molecules are also investigated in Refs. [564, 664, 665]. One can see that the $\bar{D}^{(*)}\Xi_c$ channels, $\bar{D}^{(*)}\Xi'_c$ channels, and $D_s^{(*)}\Lambda_c$ channels all play a role in forming the hidden-charm strange molecules, while the role of each component is ambiguous due to the large uncertainties in the potentials.

According to the SU(3)-flavor symmetry, two-body heavy antimeson-baryon states can be decomposed into $3 \otimes 6 = 8 \oplus 10$, i.e., into the octet and decuplet representations as shown in Fig. 5. It is obvious that the $\bar{D}^{(*)}\Sigma_c^{(*)}$ system with $I = 1/2$ and $\bar{D}^{(*)}\Xi_c^{(*)}$ system with $I = 0$ belong to the octet representation and do not mix with the systems belonging to the decuplet representation. The $\bar{D}^{(*)}\Xi'_c$ system with $I = 1$ mixes with the $\bar{D}_s^{(*)}\Sigma_c^{(*)}$ system, where the proportion of each component is given by the SU(3) Clebsch-Gordan coefficients [666]. Due to the absence of information on the molecules in the decuplet representation, we only focus on the molecules in the octet representation. Employing HQFS and SU(3)-flavor symmetry, a larger family of pentaquark molecules is predicted in Table VIII, where we only show the results for scenario A of Ref. [667]. Moreover, in Table IX, we predict the HQSS partners of Table VIII.

TABLE IX. Heavy- and light-flavor symmetry partners of the LHCb pentaquark trio, $P_c(4312)$, $P_c(4440)$ and $P_c(4457)$ (or P_{c1} , P_{c2} , P_{c3} for short). These include the five-flavor pentaquarks with quark contents $\bar{b}csdu$ and $b\bar{c}sdu$. The masses of the P_c s partners are assigned a 20% uncertainty originating from the SU(3) flavor symmetry breaking.

Molecule	I	S	B_P	M_P	Partner	Molecule	I	S	B_P	M_P	Partner
$\bar{D}\Sigma_b^*$	$\frac{1}{2}$	0	$19.1^{+4.3}_{-3.7}$	$7680.7^{+3.7}_{-4.3}$	$\frac{3}{2}$	$B\Sigma_c^*$	$\frac{1}{2}$	0	$27.0^{+8.6}_{-7.3}$	$7770.6^{+7.3}_{-8.6}$	$\frac{3}{2}$
$\bar{D}^*\Sigma_b^*$	$\frac{1}{2}$	0	$41.9^{+7.8}_{-7.2}$	$7799.2^{+7.2}_{-7.8}$	$\frac{1}{2}$	$B^*\Sigma_c^*$	$\frac{1}{2}$	0	$49.1^{+11.7}_{-10.4}$	$7793.7^{+10.4}_{-11.7}$	$\frac{1}{2}$
$\bar{D}^*\Sigma_b^*$	$\frac{1}{2}$	0	$29.2^{+6.3}_{-5.6}$	$7811.9^{+5.6}_{-6.3}$	$\frac{3}{2}$	$B^*\Sigma_c^*$	$\frac{1}{2}$	0	$35.6^{+9.8}_{-8.5}$	$7807.3^{+8.5}_{-9.8}$	$\frac{3}{2}$
$\bar{D}^*\Sigma_b^*$	$\frac{1}{2}$	0	$11.1^{+4.3}_{-3.6}$	$7830.0^{+3.6}_{-4.3}$	$\frac{5}{2}$	$B^*\Sigma_c^*$	$\frac{1}{2}$	0	$15.6^{+7.0}_{-5.8}$	$7827.3^{+5.8}_{-7.0}$	$\frac{5}{2}$
$\bar{D}\Xi_b^*$	0	-1	$21.6^{+17.7}_{-9.7}$	$7799.5^{+9.7}_{-17.7}$	$\frac{3}{2}$	$B\Sigma_b^*$	$\frac{1}{2}$	0	$46.9^{+21.0}_{-16.9}$	$11065.2^{+16.9}_{-21.0}$	$\frac{3}{2}$
$\bar{D}^*\Xi_b^*$	0	-1	$42.2^{+21.7}_{-19.6}$	$7920.2^{+19.6}_{-21.7}$	$\frac{1}{2}$	$B^*\Sigma_b^*$	$\frac{1}{2}$	0	$72.9^{+26.0}_{-21.8}$	$11084.3^{+21.8}_{-26.0}$	$\frac{1}{2}$
$\bar{D}^*\Xi_b^*$	0	-1	$29.4^{+17.4}_{-15.3}$	$7932.9^{+15.3}_{-17.4}$	$\frac{3}{2}$	$B^*\Sigma_b^*$	$\frac{1}{2}$	0	$57.2^{+23.0}_{-18.9}$	$11100.0^{+18.9}_{-23.0}$	$\frac{3}{2}$
$\bar{D}^*\Xi_b^*$	0	-1	$11.3^{+10.5}_{-8.3}$	$7951.1^{+8.3}_{-10.5}$	$\frac{5}{2}$	$B^*\Sigma_b^*$	$\frac{1}{2}$	0	$32.4^{+18.3}_{-14.3}$	$11124.8^{+14.3}_{-18.3}$	$\frac{5}{2}$
$B\Xi_b^*$	0	-1	$47.2^{+27.5}_{-23.8}$	$11186.1^{+23.8}_{-27.5}$	$\frac{3}{2}$	$B\Xi_c^*$	0	-1	$28.4^{+17.6}_{-15.4}$	$7896.7^{+15.4}_{-17.6}$	$\frac{3}{2}$
$B^*\Xi_b^*$	0	-1	$73.3^{+35.3}_{-31.7}$	$11205.2^{+31.7}_{-35.3}$	$\frac{1}{2}$	$B^*\Xi_c^*$	0	-1	$50.9^{+24.9}_{-22.7}$	$7919.4^{+22.7}_{-24.9}$	$\frac{1}{2}$
$B^*\Xi_b^*$	0	-1	$57.6^{+30.6}_{-27.0}$	$11220.9^{+27.0}_{-30.6}$	$\frac{3}{2}$	$B^*\Xi_c^*$	0	-1	$37.1^{+20.5}_{-18.4}$	$7933.2^{+18.4}_{-20.5}$	$\frac{3}{2}$
$B^*\Xi_b^*$	0	-1	$32.7^{+23.0}_{-19.3}$	$11245.8^{+19.3}_{-23.0}$	$\frac{5}{2}$	$B^*\Xi_c^*$	0	-1	$16.7^{+13.4}_{-11.2}$	$7953.6^{+11.2}_{-13.4}$	$\frac{5}{2}$

In Ref. [667], we assumed that the octet representation is the low energy configuration to predict a larger set of pentaquark molecules. Among these pentaquark molecules, the pentaquark states with five different flavors [668] and hidden-charm double strangeness [669, 670] were investigated. In particular, unified models have been proposed to describe hidden-charm and hidden-charm strange pentaquark states as meson-baryon molecules [163, 662, 671–673].

In the following, we discuss the applications of HADS in the $\bar{D}^{(*)}\Sigma_c^{(*)}$ system. Via HADS, one can relate the $\bar{D}^{(*)}\Sigma_c^{(*)}$ system with the $\Xi_{cc}^{(*)}\Sigma_c^{(*)}$ system as shown in Fig. 6. In the heavy quark limit, the contact-range potentials of the $\Xi_{cc}^{(*)}\Sigma_c^{(*)}$ system share the same low-energy constants C_a and C_b as those of the $\bar{D}^{(*)}\Sigma_c^{(*)}$ system. Therefore, with the same inputs as the $\bar{D}^{(*)}\Sigma_c^{(*)}$ system, we can predict the mass spectrum of the $\Xi_{cc}^{(*)}\Sigma_c^{(*)}$ system. The Ξ_{cc}^* baryon has not yet been discovered; therefore, its mass is unknown. As a result, we turn to lattice QCD for help. The lattice QCD simulations yield a relationship $m_{\Xi_{cc}^*} - m_{\Xi_{cc}} = \frac{3}{4}(m_{D^*} - m_D)$ [674–677], which helps determine the mass of Ξ_{cc}^* as $m_{\Xi_{cc}^*} = 3727$ MeV. In Table X, we present the mass spectrum of the $\Xi_{cc}^{(*)}\Sigma_c^{(*)}$ system with a 25% uncertainty in scenario A and scenario B. One can see a complete HQSS multiplet of hadronic molecules composed of triply charmed dibaryons,

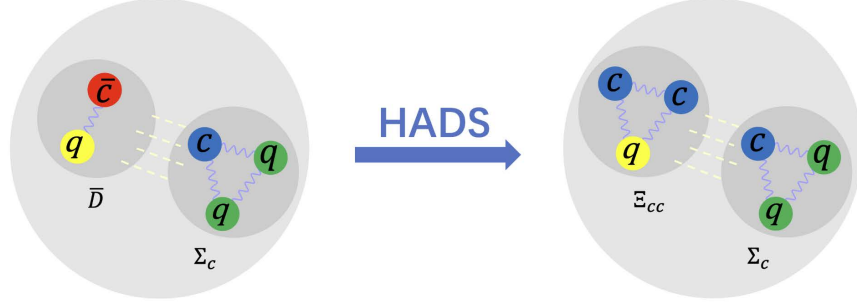


FIG. 6. HADS relates the $\bar{D}^{(*)}\Sigma_c^{(*)}$ system with the $\Xi_{cc}^{(*)}\Sigma_c^{(*)}$ system.

consistent with the results of the OBE model [678].

TABLE X. Mass spectrum (in units of MeV) of triply charmed dibaryons composed of a doubly charmed baryon (Ξ_{cc} , Ξ_{cc}^*) and a singly charmed baryon (Σ_c , Σ_c^*) for cutoffs $\Lambda = 0.5$ GeV and $\Lambda = 1$ GeV. The 25% uncertainty induced by HADS is considered in the contact-range potentials of the $\Xi_{cc}^{(*)}\Xi_c'^{(*)}$ system.

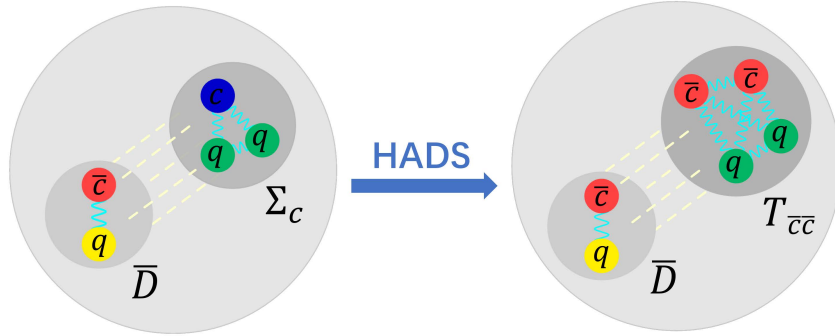
State	J^P	Threshold	$\Lambda(\text{GeV})$	B.E(Scenario A)	B.E(Scenario B)
$\Xi_{cc}\Sigma_c$	0^+	6074.9	0.5(1)	$10.0^{+7.9}_{-6.4}$ ($17.9^{+20.8}_{-14.4}$)	$30.4^{+15.5}_{-14.2}$ ($43.2^{+33.1}_{-27.2}$)
$\Xi_{cc}\Sigma_c$	1^+	6074.9	0.5(1)	$18.4^{+11.3}_{-9.9}$ ($28.3^{+26.3}_{-20.1}$)	$20.7^{+12.1}_{-10.8}$ ($31.2^{+27.7}_{-21.6}$)
$\Xi_{cc}\Sigma_c^*$	1^+	6139.5	0.5(1)	$11.3^{+8.4}_{-7.0}$ ($20.0^{+25.4}_{-17.2}$)	$29.6^{+15.1}_{-13.8}$ ($42.8^{+32.7}_{-26.9}$)
$\Xi_{cc}\Sigma_c^*$	2^+	6139.5	0.5(1)	$20.0^{+11.8}_{-10.4}$ ($30.7^{+27.2}_{-21.2}$)	$20.0^{+11.8}_{-10.4}$ ($30.8^{+27.3}_{-21.3}$)
$\Xi_{cc}^*\Sigma_c$	1^+	6180.9	0.5(1)	$28.2^{+14.7}_{-13.4}$ ($41.0^{+32.0}_{-26.0}$)	$12.2^{+8.8}_{-7.4}$ ($21.0^{+22.4}_{-16.2}$)
$\Xi_{cc}^*\Sigma_c$	2^+	6180.9	0.5(1)	$10.2^{+8.0}_{-6.5}$ ($18.5^{+21.0}_{-14.8}$)	$30.7^{+15.5}_{-14.2}$ ($44.1^{+33.3}_{-27.5}$)
$\Xi_{cc}^*\Sigma_c^*$	0^+	6245.5	0.5(1)	$35.0^{+16.8}_{-15.6}$ ($50.2^{+35.6}_{-29.9}$)	$7.6^{+6.7}_{-5.3}$ ($15.8^{+19.2}_{-13.0}$)
$\Xi_{cc}^*\Sigma_c^*$	1^+	6245.5	0.5(1)	$29.9^{+15.2}_{-13.9}$ ($43.7^{+32.9}_{-27.2}$)	$11.5^{+8.5}_{-7.0}$ ($20.7^{+22.0}_{-15.9}$)
$\Xi_{cc}^*\Sigma_c^*$	2^+	6245.5	0.5(1)	$20.3^{+11.8}_{-10.5}$ ($31.6^{+27.5}_{-21.6}$)	$20.3^{+11.8}_{-10.5}$ ($31.6^{+27.5}_{-21.6}$)
$\Xi_{cc}^*\Sigma_c^*$	3^+	6245.5	0.5(1)	$7.6^{+6.7}_{-5.3}$ ($15.8^{+19.2}_{-13.0}$)	$35.0^{+16.8}_{-15.6}$ ($50.2^{+35.6}_{-30.0}$)

One can see that the triply charmed dibaryon molecules are tied to the molecular nature of the pentaquark states. In other words, if one can obtain information on the $\Xi_{cc}^{(*)}\Sigma_c^{(*)}$ molecules, one can probe the nature of the pentaquark states. We do not expect to see experimental discoveries soon because of the low production rates of the triply charmed dibaryon molecules. Luckily, there exist lattice QCD simulations of the $\Xi_{cc}^{(*)}\Sigma_c^{(*)}$ system [679]. However, the lattice QCD results suffer from large uncertainties. If, in the future, lattice QCD simulations can yield the mass splitting of the $\Xi_{cc}\Sigma_c$ doublet, the uncertainties can be largely reduced. The

TABLE XI. Masses (in units of MeV) of $T_{c\bar{c}}^1$, $T_{c\bar{c}}^2$, and $T_{c\bar{c}}^3$ in several models and their averages.

Tetraquark	[61]	[63]	[73]	[585]	A.V
$T_{c\bar{c}}^0$	3999.8	4132	4032	3969.2	4033.3
$T_{c\bar{c}}^1$	4124.0	4151	4117	4053.2	4111.3
$T_{c\bar{c}}^2$	4194.9	4185	4179	4123.8	4170.7

relative sign for the mass splitting of the $\Xi_{cc}\Sigma_c$ doublet is the most crucial information because the sign of the mass splitting of the $\Xi_{cc}\Sigma_c$ doublet is opposite in scenarios A and B. As a result, one can obtain the spin configuration of $P_c(4440)$ and $P_c(4457)$ from the mass splitting of the $\Xi_{cc}\Sigma_c$ doublet [651], which is a model-independent approach to determine the spins of $P_c(4440)$ and $P_c(4457)$ in the molecular picture. Ref. [680] found that the mass of $J^P = 0^+ \Xi_{cc}\Sigma_c$ is larger than that of $J^P = 1^+ \Xi_{cc}\Sigma_c$ in the QCD sum rule approach, which agrees with the OBE model [681] but differs from the OBE model with the delta potential removed [678]. Similar results are found for the $\bar{D}^{(*)}\Sigma_c^{(*)}$ OBE potentials [149]. These studies motivated discussions on whether the delta potential should be removed [654]. Similarly, in terms of HADS, one can relate the $\bar{D}^{(*)}\Xi_c'^{(*)}$ system with the $\Xi_{cc}^{(*)}\Xi_c'^{(*)}$ system, which is the same as relating the $\Xi_{cc}^{(*)}\Sigma_c^{(*)}$ system with the $\Xi_{cc}^{(*)}\Xi_c'^{(*)}$ system via the SU(3)-flavor symmetry. Some states of the $\Xi_{cc}^{(*)}\Xi_c'^{(*)}$ system were investigated in the OBE model [681]. Considering HQFS, we obtain the mass spectrum of the $\Xi_{bb}^{(*)}\Sigma_b^{(*)}$ system, which are shown in Table III of Ref. [678].

FIG. 7. HADS relates the $\bar{D}^{(*)}\Sigma_c^{(*)}$ system with the $\bar{D}^{(*)}T_{c\bar{c}}^{(*)}$ system.

HADS relates the $\Sigma_c^{(*)}$ baryons with the doubly charmed tetraquark states $T_{c\bar{c}}$. Refs. [60, 61, 64] investigated the mass spectrum of the $T_{c\bar{c}}$ states via HADS. We note that the $T_{c\bar{c}}$ states predicted via HADS are different from the $T_{cc}(3875)$ discovered by the LHCb Collaboration. In terms of HADS, the isospin of $T_{c\bar{c}}$ equals 1, while isospin 0 is favored for the $T_{cc}(3875)$ experimentally. Using HADS, we relate the $\bar{D}^{(*)}\Sigma_c^{(*)}$

system with the $\bar{D}^{(*)}T_{\bar{c}\bar{c}}^{(*)}$ system as shown in Fig. 7, where the masses of $T_{\bar{c}\bar{c}}$ are taken to be the average of several theoretical predictions [61, 63, 73, 585]. In the heavy quark limit, the $\bar{D}^{(*)}\Sigma_c^{(*)}$ and $\bar{D}^{(*)}T_{\bar{c}\bar{c}}^{(*)}$ systems share the same low-energy constants. In Table XII, we present the mass spectrum of the $\bar{D}^{(*)}T_{\bar{c}\bar{c}}^{(*)}$ system in scenarios A and B. The $\bar{D}^{(*)}T_{\bar{c}\bar{c}}^{(*)}$ molecules belong to the new kind of hadronic molecules composed of a conventional hadron and a compact tetraquark state [682]. The $\bar{D}^{(*)}T_{\bar{c}\bar{c}}^{(*)}$ molecules contain the same quark contents as the DDD^* molecules and $\bar{\Omega}_{ccc}p$ hadronic atom. However, these three kinds of molecules are bound by different mechanisms. Experimental searches for $\bar{D}^{(*)}T_{\bar{c}\bar{c}}^{(*)}$ molecules would help verify the molecular nature of the pentaquark states and the existence of compact tetraquark states.

TABLE XII. Binding energies (in units of MeV) of the $\bar{D}^{(*)}T_{\bar{c}\bar{c}}^{(*)}$ molecules in scenarios A and B obtained with single-channel potentials. The numbers inside and outside the brackets correspond to $\Lambda = 0.75$ GeV and $\Lambda = 1.5$ GeV. The superscripts and subscripts are obtained by allowing for a 25% breaking of HADS.

Molecule	J^P	Threshold	B.E.(Scenario A)	B.E.(Scenario B)
$\bar{D}T_{\bar{c}\bar{c}}^0$	0^-	5900.3	$24.1^{+39.4}_{-22.5}(16.5^{+16.1}_{-12.1})$	$32.1^{+44.9}_{-28.3}(23.3^{+19.3}_{-15.4})$
$\bar{D}T_{\bar{c}\bar{c}}^1$	1^-	5978.3	$24.7^{+39.7}_{-23.0}(16.8^{+16.2}_{-12.2})$	$32.8^{+45.3}_{-28.8}(23.6^{+19.4}_{-15.5})$
$\bar{D}T_{\bar{c}\bar{c}}^2$	2^-	6037.7	$25.2^{+40.0}_{-23.3}(17.0^{+16.2}_{-12.3})$	$33.4^{+45.5}_{-29.1}(23.8^{+19.4}_{-15.6})$
$\bar{D}^*T_{\bar{c}\bar{c}}^0$	1^-	6042.3	$29.5^{+42.1}_{-26.2}(18.6^{+16.7}_{-13.0})$	$38.2^{+47.6}_{-32.0}(25.6^{+19.9}_{-16.3})$
$\bar{D}^*T_{\bar{c}\bar{c}}^1$	0^-	6120.3	$43.7^{+50.7}_{-35.3}(29.7^{+21.6}_{-18.0})$	$26.1^{+39.6}_{-23.8}(15.6^{+15.2}_{-11.4})$
$\bar{D}^*T_{\bar{c}\bar{c}}^1$	1^-	6120.3	$36.8^{+46.6}_{-31.0}(24.1^{+19.2}_{-15.6})$	$32.4^{+43.8}_{-28.1}(20.6^{+17.6}_{-13.9})$
$\bar{D}^*T_{\bar{c}\bar{c}}^1$	2^-	6120.3	$24.2^{+38.2}_{-22.3}(14.0^{+14.4}_{-10.6})$	$46.1^{+52.1}_{-36.7}(31.6^{+22.4}_{-18.8})$
$\bar{D}^*T_{\bar{c}\bar{c}}^2$	1^-	6179.7	$51.7^{+55.0}_{-39.8}(35.8^{+24.0}_{-20.5})$	$20.9^{+35.7}_{-19.8}(11.2^{+12.8}_{-9.0})$
$\bar{D}^*T_{\bar{c}\bar{c}}^2$	2^-	6179.7	$37.4^{+46.8}_{-31.3}(24.3^{+19.3}_{-15.6})$	$32.9^{+44.0}_{-28.5}(20.8^{+17.7}_{-14.0})$
$\bar{D}^*T_{\bar{c}\bar{c}}^2$	3^-	6179.7	$19.0^{+34.3}_{-18.3}(9.8^{+12.0}_{-8.1})$	$54.3^{+56.4}_{-41.3}(37.8^{+24.8}_{-21.3})$

In summary, identifying the $P_c(4312)$, $P_c(4440)$, and $P_c(4457)$ as the $\bar{D}^{(*)}\Sigma_c$ bound states in two spin assignments, we predicted a complete HQSS multiplet of $\bar{D}^{(*)}\Sigma_c^{(*)}$ hadronic molecules. Based on the $\bar{D}^{(*)}\Sigma_c^{(*)}$ molecular picture, we obtained the $\bar{D}^{(*)}\Sigma_c^{(*)}$ multiplet of hadronic molecule via the G -parity transformation, the $\bar{D}^{(*)}\Xi_c'^{(*)}$ multiplet of hadronic molecules via the SU(3)-flavor symmetry, $B^{(*)}\Sigma_c^{(*)}$, $\bar{D}^{(*)}\Sigma_b^{(*)}$, $B^{(*)}\Sigma_b^{(*)}$ multiplet of hadronic molecules via HQFS, and $B^{(*)}\Xi_c'^{(*)}$, $\bar{D}^{(*)}\Xi_b'^{(*)}$, and $B^{(*)}\Xi_b'^{(*)}$ multiplets of hadronic molecules via the SU(3)-flavor symmetry and HQFS. Moreover, assuming the $P_{cs}(4338)$ and $P_{cs}(4459)$ as the $\bar{D}^{(*)}\Xi_c$ bound states, we discussed the HQSS multiplet of hadronic molecules composed of $\bar{D}^{(*)}\Xi_c$, where coupled-channel effects play an important role. With HADS, we obtained the $\Xi_{cc}^{(*)}\Sigma_c^{(*)}$ and $\Xi_{cc}^{(*)}\Xi_c^{(*)}$ multiplets of hadronic molecules composed of the triply charmed dibaryons, as well

as a new kind of $\bar{D}^{(*)}T_{cc}^{(*)}$ hadronic molecules composed of the compact doubly charmed tetraquark and charmed mesons. In particular, we proposed a model-independent approach to clarify the molecular nature of $P_c(4312)$, $P_c(4440)$, and $P_c(4457)$ by studying their partners related with relevant symmetries, and determined the spins of $P_c(4440)$ and $P_c(4457)$ from the mass splittings of the $\Xi_{cc}\Sigma_c$ doublet.

3. $\bar{D}^{(*)}D^{(*)}$ molecules

In the heavy quark limit, the $\bar{D}^{(*)}D^{(*)}$ system contains six degenerate states, and the contact-range potentials of the $\bar{D}^{(*)}D^{(*)}$ system are parameterized by two parameters C_a and C_b . In the isoscalar sector, the $X(3872)$ is assumed as a $\bar{D}D^*$ bound state with the quantum numbers $J^{PC} = 1^{++}$ [91, 147, 179, 255, 257, 683], which can determine the sum of C_a and C_b . The contact-range potential of the $J^{PC} = 1^{++}\bar{D}D^*$ system is the same as that of the $J^{PC} = 2^{++}\bar{D}^*D^*$ system. As a result, HQSS predicts a $J^{PC} = 2^{++}\bar{D}^*D^*$ bound state with a binding energy of 5 MeV, consistent with the OBE model [257]. However, one can not fully determine the mass spectrum of the $\bar{D}^{(*)}D^{(*)}$ system because there exists only one input. In view of this situation, one can turn to the light meson saturation approach for help. For the $\bar{D}^{(*)}\Sigma_c^{(*)}$ system, with the light meson saturation approach one can obtain the ratio of C_b to C_a as

$$\frac{C_b^{\text{sat}(V)}}{C_a^{\text{sat}(V+\sigma)}} \simeq 0.123, \quad (8)$$

which is consistent with the reference value determined in the contact-range EFT approach for scenario B, i.e., $\frac{C_b}{C_a} = 0.158$. One can see that the light meson saturation approach works well in estimating the ratio of C_b to C_a .

Using the light meson saturation approach, one can estimate the ratio of C_b to C_a of $\bar{D}^{(*)}D^{(*)}$, i.e., $C_b/C_a = 0.35$ [684]. This shows that the spin-spin term of the $\bar{D}^{(*)}D^{(*)}$ interaction plays a more important role than those of the $\bar{D}^{(*)}\Sigma_c^{(*)}$ system. With the sum of C_a and C_b , one can fix C_a and C_b . In Table XIII, we present the mass spectrum of the $\bar{D}^{(*)}D^{(*)}$ system and their scattering lengths. For the convention of the scattering length, please refer to Eq.(D15). For some channels with no bound states, we search for virtual poles in the unphysical sheet that is close to the real axis. The potentials for the bound states are stronger than those for the virtual states. It is worth noting that the ratio estimated in the light meson saturation mechanism suffers from unquantified uncertainties. Therefore, the results for the $\bar{D}^{(*)}D^{(*)}$ system need further investigations. Ref. [453] systematically analysed the $\bar{D}^{(*)}D^{(*)}$ molecules. The results depend on the cutoff in the form factors and the interpretation for the newly discovered exotic state $X(3960)$. In the isoscalar sector, in addition to the $J^{PC} = 1^{++}\bar{D}D^*$ and $J^{PC} = 2^{++}\bar{D}^*D^*$ molecules, the $D\bar{D}$ channel is close to forming a bound state, but it is bound in other approaches [161, 453, 456]. We note that in the local

TABLE XIII. Scattering lengths (a in units of fm), binding energies (B in units of MeV if bound states exist) and mass spectra (M in units of MeV) of prospective isoscalar heavy antimeson-meson molecules. The \dagger symbol indicates that there is no bound state. The subscript V denotes the existence of a virtual state. The uncertainties originate from the HQSS breaking of the order 15%.

molecule	$I J^{PC}$	a (fm)	B (MeV)	M (MeV)
$D\bar{D}$	$0 \ 0^{++}$	$-20.5^{+(27.5, \infty)}_{+(-\infty, 17.2)}$	0.1^V	3733.9^V
$D\bar{D}^* + D^*\bar{D}$	$0 \ 1^{++}$	$2.7^{+2.8}_{-0.7}$	Input	Input
$D\bar{D}^* - D^*\bar{D}$	$0 \ 1^{+-}$	$-1.3^{+0.4}_{-0.8}$	7.9^V	3868.1^V
$D^*\bar{D}^*$	$0 \ 0^{++}$	$-0.3^{+0.1}_{-0.1}$	\dagger	\dagger
$D^*\bar{D}^*$	$0 \ 1^{+-}$	$-1.5^{+0.5}_{-1.0}$	6.3^V	4011.7^V
$D^*\bar{D}^*$	$0 \ 2^{++}$	$2.5^{+1.9}_{-0.6}$	$4.9^{+5.3}_{-3.6}$	4013.1

hidden gauge approach [159], these states bind more than their counterparts in other approaches.

In the heavy quark limit, the contact-range potentials of the $\bar{B}^{(*)}B^{(*)}$ and $B^{(*)}D^{(*)}$ systems are the same as those of the $\bar{D}^{(*)}D^{(*)}$ system. Therefore, assuming $X(3872)$ as a \bar{D}^*D bound state, we predict the mass spectrum and scattering lengths of the $\bar{B}^{(*)}B^{(*)}$ and $B^{(*)}D^{(*)}$ systems in Table XIV.⁴ These systems are more bound because the reduced masses are larger. Among these molecules, the X_b as a \bar{B}^*B bound state is viewed as the HQFS partner of $X(3872)$. The existence of X_b is crucial to establishing the molecular nature of $X(3872)$ [179, 254, 257]. The same can be said about $X_2(4013)$. Experimental searches for X_b and X_2 are ongoing, but no conclusive results exist yet [260, 332].

TABLE XIV. Same as Table XIII but for the $\bar{B}^{(*)}B^{(*)}$ and $B^{(*)}B^{(*)}$ systems.

molecule	$I J^{PC}$	a (fm)	B (MeV)	M (MeV)
$B\bar{B}$	$0 \ 0^{++}$	1.1	20.5	10538.4
$B\bar{B}^* + B^*\bar{B}$	$0 \ 1^{++}$	1.0	38.3	10565.8
$B\bar{B}^* - B^*\bar{B}$	$0 \ 1^{+-}$	1.6	6.0	10598.2
$B^*\bar{B}^*$	$0 \ 0^{++}$	-3.5	0.5^V	10648.9^V
$B^*\bar{B}^*$	$0 \ 1^{+-}$	1.6	6.0	10643.4
$B^*\bar{B}^*$	$0 \ 2^{++}$	1.0	38.5	10610.9

In the SU(3)-flavor symmetry limit, the $\bar{P}^{(*)}P^{(*)}$ system contains both a singlet and an octet irreducible

⁴ We note that similar results are obtained in Ref. [685] using heavy quark symmetry and the local hidden gauge approach.

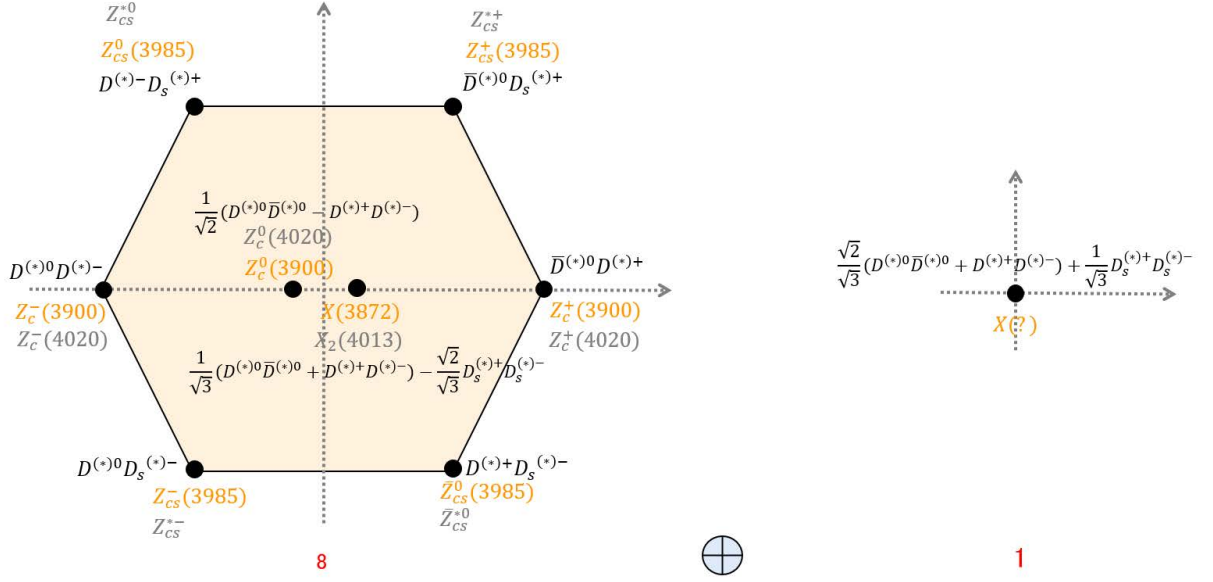


FIG. 8. $Z_c(3900)$, $Z_{cs}(3985)$, $X(3872)$ as parts of the SU(3)-flavor $\bar{D}_s^{(*)}D_s^{(*)}$ multiplet of hadronic molecules, and the representations in grey referring to their corresponding HQSS partners.

representation as shown in Fig. 8. In both representations, they contain $\bar{D}^{(*)}D^{(*)}$ and $\bar{D}_s^{(*)}D_s^{(*)}$ components, which indicates that the $\bar{D}_s^{(*)}D_s^{(*)}$ system affects the behaviors of isoscalar hadronic molecules. In Refs. [453, 686–688], the authors employ SU(3)-flavor symmetry and HQSS to study the molecules near the $\bar{D}^{(*)}D^{(*)}$ and $\bar{D}_s^{(*)}D_s^{(*)}$ mass thresholds, where the results depend sensitively on the inputs. In general, with ideal mixing, the octet and singlet configurations specify the $\bar{D}_s^{(*)}D_s^{(*)}$ and $\bar{D}^{(*)}D^{(*)}$ components [147]. In the meson exchange theory, the strength of the $\bar{D}_s^{(*)}D_s^{(*)}$ potentials are weaker than that of the isoscalar $\bar{D}^{(*)}D^{(*)}$ potentials [147, 689], leading to the nonexistence of $\bar{D}_s^{(*)}D_s^{(*)}$ bound states [161]. Recently, lattice QCD simulations obtained a \bar{D}_sD_s bound state [456], which is also found in the local hidden gauge approach [457]. It can be seen that the precise $\bar{D}^{(*)}D^{(*)}$ and $\bar{D}_s^{(*)}D_s^{(*)}$ interactions, and particularly the SU(3) flavor symmetry breaking, are important to probe the nature of exotic states near their mass thresholds. In particular, the impact of compact configurations such as excited charmonium components and compact tetraquark components on the $\bar{D}^{(*)}D^{(*)}$ and $\bar{D}_s^{(*)}D_s^{(*)}$ mass thresholds, often expressed as effective potentials, were not included in our studies. In particular, the $\chi_{c0}(3915)$ and the newly discovered $X(3960)$ are located in the vicinity of the \bar{D}_sD_s mass threshold as shown in Fig. 9. This indicates that the couplings between the \bar{D}_sD_s mass threshold and the bare $\chi_{c0}(2P)$ component may affect the physical state around this energy region.

Via HADS, one can relate the $D^{(*)}\bar{D}^{(*)}$ system with the $D^{(*)}\Xi_{cc}^{(*)}$ system, as shown in Fig. 10. In the heavy quark limit, the $D^{(*)}\bar{D}^{(*)}$ and $D^{(*)}\Xi_{cc}^{(*)}$ systems share the same couplings C_a and C_b . With the

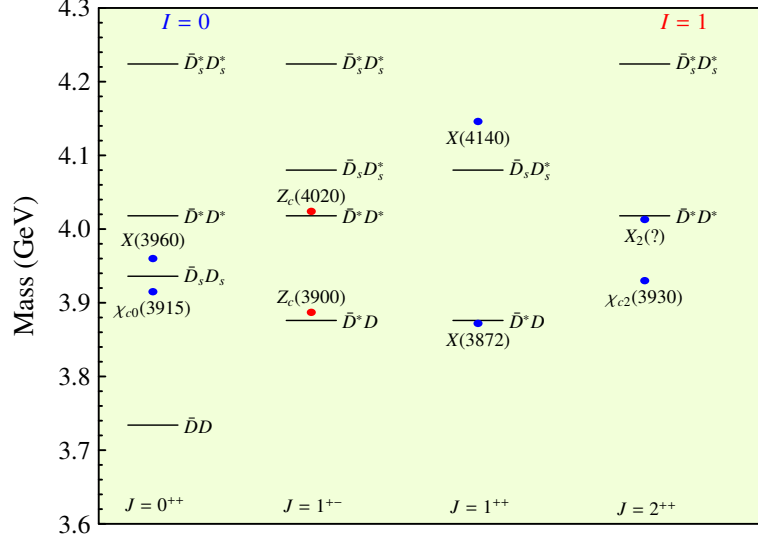


FIG. 9. Locations of isoscalar (blue) and isovector (red) hadronic molecular candidates with respect to the $\bar{D}^{(*)}D^{(*)}$ and $\bar{D}_s^{(*)}D_s^{(*)}$ mass thresholds.

couplings obtained, one can calculate the binding energies and scattering lengths of the $D^{(*)}\Xi_{cc}^{(*)}$ system, which are shown in Table XV. One can see that the $D^{(*)}\Xi_{cc}^{(*)}$ states are more bound than the $D^{(*)}\bar{D}^{(*)}$ states due to the larger reduced masses of the $D^{(*)}\Xi_{cc}^{(*)}$ system. We predict two bound states $J^P = 1/2^- \bar{D}^*\Xi_{cc}$ and $J^P = 5/2^- \bar{D}^*\Xi_{cc}^*$, consistent with the results of Refs. [607, 690, 691]. The minimum quark content of the $D^{(*)}\Xi_{cc}^{(*)}$ molecules are ccc , which could mix with excited fully charmed baryons. It means the exotic charmonium states have strong couplings to a pair of charmed mesons. In terms of HQFS, one can expect a more bound system composed of $B^{(*)}\Xi_{bb}^{(*)}$.

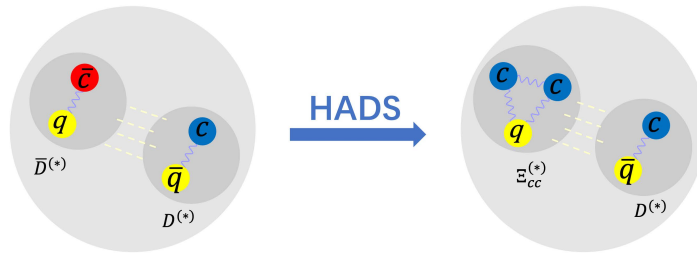


FIG. 10. HADS relates the $\bar{D}^{(*)}\Sigma_c^{(*)}$ system with the $\bar{D}^{(*)}T_{cc}^{(*)}$ system.

The leading-order $\bar{D}^{(*)}D^{(*)}$ contact potentials for the isovector sector are the same as those for the isoscalar sector. With the light meson saturation mechanism, we find that the isovector $\bar{D}^{(*)}D^{(*)}$ potentials are less attractive than their isoscalar counterparts. In the local hidden gauge approach [526], Aceti et al.

TABLE XV. Scattering lengths (a in units of fm), binding energies (B in units of MeV, if bound states exist) and mass spectra (M in units of MeV) of prospective isoscalar heavy meson-baryon molecules. The superscript V denotes the existence of virtual states, the \dagger symbol denotes that the system is unbound, and the $?$ symbol indicates that the system is bound with the central value of the potential and can become unbound if the potential is made less attractive within the range specified in the text. The uncertainties originate from the HADS breaking of the order 30%.

molecule	I	J^{PC}	a (fm)	B (MeV)	M (MeV)
$D\Xi_{cc}$	0	$1/2^-$	$3.3_{-1.5}^{+9.1}$	$2.0_{\dagger}^{+7.3}$?
$D\Xi_{cc}^*$	0	$3/2^-$	$3.2_{-1.4}^{+9.5}$	$2.1_{\dagger}^{+7.5}$?
$D^*\Xi_{cc}$	0	$1/2^-$	$1.8_{-0.5}^{+3.5}$	$8.7_{-8.1}^{+13.3}$	5621.3
$D^*\Xi_{cc}$	0	$3/2^-$	$4.7_{-2.7}^{+8.0}$	$0.9_{\dagger}^{+5.3}$?
$D^*\Xi_{cc}^*$	0	$1/2^-$	$-0.9_{-0.9}^{+0.4}$	11.2^V	5724.6^V
$D^*\Xi_{cc}^*$	0	$3/2^-$	$22.8_{-22.0}^{+24.6}$	$0_{\dagger}^{+2.8}$?
$D^*\Xi_{cc}^*$	0	$5/2^-$	$1.6_{-0.4}^{+1.7}$	$12.9_{-10.9}^{+15.9}$	5723.2

argued that due to the OZI rule, the light meson exchange for the \bar{D}^*D system with $I = 1$ is suppressed. The two-pion exchange contributions are much smaller than the heavy meson exchange contributions, which shows that the isovector \bar{D}^*D potential is weak. In addition, the OBE model showed that the isovector \bar{D}^*D system can not form a bound state [257]. Therefore, one expects either a virtual state or a resonance in the isovector \bar{D}^*D system. In Ref. [153], He et al. employed the meson exchange model to obtain the potentials of the $J/\psi\pi - \bar{D}^*D$ system and assigned the $Z_c(3900)$ as a virtual state. They found that the inelastic potential $J/\psi\pi - \bar{D}^*D$ plays a minor role. In Ref. [513], Wang et al. employed the chiral EFT approach to obtain the \bar{D}^*D and \bar{D}^*D^* potentials up to the next-to-leading order. Then, they fitted the experimental invariant mass distributions. Later, they introduced the $J/\psi\pi$ channel, and reproduced the masses and widths of $Z_c(3900)$ and $Z_c(4020)$ with the contact potentials [514]. In Ref. [516], Du et al. argued that $Z_c(3900)$ and $Z_c(4020)$ could be either virtual states or resonant states with contact potentials by fitting the experimental data. Therefore, virtual states or resonant states are likely to exist in the isovector $\bar{D}^{(*)}D^{(*)}$ system.

In principle, with only C_a and C_b , the contact potentials can not generate resonant states in the single-channel case. If a q^2 term is included, i.e., $C_a + D_a \cdot q^2$ [181, 514, 692], resonances can be dynamically generated. Experimentally, the two tetraquark states $Z_c(3900)$ and $Z_c(4020)$ are located above the \bar{D}^*D and \bar{D}^*D^* mass thresholds, which can be naturally interpreted as $\bar{D}^*D^{(*)}$ resonant states [513, 514]. Assuming $Z_c(3900)$ as a $J^{PC} = 1^{+-} \bar{D}D^*$ resonance, one can determine $C_a = -7 \text{ GeV}^{-2}$ and $D_a = -220$

TABLE XVI. Pole positions of $\bar{D}D^*$, \bar{D}^*D^* , $\bar{D}D_s^*$, and $\bar{D}^*D_s^*$ with $J^{PC} = 1^{+-}$ for a cutoff of $\Lambda = 1$ GeV. The subscript V denotes the existence of virtual states.

molecule	I	J^{PC}	$m - \frac{\Gamma}{2}$ (MeV)	Experimental data (MeV)
$D\bar{D}^*$	1	1^{+-}	Input	3888.4+14.2 <i>i</i>
$D^*\bar{D}^*$	1	1^{+-}	4029.2+12.9 <i>i</i>	4024.1+6.5 <i>i</i>
$D_s\bar{D}^*$	$\frac{1}{2}$	1^{+-}	3988.5+13.2 <i>i</i>	3982.5+6.4 <i>i</i>
$D_s^*\bar{D}^*$	$\frac{1}{2}$	1^{+-}	4131.5+12.0 <i>i</i>	-
$B\bar{B}^*$	1	1^{+-}	10602 ^V	10608.4+7.8 <i>i</i>
$B^*\bar{B}^*$	1	1^{+-}	10648 ^V	10653.2+7.2 <i>i</i>

GeV⁻⁴ for a cutoff $\Lambda = 1$ GeV. Via HQSS and SU(3)-flavor symmetry, one can relate the $\bar{D}D^*$ channel with the \bar{D}^*D^* , $\bar{D}D_s^*$, and $\bar{D}^*D_s^*$ channels. Therefore, with the parameters obtained, we predict the molecular states in the \bar{D}^*D^* , $\bar{D}D_s^*$, and $\bar{D}^*D_s^*$ systems in Table XVI, where the \bar{D}^*D^* and $\bar{D}D_s^*$ resonant states likely correspond to the exotic states of $Z_c(4020)$ [489] and $Z_{cs}(3985)$ discovered by the BESIII Collaboration [495]. In contrast, the $\bar{D}^*D_s^*$ resonant state has not yet been discovered. Here we only discuss the resonant states with the quantum numbers $J^{PC} = 1^{+-}$. Moreover, with HQFS, one can relate the $\bar{D}D^*$ and \bar{D}^*D^* systems with the $\bar{B}B^*$ and \bar{B}^*B^* systems. With the same inputs, we predict the poles near the $\bar{B}B^*$ and \bar{B}^*B^* mass thresholds, i.e., virtual states [513]. Since the $\bar{B}^*B^{(*)}$ reduced mass is larger, the isovector $\bar{B}^*B^{(*)}$ molecules are more bound, resulting in virtual $\bar{B}B^*$ and \bar{B}^*B^* states. We note that other channels composed of a charmonium state and a light meson may also play a role in generating these molecules.

TABLE XVII. Masses of DD^* , D^*D^* , DD_s^* , and $D^*D_s^*$ with $J^P = 1^+$ for a cutoff of $\Lambda = 1$ GeV.

molecule	I	J^{PC}	m (MeV)	Experimental data (MeV)
DD^*	0	1^+	Input	3874.73
D^*D^*	0	1^+	4015.3	-
D_sD^*	$\frac{1}{2}$	1^+	3975.2	-
$D_s^*D^*$	$\frac{1}{2}$	1^+	4118.3	-
BB^*	0	1^+	10551.2	-
B^*B^*	0	1^+	10596.1	-

Finally, we discuss the open-charm $D^{(*)}D^{(*)}$ molecules. Because of the Bose-Einstein statistics, the quantum numbers of the $D^{(*)}D^{(*)}$ system satisfy $(-1)^{I+S+L+1} = 1$. In the isoscalar sector, there exist

only two states in contrast with the $\bar{D}^{(*)}D^{(*)}$ system, i.e., $J^P = 1^+ DD^*$ and $J^P = 1^+ D^*D^*$. In the heavy quark limit, the DD^* contact interaction is the same as that of D^*D^* . Unlike its hidden-charm counterpart, the isospin-breaking effect is expected to be small due to the smaller mass splitting of the two components of the D^*D channel. Identifying the $T_{cc}(3875)$ discovered by the LHCb Collaboration as a DD^* bound state, one can determine the coupling $C_{DD} = -18.215 \text{ GeV}^{-2}$ for a cutoff $\Lambda = 1 \text{ GeV}$. With the coupling obtained, one predicts a D^*D^* bound state with a binding energy of 1.9 MeV, in agreement with Refs. [581, 693].

With SU(3)-flavor symmetry, we obtain two $D_s D^*$ and $D_s^* D^*$ bound states with binding energies of 1.6 MeV and 2.6 MeV, consistent with the results of the chiral unitary approach [693]. The $D_s D^*$ and $D_s^* D^*$ systems can bind via the one-kaon exchange. On the other hand, there is essentially no light-meson exchange allowed for the $D_s^* \bar{D}$ system. Therefore, the strength of the $D_s^* \bar{D}$ interaction is very weak [529, 694], which indicates there are no bound states around the $D_s^* \bar{D}$ mass threshold. Along the same line, with HQFS, we predict two $B^* B$ and $B^* B^*$ bound states with binding energies of 53.0 MeV and 53.3 MeV as shown in Table XVII. This shows that the HQSS works well in the bottom sector. Regarding quark rearrangements, the doubly heavy tetraquark molecules are also likely to be compact doubly heavy tetraquark states. The quark model predictions for the doubly charmed tetraquark state are above the D^*D mass threshold [59, 60, 695], which supports the molecular interpretation for the $T_{cc}(3875)$. The lattice QCD simulations of the D^*D interaction resulted in a virtual state [567], which indicates that the D^*D interaction is attractive but not very strong. However, the quark model predictions for the doubly bottomed tetraquark state are below the BB mass threshold [585, 696]. The light meson saturation mechanism shows that the hidden-charm dimeson molecules are more bound than the open-charm dimeson molecules. However, the hidden-charm pentaquark states are less bound than their open-charm partners [634, 658].

According to the above studies, we can obtain some universal conclusions regarding the strengths of the potentials of a given system.

1. As a given system's total isospin decreases, its potential becomes stronger. For instance, the DK $I = 0$ interaction is more attractive than the $I = 1$ one.
2. A system with a pair of a light quark and a light antiquark experiences stronger attraction than that with a pair of light quarks or a pair of light antiquarks. For instance, the DK attraction is stronger than the $\bar{D}K$ one.

4. $\bar{D}^{(*)}D_{1,2}$ and $B_c\bar{B}_c$ molecules

In the previous section, we discussed the final-state contributions of a pair of ground-state charmed mesons to the X and Z charmoniumlike states. We note that their contributions to the Y charmoniumlike states are minor due to the conservation of angular momentum. On the other hand, the Y charmoniumlike states with the quantum numbers $J^{PC} = 1^{--}$ strongly couple to either a pair of ground-state and excited charmed meson, such as $\bar{D}^{(*)}D_{1,2}(D_{0,1})$, or a pair of charmed baryon and anti-baryon (denoted by $B_c\bar{B}_c$), such as $\Lambda_c\bar{\Lambda}_c$ and $\Sigma_c\bar{\Sigma}_c$. In the heavy quark limit, the P -wave charmed mesons are classified as two doublets of $(D_0, D_1(2430))$ and $(D_1(2420), D_2)$, while the widths of the former one are so broad that they are not good candidates for the constituents of hadronic molecules. In the following, we discuss only two such kinds of molecules: $\bar{D}^{(*)}D_{1,2}$ and $\Sigma_c^{(*)}\bar{\Sigma}_c^{(*)}$.

TABLE XVIII. Mass spectrum of the $\bar{D}^{(*)}D_{1,2}$ system.

Molecule	J^{PC}	Wave function	Mass(A) (MeV)	Mass(B) (MeV)
$\bar{D}D_1$	1^{-+}	$\frac{1}{\sqrt{2}}(\bar{D}D_1 + D\bar{D}_1)$	—	—
$\bar{D}D_1$	1^{--}	$\frac{1}{\sqrt{2}}(\bar{D}D_1 - D\bar{D}_1)$	Input	4087.5
$\bar{D}D_2$	2^{-+}	$\frac{1}{\sqrt{2}}(\bar{D}D_2 + D\bar{D}_2)$	—	4031.8
$\bar{D}D_2$	2^{--}	$\frac{1}{\sqrt{2}}(\bar{D}D_2 - D\bar{D}_2)$	4317.5	4237.6
\bar{D}^*D_1	0^{-+}	$\frac{1}{\sqrt{2}}(\bar{D}^*D_1 + D^*\bar{D}_1)$	—	—
\bar{D}^*D_1	0^{--}	$\frac{1}{\sqrt{2}}(\bar{D}^*D_1 - D^*\bar{D}_1)$	—	—
\bar{D}^*D_1	1^{-+}	$\frac{1}{\sqrt{2}}(\bar{D}^*D_1 - D^*\bar{D}_1)$	—	4236.1
\bar{D}^*D_1	1^{--}	$\frac{1}{\sqrt{2}}(\bar{D}^*D_1 + D^*\bar{D}_1)$	4428.5	Input
\bar{D}^*D_1	2^{-+}	$\frac{1}{\sqrt{2}}(\bar{D}^*D_1 + D^*\bar{D}_1)$	4418.5	4336.5
\bar{D}^*D_1	2^{--}	$\frac{1}{\sqrt{2}}(\bar{D}^*D_1 - D^*\bar{D}_1)$	4369.0	4240.1
\bar{D}^*D_2	1^{-+}	$\frac{1}{\sqrt{2}}(\bar{D}^*D_2 + D^*\bar{D}_2)$	—	—
\bar{D}^*D_2	1^{--}	$\frac{1}{\sqrt{2}}(\bar{D}^*D_2 - D^*\bar{D}_2)$	—	—
\bar{D}^*D_2	2^{--}	$\frac{1}{\sqrt{2}}(\bar{D}^*D_2 + D^*\bar{D}_2)$	—	—
\bar{D}^*D_2	2^{-+}	$\frac{1}{\sqrt{2}}(\bar{D}^*D_2 - D^*\bar{D}_2)$	4466.0	4399.6
\bar{D}^*D_2	3^{-+}	$\frac{1}{\sqrt{2}}(\bar{D}^*D_2 + D^*\bar{D}_2)$	—	—
\bar{D}^*D_2	3^{--}	$\frac{1}{\sqrt{2}}(\bar{D}^*D_2 - D^*\bar{D}_2)$	4251.3	4033.3

In the heavy quark limit, the contact-range potentials of the $\bar{D}^{(*)}D_{1,2}$ system are characterized by four

parameters. In terms of the products of spin operators, they can be written as

$$V = D_a + S_1 \cdot S_2 D_b + S_{12} \cdot S_{12} C_a + Q_{ij} Q_{ij} C_b, \quad (9)$$

where D_a and D_b characterise the potentials of the direct scattering process, and C_a and C_b the cross scattering process. In principle, one needs experimental data to fix these parameters. However, in the R -value scan, only the states $Y(4220)$ and $Y(4360)$ are difficult to be understood as conventional charmonium states [697], which are around the $\bar{D}D_1$ and \bar{D}^*D_1 mass thresholds. For a cutoff of $\Lambda = 1$ GeV, the parameters of the $\bar{D}D_1$ and \bar{D}^*D_1 contact-range potentials are determined to be 34.3 GeV^{-2} and 32.0 GeV^{-2} , which reflects HQSS in the $\bar{D}D_1$ and \bar{D}^*D_1 contact-range potentials. Therefore, it is natural to expect that $Y(4220)$ and $Y(4360)$ are $\bar{D}D_1$ and \bar{D}^*D_1 molecules [483, 484]. With the molecular assumptions for $Y(4220)$ and $Y(4360)$, one can not fix the four parameters of the $\bar{D}^{(*)}D_{1,2}$ system. We further resort to the light meson saturation approach, which determines the ratios of these parameters well. In the isospin limit, the flavor wave function of $\bar{D}^*D_{1,2}$ is $|\bar{P}T(\eta)\rangle = \frac{1}{\sqrt{2}}(|\bar{P}T\rangle + \eta|P\bar{T}\rangle)$ with the charge parity $C = \eta(-1)^{S-S_P-S_T}$. For $\eta = 1$, we obtain the ratios

$$\frac{D_b^{sat}}{D_a^{sat}} = 0.53, \quad \frac{C_a^{sat}}{D_a^{sat}} = -0.76, \quad \frac{C_b^{sat}}{D_a^{sat}} = -0.20. \quad (10)$$

For $\eta = -1$, we obtain the ratios

$$\frac{D_b^{sat}}{D_a^{sat}} = 0.74, \quad \frac{C_a^{sat}}{D_a^{sat}} = -1.07, \quad \frac{C_b^{sat}}{D_a^{sat}} = -0.28. \quad (11)$$

One can see that C_a and D_b are more than 50% of D_a , which induces large mass splittings between the multiplet of hadronic molecules. Assuming $Y(4220)$ as a $\bar{D}D_1$ bound state, the flavor wave function is $\frac{1}{\sqrt{2}}(\bar{D}D_1 - D\bar{D}_1)$ and the contact-range potential is $D_a - C_a$. Together with the ratio obtained in the light meson saturation approach, one further obtains $D_a = -16.57 \text{ GeV}^{-2}$ and $C_a = 17.73 \text{ GeV}^{-2}$. At last, one obtains $D_b = -12.26 \text{ GeV}^{-2}$ and $C_b = 4.64 \text{ GeV}^{-2}$. Identifying $Y(4360)$ as a \bar{D}^*D_1 bound state, one can obtain the sum of $D_a - \frac{5}{6}D_b - \frac{1}{4}C_a - \frac{5}{4}C_b = -32.0 \text{ GeV}^{-2}$. With the ratios obtained in the light meson saturation approach, one can determine $D_a = -32.05 \text{ GeV}^{-2}$, $D_b = -16.67 \text{ GeV}^{-2}$, $C_a = 24.36 \text{ GeV}^{-2}$, and $C_b = 6.41 \text{ GeV}^{-2}$. One can see that the latter values are smaller than the former ones, which indicates that the signs of contact potentials are consistent in both cases. We show the mass spectrum of the $\bar{D}^*D_{1,2}$ system for the two cases in Table XVIII. Case A refers to the former fitted parameters, and Case B to the latter. The results in Case B are more bound such that the mass of $Y(4220)$ shifts to 4088. Assuming that $Y(4220)$ and $Y(4360)$ are $\bar{D}D_1$ and \bar{D}^*D_1 bound states, the difference of Case A and Case B can be attributed to the unknown couplings between excited charmed mesons and light mesons. The light meson saturation mechanism does not work for this system. It is worth noting that the two states $J^{PC} = 2^{--}$

\bar{D}^*D_1 and $J^{PC} = 3^{--} \bar{D}^*D_2$ are bound in both cases. The impact of the $\bar{D}^{(*)}D_{1,2}$ coupled channels on the charmonium vector states is not clear due to the unknown interactions of the $\bar{D}^{(*)}D_{1,2}$ system. It is necessary to construct the precise interactions of the $\bar{D}^{(*)}D_{1,2}$ system in the future. In Ref. [480], Dong et al. adopted the meson exchange model to assign $Y(4260)$ as a $J^{PC} = 1^{--} \bar{D}D_1$ bound state and predicted its C -parity partner, a $J^{PC} = 1^{-+} \bar{D}D_1$ bound state with a large binding energy, which is different from our results.

In addition, a molecule composed of the ground-state charmed meson D and the excited charmed meson with strangeness $D_{s0}^*(2317)$ is likely to exist. In Ref. [698], the potentials of $DD_{s0}^*(2317)$ and $DD_{s1}(2460)$ are generated via the one kaon exchange, and their binding energies are calculated. Three-body hadrons could also form these two molecules: DDK and DD^*K in terms of quark contents, which will be discussed in the next section. In addition, the vector charmonium state $Y(4630)$ is explained as a $\bar{D}_s^*D_{s1}(2536)$ molecule [699, 700], where the η and ϕ exchanges are responsible for the $\bar{D}_s^*D_{s1}(2536)$ interactions.

Several Y states around 4.6 GeV were discovered experimentally, such as $Y(4630)$ [471] and $Y(4660)$ [346], which show strong coupling to the $\bar{\Lambda}_c\Lambda_c$ channel. Up to now, there exists no vector charmonium state around 4.9 GeV, i.e., in the vicinity of the $\bar{\Sigma}_c\Sigma_c$ mass threshold. In this section, we investigate the mass spectrum of the $\Sigma_c^{(*)}\bar{\Sigma}_c^{(*)}$ system. The contact-range potentials of the $\Sigma_c^{(*)}\bar{\Sigma}_c^{(*)}$ system are parameterised with three parameters: E_a , E_b , and E_c ,

$$V = E_a + S_1 \cdot S_2 E_b + Q_{ij}Q_{ji}E_c, \quad (12)$$

where E_a , E_b , and E_c represent the electric charge, magnetic dipole, and electric quadrupole terms, which are constructed by the products of irreducible tensors built from the light-spin operators.

Since no experimental data is available, one can not determine E_a and E_b . Often, one resorts to phenomenological models such as the OBE model to predict the mass spectrum of the $\Sigma_c^{(*)}\Sigma_c^{(*)}$ system [701]. On the other hand, relying on the light meson saturation mechanism, one can also understand the $\Sigma_c^{(*)}\bar{\Sigma}_c^{(*)}$ system qualitatively. Following Ref. [182], the couplings of E_a , E_b , and E_c are saturated in the following way

$$\begin{aligned} E_a^{sat(\sigma)}(\Lambda \sim m_\sigma) &\propto -\frac{g_{\sigma 2}^2}{m_\sigma^2}, \\ E_a^{sat(V)}(\Lambda \sim m_V) &\propto \frac{g_{v2}^2}{m_v^2}(\eta + \vec{T}_1 \cdot \vec{T}_2), \\ E_b^{sat(V)}(\Lambda \sim m_V) &\propto \frac{f_{v2}^2}{6M^2}(\eta + \vec{T}_1 \cdot \vec{T}_2), \\ E_c^{sat(V)}(\Lambda \sim m_V) &\propto \frac{h_v^2}{36M^4}m_V^2(\eta + \vec{T}_1 \cdot \vec{T}_2), \end{aligned} \quad (13)$$

where $\eta = +1$ is for the $\Sigma_c^{(*)}\Sigma_c^{(*)}$ systems and $\eta = -1$ is for the $\Sigma_c^{(*)}\bar{\Sigma}_c^{(*)}$ system. With the relevant values

TABLE XIX. Likely bound states in the $\Sigma_c^{(*)}\bar{\Sigma}_c^{(*)}$ system.

Molecule	J^{PC}	Potential	Attractive?
$\Sigma_c\bar{\Sigma}_c$	0^{-+}	$C_0 - \frac{4}{3}C_1$?
$\Sigma_c\bar{\Sigma}_c$	1^{--}	$C_0 + \frac{4}{9}C_1$	likely
$\bar{\Sigma}_c^*\Sigma_c$	1^{--}	$C_0 - \frac{11}{9}C_1 + 5C_2$?
$\bar{\Sigma}_c^*\Sigma_c$	1^{-+}	$C_0 - C_1 - 5C_2$?
$\bar{\Sigma}_c^*\Sigma_c$	2^{-+}	$C_0 + \frac{1}{3}C_1 - C_2$	likely
$\bar{\Sigma}_c^*\Sigma_c$	2^{--}	$C_0 + C_1 + C_2$	likely
$\bar{\Sigma}_c^*\Sigma_c^*$	0^{-+}	$C_0 - \frac{5}{3}C_1 + 5C_2$?
$\bar{\Sigma}_c^*\Sigma_c^*$	1^{--}	$C_0 - \frac{11}{9}C_1 + C_2$?
$\bar{\Sigma}_c^*\Sigma_c^*$	2^{-+}	$C_0 - \frac{1}{3}C_1 - 3C_2$?
$\bar{\Sigma}_c^*\Sigma_c^*$	3^{--}	$C_0 + C_1 + C_2$	likely

of Table XLV and the coupling $h_v = \eta g_v$ with $\eta = 0$ [149], we obtain the ratios of the $\Sigma_c^{(*)}\bar{\Sigma}_c^{(*)}$ system:

$$\frac{E_b^{sat}}{E_a^{sat}} = 0.19, \quad \frac{E_c^{sat}}{E_a^{sat}} = 0, \quad (14)$$

which indicates that the E_c term can be safely neglected. Moreover, we obtain the ratios of the $\Sigma_c^{(*)}\Sigma_c^{(*)}$ system:

$$\frac{E_b^{sat}}{E_a^{sat}} = 0.10, \quad \frac{E_c^{sat}}{E_a^{sat}} = 0. \quad (15)$$

The E_a term provides attraction. According to the light meson saturation mechanism, the E_b term also provides attraction [182]. As shown in Table XIX, we can anticipate that the $J^{PC} = 1^{--}\bar{\Sigma}_c\Sigma_c$, $J^{PC} = 2^{--}\bar{\Sigma}_c\Sigma_c^*$, $J^{PC} = 2^{-+}\bar{\Sigma}_c\Sigma_c^*$, and $J^{PC} = 3^{--}\bar{\Sigma}_c^*\Sigma_c^*$ systems bind, where the state $J^{PC} = 3^{--}\bar{\Sigma}_c^*\Sigma_c^*$ is the most bound. The $\Sigma_c^{(*)}\bar{\Sigma}_c^{(*)}$ system can be decomposed into isopin eigenstates with isospin 0, 1, or 2. Referring to the light meson saturation approach, we find that the $\Sigma_c^{(*)}\bar{\Sigma}_c^{(*)}$ system is more bound as the isospin decreases. In this picture, one can estimate the potential strength of the $\Sigma_c^{(*)}\bar{\Sigma}_c^{(*)}$ system, which is helpful to understand the relevant hadron-hadron interactions and explore Y states near the $\Sigma_c^{(*)}\bar{\Sigma}_c^{(*)}$ mass threshold. In Ref. [702], Lee et al. found that the $J^{PC} = 1^{--}\bar{\Sigma}_c\Sigma_c$ system is more bound than the $J^{PC} = 0^{-+}\bar{\Sigma}_c\Sigma_c$ system, consistent with our conclusion. In terms of the light meson saturation mechanism, we find that the ratio of E_b/E_a for the $\Sigma_c^{(*)}\bar{\Sigma}_c^{(*)}$ system is larger than that for the $\Sigma_c^{(*)}\Sigma_c^{(*)}$ system, which hints at a large mass splitting for the $\Sigma_c^{(*)}\bar{\Sigma}_c^{(*)}$ system than for the $\Sigma_c^{(*)}\Sigma_c^{(*)}$ system. Moreover, the $\Sigma_c^{(*)}\bar{\Sigma}_c^{(*)}$ molecules are more bound than the $\Sigma_c^{(*)}\Sigma_c^{(*)}$ molecules.

C. Strong and radiative decays

The decay patterns of hadronic molecules are essential in revealing their nature. The likely decay modes of the predicted multiplets can help plan future experiments. In this review, we only focus on strong decays and radiative decays. The decay modes include two-body decays and three-body decays. The three-body decays of hadronic molecules always proceed via one of their unstable constituents at tree level. The triangle diagrams describe the two-body decays of hadronic molecules, equal to inelastic scatterings. Due to the small phase space, the widths of the three-body decays of hadronic molecules are often smaller than those of the two-body decays.

1. Three-body decays

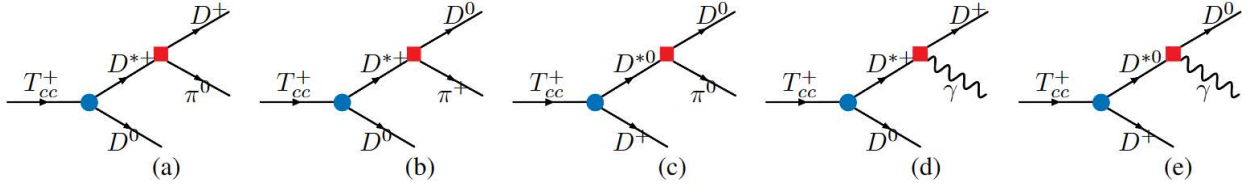


FIG. 11. Tree-level diagrams for the strong decays of $T_{cc}^+ \rightarrow D^+\pi^0(D^{*+})D^0$ (a), $T_{cc}^+ \rightarrow D^0\pi^+(D^{*+})D^0$ (b), and $T_{cc}^+ \rightarrow D^0\pi^0(D^{*0})D^+$ (c) as well as radiative decays of $T_{cc}^+ \rightarrow D^+\gamma(D^{*+})D^0$ (d) and $T_{cc}^+ \rightarrow D^0\gamma(D^{*0})D^+$ (e).

The decay of the doubly charmed tetraquark state $T_{cc}(3875)$ is a typical example of three-body decays. As a D^*D bound state, it can decay into $DD\pi(\gamma)$ via an off-shell D^* decaying into $D\pi(\gamma)$ as shown in Fig. 11. One should note that this is the dominant decay mode of T_{cc} since two-body decays are not allowed for T_{cc} as a D^*D bound state due to parity and momentum conservations. We employ the Lagrangian approach to calculate the decay widths of $T_{cc} \rightarrow DD\pi(\gamma)$. For the D^*D system, the difference between the $D^{*0}D^+$ and $D^{*+}D^0$ mass thresholds is about 1 MeV, which indicates that the isospin breaking in the T_{cc} couplings to $D^{*0}D^+$ and $D^{*+}D^0$ is small. Therefore, we estimate the T_{cc} couplings to its constituents D^*D by the compositeness condition in the isospin limit [571], consistent with Refs [178, 573, 581]. Then, we estimated the sum of its radiative and strong decay widths to be 63 keV, consistent with the experimental data. In other words, our results support the molecular interpretation for $T_{cc}(3875)$. Considering final-state interactions, the decay modes of Fig. 11 can result in triangle diagrams, which are of the next-to-leading order in the Language of EFTs. As a result, the contribution of such triangle diagrams can be treated perturbatively. In Ref. [175], the contribution of the triangle diagram is estimated to be 20% of the tree diagram.

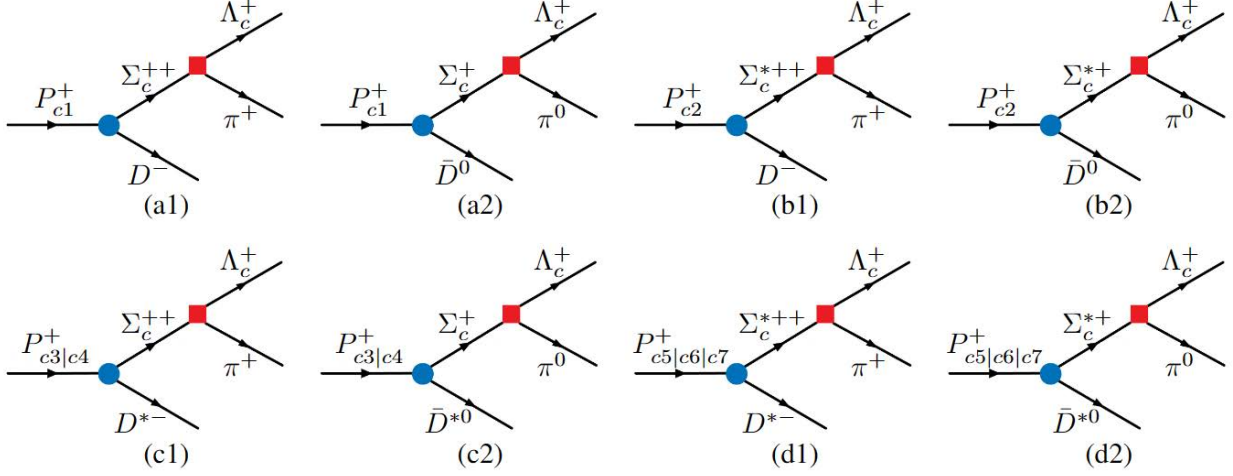


FIG. 12. Tree-level diagrams for the decays of $P_{c1} \rightarrow \bar{D}\Sigma_c \rightarrow \bar{D}\Lambda_c\pi$ (a), $P_{c2} \rightarrow \bar{D}^*\Sigma_c \rightarrow \bar{D}\Lambda_c\pi$ (b), $P_{c3|c4} \rightarrow \bar{D}^*\Sigma_c \rightarrow \bar{D}^*\Lambda_c\pi$ (c), and $P_{c5|c6|c7} \rightarrow \bar{D}^*\Sigma_c^* \rightarrow \bar{D}^*\Lambda_c\pi$ (d).

Considering HQSS, it is natural to expect a D^*D^* bound state. Because the D^*D^* molecules are located below the mass threshold by about 2 MeV, the phase space for its decay into $D^*D\pi$ and $D\pi D\pi$ is small. Therefore, the D^*D^* molecule dominantly decays into D^*D . In Ref. [693], Dai et al. estimated the partial decay width to be around 2 MeV, much larger than the T_{cc} width. The widths of three-body decays and four-body decays of the D^*D^* molecules are estimated to be around 65 keV, much smaller than that of the two-body decay [703, 704]. The decay modes of the D^*D^* molecule are more abundant than those of the D^*D molecule. According to SU(3)-flavor symmetry, the decay modes of the D^*D_s and $D_s^*D^*$ molecule are similar to those of the D^*D and D^*D^* molecules.

Identified as a \bar{D}^*D bound state, the $X(3872)$ cannot decay into a pair of charmed mesons, the same as the T_{cc} , resulting in a narrow width. We note that the $X(3872)$ is located almost exactly in the $\bar{D}^{*0}D^0$ mass threshold. Whether the $X(3872)$ is located above or below the $\bar{D}^{*0}D^0$ mass threshold remains undetermined, which would heavily affect its decay behavior. Since the $X(3872)$ can decay into charmonium and light mesons but T_{cc} can not, the width of the $X(3872)$ should be larger than that of T_{cc} . Regarding the $X(3872)$ as a $\bar{D}^{*0}D^{*0}-D^{*-}D^+$ molecule, the widths of the three-body decay of $X(3872) \rightarrow \bar{D}D\pi(\gamma)$ are estimated to be tens of keV, a bit smaller than that of T_{cc} as a D^*D molecule [705, 706], which account for only several percent of its total width.

The three-body decays of the $\bar{D}^{(*)}\Sigma_c^{(*)}$ molecules can proceed as shown in Fig. 12. The binding energies of the $\bar{D}^*\Sigma_c^{(*)}$ molecules relative to their mass thresholds are around 4-20 MeV [401, 547], while the mass thresholds of the $\bar{D}\pi\Sigma_c^{(*)}$ are 5 MeV less than those of the $\bar{D}^*\Sigma_c^{(*)}$, which implies that the decays of $\bar{D}^*\Sigma_c^{(*)}$ molecules into $\bar{D}\pi\Sigma_c^{(*)}$ via off-shell \bar{D}^* mesons are heavily suppressed or forbidden. The phase space for

TABLE XX. Partial decay widths (in units of MeV) of $P_c^+ \rightarrow D^{(*)-}\Lambda_c^+\pi^+$ and $P_c^+ \rightarrow \bar{D}^{(*)0}\Lambda_c^+\pi^0$ in Fig. 12 in scenario A and scenario B for a cutoff $\Lambda = 1.5$ GeV.

Scenario	A	A	B	B
Mode	$D^{(*)-}\Lambda_c^+\pi^+$	$\bar{D}^{(*)0}\Lambda_c^+\pi^0$	$D^{(*)-}\Lambda_c^+\pi^+$	$\bar{D}^{(*)0}\Lambda_c^+\pi^0$
P_{c1}	0.051	0.201	0.030	0.129
P_{c2}	2.670	2.859	2.164	2.251
P_{c3}	0.002	0.038	0.566	1.964
P_{c4}	0.189	0.655	0.001	0.013
P_{c5}	2.751	2.435	7.087	6.490
P_{c6}	3.567	3.188	4.539	4.156
P_{c7}	2.991	2.739	1.352	1.195

the $\Sigma_c^{(*)} \rightarrow \Lambda_c\pi$ is more than 30 MeV so that the tree-level decays of $\bar{D}^{(*)}\Sigma_c^{(*)} \rightarrow \bar{D}^{(*)}(\Sigma_c^{(*)} \rightarrow \Lambda_c\pi) \rightarrow \bar{D}^{(*)}\Lambda_c\pi$ are allowed, as shown in Fig. 12. Using the masses obtained in Ref. [547], we predict the decays of pentaquark molecules into $\bar{D}^{(*)}\Lambda_c\pi$. The decay width of $P_c(4312)$ into $\bar{D}\Lambda_c\pi$ is about hundreds of keV, which accounts for 2% – 3% of its total width. The decay width of $P_c(4457)$ into $\bar{D}\Lambda_c\pi$ is up to several MeV, while for $P_c(4440)$ it is only tens of keV. The partial decay width of $P_c(4457)$ accounts for tens of percent of its total width, while for $P_c(4440)$, it accounts for less than one percent. In addition, we predict the partial decay widths of the other four molecules into $\bar{D}^{(*)}\Lambda_c\pi$, which are about several MeV, some of which are even up to tens of MeV, in agreement with the results of Ref. [545]. It should be noted that it is difficult to observe P_{c7} in the $J/\psi p$ invariant mass distribution where only the D -wave $J/\psi p$ is allowed, while it may be detected via its three-body decays. Taking into account the final-state rescattering of Fig. 12, the tree diagrams will convert into the triangle diagrams as shown in Fig. 2 of Ref. [549], which only contribute to the widths of P_c states by several keV at most. Similarly, the $\bar{D}^{(*)}\Xi_c'^{(*)}$ molecules can decay into $\bar{D}^{(*)}\Xi_c\pi$, and the partial decay widths should be similar to the P_c states in terms of SU(3) flavor symmetry.

Assuming $Y(4220)$ and $Y(4360)$ as the $\bar{D}D_1$ and \bar{D}^*D_1 bound states, they can decay into $\bar{D}D^*\pi(\gamma)$ and $\bar{D}^*D^*\pi(\gamma)$ via an off-shell D_1 meson as shown in Fig. 13. The widths of the decays $Y(4220) \rightarrow D\bar{D}^*\pi(\gamma)$ and $Y(4360) \rightarrow D^*\bar{D}^*\pi(\gamma)$ are shown in Table XXI, indicating that the radiative decays of $Y(4220)$ and $Y(4360)$ are larger than those of pionic decays by one order of magnitude. In Ref. [707], Wang estimated the width of the partial decay $Y(4220) \rightarrow \bar{D}D^*\pi$ up to be 0.12 MeV assuming $Y(4220)$ as the compact tetraquark state, smaller than that obtained assuming $Y(4220)$ as the hadronic molecule,

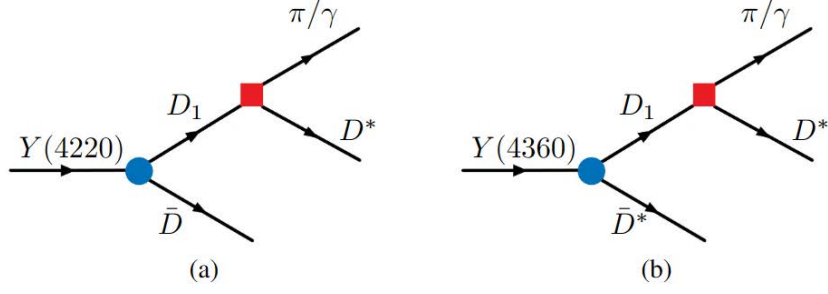


FIG. 13. Tree diagrams of $Y(4220) \rightarrow D\bar{D}^*\pi(\gamma)$ and $Y(4360) \rightarrow D^*\bar{D}^*\pi(\gamma)$.

which indicate that there exists prominent difference for the width of the decay $Y(4220) \rightarrow \bar{D}D^*\pi$ in two scenarios of $Y(4220)$. The $Y(4220)$ and $Y(4360)$ can decay into the final states with hidden charm number $J/\psi\pi\pi$, $J/\psi KK$, and $h_c\pi\pi$ as well [707], which generally proceed via the triangle mechanism, e.g., the final states of $\bar{D}^{(*)}$ and D^* in Fig. 13 rescattering into $J/\psi\pi$ and $h_c\pi$.

TABLE XXI. Widths (in units of MeV) of the partial decays of $Y \rightarrow \bar{D}^{(*)}D^*\pi(\gamma)$ and $Y \rightarrow D^{(*)}\bar{D}^*\pi(\gamma)$.

Molecules	$\bar{D}^{(*)}D^*\pi$	$D^{(*)}\bar{D}^*\pi$	$\bar{D}^{(*)}D^*\gamma$	$D^{(*)}\bar{D}^*\gamma$
$Y(4220)$	1.84	1.84	0.12	0.12
$Y(4360)$	3.21	3.21	0.21	0.21

2. Two-body decays

In general, two-body decay modes dominate the decays of hadronic molecules because they have ample phase space. Two methods can be employed to calculate the two-body decay widths. The first is to construct coupled-channel potentials constrained by symmetries, such as the chiral Lagrangian with SU(3)-flavor symmetry [123, 125, 183] and SU(4) symmetry [366], the local hidden gauge Lagrangian with SU(2)-flavor symmetry [708], SU(3)-flavor symmetry [158] or SU(4)-flavor symmetry [154, 159], the contact-range potentials with HQSS [255, 546, 630], and some phenomenological models [654, 709]. The second is to develop models, such as triangle diagrams [385, 545, 548, 710–712]. The former can account for both the masses and widths of exotic states, but the latter can only deal with the widths. An initial particle decaying into two final particles at the quark level can be described by three-point correlation functions in the QCD sum rules, which can extract the initial particle's couplings to the two final particles and then obtain the corresponding decay widths [77, 713–715].

A typical example is the two-body decays of the pentaquark states. From HQSS, the $\bar{D}^{(*)}\Sigma_c^{(*)} \rightarrow J/\psi(\eta_c)N$ interactions are only related to the spin of the light quark $1/2$, denoted by one coupling: $g_2 = \langle \bar{D}^{(*)}\Sigma_c^{(*)} | 1_H \otimes 1/2_L \rangle = \langle \bar{D}^{(*)}\Sigma_c^{(*)} | 0_H \otimes 1/2_L \rangle$. Similarly, one can express the $\bar{D}^{(*)}\Lambda_c \rightarrow J/\psi(\eta_c)N$ interactions by a second parameter: $g_1 = \langle \bar{D}^{(*)}\Lambda_c | 1_H \otimes 1/2_L \rangle = \langle \bar{D}^{(*)}\Lambda_c | 0_H \otimes 1/2_L \rangle$. As for the $\bar{D}^{(*)}\Sigma_c^{(*)} \rightarrow \bar{D}^{(*)}\Lambda_c$ interactions, they depend only on one coupling constant in the heavy quark limit. Therefore, we parameter the $\bar{D}^{(*)}\Sigma_c^{(*)} \rightarrow \bar{D}^{(*)}\Lambda_c$ potential by one coupling: $C'_b = \langle \bar{D}^{(*)}\Sigma_c^{(*)} | \bar{D}^{(*)}\Lambda_c \rangle$. The potentials of $J/\psi N \rightarrow J/\psi N$, $J/\psi N \rightarrow \eta_c N$ and $\eta_c N \rightarrow \eta_c N$ are suppressed due to the Okubo-Zweig-Iizuka (OZI) rule, which is also supported by lattice QCD simulations [716]. Combining the two parameters C_a and C_b characterising the $\bar{D}^{(*)}\Sigma_c^{(*)} \rightarrow \bar{D}^{(*)}\Sigma_c^{(*)}$ interactions, the $\bar{D}^{(*)}\Sigma_c^{(*)}$, $\bar{D}^*\Lambda_c$, $\bar{D}\Lambda_c$, $J/\psi p$, and $\eta_c p$ coupled-channel interactions are parameterised by the following parameters C_a , C_b , C'_b , g_1 , and g_2 , which are determined by reproducing the masses and widths of $P_c(4312)$, $P_c(4440)$, and $P_c(4457)$ in two scenarios A and B [232].

In Table XXII, we present the pole positions of the hidden-charm pentaquark molecules and the couplings to their constituents. From the obtained pole positions of $P_c(4312)$, $P_c(4440)$, and $P_c(4457)$, it is evident that scenario A, yielding results consistent with the experimental data, is more preferred than Scenario B, which is quite different from the single-channel study [547]. Our study shows that the coupled-channel effects can help distinguish the two possible scenarios. In a similar approach but without considering the $\bar{D}^{(*)}\Lambda_c$ channels, Scenario A is still slightly more preferred than Scenario B [549]. We note in passing that the chiral unitary model [186] also prefers scenario A. We further note that the coefficients in the contact-range potentials are derived assuming the HQSS, while the HQSS breaking is not considered. In Ref. [375], it was shown that the tensor term of the one-pion exchange potentials plays a crucial role in describing the widths of the pentaquark molecules, while the D -wave potentials are neglected in this work. Therefore, we can not conclude which scenario is more favorable. In Refs. [231, 717], Burns et al. proposed another case, named Scenario C, which corresponds to a particular case of Scenario B, where the $J^P = 1/2^-$ $\bar{D}^*\Sigma_c \rightarrow \bar{D}^*\Sigma_c$ potential is not strong enough to form a bound state. Therefore, $P_c(4457)$ is interpreted as a kinetic effect rather than a genuine state. From their values of C_a and C_b [231], the ratio C_b/C_a is determined to be around 0.5, which implies the emergence of a sizeable spin-spin interaction, inconsistent with the principle of EFTs. It is no surprise that such a large spin-spin interaction breaks the completeness of the multiplet picture of hidden-charm pentaquark molecules [161, 176, 177, 186, 375, 545, 547, 654, 709, 718].

From the couplings obtained in Table XXII, the partial decay widths of pentaquark molecules, as well as the corresponding branching fractions, are predicted in Scenario A and Scenario B as shown in Table XXIII. One can see that the branching fractions of the decays $P_c \rightarrow \bar{D}^{(*)}\Lambda_c$ in Scenario A are larger than those in Scenario B. In comparison, the branching fractions of the decays $P_c \rightarrow J/\psi p$ and $P_c \rightarrow \eta_c p$ in Scenario

TABLE XXII. Pole positions(in units of MeV) of six hidden-charm pentaquark molecules and the couplings to their constituents in Scenario A and Scenario B.

Scenario		A				
Name	P_{c1}	P_{c2}	P_{c3}	P_{c4}	P_{c5}	P_{c6}
Molecule	$\bar{D}\Sigma_c$	$\bar{D}\Sigma_c^*$	$\bar{D}^*\Sigma_c$	$\bar{D}^*\Sigma_c$	$\bar{D}^*\Sigma_c^*$	$\bar{D}^*\Sigma_c^*$
J^P	$\frac{1}{2}^-$	$\frac{3}{2}^-$	$\frac{1}{2}^-$	$\frac{3}{2}^-$	$\frac{1}{2}^-$	$\frac{3}{2}^-$
Pole (MeV)	4310.6+3.5 <i>i</i>	4372.8 +2.7 <i>i</i>	4440.6+8.6 <i>i</i>	4458.4+0.7 <i>i</i>	4500.0+9.9 <i>i</i>	4513.2+7.7 <i>i</i>
$g_{P_c\Sigma_c^*\bar{D}^*}$	-	-	-	-	2.686	2.194
$g_{P_c\Sigma_c\bar{D}^*}$	-	-	2.554	1.082	0.141	0.218
$g_{P_c\Sigma_c^*\bar{D}}$	-	2.133	-	0.179	-	0.237
$g_{P_c\Sigma_c\bar{D}}$	2.089	-	0.254	-	0.139	-
$g_{P_c\Lambda_c\bar{D}^*}$	0.234	0.074	0.177	0.050	0.110	0.241
$g_{P_c\Lambda_c\bar{D}}$	0.014	-	0.158	-	0.207	-
$g_{P_cJ/\psi N}$	0.251	0.454	0.584	0.103	0.434	0.532
$g_{P_c\eta_c N}$	0.420	-	0.261	-	0.527	-
Scenario		B				
Name	P_{c1}	P_{c2}	P_{c3}	P_{c4}	P_{c5}	P_{c6}
Molecule	$\bar{D}\Sigma_c$	$\bar{D}\Sigma_c^*$	$\bar{D}^*\Sigma_c$	$\bar{D}^*\Sigma_c$	$\bar{D}^*\Sigma_c^*$	$\bar{D}^*\Sigma_c^*$
J^P	$\frac{1}{2}^-$	$\frac{3}{2}^-$	$\frac{1}{2}^-$	$\frac{3}{2}^-$	$\frac{1}{2}^-$	$\frac{3}{2}^-$
Pole (MeV)	4309.9+4 <i>i</i>	4365.8+6.2 <i>i</i>	4458.4+4.5 <i>i</i>	4441.4+1.1 <i>i</i>	4521.6+7.5 <i>i</i>	4522.5+3.7 <i>i</i>
$g_{P_c\Sigma_c^*\bar{D}^*}$	-	-	-	-	1.841	1.621
$g_{P_c\Sigma_c\bar{D}^*}$	-	-	1.679	2.462	0.107	0.143
$g_{P_c\Sigma_c^*\bar{D}}$	-	2.451	-	0.099	-	0.171
$g_{P_c\Sigma_c\bar{D}}$	2.072	-	0.161	-	0.131	-
$g_{P_c\Lambda_c\bar{D}^*}$	0.392	0.090	0.247	0.159	0.232	0.223
$g_{P_c\Lambda_c\bar{D}}$	0.020	-	0.191	-	0.281	-
$g_{P_cJ/\psi N}$	0.263	0.704	0.277	0.168	0.314	0.312
$g_{P_c\eta_c N}$	0.413	-	0.164	-	0.328	-

A are smaller than those in Scenario B. One can see that the two-body partial decays are uncertain due to the uncertainties of the $\bar{D}^{(*)}\Sigma_c^{(*)} \rightarrow \bar{D}^{(*)}\Lambda_c$ interactions and $\bar{D}^{(*)}\Sigma_c^{(*)} \rightarrow J/\psi(\eta_c)N$ interactions using the contact-range EFT approach. Such partial decay widths can not discriminate which scenario is better due

TABLE XXIII. Two-body partial decay widths (in units of MeV) of hidden-charm pentaquark molecules as well as their branching fractions in Scenario A and Scenario B .

Scenario		A				
Molecule	P_{c1}	P_{c2}	P_{c3}	P_{c4}	P_{c5}	P_{c6}
$\Gamma_2(\Sigma_c \bar{D}^*)$	-	-	-	-	0.50 (2.52 %)	1.38 (8.87 %)
$\Gamma_3(\Sigma_c^* \bar{D})$	-	-	-	1.14 (73.23 %)	-	2.62 (16.87 %)
$\Gamma_4(\Sigma_c \bar{D})$	-	-	2.87 (16.59 %)	-	1.04 (5.29 %)	-
$\Gamma_5(\Lambda_c \bar{D}^*)$	0.83 (11.71 %)	0.19 (3.48 %)	1.44 (8.33 %)	0.12 (7.82 %)	0.65 (3.32 %)	3.24 (20.81 %)
$\Gamma_6(\Lambda_c \bar{D})$	0.01 (0.14 %)	-	1.60 (9.22 %)	-	2.98 (15.14 %)	-
$\Gamma_7(J/\psi N)$	1.43 (20.22 %)	5.16 (96.52 %)	9.29 (53.64 %)	0.29 (18.95 %)	5.46 (27.73 %)	8.31 (53.45 %)
$\Gamma_8(\eta_c N)$	4.81 (67.93 %)	-	2.12 (12.23 %)	-	9.06 (45.98 %)	-
Scenario		B				
Molecule	P_{c1}	P_{c2}	P_{c3}	P_{c4}	P_{c5}	P_{c6}
$\Gamma_2(\Sigma_c \bar{D}^*)$	-	-	-	-	0.36 (2.17 %)	0.64 (8.30 %)
$\Gamma_3(\Sigma_c^* \bar{D})$	-	-	-	0.31 (13.63 %)	-	1.41 (18.19 %)
$\Gamma_4(\Sigma_c \bar{D})$	-	-	1.23 (12.88 %)	-	0.98 (5.92 %)	-
$\Gamma_5(\Lambda_c \bar{D}^*)$	2.27 (26.71 %)	0.26 (2.10 %)	2.97 (30.92 %)	1.17 (52.05 %)	3.05 (18.48 %)	2.82 (36.37 %)
$\Gamma_6(\Lambda_c \bar{D})$	0.02 (0.23 %)	-	2.40 (25.03 %)	-	5.65 (34.18 %)	-
$\Gamma_7(J/\psi N)$	1.57 (18.45 %)	12.28 (97.90 %)	2.13 (22.26 %)	0.77 (34.33 %)	2.92 (17.67 %)	2.88 (37.14 %)
$\Gamma_8(\eta_c N)$	4.65 (54.61 %)	-	0.85 (8.86 %)	-	3.57 (21.58 %)	-

to the slight differences in their values between Scenario A and Scenario B. Up to now, no suitable physical observable can discriminate the two scenarios.

The triangle mechanism has been applied to study the decay of the pentaquark molecules. In Ref. [548],

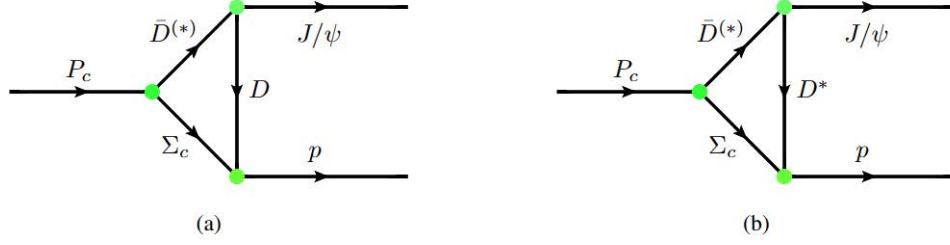


FIG. 14. Triangle diagrams for the decays of $P_c \rightarrow J/\psi p$.

assuming the three pentaquark states as $\bar{D}^{(*)}\Sigma_c$ molecules, we constructed the triangle diagrams connecting the $\bar{D}^{(*)}\Sigma_c$ channels to the $J/\psi p$ channels by exchanging the $D^{(*)}$ mesons as shown in Fig. 14. With reasonable parameters, we can reproduce the widths of $P_c \rightarrow J/\psi p$. Similarly, Lin et al. systematically investigated the decays of the $\bar{D}^{(*)}\Sigma_c^{(*)}$ molecules [545], which considered more partial decay modes of the $\bar{D}^{(*)}\Sigma_c^{(*)}$ molecules. The latter work pointed out that the decays into the $\bar{D}^*\Lambda_c$ channel are the most important. We note that the meson exchange theory has been tested for light meson exchanges but remains to be verified for heavy meson exchanges, especially when both heavy and light mesons can be exchanged. The meson exchange theory dictates that charmed mesons are responsible for short-range interactions of 0.1 fm. However, charmed meson exchanges can not adequately describe such interactions because one gluon exchange may play a role. In Ref. [157], the strength of the short-range potential provided by the one gluon exchange is much stronger than that provided by the heavy meson exchanges. The origin of such short-range interactions remains unclear.

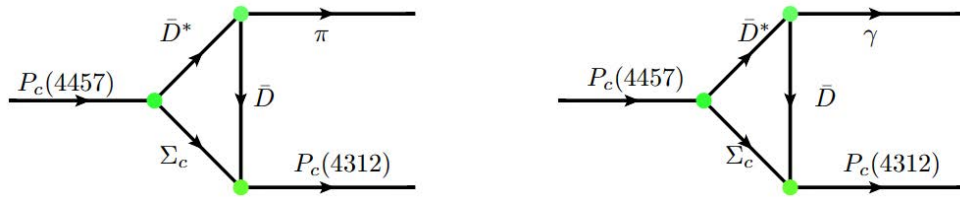


FIG. 15. Triangle diagram of pionic and radiative decays of $P_c(4457)$ to $P_c(4312)$ with the spin of $P_c(4457)$ being either 1/2 or 3/2.

Pionic or radiative decays can relate members of the multiplet of hadronic molecules. We further investigated the radiative decays of the pentaquark molecules with the triangle diagrams. According to the LHCb measurements [719], the mass splitting between $P_c(4440)$ and $P_c(4312)$ is 128 MeV, which is less than the pion mass. Therefore, the decay of $P_c(4440) \rightarrow P_c(4312)\pi$ is forbidden due to phase space. The mass splitting between $P_c(4457)$ and $P_c(4312)$ is 145 MeV, accordingly the $P_c(4457) \rightarrow P_c(4312)\pi$ decay

is allowed. Moreover, the radiative decays of $P_c(4457) \rightarrow P_c(4312)\gamma$ and $P_c(4440) \rightarrow P_c(4312)\gamma$ are both allowed as shown in Fig. 15. The widths of the pionic decays of $P_c(4457)$ to $P_c(4312)$ are estimated to be the order of hundreds of keV, while those of radiative decays are about 1 keV. The ratio of the former to the latter agrees with the ratio of the pionic decay of $D^* \rightarrow D\pi$ to that of the radiative decay, indicating that such a ratio can help verify the molecular nature of pentaquark states. In the triangle diagram mechanism, all the couplings are well constrained by experimental data, which largely reduces the uncertainties of the results. Therefore, such results are reliable. In addition to the above decays, the $\bar{D}^*\Sigma_c$ molecules can decay into $\bar{D}^*\Sigma_c$ and $\bar{D}\Sigma_c$ molecules together with a π and a photon [720]. For the radiative decays of $P_c(4457) \rightarrow P_c(4312)$, our results are consistent with the quark model results [721].

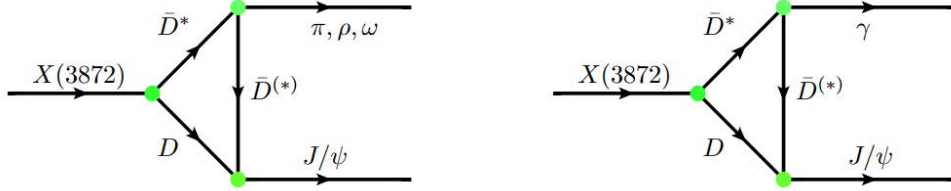


FIG. 16. Triangle diagram of pionic and radiative decays of $X(3872)$ to charmonium states.

With the triangle mechanism, the decays of $X(3872)$ as a \bar{D}^*D molecule have been extensively studied. Refs. [440, 722] investigated the pionic and radiative decays of $X(3872)$ to J/ψ and $\psi(2S)$ as shown in Fig. 16, where based on the triangle diagrams some more complex processes are explored. Ref. [141] constructed the triangle mechanism to study the decays of $X(3872) \rightarrow J/\psi\pi\pi$ and $X(3872) \rightarrow J/\psi\pi\pi\pi$ and $\pi^0\chi_{cJ}$, suggesting that the isospin breaking effect can be attributed to the isospin breaking and the loop functions of the \bar{D}^*D neutral and charged components, where the secondary decays of $\rho \rightarrow \pi\pi$ and $\omega \rightarrow \pi\pi\pi$ are considered in the triangle diagrams. However, the two-body decays of the $J^{PC} = 1^{++}$ \bar{D}^*D molecule can not contain open-charm mesons, similar to the decay of T_{cc} . Very recently, Wang et al. estimated the widths of $X(3872)$ decaying into a pair of light mesons, showing that these branching ratios are around several percent of its total width [723]. For the $X_2(4013)$ as the HQSS partner of $X(3872)$, the strong [724] and radiative [725] decays have been investigated via the triangle diagrams, where the former decays into $\bar{D}D$ and \bar{D}^*D , and the latter radiatively decays into charmonium states. Because the meson exchange theory does not work for the inelastic potentials $\bar{D}^{(*)}D^{(*)} \rightarrow J/\psi(\chi_{c1})\rho(\omega)$, it is difficult to construct a coupled-channel framework to study the two-body decays of $X(3872)$ and $X_2(4013)$. In principle, the strong decays of $J^{PC} = 0^{++}$ $\bar{D}D$, $J^{PC} = 1^{+-}$ \bar{D}^*D^* , and $J^{PC} = 0^{++}$ \bar{D}^*D^* bound states as the HQSS partners of the $J^{PC} = 1^{++}$ \bar{D}^*D state can proceed via the triangle diagrams as well, which have

been investigated with the vector-vector interaction within the local hidden gauge framework [159]. The radiative and pionic decays between the multiplet members of $\bar{D}^{(*)}D^{(*)}$ hadronic molecules are naturally expected [726].

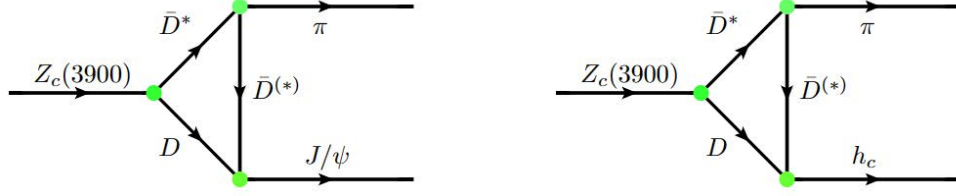


FIG. 17. Triangle diagram for the pionic decay of $Z_c(3900)$ to the charmonium states.

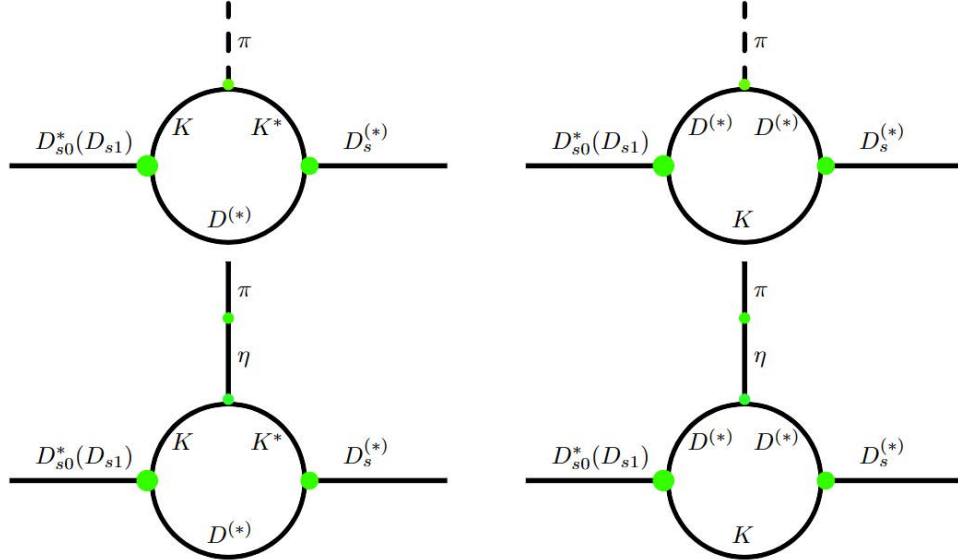


FIG. 18. Decays of $D_{s0}^* \rightarrow D_s \pi$ and $D_{s1}^* \rightarrow D_s^* \pi$ studies in Refs. [385, 386].

Next, we discuss the decays of the isovector doublet of \bar{D}^*D and \bar{D}^*D^* molecules. Employing the triangle diagram shown in Fig. 17, Refs. [727, 728] estimated the decay width of $Z_c(3900)$ into a charmonium state plus a π , where the $Z_c(3900)$ couplings to the \bar{D}^*D is estimated by saturating the width of $Z_c(3900)$. We note that the \bar{D}^*D channel contributes to both the mass and width of $Z_c(3900)$, while the approach of saturating the width does not consider the contribution of the real part of the potential, which needs further discussions. Similar decay modes of $Z_c(4020)$, regarded as a \bar{D}^*D^* molecule and the HQSS partner of $Z_c(3900)$, were investigated through the triangle diagram [727, 729]. In the molecular picture, the radiative decays of $Z_c(4020)$ and $Z_c(3900)$ were investigated using the triangle diagram mechanism [730, 731].

Using the same approach, the decays of the SU(3)-flavor partner of $Z_c(3900)$, e.g., $Z_{cs}(3985)$, have been studied [732].

The dominant decays of $D_{s0}^* \rightarrow D_s \pi$ and $D_{s1} \rightarrow D_s^* \pi$ break the isospin symmetry. In Refs. [385, 386], these decays proceed via the diagrams shown in Fig. 18, named the “Direct” diagrams and the “ $\pi^0 - \eta$ mixing” diagrams, and their results indicate that the former decay modes play the dominant role. The widths of the partial decays $D_{s0}^* \rightarrow D_s \pi$ and $D_{s1} \rightarrow D_s^* \pi$ in this picture are estimated to be 80 keV and $50 \sim 80$ keV, respectively, consistent with the results of the EFT approach [733]. In Ref. [734], the radiative and pionic decays of the D_{s1} to D_{s0}^* were investigated via the triangle diagrams.

D. Production mechanisms

Studies of the production mechanisms of exotic states can help reveal their internal structure and provide useful guidance to experimental searches for their partners. Up to now, exotic states have often been discovered in inclusive and exclusive processes. The well-known exotic states, such as $D_{s0}^*(2317)$ and T_{cc} , are discovered in the inclusive process. The $X(3872)$ and P_c states are discovered in the exclusive process. The inclusive process’s intermediate processes are unclear, but they have been studied in statistical models by simulating the production of hadronic molecules. For the exclusive process, the exotic states with the charm quark constituent are produced in the b -flavored hadrons via the decay $b \rightarrow c\bar{c}s$ at the quark level as shown in Table XXIV, which can be studied in the effective Lagrangian approach. In this review, we mainly focus on the exclusive processes.

From the perspective of the interactions, the production process of an exotic state in b -flavored hadron can be factorized into short-distance and long-distance interactions, corresponding to weak and strong interactions. The weak interaction is encoded in the non-leptonic decays that can be described by the naive factorization approach, which generally includes the T and C diagrams of the topological diagrammatic approach [736–738]. The strong interaction is encoded in the final-state interactions described by the meson exchange theory. With these interactions determined, the triangle diagram mechanism can account for the production of exotic states in heavy hadron decays. Such a mechanism has been widely applied to study the branching fractions and CP violations of charmed hadrons [229, 739, 740]. This mechanism predicted large branching fractions for the weak decays of doubly charmed baryons, taking into account the final-state interactions, which provide valuable guidance for the experimental discovery of the Ξ_{cc} [741]. Being applied to the production of multiplets of hadronic molecules, it will not only check the molecular nature of these states but also provide guidance to search for its partners experimentally in a similar process.

TABLE XXIV. Productions of exotic states in b -flavored hadron decays [735].

Decay modes	Branching fractions
$B^+ \rightarrow D_{s0}^*(2317)^+ \bar{D}^0$	$0.83_{-0.15}^{+0.25} \times 10^{-3}$
$B^+ \rightarrow D_{s0}^*(2317)^+ \bar{D}^{*0}$	$(0.90 \pm 0.68) \times 10^{-3}$
$B^+ \rightarrow D_{s1}(2460)^+ \bar{D}^0$	$(3.28 \pm 0.78) \times 10^{-3}$
$B^+ \rightarrow D_{s1}(2460)^+ \bar{D}^{*0}$	$(10.5 \pm 2.4) \times 10^{-3}$
$B^+ \rightarrow X(3872)K^+$	$2.06_{-0.49}^{+0.61} \times 10^{-4}$
$B^+ \rightarrow X(3872)K^{*+}$	$1.2_{-2.7}^{+2.9} \times 10^{-4}$
$B^+ \rightarrow X(3872)K^0\pi^+$	$3.0_{-1.1}^{+1.6} \times 10^{-4}$
$B_s^0 \rightarrow X(3872)\phi$	$(1.1 \pm 0.4) \times 10^{-4}$
$B^+ \rightarrow X(3915)K^+$	$(0.4 \pm 1.6) \times 10^{-4}$
$B^+ \rightarrow (Y(3940) \rightarrow J/\psi\omega)K^+$	$3.0_{-0.67}^{+0.86} \times 10^{-5}$
$B^+ \rightarrow (Y(4260) \rightarrow J/\psi\pi^+\pi^-)K^+$	$(2.00 \pm 0.73) \times 10^{-5}$
$B^+ \rightarrow (\chi_{c1}(4140) \rightarrow J/\psi\phi)K^+$	$0.66_{-0.27}^{+0.37} \times 10^{-5}$
$B^+ \rightarrow (\chi_{c1}(4274) \rightarrow J/\psi\phi)K^+$	$0.31_{-0.16}^{+0.24} \times 10^{-5}$
$\Lambda_b^0 \rightarrow P_c(4380)^+\pi^-$	$0.162_{-0.070}^{+0.095} \times 10^{-4}$
$\Lambda_b^0 \rightarrow P_c(4380)^+K^-$	$3.2_{-1.8}^{+7.4} \times 10^{-4}$
$\Lambda_b^0 \rightarrow P_c(4457)^+\pi^-$	$0.051_{-0.025}^{+0.032} \times 10^{-4}$
$\Lambda_b^0 \rightarrow P_c(4457)^+K^-$	$1.5_{-0.9}^{+2.6} \times 10^{-4}$
$\Lambda_b^0 \rightarrow Z_c(4200)^-p$	$0.24_{-0.15}^{+0.14} \times 10^{-4}$

1. Production rates of DK and D^*K molecules

At first, we start with the productions of $D_{s0}^*(2317)$ and $D_{s1}(2460)$ in B decays. Within the molecular picture, the productions of $D_{s0}^*(2317)$ and $D_{s1}(2460)$ in b -flavored hadron decays have been discussed [388, 638, 742]. Assuming the production mechanism of $D_{s0}^*(2317)$ and $D_{s1}(2460)$ in B decays are similar to those of ground-state mesons $D_s^{(*)}$ in B decays, the decays of $B \rightarrow \bar{D}^{(*)}D_{s0}^*(D_{s1})$ and $B \rightarrow \bar{D}^{(*)}D_s^{(*)}$ proceed via the W -boson external emission at the quark level, which can be described by the naive factorization approach [391, 743–747]. The decay constants of $D_{s0}^*(2317)$ and $D_{s1}(2460)$ reflect their internal structure, which are estimated to be $f_{D_{s0}^*} = 58.74$ MeV and $f_{D_{s1}} = 133.76$ MeV in the molecular picture. In particular, once the decay constants of $D_{s0}^*(2317)$ and $D_{s1}(2460)$ are obtained [638], their

TABLE XXV. Branching fractions of (10^{-3}) of $D_{s0}^*(2317)$ and $D_{s1}(2460)$ in b -flavored hadron decays.

Decay modes	Branching fractions	Decay modes	Branching fractions
$B^+ \rightarrow \bar{D}^0 D_{s0}^{*+}(2317)$	0.48	$B_s^0 \rightarrow D_s D_{s0}^*(2317)$	0.47
$B^+ \rightarrow \bar{D}^{*0} D_{s0}(2317)$	0.39	$B_s^0 \rightarrow D_s^* D_{s0}(2317)$	0.27
$B^+ \rightarrow \bar{D}^0 D_{s1}(2460)$	1.39	$B_s^0 \rightarrow D_s D_{s1}(2460)$	1.18
$B^+ \rightarrow \bar{D}^{*0} D_{s1}(2460)$	4.36	$B_s^0 \rightarrow D_s^* D_{s1}(2460)$	4.11
$\Lambda_b \rightarrow \Lambda_c D_{s0}^*(2317)$	0.70	$\Xi_b \rightarrow \Xi_c D_{s0}^*(2317)$	0.58
$\Lambda_b \rightarrow \Lambda_c D_{s1}(2460)$	4.34	$\Xi_b \rightarrow \Xi_c D_{s1}(2460)$	4.29

production rates in B_s , Λ_b , and Ξ_b decays can be straightforwardly calculated using the naive factorization approach as shown in Table XXV. One can see that the production rates of $D_{s0}^*(2317)$ and $D_{s1}(2460)$ in b -flavored baryon decays are larger than those in b -flavored meson decays, which imply that these exotic states are likely to be detected in heavy baryons in the future. The obtained branching fractions of the decays $B \rightarrow \bar{D}^{(*)} D_{s0}^*(D_{s1})$ are smaller than the experimental data, which indicate that $D_{s0}^*(2317)$ and $D_{s1}(2460)$ can contain other components other than the DK and D^* components, such as the bare $c\bar{s}$ components.

TABLE XXVI. Decay constants of $D_{s0}^*(2317)$ and $D_{s1}(2460)$ as excited $c\bar{s}$ states (in units of MeV).

Decay Constants	$f_{D_{s0}^*}$	$f_{D_{s1}}$
QCD sum rule [748]	333 ± 20	345 ± 17
Quark model [390]	110	233
Salpeter method [749]	112	219
covariant light-front quark model [750]	$74.4^{+10.4}_{-10.6}$	159^{+36}_{-32}
Lattice QCD [116]	114(2)(0)(+5)(10)	194(3)(4)(+5)(10)

According to the recent study [46], the DK and D^*K molecular components account for 70% and 50% of the total wave functions of $D_{s0}^*(2317)$ and $D_{s1}(2460)$. As a result, we have embodied other components, such as the $c\bar{s}$ configuration, into the total wave functions. With the experimental branching fractions of the decays of $B^+ \rightarrow \bar{D}^0 D_{s0}^{*+}(2317)$ and $B^+ \rightarrow \bar{D}^0 D_{s1}^{*+}(2460)$, we can obtain the decay constants $f_{D_{s0}^*} = 75.83$ MeV and $f_{D_{s1}} = 199.75$ MeV. With the values of $f_{D_{s0}^*}^M = 58.74$ MeV and $f_{D_{s1}}^M = 133.76$ MeV in the molecular picture and their molecular components in the total wave function, i.e., 70% and 50%, one can obtain the decay constants $f_{D_{s0}^*}^E = 115.71$ MeV and $f_{D_{s1}}^E = 265.74$ MeV, which correspond to the D_{s0}^* and D_{s1} as pure excited $c\bar{s}$ states. The estimated values for the decay constants of $D_{s0}^*(2317)$ and $D_{s1}(2460)$ are

consistent with other approaches shown in Table XXVI, which indicates that the $D_{s0}^*(2317)$ and $D_{s1}(2460)$ are composed of a $D^{(*)}K$ component and a $c\bar{s}$ component from the perspective of the branching fractions of the weak decays.

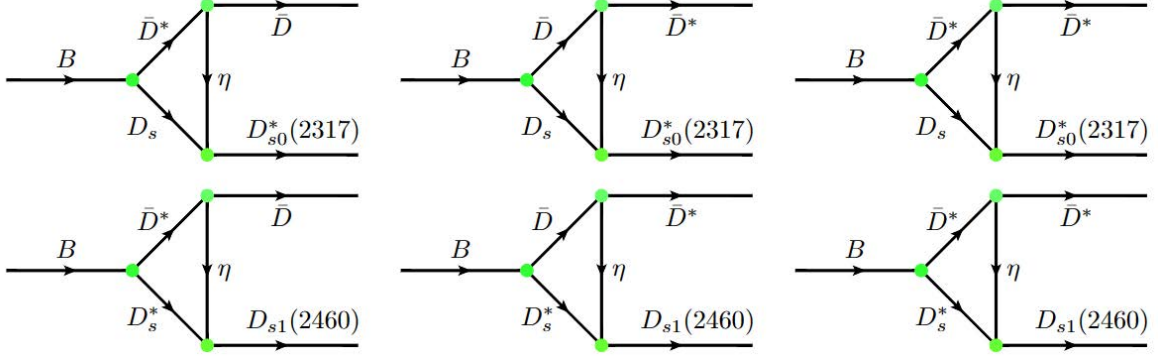


FIG. 19. Triangle diagrams accounting for the decays of $B \rightarrow \bar{D}^{(*)} D_{s0}^*(2317)$ and $B \rightarrow \bar{D}^{(*)} D_{s1}(2460)$.

In addition to the naive factorization approach, one can adopt the triangle diagram mechanism to investigate the above decays, where the B meson firstly weakly decays into $D_s^{(*)}$ and $\bar{D}^{(*)}$, then the latter scatter into $\bar{D}^{(*)}$ and η , and finally the $D_s^{(*)}\eta$ interactions dynamically generate the $D_{s0}^*(2317)$ and $D_{s1}(2460)$ as shown in Fig. 19. We should note that other triangle diagrams with weak decays $B \rightarrow J/\psi(\eta_c)K$ were also considered in the study [742], which actually leads to double counting since the decays $B \rightarrow \bar{D}^{(*)} D_s^{(*)}$ contribute to the decays $B \rightarrow J/\psi(\eta_c)K$. These Feynman diagrams can be calculated using the effective Lagrangian approach. In Ref. [742], the effective Wilson coefficients are determined by reproducing the branching fractions of the weak decays, which are a bit smaller than the value of $a_1 = 1.07$ obtained at the charm quark scale [739, 751]. In Table XXVII, we present the branching fractions of the weak decays $B \rightarrow \bar{D}^{(*)} D_{s0}^*(2317)$ and $B \rightarrow \bar{D}^{(*)} D_{s1}(2460)$ obtained using the triangle diagram mechanism, in comparison with those obtained in the naive factorization approach [638]. One can see that the results are of the same order of magnitude, but the difference can be as large as a factor of two.

TABLE XXVII. Branching fractions (10^{-3}) of $B \rightarrow \bar{D}^{(*)} D_{s0}^*(2317)$ and $B \rightarrow \bar{D}^{(*)} D_{s1}(2460)$.

decay modes	Triangle Mechanism [742]	Naive Factorization [638]
$B^+ \rightarrow \bar{D}^0 D_{s0}^{*+}(2317)$	0.55	0.48
$B^+ \rightarrow \bar{D}^{*0} D_{s0}^{*+}(2317)$	0.59	0.39
$B^+ \rightarrow \bar{D}^0 D_{s1}^+(2460)$	0.35	1.39
$B^+ \rightarrow \bar{D}^{*0} D_{s1}^+(2460)$	2.12	4.36

2. Production rates of \bar{D}^*D and \bar{D}^*D^* molecules

In this section, we focus on the production mechanism of the $\bar{D}^*D^{(*)}$ molecules. In Ref. [448], Guo et al. proposed to produce $X(3872)$ as a $\bar{D}D^*$ molecule via the radiative decay of the excited vector charmonium states. Later, using a similar approach, they investigated the production rates of \bar{D}^*D^* molecules (the HQSS partners of \bar{D}^*D molecules) [752]. In addition, Dong et al. employed the effective Lagrangian approach to estimate the decay widths of $Y(4260) \rightarrow X(3872)\gamma$ in the molecular picture [478]. Braaten et al. analysed the mass distribution of $X(3872)\gamma$ in the process of $e^+e^- \rightarrow X(3872)\gamma$ and found a narrow peak around 4.23 GeV due to the triangle singularity [753, 754], where $X(3872)$ is treated as a weakly $\bar{D}^{*0}D^0$ bound state and the narrow peak structure around 4.23 GeV possibly corresponds to the $Y(4220)$ observed by the BESIII Collaboration [333]. The BESIII Collaboration observed the radiative transition process $Y(4260) \rightarrow X(3872)\gamma$ in the process $e^+e^- \rightarrow X(3872)\gamma$ [325]. Such studies show that the isoscalar $\bar{D}D^{(*)}$ molecules can be produced in e^+e^- collisions.

The $X(3872)$ can be produced in B decays. In Refs. [207, 755], Braaten et al. proposed a mechanism to estimate the branching fractions of $B \rightarrow X(3872)K$, where the B meson first weakly decays into \bar{D}^*DK , and then $X(3872)$ is dynamically generated via the \bar{D}^*D rescattering. Recently, they calculated the production rate of $X(3872)$ in the decay of $B \rightarrow X(3872)\pi K$ via the triangle diagram, where the B meson first weakly decays into \bar{D}^*D^*K , then \bar{D}^* or D^* meson decays into $\bar{D}\pi$ or $D\pi$, and finally $X(3872)$ is dynamically generated in the \bar{D}^*D channel [756]. Moreover, they obtained a narrow structure near the mass threshold of \bar{D}^*D^* by analyzing the $X(3872)\pi$ mass distribution of the decay of $B \rightarrow X(3872)\pi K$ [756], which was assigned as a triangle singularity in other studies [757, 758]. Nevertheless, identifying $X(3872)$ as a pure $c\bar{c}$ charmonium, Meng et al. calculated the decay of $B \rightarrow X(3872)K$ in the QCD factorization approach. They claimed that the branching ratio of $Br(B^+ \rightarrow X(3872)K^+)$ is equal to that of $Br(B^0 \rightarrow X(3872)K^0)$ [446]. However, the Belle Collaboration estimated the ratio to be [404]:

$$\frac{Br(B^0 \rightarrow X(3872)K^0)}{Br(B^+ \rightarrow X(3872)K^+)} = 0.50 \pm 0.14 \pm 0.04, \quad (16)$$

which shows large isospin breaking and can be understood in the molecular picture [447, 759].

In Ref. [760], Chen et al. adopted the compositeness theorem proposed by Weinberg in effective field theories to study the near-mass-threshold lineshape of the \bar{D}^0D^{*0} mass distribution of $B \rightarrow \bar{D}^0D^{*0}K$ using the experimental data, where the short-range and long-range production mechanism of $X(3872)$ are accounted for by the short-distance vertex of the B decay and the \bar{D}^0D^{*0} rescattering into the $X(3872)$ via the weak decay $B \rightarrow \bar{D}^0D^{*0}K$. The non-vanishing value of $Z = 0.19$ indicated that $X(3872)$ contains a sizable molecular component. In Ref. [761], Wang et al. investigated the short-distance $c\bar{c}$ component of

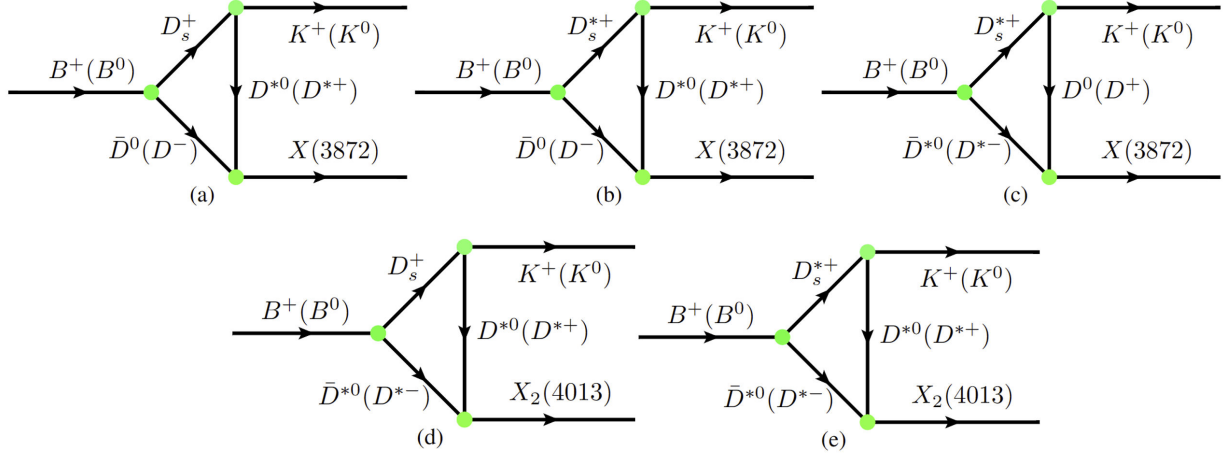


FIG. 20. Triangle diagrams accounting for (a-c) $B^+(B^0) \rightarrow D_s^{(*)+} \bar{D}^{(*)0}(D^{(*)+}) \rightarrow X(3872)K^+(K^0)$ and (d-e) $B^+(B^0) \rightarrow D_s^{(*)+} \bar{D}^{(*)0}(D^{(*)+}) \rightarrow X_2(4013)K^+(K^0)$.

$X(3872)$ in the semileptonic and nonleptonic B_c decays.

The $X(3872)$ production in heavy ion collisions has also been studied. In Refs. [238, 762], the authors suggested measuring the productions of exotic states such as $X(3872)$ in relativistic heavy ion collisions since the yields of exotic states estimated in the coalescence model are tied to their internal structure. In Ref. [243], Zhang et al., assuming $X(3872)$ as either a molecule or a tetraquark state, computed the yield of $X(3872)$ in Pb-Pb collisions and claimed that the obtained physical observables with two order-of-magnitude difference in two different pictures can help reveal the internal structure of $X(3872)$, which are pretty different from the results of Ref. [763]. Recently, the CMS Collaboration reported the first evidence of $X(3872)$ in relativistic heavy ion collisions and pointed out that the obtained ratio between the $X(3872)$ and $\phi(2S)$ yields helps clarify the nature of $X(3872)$ [400]. In addition, Kamiya et al. studied the correlation functions of \bar{D}^*D in heavy ion collisions to investigate the nature of $X(3872)$ [285].

In comparison with the $X(3872)$, the $Z_c(3900)$ does not have many production modes. The D0 Collaboration observed the signal of $Z_c(3900)$ in the $J/\psi\pi^\pm$ mass distribution in the semi-inclusive decays of b -flavored hadrons [494] except that it is produced in electron-positron collisions. Following the discovery in the semi-inclusive decays of b -flavored hadrons, Wu et al. investigated the production of $Z_c(3900)$ in the B_c decay, which can be accessed at large colliders [764]. Based on the discovery of $Z_c(3900)$ via the $Y(4260)$, many works described the lineshape of $J/\psi\pi$ and $\pi\pi$ mass distribution and reproduced the $Z_c(3900)$ peak with the assumption that $Y(4260)$ is strongly coupled to a pair of charmed mesons [475, 477, 525], where $Z_c(3900)$ is regarded as a kinetic effect rather than a genuine state. However, the production of $Z_c(3900)$ in B decays remains unobserved. The Belle Collaboration observed no signal of $Z_c(3900)$ in the decay

TABLE XXVIII. Branching fractions (10^{-4}) of $B^{+(0)} \rightarrow X(3872)/X_2(4013)K^{+(0)}$ and $B^{+(0)} \rightarrow Z_c(3900)/Z_c(4020)K^{+(0)}$ and ratios $\mathcal{B}(B^0 \rightarrow)/\mathcal{B}(B^+ \rightarrow)$.

Decay modes	Our predictions	Exp. [766]	Ratio	Exp. data [766]
$B^+ \rightarrow X(3872)K^+$	1.49 ± 0.62	2.1 ± 0.7	0.62 ± 0.13	0.52 ± 0.26
$B^0 \rightarrow X(3872)K^0$	0.93 ± 0.39	1.1 ± 0.4		
$B^+ \rightarrow X_2(4013)K^+$	0.23 ± 0.08	—	0.75 ± 0.16	—
$B^0 \rightarrow X_2(4013)K^0$	0.17 ± 0.06	—		
$B^+ \rightarrow Z_c(3900)K^+$	0.21 ± 0.11	$< 4.7 \times 10^{-5}$	0.63 ± 0.29	—
$B^0 \rightarrow Z_c(3900)K^0$	0.13 ± 0.07	—		
$B^+ \rightarrow Z_c(4020)K^+$	0.0095 ± 0.0033	$< 1.6 \times 10^{-5}$	1.05 ± 0.14	—
$B^0 \rightarrow Z_c(4020)K^0$	0.0100 ± 0.0034	—		

$B \rightarrow J/\psi\pi K$ [491] or in the decay $B \rightarrow \bar{D}^* DK$ [328].

Recently, we systematically studied the production rates of $\bar{D}^* D$ and $\bar{D}^* D^*$ molecules in B decays in a unified framework. The production mechanism of $\bar{D}^* D$ and $\bar{D}^* D^*$ molecules via the triangle diagrams are shown in Fig. 20. First, the B meson weakly decays into a pair of charmed mesons $D_s^{(*)}$ plus $\bar{D}^{(*)}$, which proceed via the W -emission mechanism at the quark level. The strength of the W -emission mechanism is usually the largest [233, 234, 765]. Then, the charmed-strange mesons $D_s^{(*)}$ scatter into the charmed mesons $D^{(*)}$ and a kaon. Finally, the $\bar{D} D^*$ and $\bar{D}^* D^*$ molecules are dynamically generated via the final-state interactions. The isoscalar and isovector $\bar{D} D^*$ molecules refer to $X(3872)$ and $Z_c(3900)$, and isoscalar and isovector $\bar{D}^* D^*$ molecules to $X_2(4013)$ and $Z_c(4020)$. The effective Lagrangian approach is adopted to calculate the production rates.

Our results show that the branching ratios of the decays $B^+ \rightarrow X(3872)K^+$ and $B^0 \rightarrow X(3872)K^0$ are $(0.63 \sim 2.39) \times 10^{-4}$ and $(0.42 \sim 1.56) \times 10^{-4}$, consistent with the experimental data. The branching ratios of $B^+ \rightarrow Z_c(3900)K^+$ and $B^0 \rightarrow Z_c(3900)K^0$ are of the order of 10^{-5} , smaller than the experimental upper limits. Moreover, we predicted the branching ratios of the decays $B \rightarrow X_2(4013)K$ and $B \rightarrow Z_c(4020)K$ to be the order of 10^{-5} and 10^{-6} . We obtained a hierarchy for the production rates of all $\bar{D}^* D$ and $\bar{D}^* D^*$ molecules in B decays, which can help clarify the nature of XZ states in these energy regions.

We emphasize that the ratios of branching fractions are more certain than the absolute branching fractions in our model. We obtained the ratio $\mathcal{B}[B^+ \rightarrow X(3872)K^+]/\mathcal{B}[B^0 \rightarrow X(3872)K^0] = 0.66$, consistent with the experimental data. Our results show that the large isospin-breaking effect is attributed to the isospin breaking of the $\bar{D}^* D$ neutral and charged components. Considering HQSS, we predict the ratio

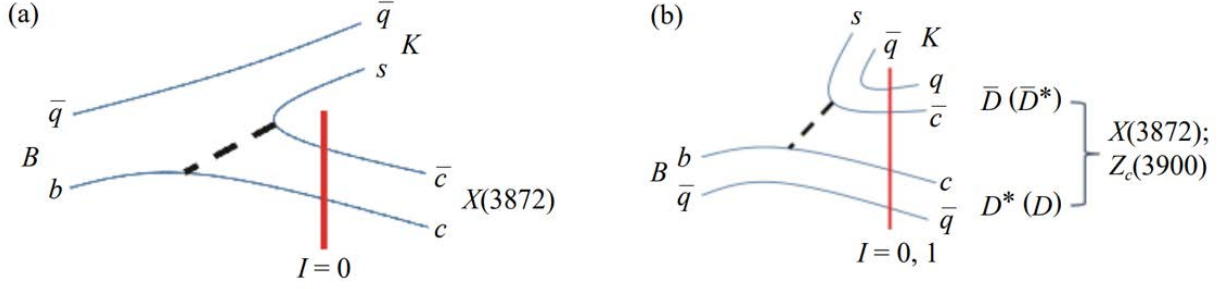


FIG. 21. Short-distance component of $X(3872)$ allows its production directly via a $c\bar{c}$ configuration in (a), while $X(3872)$ and $Z_c(3900)$ can both be produced via the long-distance $\bar{D}^* D$ component.

TABLE XXIX. Ratios of the couplings in particle basis to the couplings in isospin basis.

Molecules	$D^{*+} D^-$	$D^+ D^{*-}$	$D^{*0} \bar{D}^0$	$D^0 \bar{D}^{*0}$
$X(3872)$	1/2	-1/2	1/2	-1/2
$Z_c(3900)$	1/2	1/2	-1/2	-1/2
Molecules	$D^{*+} D^{*-}$	$D^{*0} \bar{D}^{*0}$		
$X_2(4013)$	$1/\sqrt{2}$	$1/\sqrt{2}$		
$Z_c(4020)$	$1/\sqrt{2}$	$-1/\sqrt{2}$		

$\mathcal{B}[B^+ \rightarrow X_2(4013)K^+]/\mathcal{B}[B^0 \rightarrow X_2(4013)K^0] = 0.35$, which shows larger isospin breaking effects. In addition, our results show that the branching fractions of $\mathcal{B}[B \rightarrow Z_c(3900)K]$ are smaller than those of $\mathcal{B}[B \rightarrow X(3872)K]$ by one order of magnitude, which provides a natural explanation why $Z_c(3900)$ has not been observed in B decays. We note that only the amplitude of Fig. 20 (a) and that of Fig. 20 (c) contribute to the decays of the B meson into the $\bar{D}^* D$ molecules, while the contribution of Fig. 20 (b) is accidentally small. The signs of the amplitude of Fig. 20 (a) and that of Fig. 20 (c) depend on the relative sign between the charged and neutral components in the wave functions of the $\bar{D}^* D$ molecules. From Table XXIX, one can see that the sign is opposite for the isoscalar molecules but the same for the isovector molecules. As the two amplitudes for the isoscalar molecules add constructively, but those for the isovector molecules add destructively, the $Z_c(3900)$ production rates in B decays are lower than those of $X(3872)$ in B decays. We note that Ref. [767] proposed a different mechanism to explain why the $Z_c(3900)$ production rates in B decays are lower than those of $X(3872)$. As shown in Fig. 21, the $Z_c(3900)$ containing the $\bar{D}^* D$ component can not be produced directly in the short-distance process but can be produced in the long-distance process, while $X(3872)$ containing the $c\bar{c}$ component and $\bar{D}^* D$ component can be produced via both the

short-distance and long-distance processes. Therefore, the $X(3872)$ can be observed, but $Z_c(3900)$ can not in high-energy productions.

We only considered the contribution of the $\bar{D}^* D^{(*)}$ channel to the XZ states. However, other channels, such as $\bar{D}_s D_s$, $\bar{D}^* D^*$, and $\bar{D}_s^* D_s^*$, may play a role in forming the $X(3872)$ [139, 688]. Moreover, the $X(3872)$ may contain a $c\bar{c}$ component [120]. With only the $\bar{D}^* D$ contribution, we can well describe the production rates of $X(3872)$ in B decays, which further supports that $X(3872)$ contains a sizable $\bar{D}^* D$ molecular component. Our predictions for the production rates of the other $\bar{D}^* D^{(*)}$ molecules in B decays are crucial to verify the molecular nature of $Z_c(3900)$, $X_2(4013)$, and $Z_c(4020)$.

TABLE XXX. Branching fractions of $B \rightarrow X_{s\bar{s}/q\bar{q}}/X(3960)K^+$ where $X_{s\bar{s}/q\bar{q}}$ is a bound state of $D_s^+ D_s^-$ or $\bar{D}D$.

Decay modes	Our results	Exp [401]
$B^+ \rightarrow X_{s\bar{s}} K^+$	$(2.1 \sim 17.0) \times 10^{-4}$	$\text{Br}(B^+ \rightarrow \chi_{c0}(3915) K^+) < 2.8 \times 10^{-4}$
$B^+ \rightarrow (X_{q\bar{q}} \rightarrow \eta_c \eta) K^+$	$(0.9 \sim 6.7) \times 10^{-4}$	$\text{Br}(B^+ \rightarrow \eta_c \eta K^+) < 2.2 \times 10^{-4}$
$B^+ \rightarrow X(3960) K^+$	$< 2.4 \times 10^{-4}$	-

Similarly, another HQSS partner, e.g., the $\bar{D}D$ molecule, can also be produced in B decays, which proceed via the triangle diagram mechanism shown in Fig. 2 of Ref. [692]. Since the existence of the $\bar{D}D$ molecule still needs experimental verification, we show the branching fractions of the $\bar{D}D$ molecule in B decays as a function of the $\bar{D}D$ molecule mass. Our results show that its branching fraction is 10^{-4} , likely to be observed in current experiments. More precise data for B decays are helpful to verify the molecular nature of the $\bar{D}D$ molecule. Using the same framework, we calculated the branching fractions of the $\bar{D}_s D_s$ molecule as a bound state or a resonant state in B decays. The results are shown in Table XXX.

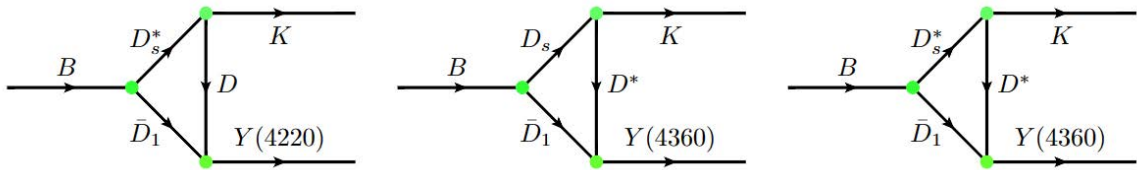


FIG. 22. Triangle diagrams accounting for $B \rightarrow KY(4220)$ and $B \rightarrow KY(4360)$.

Next, we will comment on the productions of Y states in B decays. As discussed above, the $Y(4220)$ and $Y(4360)$ can be viewed as a doublet of $\bar{D}D_1$ hadronic molecules. Similarly, one can study the productions of $\bar{D}D_1$ molecules in B decays via the triangle diagram mechanism as shown in Fig. 22. With the effective

Lagrangian approach, one can obtain the branching fractions of the decays $B \rightarrow Y(4220)K$ and $B \rightarrow Y(4360)K$, which we plan as a future work.

From our above analysis, we conclude that the charmonium-like states (also named the XYZ states) can be produced in B decays via the triangle diagrams because the XYZ states have strong couplings to pairs of charmed mesons.

3. Production rates of the pentaquark states

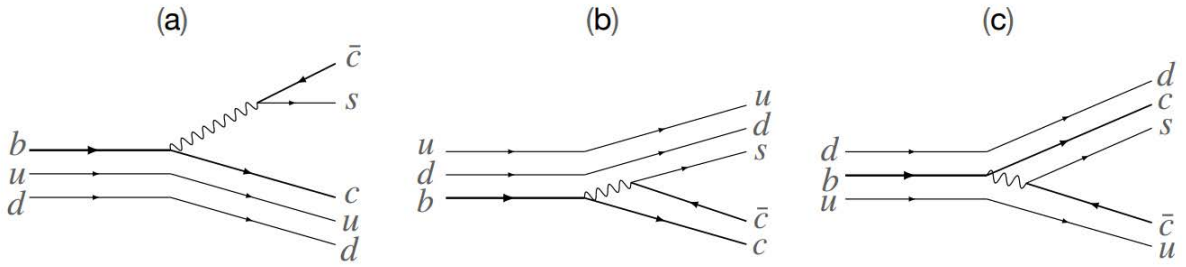


FIG. 23. Three possible topologies for the Cabibbo-favored weak decay $b \rightarrow c\bar{c}s$.

The pentaquark states were discovered in the Λ_b decay in pp collisions. To understand their production, it is necessary to understand the weak decays of Λ_b . At the quark level, there are three possible topologies for the Cabibbo-favored weak decay ($b \rightarrow c\bar{c}s$) as shown in Fig. 23, which correspond to the decays of $\Lambda_b \rightarrow \bar{D}_s\Lambda_c$, $\Lambda_b \rightarrow J/\psi\Lambda$, and $\Lambda_b \rightarrow \bar{D}\Xi_c$ at the hadron level. Such weak decays proceed via the external W-emission mechanism shown in Fig. 23 (a) and the internal W-conversion mechanism shown in Fig. 23 (b) and (c). The former is color-favored, while the latter is suppressed, indicating that topology (a) is responsible for the production of the pentaquark states. The branching fractions for topology (a) and (b) are $\mathcal{B}(\Lambda_b \rightarrow \bar{D}_s\Lambda_c) = 1.1 \pm 1.0\%$ and $\mathcal{B}(\Lambda_b \rightarrow J/\psi\Lambda) = (3.72 \pm 1.07) \times 10^{-4}$ [231]. The branching fraction for topology (c) is naively estimated to be $\mathcal{B}(\Lambda_b \rightarrow \bar{D}\Xi_c) = 2.5 \times 10^{-4}$ [655]. One can see that topologies (b) and (c) are smaller than topology (a) by a factor of 50. Based on these weak decay vertices, the pentaquark molecules can be generated via the triangle diagrams shown in Fig. 24. The topologies (b) and (c) can mix via topology (a), which can lead to double counting if they are considered simultaneously. Therefore, topology (a) is usually adopted to produce the pentaquark molecules.

In Ref. [228], Wu et al. constructed the triangle mechanism where the Λ_b baryon weakly decays into $D_s^{(*)}\Sigma_c$, then $D_s^{(*)}$ scatter into $\bar{D}^{(*)}K$, and finally the $\bar{D}^{(*)}\Sigma_c$ molecules are dynamically generated as shown in Fig. 25. We note that the Λ_b decay into $\Sigma_c^{(*)}$ is highly suppressed due to the fact the light quark

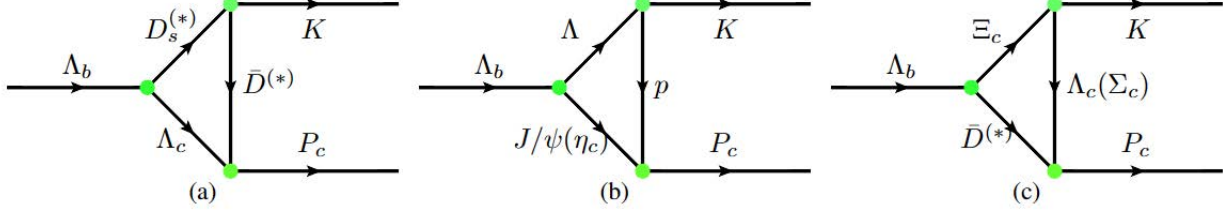


FIG. 24. The triangle diagram generating the pentaquark molecules based on the weak vertices of Fig. 23.

pair transition between a symmetric and antisymmetric spin-flavor configuration is forbidden [768, 769], which indicates that the production of pentaquark molecules is difficult (if not impossible) via the weak decays of $\Lambda_b \rightarrow D_s^{(*)} \Sigma_c$ ⁵. For the vertices of the molecules, the $\bar{D}^{(*)} \Sigma_c^{(*)}$, $\bar{D}^{(*)} \Lambda_c$, $J/\psi p$ and $\eta_c p$ channels contribute to the pentaquark molecules. However, the relative importance of each component remains uncertain, especially that of $\bar{D}^{(*)} \Lambda_c$. According to Ref. [186], the $\bar{D}^{(*)} \Lambda_c$, $\eta_c p$, and $J/\psi p$ channels are less important. However, Refs. [375, 709] claim that the $\bar{D}^{(*)} \Lambda_c$ contributions are sizable. If the weak vertices involve $\mathcal{B}(\Lambda_b \rightarrow D_s^{(*)} \Lambda_c)$, then the vertices generating the molecules are small. On the other hand, if one takes the dominant vertices to generate the molecules, one needs to introduce the unknown weak vertex $\mathcal{B}(\Lambda_b \rightarrow D_s^{(*)} \Sigma_c)$. Based on the obtained couplings of the pentaquark molecules to their components in Scenario A and Scenario B, we employ the effective Lagrangian approach to calculate the branching fractions of the decays $\Lambda_b \rightarrow P_c K$ as shown in Table XXXI. Since the pentaquark molecules are generated by the S -wave $\bar{D}^{(*)} \Lambda_c$ interactions, only the pentaquark molecules with $J^P = \frac{1}{2}^-$ and $J^P = \frac{3}{2}^-$ are produced in our model, which indicates that the production rate of the pentaquark molecule with $J^P = \frac{5}{2}^-$ in Λ_b decay is low.

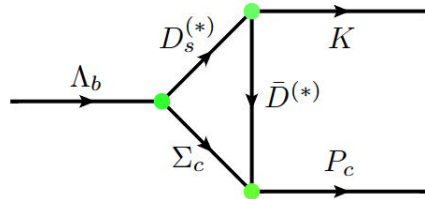


FIG. 25. Triangle diagram of $\Lambda_b \rightarrow D_s^{(*)} \Sigma_c \rightarrow P_c K$.

The products of the branching fractions $\mathcal{B}(\Lambda_b^0 \rightarrow P_\psi^{N+} K^-)$ and the branching fractions $\mathcal{B}(P_\psi^{N+} \rightarrow$

⁵ In Ref. [228], the $\Lambda_b \rightarrow \Sigma_c$ transition is assumed to be proportional to the $\Lambda_b \rightarrow \Lambda_c$ transition, characterized by an unknown parameter R . By reproducing the experimental production rates of the pentaquark molecules, R is found to be about 0.1.

TABLE XXXI. Branching fractions (10^{-6}) of Λ_b decay into a K meson and a hidden-charm pentaquark molecule in Scenario A and Scenario B.

Scenario		A					
Molecule		$P_{\psi 1}^N$	$P_{\psi 2}^N$	$P_{\psi 3}^N$	$P_{\psi 4}^N$	$P_{\psi 5}^N$	$P_{\psi 6}^N$
$\mathcal{B}(\Lambda_b \rightarrow P_{\psi}^N K)$		35.18	1.49	15.30	0.48	6.37	9.01
Scenario		B					
Molecule		$P_{\psi 1}^N$	$P_{\psi 2}^N$	$P_{\psi 3}^N$	$P_{\psi 4}^N$	$P_{\psi 5}^N$	$P_{\psi 6}^N$
$\mathcal{B}(\Lambda_b \rightarrow P_{\psi}^N K)$		98.88	2.27	27.23	5.21	21.69	7.43

$J/\psi p$) have been measured:

$$\begin{aligned}
\mathcal{B}(\Lambda_b^0 \rightarrow P_{\psi}^N (4312)^+ K^-) \cdot \mathcal{B}(P_{\psi}^N (4312)^+ \rightarrow J/\psi p) &= 0.96_{-0.39}^{+1.13} \times 10^{-6}, \\
\mathcal{B}(\Lambda_b^0 \rightarrow P_{\psi}^N (4440)^+ K^-) \cdot \mathcal{B}(P_{\psi}^N (4440)^+ \rightarrow J/\psi p) &= 3.55_{-1.24}^{+1.43} \times 10^{-6}, \\
\mathcal{B}(\Lambda_b^0 \rightarrow P_{\psi}^N (4457)^+ K^-) \cdot \mathcal{B}(P_{\psi}^N (4457)^+ \rightarrow J/\psi p) &= 1.70_{-0.71}^{+0.77} \times 10^{-6}.
\end{aligned} \tag{17}$$

To compare with the experiments, we have estimated the products $\mathcal{B}(\Lambda_b^0 \rightarrow P_{\psi}^{N+} K^-) \cdot \mathcal{B}(P_{\psi}^{N+} \rightarrow J/\psi p)$ in Scenario A and Scenario B by first estimating the branching fractions of the decays $P_c \rightarrow J/\psi p$. Since the main uncertainties of our results are from the couplings of the pentaquark molecules to the $\bar{D}^{(*)}\Lambda_c$ and $J/\psi p$, we have adopted the couplings determined by the ChUA to calculate these values [770], which actually correspond to our results of scenario A as shown in Table XXXII. Our results show that the production rate of $P_c(4457)$ in the Λ_b decay in Scenario A, the production rate of $P_c(4312)$ in Scenario B, and the production rate of $P_c(4440)$ in the ChUA, deviate much from the experimental data, which indicates that the production rates of $P_c(4312)$, $P_c(4440)$, and $P_c(4457)$ in the Λ_b decays can not be simultaneously described in the triangle diagram mechanism. Nevertheless, the production mechanism of these three pentaquark states via the triangle diagram can qualitatively reproduce the experimental data, which further corroborates the hadronic molecular picture of these pentaquark states.

These hidden-char pentaquark molecules are observed in the $J\psi p$ invariant mass distribution, and one can also expect to see them in the $\bar{D}^*\Lambda_c$ invariant mass distribution. As a byproduct, with the branching fractions of the decays $P_c \rightarrow \bar{D}^{(*)}\Lambda_c$ we predicted the products of $\mathcal{B}(\Lambda_b \rightarrow P_{\psi}^N K) \cdot \mathcal{B}(P_{\psi}^N \rightarrow \bar{D}^{(*)}\Lambda_c)$ in Scenario A and Scenario B. We can see that the branching fractions of the pentaquark molecules in the decays $\Lambda_b \rightarrow (P_{\psi}^N \rightarrow J/\psi p)K$ and $\Lambda_b \rightarrow (P_{\psi}^N \rightarrow \bar{D}^*\Lambda_c)K$ are similar except for $P_{\psi 2}^N$. The branching fraction $\mathcal{B}[\Lambda_b \rightarrow (P_{\psi 2}^N \rightarrow \bar{D}^*\Lambda_c)K]$ is smaller than the branching fraction $\mathcal{B}[\Lambda_b \rightarrow (P_{\psi 2}^N \rightarrow J/\psi p)K]$ by two orders of magnitude. We encourage experimental searches for these pentaquark states in the $\bar{D}^*\Lambda_c$

TABLE XXXII. Branching fractions (10^{-6}) of the decays $\Lambda_b \rightarrow (P_\psi^N \rightarrow J/\psi p)K$ in Scenario A and Scenario B.

Scenario		A					
Molecule		$P_{\psi 1}^N$	$P_{\psi 2}^N$	$P_{\psi 3}^N$	$P_{\psi 4}^N$	$P_{\psi 5}^N$	$P_{\psi 6}^N$
Ours		7.11	1.44	8.21	0.09	1.77	4.82
ChUA [770]		1.82	8.62	0.13	0.83	0.04	2.36
Exp		0.96	-	3.55	1.70	-	-

Scenario		B					
Molecule		$P_{\psi 1}^N$	$P_{\psi 2}^N$	$P_{\psi 3}^N$	$P_{\psi 4}^N$	$P_{\psi 5}^N$	$P_{\psi 6}^N$
Ours		18.24	2.22	6.06	1.79	3.83	2.76
ChUA [770]		-	-	-	-	-	-
Exp		0.96	-	1.70	3.55	-	-

invariant mass distributions of the Λ_b decays.

TABLE XXXIII. Branching fractions(10^{-6}) of the decays $\Lambda_b \rightarrow (P_\psi^N \rightarrow \bar{D}^* \Lambda_c)K$ in Scenario A and Scenario B.

Scenario		A					
Molecule		$P_{\psi 1}^N$	$P_{\psi 2}^N$	$P_{\psi 3}^N$	$P_{\psi 4}^N$	$P_{\psi 5}^N$	$P_{\psi 6}^N$
Ours		4.12	0.05	1.27	0.00	0.21	1.87

Scenario		B					
Molecule		$P_{\psi 1}^N$	$P_{\psi 2}^N$	$P_{\psi 3}^N$	$P_{\psi 4}^N$	$P_{\psi 5}^N$	$P_{\psi 6}^N$
Ours		26.41	0.05	8.42	2.71	4.01	2.70

The hidden-charm pentaquark states have only been observed in the exclusive b decays in proton-proton collisions. The productions of pentaquark states in other processes have been proposed. In Refs. [246–248, 771, 772], the authors claimed that the hidden-charm pentaquark states can be produced in the J/ψ photoproduction off proton. This process could distinguish whether these pentaquark states are genuine states or anomalous triangle singularities. Moreover, it is suggested that the hidden-charm pentaquark states can be produced in e^+e^- collisions [773] and antiproton-deuteron collisions [774]. Based on Monte Carlo simulations, the inclusive production rates of these pentaquark states are estimated in proton-proton collisions [775, 776] and electron-proton collisions [777], which are helpful for future experimental searches for the pentaquark states.

IV. THREE-BODY HADRONIC MOLECULES

Nowadays, using nucleons as degrees of freedom and with the two-body NN interaction determined by the nucleon-nucleon scattering data and the residual small NNN interaction, ab initio calculations can reproduce most of the ground-state and low-lying excited states of light nuclei [778–780]. Adding hyperons to the nuclear system, one ends up with hypernuclei. Following the same approach, the properties of hypernuclei can also be understood very well [781–783]. Such a picture can be extended to other three-body hadronic systems based on the molecular candidates discovered experimentally, such as $X(3872)$, $D_{s0}^*(2317)$, the P_c pentaquark states, and $T_{cc}^+(3875)$ mentioned above. The idea is that if one exotic hadron C is a bound state of two conventional hadrons A and B , then with the same interaction between A and B which leads to the formation of C , one can study the three-body ABB and AAB systems and check whether they can form bound/resonant states. If the ABB or AAB system binds, then an experimental (or lattice QCD) confirmation on the existence of this state can unambiguously verify the molecular picture for the exotic state C , i.e., it is dominantly a hadronic molecule of A and B . Conversely, studies on multi-hadron states can also illuminate the relevant hadron-hadron interactions. It should be noted that the binding of a three-body system is not only determined by the interactions but also by other factors such as their masses and quantum numbers. A small reduced mass can increase the kinematic energy barrier and make the systems difficult to bind. Quantum numbers such as spin and isospin in multi-body systems can also significantly affect the bindings of multi-hadron systems. In the case that AA (BB) is not bound, the binding of AB is not a sufficient but necessary condition for the binding of AAB (ABB) [271].

There have been many studies of three-body systems containing nucleons and hyperons. For instance, Refs. [784–788] studied the possible existence of nonstrange tribaryons including NNN [785, 788], $NN\Delta$ [785, 788], $N\Delta\Delta$ [786, 788] and $\Delta\Delta\Delta$ [784, 787, 788] systems. The strange tribaryons have also been studied, including single strangeness ΛNN and ΣNN [789–791], double strangeness $\Lambda\Lambda N$ and ΞNN [792–796], and multi strangeness $N\Xi\Xi$ [796], ΩNN and $\Omega\Omega N$ [797, 798]. On the experimental side, a strange tribaryon $S^0(3115)$ was reported in the ^4He (stopped K^- , p) reaction, which mainly decays into ΣNN [799]. In Ref. [800], this strange tribaryon is explained as a nonquark state. Other searches for strange tribaryons have also been performed [801–804].

A particularly relevant line of research is the studies on the clusters of different numbers of antikaons and nucleons [805–814]. The $\Lambda(1405)$ can be considered as a quasibound $\bar{K}N$ state [815, 816], from which one can deduce that the $\bar{K}N$ interaction is strongly attractive. In such a case, it is natural to expect the existence of a $\bar{K}NN$ bound state. The $\bar{K}\bar{K}N$ system was found to bind with a binding energy of $10 \sim 33$ MeV [812], and the $K\bar{K}N$ systems were also found bound in Ref. [817] with the fixed-center

approximation and in Ref. [818] with a variational approach. In Ref. [813], multi-hadron states composed of an antikaon and different numbers of nucleons, i.e., $\bar{K}NN$, $\bar{K}NNN$, $\bar{K}NNNN$, and $\bar{K}NNNNN$, were found to bind with binding energies of $25 \sim 28$ MeV, $45 \sim 50$ MeV, $68 \sim 76$ MeV, and $70 \sim 81$ MeV.

In this short review, we focus on possible three-body systems that help reveal the nature of the many two-body exotic hadrons covered in this review, especially in the heavy flavor sector. In the charm sector, there are many studies about multi-hadron systems. Most of them are based on the molecular nature assumptions of discovered exotic states, including $X(3872)$ as a $D\bar{D}^*$ molecule, $D_{s0}^*(2317)$ as a DK molecule, the P_c pentaquark states as $D\bar{\Sigma}_c^{(*)}$ molecules, and $T_{cc}^+(3875)$ as a DD^* molecule. With these assumptions and the two-body hadron-hadron interactions, multi-hadron systems such as $D^{(*)}D^{(*)}(\bar{D}^{(*)})K$, $\bar{D}\bar{D}^{(*)}\Sigma_c$, and $D^{(*)}D^{(*)}D^{(*)}$ have been studied and found to form bound/resonant states. Their masses, decays, and productions have been studied, which provide valuable information for future experimental searches. Extending the studies from the charm sector to the bottom sector is straightforward, employing the so-called heavy quark flavor symmetry. Since multi-hadron bound/resonant states in the bottom sector are more difficult to observe experimentally, we mainly focus on the charm sector.

A. $DD(\bar{D})K$ molecules

As discussed in Sec. III, the $D_{s0}^*(2317)$ and $D_{s1}(2460)$ can be explained as DK and D^*K molecules. Adding a D meson to the DK system, one can study the DDK system and search for likely bound states by solving the Schrödinger equation via the Gaussian Expansion Method(GEM). The Jacobi coordinates for the DDK system are shown in Fig. 40, where the symbols N_1 , N_2 , and N_3 denote D , D , and K mesons, respectively. In Ref. [273], the DD potential is described by the OBE model, and the DK potential containing a leading-order attractive potential and a next-to-leading order repulsive correction is determined by reproducing the $D_{s0}^*(2317)$ as a DK bound state with a binding energy of 45 MeV. A DDK bound state is found below the three-body mass threshold by $67 \sim 72$ MeV, which is also below the $DD_{s0}^*(2317)$ mass threshold. Therefore, if the $D_{s0}^*(2317)$ is assumed as a DK bound state, a DDK bound state is expected. In other words, the existence of a DDK molecule can help verify the molecular nature of $D_{s0}^*(2317)$. The DDK system is found to bind with a binding energy of about 90 MeV in the three-body coupled-channel DDK , $DD_s\pi$, and $DD_s\eta$ system by solving the Faddeev equations in Ref. [819] and about 70 MeV in finite volume [820], which are consistent with the results of Ref. [273]. In addition, Ref. [821] points out that the KK repulsive interaction, which is the same magnitude as the DK attraction, prevents the DKK system from binding.

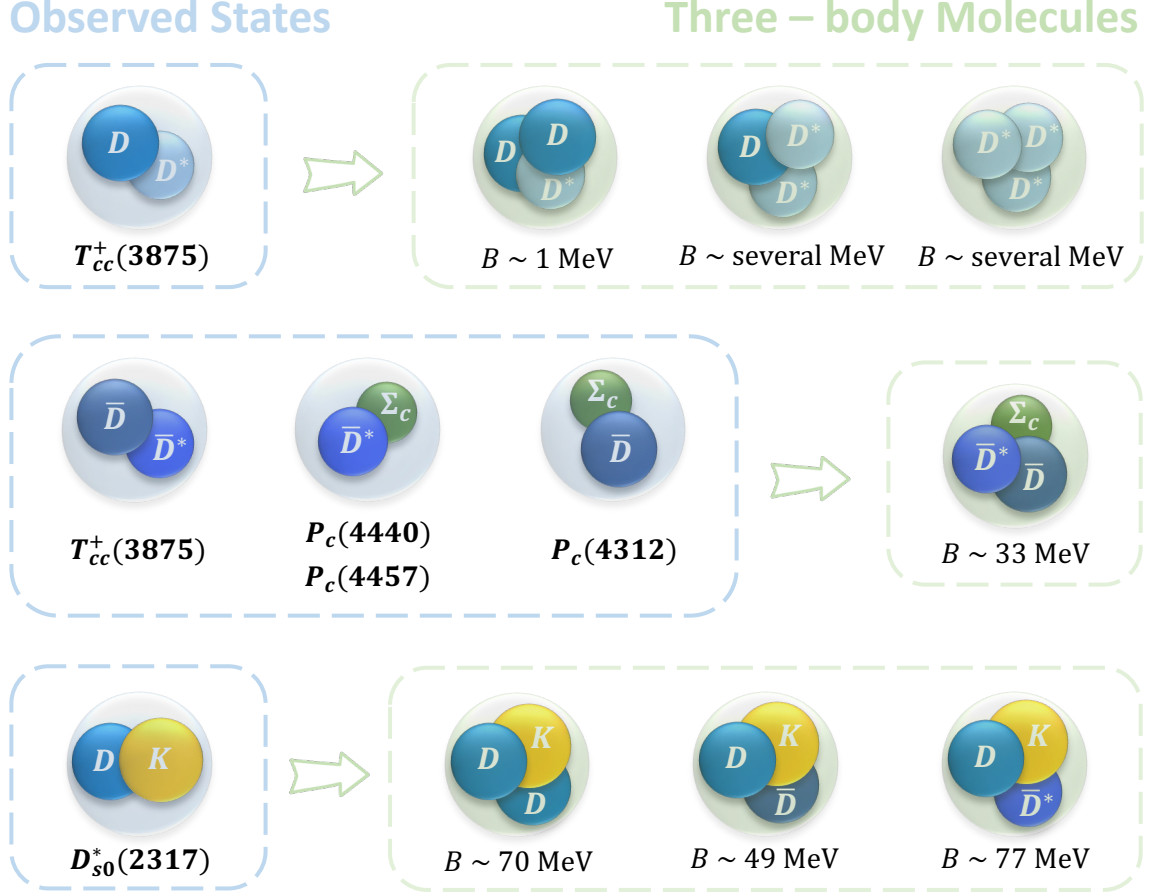


FIG. 26. Three-body hadronic molecules based on the assumption that the observed states are two-body hadronic molecules.

Since the DDK bound state carries double charm, it is difficult to be produced experimentally. If we replace one of the charmed D mesons with an anti-charmed \bar{D} meson, we have a hidden-charm system of $D\bar{D}K$, which is more likely to be produced experimentally. Therefore, we investigate the three-body systems of $D\bar{D}K$ and $D\bar{D}^*K$ in the same approach [822]. One should note that according to chiral perturbation theory, the $\bar{D}K$ interaction in the isospin zero channel is only half that of the DK interaction. Caution should be taken when one transforms the Weinberg-Tomozawa chiral potential from momentum space to coordinate space. In particular, no $\bar{D}K$ bound state with isospin zero [272] exists. Two bound states $D\bar{D}K$ and $D\bar{D}^*K$ are obtained with the binding energies of 49 MeV and 77 MeV, which are also below the $D_{s0}^*(2317)\bar{D}$ and $D_{s1}(2460)\bar{D}$ mass thresholds, in agreement with Refs. [823–825]. The minimum quark contents of such molecules are the same as those of hidden-charm tetraquark states with strangeness Z_{cs} , while the parity of Z_{cs} is different from that of the $D\bar{D}^{(*)}K$ molecules. Therefore, the $D\bar{D}^{(*)}K$ molecules

can be regarded as excited states of Z_{cs} . We should note that the existence of the $D\bar{D}K$ molecule is heavily tied to the DK interaction, which, in other words, indicates that the existence of the $D\bar{D}K$ molecule would verify or refute the molecular nature of $D_{s0}^*(2317)$. Therefore, we strongly recommend experimental searches for the $D\bar{D}K$ molecule, particularly at the Belle II experiment [245].

TABLE XXXIV. Masses and binding energies (in units of MeV) of the $D\bar{D}K$ and $D\bar{D}^*K$ bound states, in comparison with the results of other works.

	Ref. [822]	Ref. [823]	Ref. [824]
$\frac{1}{2}(0^-) D\bar{D}K$	$4181.2^{+2.4}_{-1.4}(B_3 \simeq 48.9^{+1.4}_{-2.4})$	-	-
$\frac{1}{2}(1^-) D\bar{D}^*K$	$4294.1^{+6.6}_{-3.1}(B_3 \simeq 77.3^{+3.1}_{-6.6})$	$4317.92^{+6.13}_{-6.55}(B_3 \simeq 53.52^{+6.55}_{-6.13})$	$4307 \pm 2(B_3 \simeq 64 \pm 2)$

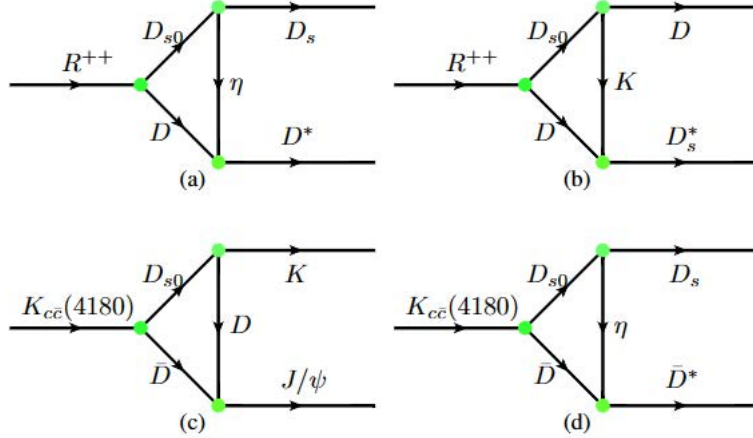


FIG. 27. Triangle diagram representing the decays of the R^{++} state to $D_s D^*$ (a) and DD_s^* (b) and the $K_{c\bar{c}}(4180)$ state to $J/\psi K$ (c) and $D_s \bar{D}^*$ (d).

Identifying the $D_{s0}^*(2317)$ as a DK bound state, we predicted several relevant three-body bound states, e.g., DDK , $D\bar{D}K$ and $D\bar{D}^*K$. We further investigated the strong decay of these three hadronic molecules to guide experimental searches for them. Their decays are similar to the two-body molecules. That is to say; the three-body molecules can be viewed as quasi-two-body molecules. The proportion of each configuration can be described by their wave function. Since the DD interaction is quite weak, the DDK molecule can be regarded as a $DD_{s0}^*(2317)$ molecule. The partial decay width of the $DD_{s0}^*(2317)$ molecule to three-body final states is small due to the small widths of its constituents. Nevertheless, the $DD_{s0}^*(2317)$ can scatter into DD_s^* or D^*D_s , and the orbital angular momentum between the final states is P -wave. The contact-range approach cannot solve the $DD_{s0}^*(2317) - D^*D_s$ coupled-channel problem due to several

unknown parameters. We resort to the triangle diagram depicting the $DD_{s0}^*(2317)$ molecule transition to the DD_s^* or D^*D_s via exchanges of a K meson or an η meson as shown in Fig. 27. Using the effective Lagrangian, we estimated the widths of the DDK molecule to be the order of several MeV [826]. As for the $D\bar{D}K$ molecule, the $D_{s0}^*(2317)\bar{D}$ configuration accounts for 86.8% of its wave function, and thus its three-body decay behavior is similar to that of $D_{s0}^*(2317)D$. For the two-body decay, the $D\bar{D}K$ molecule can decay into $J/\psi K$ and $D_s\bar{D}^*$ via exchanges of D and η mesons as shown in Fig. 27. Using the effective Lagrangian approach, we estimated the partial decay widths of $D\bar{D}K \rightarrow J/\psi K$ and $D\bar{D}K \rightarrow \bar{D}_s D^*$ to be about 0.5 MeV and 0.2 MeV.

It is easy to realize that the DDK molecule contains two charm quarks, leading to low production yields. This is consistent with the null result of the Belle Collaboration [827]. Similar to T_{cc} , the DDK molecule will likely be detected in the inclusive process. In the exclusive process, the DDK molecule can be produced in the semi-inclusive decays of b -flavored hadrons, such as the B_c meson. Very recently, Li et al. estimated the production rates of DD^* and $D_s D^*$ molecules in the B_c decays [828]. Due to the low production rate of the B_c meson, searches for the DDK molecule via the B_c decay is difficult. The hidden-charm $D\bar{D}K$ molecule can be observed in the exclusive process, such as the B meson decay. The B meson first decays into $\bar{D}^{(*)}D_{s0}^*(2317)$, then $\bar{D}^{(*)}$ meson scatters into $\bar{D}\pi$, and finally the $K_{c\bar{c}}(4180)$ is dynamically generated by the $\bar{D}D_{s0}^*(2317)$ interaction. This should be explicitly studied in the future.

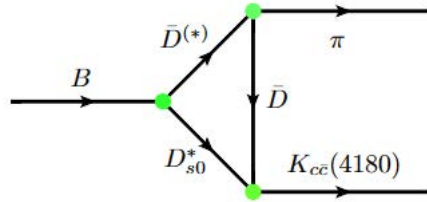


FIG. 28. The triangle diagram of $B \rightarrow \bar{D}^{(*)}D_{s0}^* \rightarrow K_{c\bar{c}}(4180)\pi$.

B. $\bar{D}\bar{D}^*\Sigma_c$ molecules

Since the three pentaquark states $P_c(4312)$, $P_c(4440)$, and $P_c(4457)$ are widely viewed as $\bar{D}^{(*)}\Sigma_c$ bound states, it is interesting to investigate the three-body hadron system $\bar{D}\bar{D}^*\Sigma_c$, where the $\bar{D}\bar{D}^*$ interaction is determined by reproducing the mass of $T_{cc}^+(3875)$ as a DD^* bound state. The Jacobi coordinates for the $\bar{D}\bar{D}^*\Sigma_c$ system are shown in Fig. 40, where the symbols N_1 , N_2 , and N_3 denote \bar{D} , \bar{D}^* , and Σ_c , respectively. The $\bar{D}\bar{D}^*$ and $\bar{D}^{(*)}\Sigma_c$ interactions are described in the OBE model, where the cutoffs Λ_P and Λ_T are determined by reproducing the masses of P_c s and $T_{cc}^+(3875)$. To accommodate the so-induced uncertain-

TABLE XXXV. Binding energies (in units of MeV), expectation values of the Hamiltonian (potential and kinetic energies) (in units of MeV) and root-mean-square radii (in units of fm) of the $\bar{D}\bar{D}^*\Sigma_c$ system obtained in the three cases detailed in the main text.

$I(J^P)$	B	T	$V_{\bar{D}^*\Sigma_c}$	$V_{\bar{D}\Sigma_c}$	$V_{\bar{D}\bar{D}^*}$	$r_{\bar{D}^*\Sigma_c}$	$r_{\bar{D}\Sigma_c}$	$r_{\bar{D}\bar{D}^*}$
Case I $\Lambda_P = \Lambda_T = 0.998$ GeV								
$1(\frac{1}{2}^+)$	10.86	65.41	-19.64	-21.69	-34.94	1.42	1.41	1.36
$1(\frac{3}{2}^+)$	7.06	52.18	-19.66	-10.46	-29.12	1.62	1.81	1.64
Case II $\Lambda_T = 0.998$ GeV $\Lambda_P = 1.16$ GeV								
$1(\frac{1}{2}^+)$	37.24	116.16	-41.53	-72.44	-39.43	1.00	0.88	1.03
$1(\frac{3}{2}^+)$	29.63	92.50	-81.32	-21.67	-19.15	0.91	1.36	1.40
Case III $\Lambda_P = \Lambda_T = 1.16$ GeV								
$1(\frac{1}{2}^+)$	63.07	169.01	-52.14	-66.03	-113.91	0.83	0.82	0.75
$1(\frac{3}{2}^+)$	46.94	141.01	-61.84	-25.27	-100.84	0.91	1.02	0.86

ties, we take three sets of cutoff values to search for three-body bound states: Case I: $\Lambda_T=\Lambda_P=0.998$ GeV; Case II: $\Lambda_T=0.998$ GeV, $\Lambda_P=1.16$ GeV; and Case III: $\Lambda_T=\Lambda_P=1.16$ GeV. One can see that we obtained two three-body bound states of $\bar{D}\bar{D}^*\Sigma_c$ with $I(J^P) = 1(1/2^+)$ and $I(J^P) = 1(3/2^+)$, and of binding energies 37.24 MeV and 29.63 MeV below the $\bar{D}\bar{D}^*\Sigma_c$ mass threshold [829].

The mass splitting of the three-body $\bar{D}\bar{D}^*\Sigma_c$ doublet in case III larger than that of case II implies that the strength of the $\bar{D}\bar{D}^*$ potential affects the mass splitting. The mass splitting as a function of the cutoff of the $\bar{D}\bar{D}^*$ potential is presented in Fig. 29. It is obvious that the mass splitting increases with the strength of the $\bar{D}\bar{D}^*$ potential. Interestingly, the positive mass splitting means that the mass of the spin $3/2$ $\bar{D}\bar{D}^*\Sigma_c$ bound state is larger than that of its spin $1/2$ counterpart. While in this case the mass of the $J^P = \frac{1}{2}^-$ $\bar{D}^*\Sigma_c$ system is larger than that of the $J^P = \frac{3}{2}^-$ $\bar{D}^*\Sigma_c$ system [149]. That is, the mass splitting of the three-body $\bar{D}\bar{D}^*\Sigma_c$ doublet is oppositely correlated to the mass splitting of the two-body $\bar{D}^*\Sigma_c$ bound states, which offers a non-trivial way to check the molecular nature of the involved states.

TABLE XXXVI. Weights of each Jacobian channel in the $\bar{D}\bar{D}^*\Sigma_c$ system for Case II

$I(J^P)$	$\bar{D}^*\Sigma_c - \bar{D}$	$\bar{D}\Sigma_c - \bar{D}^*$	$\bar{D}\bar{D}^* - \Sigma_c$
$1(\frac{1}{2}^+)$	19.18 %	52.42 %	28.40 %
$1(\frac{3}{2}^+)$	78.39 %	8.09 %	13.52 %

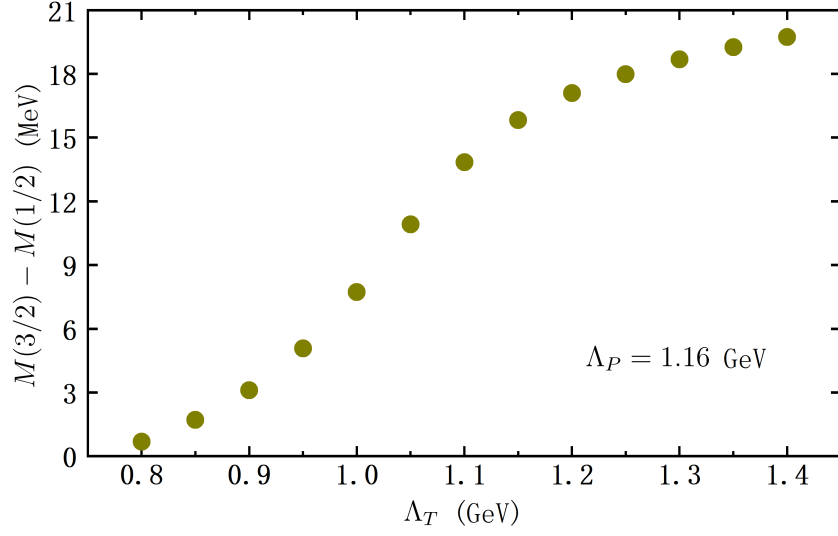


FIG. 29. Mass splitting of the three-body $\bar{D}\bar{D}^*\Sigma_c$ doublet as a function of the cutoff of the $\bar{D}\bar{D}^*$ potential for fixed $\Lambda_P = 1.16$ GeV.

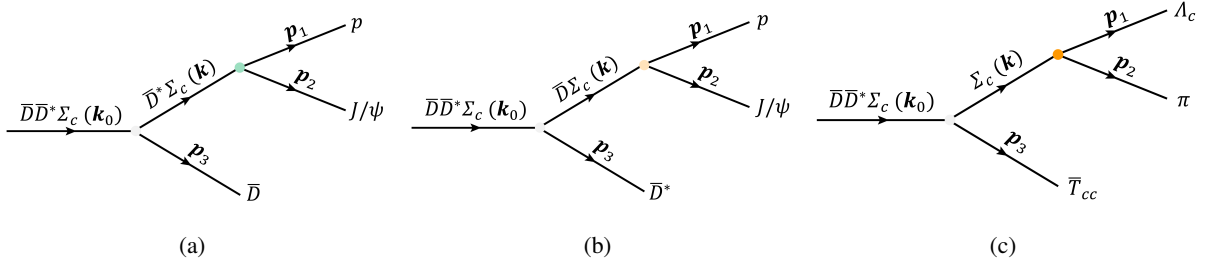


FIG. 30. Tree level diagrams for the three-body $\bar{D}\bar{D}^*\Sigma_c$ bound states decaying into $J/\psi p \bar{D}$ (a), $J/\psi p \bar{D}^*$ (b), and $\pi \Lambda_c \bar{T}_{cc}$ (c).

Such $\bar{D}\bar{D}^*\Sigma_c$ bound states can be regarded as suppositions of three quasi two-body bound states, $P_{c2}(P_{c3})\bar{D}$, $P_{c1}\bar{D}^*$, and $\bar{T}_{cc}\Sigma_c$. The weight of each configuration equals the weight of the corresponding Jacobian channel. They are tabulated in Table XXXVI for Case II. We treated $P_{c2/c3}$, P_{c1} , and Σ_c as unstable particles compared with the \bar{D} , \bar{D}^* , and \bar{T}_{cc} particles [401, 566] so that these unstable particles can further decay into two other particles. The decay modes of the three-body bound states $\bar{D}\bar{D}^*\Sigma_c$ into $J/\psi p \bar{D}$, $J/\psi p \bar{D}^*$, and $\Lambda_c \pi \bar{T}_{cc}$, are shown in Fig. 30. The $\bar{D}\bar{D}^*\Sigma_c$ states will not couple to a pair of traditional hadrons since its minimum number of valence quarks is seven. As a result, they can only decay into at least three traditional hadrons, which means the decay mechanism shown in Fig. 30 should play a dominate role.

TABLE XXXVII. Partial decay widths of the $\bar{D}\bar{D}^*\Sigma_c$ molecules.

Modes	Fig. 30(a)		Fig. 30(b)		Fig. 30(c)	
	$H_{q1} \rightarrow J/\psi p \bar{D}$	$H_{q2} \rightarrow J/\psi p \bar{D}$	$H_{q1} \rightarrow J/\psi p \bar{D}^*$	$H_{q2} \rightarrow J/\psi p \bar{D}^*$	$H_{q1} \rightarrow \bar{T}_{cc}\Lambda_c\pi$	$H_{q2} \rightarrow \bar{T}_{cc}\Lambda_c\pi$
Value	2.4 MeV	0.7 MeV	2.0 MeV	0.3 MeV	0.05 keV	0.5 keV

The partial decay widths of the two three-body bound states, H_{q1} and H_{q2} are listed in Table XXXVII. One can find that the partial widths of the bound state with $J = 1/2$ decaying into $J/\psi p \bar{D}$ and $J/\psi p \bar{D}^*$ are much larger than those of the $J = 3/2$ state, which indicates that the $J/\psi p \bar{D}$ and $J/\psi p \bar{D}^*$ decay modes can help us to discriminate the spins of the H_{q1} and H_{q2} molecules. However, the partial widths of both H_{q1} and H_{q2} decaying into $\bar{T}_{cc}\Lambda_c\pi$ are rather small due to the small phase spaces. Note that there exist some uncertainties about the partial decay widths given in Table XXXVII because the partial decay widths of the three pentaquark states decaying into $J/\psi p$ are not precisely known [770]. However, we suggest to search for them in the $J/\psi p \bar{D}^*$ or $J/\psi p \bar{D}$ mass distributions.

C. $D^{(*)}D^{(*)}D^{(*)}$ molecules

The $T_{cc}^+(3875)$ discovered by the LHCb Collaboration can be understood as a DD^* bound state [162, 175, 178, 257, 571–574, 581, 830–832]. Adding a charmed meson D into the DD^* system, it is meaningful to investigate the three-body system DDD^* , which carries the highest charm number. For such a three-body system, the Jacobi coordinates are shown in Fig. 40, where the symbols N_1 , N_2 , and N_3 denote D , D , and D^* , respectively. Using the GEM, we search for the likely DDD^* bound state by solving the Schrödinger equation. We take the OBE model to obtain the DD and DD^* interactions. Since HQSS relates the DD and DD^* systems, we take the same cutoff to obtain the DD and DD^* interactions. In addition, we consider the Coulomb interactions between the charmed mesons and then search for the DDD^* bound state. In Table XXXVIII, we present the binding energy of the DDD^* system. We obtain a DDD^* bound state with a binding energy of around 1 MeV, denoted as H_{ccc} [833]. The quark contents of the H_{ccc} state are the same as that of $\bar{D}T_{cc}$, which is a kind of hadronic molecule composed of a charmed meson and a doubly charmed tetraquark state. We find that the mass of $\bar{D}T_{cc}$ is larger than that of H_{ccc} . It is worth noting that the existence of the $\bar{D}T_{cc}$ molecule is dependent on the molecular nature of the pentaquark states [682], while the existence of H_{ccc} is dependent on the molecular nature of T_{cc} [833]. Such a state could, in principle, be observed with the upcoming LHC data and will unambiguously determine the nature of the T_{cc}^+ state.

Considering HQSS, we also investigated the D^*D^*D and $D^*D^*D^*$ systems [834]. Following the same strategy as Ref. [833], two-body interactions are derived in the OBE model, and the cutoff Λ is determined

TABLE XXXVIII. Binding energies, RMS radii and Hamiltonian expectation values of the doubly charged $I(J^P) = \frac{1}{2}(1^-)$ DDD^* state with S -wave OBE and Coulomb interactions. The uncertainties originate from HQSS breaking, as explained in the main text.

$\Lambda(\text{MeV})$	$B(\text{MeV})$	r_{DD^*}	r_{DD}	$\langle T \rangle$	$\langle V_{DD^*} \rangle$	$\langle V_{DD} \rangle$
976	$0.16^{+0.01}_{-0.01}$	$8.83^{+0.01}_{-0.23}$	$10.74^{+0.09}_{-0.08}$	$7.65^{+1.32}_{-0.52}$	$-7.81^{+0.47}_{-1.27}$	$-0.00^{+0.02}_{-0.07}$
998	$1.09^{+0.17}_{-0.13}$	$4.50^{+0.83}_{-0.65}$	$5.86^{+1.19}_{-0.92}$	$23.65^{+2.85}_{-2.03}$	$-24.14^{+2.45}_{-2.58}$	$-0.60^{+0.31}_{-0.43}$
1013	$2.22^{+0.27}_{-0.23}$	$3.15^{+0.41}_{-0.33}$	$4.04^{+0.59}_{-0.47}$	$33.34^{+2.93}_{-2.76}$	$-34.40^{+2.52}_{-2.62}$	$-1.16^{+0.46}_{-0.56}$

by reproducing the binding energy of $T_{cc}^+(3875)$. In addition, the S - D mixing and coupled-channel effects are also considered. With the GEM, we find that the $I(J^P) = \frac{1}{2}(0^-, 1^-, 2^-)$ D^*D^*D and $I(J^P) = \frac{1}{2}(0^-, 1^-, 2^-, 3^-)$ $D^*D^*D^*$ systems can form loosely bound states with binding energies of a few MeV, which could be viewed as good hadronic molecular candidates. While, the $I(J^P) = \frac{3}{2}(0^-, 1^-, 2^-)$ D^*D^*D and $I(J^P) = \frac{3}{2}(1^-, 2^-, 3^-)$ $D^*D^*D^*$ systems are more difficult to bind. We suggest searching for these molecular states in the following decay modes: a) a double-charm molecular state and a charmed meson, b) three charmed mesons, and c) three charmed mesons with several pions and photons.

In Ref. [835], the authors investigated the $D^*D^*D^*$ system considering that two D^* 's generate a $I(J^P) = 0(1^+)$ bound state [693]. By solving the Faddeev equation with the fixed center approximation, they found that the $D^*D^*D^*$ system is bound in the $I(J^P) = \frac{1}{2}(0^-, 1^-, 2^-)$ channels with binding energies of 53.1 MeV, 33.8 MeV, and 34.6 MeV. The absence of the $J^P = 3^-$ and $I = \frac{3}{2}$ states is a consequence of the fact that the D^*D^* binds only in $I(J^P) = 0(1^+)$ in their model. In addition, the $I(J^P) = \frac{1}{2}(0^-)$ state has a width of 99.7 MeV because of the $D^*D^* \rightarrow D^*D$ decays considered. It is interesting to see that in Ref. [834] the authors mention that there is no bound-state solution with $\Lambda = 1$ GeV and $J^P = 3^-$, while bound states are formed for the other J^P configurations.

D. Other heavy-flavor three-body molecules

Here, we briefly summarize studies of other heavy-flavor three-body bound states. With the same method mentioned above, i.e., GEM, many three-body systems were also studied based on the two-body interactions determined by experimentally observed states. In Ref. [840], the $\bar{D}\bar{K}$ and $\bar{D}\Sigma_c$ interactions were determined by the $D_{s0}^*(2317)$ and $P_c(4312)$ states, and the $\Sigma_c\bar{K}$ interaction was related to the $N\bar{K}$ one via chiral symmetry. The three-body $\Sigma_c\bar{D}\bar{K}$ system was found to form a bound state, named $P_{cs}^*(4739)$, with quantum numbers $I(J^P) = 1(1/2^+)$ and a binding energy of about 77.8 MeV. They also found that the $P_{cs}^*(4739)$ state can decay into $\Xi'\bar{D}$ and $\bar{D}_s^*\Sigma_c$ with partial decay widths of a few tens of MeV. In Ref. [838],

TABLE XXXIX. Summary for heavy-flavor three-body states. Energies are in units of MeV.

Components	$I(J^P)$	Results (Method)	Decay modes
DNN	$\frac{1}{2}(0^-)$	BS $\sim 3500 - 15i$ (FCA, V) [836]	$\Lambda_c \pi^- p, \Lambda_c p$ [836]
$NDK, ND\bar{K},$ $ND\bar{D}$	$\frac{1}{2}(\frac{1}{2}^+)$	BS $\sim 3050, 3150, 4400$ (FCA) [837]	\dagger
DD^*N	$\frac{1}{2}(\frac{1}{2}^+, \frac{3}{2}^+)$	BS $\sim 4773.2, 4790.7$ (GEM) [838]	$T_{cc}p, DDp + \pi(\gamma), \Xi_{cc} + \pi(\gamma),$ charmed baryon + charmed meson [838]
DD^*N	$\frac{3}{2}(-)$	difficult to form bound states (GEM) [838]	\dagger
$DK\bar{K}$	$\frac{1}{2}(0^-)$	D -like state ~ 2845.5 (FCA) [821], D -like state ~ 2900 (QCDSR, χ F) [839]	$\pi\pi D$ [821]
DKK	$\frac{1}{2}(0^-)$	no bound state (FCA) [821]	\dagger
$\bar{D}\bar{K}\Sigma_c$	$1(\frac{1}{2}^+)$	BS ~ 4738.6 (GEM) [840]	$D\Xi', D_s\Sigma_c$ [840]
$D^{(*)}$ multi ρ	...	several $D_J^{(*)}$ states (FCA) [841, 842]	\dagger
$\rho D\bar{D}$	$0(?), 1(?)$	BS $\sim 4241 - 10i, [4320 - 13i, 4256 - 14i]$ (FCA) [843]	\dagger
DDK	$\frac{1}{2}(0^-)$	BS ~ 4162 (GEM) [273], 4140 (χ F) [819], 4160 (FV) [820]	DD_s^*, D^*D_s [826]
$D\bar{D}K$	$\frac{1}{2}(0^-)$	BS ~ 4181.2 (GEM) [822], 4191 (FCA) [825]	$D_s\bar{D}^*, J/\psi K$ [822]
DD^*K	$\frac{1}{2}(1^-)$	BS ~ 4317.9 (BO) [823]	\dagger
$D\bar{D}^*K$	$\frac{1}{2}(1^-)$	BS ~ 4294.1 (GEM) [822], 4317.9 (BO) [823], 4307 (FCA) [824]	$D_s^{(*)}\bar{D}^{(*)}, J/\psi K^*$ [823, 844]
$D^*D^*\bar{K}^*$	$\frac{1}{2}(0^-, 1^-, 2^-)$	BS $\sim [4850 - 46i, 4754 - 50i],$ (FCA) [845] [4840 - 43i, 4755 - 50i]	$D^*D^*\bar{K}^*,$ $D^*D^{(*)}\bar{K}^*,$ [845] $[D^*D^*\bar{K}^*, D^*D^{(*)}\bar{K}^*]$
$\bar{D}\bar{D}^*\Sigma_c$	$1(\frac{1}{2}^+, \frac{3}{2}^+)$	BS $\sim 6292.3, 6301.5$ (GEM) [829]	$J/\psi p\bar{D}^{(*)}, \bar{T}_{cc}\Lambda_c\pi$ [829]
$J/\psi K\bar{K}$	$0(1^-)$	$Y(4260) \sim 4150 - 45i$ (χ F) [481]	\dagger
DDD^*	$\frac{1}{2}(1^-)$	BS ~ 5742.2 (GEM) [833]	$DDD\pi(\gamma)$ [833]
DD^*D^*	$\frac{1}{2}(0^-, 1^-, 2^-)$	several loosely bound states (GEM) [834]	charmed mesons + ... [834]
$D^*D^*D^*$	$\frac{1}{2}(0^-, 1^-, 2^-, 3^-)$	several loosely bound states (GEM) [834]	charmed mesons + ... [834]
$D^*D^*D^{(*)}$	$\frac{1}{2}(0^-, 1^-, 2^-)$	BS $\sim 5790.9 - 49.8i, 5990.2, 5989.4$ (FCA) [835]	
$D^*D^*\bar{D}$	$\frac{3}{2}(-)$	difficult to form bound states (GEM) [834]	\dagger
$D^*D^*\bar{D}^*$	$\frac{1}{2}(2^-)$	BS ~ 5879 (F) [846]	\dagger
$D^*D^*\bar{D}^*$	$\frac{1}{2}(3^-)$	BS ~ 6019 (F) [846]	\dagger
$\Omega_{ccc}\Omega_{ccc}\Omega_{ccc}$	$?(\frac{3}{2}^+)$	no bound state (GEM) [847]	\dagger
$\Xi_{cc}\Xi_{cc}\bar{K}$	$\frac{1}{2}(0^-)$	BS ~ 7641.8 (GEM) [848]	\dagger

Meaning of the abbreviations: BS - bound state, GEM - Gaussian expansion method, F - Faddeev equation, BO - Born-Oppenheimer approximation, FCA - Fixed center approximation, V - Variational approach, QCDSR - QCD sum rule, χ F - chiral Faddeev, FV - finite volume

the DD^* , DN , and D^*N interactions were described in the OBE model associated with the observed T_{cc}^+ , $\Sigma_c(2800)$, and $\Lambda_c(2940)$ states. Two DD^*N bound states with $I(J^P) = \frac{1}{2}(\frac{1}{2}^+)$ and $\frac{1}{2}(\frac{3}{2}^+)$ were found with only S -wave pairwise interactions. Considering the S - D mixing and coupled-channel effects, the conclusion remains unchanged. On the contrary, the $I(J^P) = \frac{3}{2}(\frac{1}{2}^+)$ and $\frac{3}{2}(\frac{3}{2}^+)$ DD^*N systems are difficult to bind. Utilizing heavy quark symmetry, Ref. [848] studied the $\Xi_{cc}\Xi_{cc}\bar{K}$ and $BB\bar{K}$ with $I(J^P) = \frac{1}{2}(0^-)$.

TABLE XL. Summary for heavy-flavor three-body states. Energies are in units of MeV.

Components	$I(J^P)$	Results (Method)	Decay modes
$B\bar{D}\bar{D}, B\bar{D}D$	$\frac{1}{2}(1^-)$	BS ~ 8955 , probable BS ~ 8960 (FCA) [849]	\dagger
$DB^*\bar{B}^*, DB\bar{B},$ $D^*B^*\bar{B}^*, D^*B\bar{B}$	$\frac{1}{2}(?)$	BS $\sim 12384, 12294, 12520, 12430$ (FCA) [850]	\dagger
BBB^*	...	probable BS (BO) [851]	\dagger
$BB^*B^* - B^*B^*B^*$	$\frac{1}{2}(2^-)$	BS ~ 15658 (F) [852]	\dagger
$\rho B^*\bar{B}^*$	$1(3^-)$	a state $\sim 10987 - 40i$ (FCA) [853]	\dagger
$BB^*\bar{K}, B\bar{B}^*\bar{K}$	$\frac{1}{2}(1^-)$	BS ~ 11014 (BO) [823]	\dagger
$BB\bar{K}$	$\frac{1}{2}(0^-)$	BS ~ 10945 (GEM) [848]	\dagger
$B\bar{B}\bar{K}$	$\frac{1}{2}(0^-)$	BS ~ 10659 (FCA) [854]	\dagger
$B^*\bar{B}^*\bar{K}$	$\frac{1}{2}(2^-)$	BS ~ 10914 (FCA) [854]	\dagger
$B\bar{B}\bar{K}^*$	$\frac{1}{2}(1^-)$	BS $\sim 11002, 11264$ (FCA) [854]	\dagger
$B^*\bar{B}^*\bar{K}^*$	$\frac{1}{2}(3^-)$	BS $\sim 11078, 11339$ (FCA) [854]	\dagger
$\bar{B}^*\bar{B}^*\bar{K}^*$	$\frac{1}{2}(0^-, 1^-, 2^-)$	BS $\sim 11413 - 88i, 11405 - 130i, 11491 - 126i$ (FCA) [855]	\dagger
$B^*B^*\bar{K}$	$\frac{1}{2}(0^+, 1^+, 2^+)$	BS ~ 11040 (F) [856]	\dagger
$\Xi_{bb}\Xi_{bb}\bar{K}$	$\frac{1}{2}(?)$	BS $\sim 20608, 20667$ (F) [856]	\dagger
$\Omega_{bbb}\Omega_{bbb}\Omega_{bbb}$	$?(\frac{3}{2}^+)$	no bound state (GEM) [847]	\dagger

Meaning of the abbreviations: BS - bound state, GEM - Gaussian expansion method, F - Faddeev equation, BO - Born-Oppenheimer approximation, FCA - Fixed center approximation

The $B(\Xi_{cc})\bar{K}$ two-body interactions were derived in chiral perturbation theory, and the interactions between two identical particles were described in the OBE model. The $\Xi_{cc}\Xi_{cc}\bar{K}$ and $BB\bar{K}$ bound states with binding energies of about 92 MeV and 109 MeV were found.

In the fixed center approximation (FCA) to the Faddeev equation, a three-body system is treated as a third particle scattering with a two-body cluster, which can be associated with an experimentally observed state. Due to its simplicity, it has been employed to study many three-body systems containing heavy quarks. Considering the $\Lambda_c(2595)$ resonance as a DN cluster, the scattering among a nucleon, a $K(\bar{K})$, and a D meson generates a $I(J^P) = \frac{1}{2}(0^-)$ DNN bound state with a mass of about 3500 MeV and a width of $20 \sim 40$ MeV [836]. A variational method (V) was employed to study the DNN system ending with similar results [836]. In Ref. [837], considering the scattering of a nucleon on the $D\bar{D}$ cluster, which corresponds to the hidden-charm resonance $X(3700)$, three relatively narrow bound or quasibound $I(J^P) = \frac{1}{2}(\frac{1}{2}^+)$ $NDK, ND\bar{K}, ND\bar{D}$ states with energies of 3050 MeV, 3150 MeV, and 4400 MeV were found. Considering the $D_1(2420)$ as a ρD cluster, and following the same strategy, the $\rho D\bar{D}$ and D -multi-

systems were studied [842, 843]. In Ref. [843], one $I = 0$ $\rho D\bar{D}$ bound state with a mass of around 4241 MeV and a width of about 20 MeV was found. While in isospin $I = 1$, two bound states were found, one with a mass around 4320 MeV and a width about 25 MeV in the $\rho - X(3700)$ scattering, and the other with a mass around 4256 MeV and a width about 28 MeV in the $\bar{D} - D_1(2420)$ scattering, which can be associated with the $X(4260)$ or $X(4360)$ states. In Ref. [842], assuming the $f_2(1270)$ as a $\rho\rho$ cluster, several D_J -like states were predicted in the D -multi ρ few-body systems. Several D_J^* -like states were also predicted in the D^* -multi ρ few-body systems assuming $D_2^*(2460)$ as a $D^*\rho$ cluster [841]. Assuming T_{cc} and $X(2900)$ states are D^*D^* and $D^*\bar{K}^*$ bound states, several $D^*D^*\bar{K}^*$ bound states were obtained with quantum numbers $I(J^P) = \frac{1}{2}(0^-, 1^-, 2^-)$, one state for $J^P = 0^-$, two states for $J^P = 1^-, 2^-$, with binding energies of $56 \sim 151$ MeV and widths of $80 \sim 100$ MeV [845]. The BD system analogous to the bound DK system was found in Ref. [857]. Therefore, Ref. [849] studied the $BD\bar{D}$ and BDD systems considering the multiple rescattering of the $D(\bar{D})$ meson with the BD cluster. They obtained a $BDD\bar{D}$ bound state with a mass of about $8928 \sim 8985$ MeV. For BDD , some clues of a bound state in the energy region $8935 \sim 8985$ MeV were found, and the results are sensitive to the theoretical uncertainties. Based on the bound $B\bar{B}$ and $B^*\bar{B}^*$ systems in isospin $I = 0$ [685], Ref. [850] studied the $D^{(*)}B^{(*)}\bar{B}^{(*)}$ systems considering that the clusterized $B\bar{B}(B^*\bar{B}^*)$ systems interact with a third particle $D^{(*)}$. As a result, they found four three-body bound states $DB^*\bar{B}^*$, $D^*B^*\bar{B}^*$, $DB\bar{B}$, and $D^*B^*\bar{B}^*$ with binding energies of about $20 \sim 30$ MeV. In addition, they found resonant bumps above the $D^{(*)}[B^{(*)}\bar{B}^{(*)}]$ thresholds with widths of about 10 MeV. Again, the results were sensitive to the theoretical uncertainties.

In addition, other methods for heavy-flavor three-body systems exist. In Ref. [839], a D -like meson with a mass of 2890 MeV and a width of about 55 MeV was predicted treating $DK\bar{K}$ as $Df_0(980)$ in two methods, i.e., QCD sum rule and chiral Faddeev equation. Similar results were obtained in Ref. [821] by the FCA, and evidence for a $I(J^P) = \frac{1}{2}(0^-)$ $DK\bar{K}$ state with a mass of about $2833 \sim 2858$ MeV, mainly made of $Df_0(980)$, was found. In Ref. [481], they studied the $J/\psi\pi\pi$ and $J/\psi K\bar{K}$ coupled channels solving the chiral Faddeev equations to investigate the existence of the $J^{PC} = 1^{--}$, $Y(4260)$ resonance. They obtained a peak of around 4150 MeV with a width of about 90 MeV. All heavy-flavor three-body states studied are collected in Table XXXIX and Table XL.

Lattice QCD simulations have also been widely employed in studies of three-body systems, but most of them focused on the light-flavor sector [858–870]. In the heavy-flavor sector, very few studies have been performed [820]. We hope to see more lattice QCD studies of heavy-flavor three-body systems.

We must note that the studies of three-body hadronic systems cannot only help reveal the nature of the relevant sub-two-body interactions such that one can verify the nature of two-body hadronic molecules but also are essential by themselves because the three-body molecules are the beginning of new kinds of

periodic tables composed of (unstable) mesons and hadrons, beyond what is well known in nuclear and hypernuclear physics. This perspective has recently been emphasized in, e.g., Ref. [271]. In particular, it has been shown that four-body systems of kaons and D mesons are likely to exist [272, 273].

V. FEMTOSCOPIC CORRELATION FUNCTIONS FOR EXOTIC HADRONS

Traditionally, hadron-hadron interactions were studied in scattering experiments. Using such techniques, we have learned a lot about the nuclear force. However, such experiments are difficult for unstable particles because of their short lifetime and the lack of suitable targets. In the last few years, femtoscopy, which measures two particle momentum correlation functions in high-energy proton-proton (pp), proton-nucleus (pA), and nucleus-nucleus (AA) collisions, has made remarkable progress in probing the strong interactions between various pairs of hadrons [279]. Historically, the femtoscopic technique can be traced back to the 1950s, when Hanbury Brown and Twiss used photon interferometry to measure the apparent angular diameter of stars [871]. Subsequently, this method was applied in heavy-ion collisions and has been proven to be helpful in exploring properties like the size of the emitting source or the time dependence of the emission process [872–876]. In the earlier studies, the efforts focused on the analysis of π or K pairs, where the quantum statistics and Coulomb force determine the behavior of the correlations.

Thanks to the small size of the particle emission source, the abundant rare hadrons produced in relativistic heavy-ion collisions, and the excellent capabilities of detectors to identify particles and measure their momenta, the measurements of momentum correlation functions have become possible in revealing the precise dynamics of the strong interactions between pairs of hadrons. Recently, the strong interactions among $\pi^\pm K^\pm$ [877], $\pi^\pm K_S^0$ [878], $K_S^0 K_S^0$ [879], $K_S^0 K^\pm$ [879–881], $K^\pm p$ [882, 883], ϕp [278], $K^\pm \Lambda$ [884, 885], pp [886], $p\Lambda^-$ [886, 887], $p\Sigma^0$ [887, 888], $p\Xi^-$ [276], $p\Omega^-$ [277], $\Lambda\Lambda$ [886, 889], $\Lambda\Xi^-$ [890], and baryon-antibaryon [891, 892] pairs have been determined by the ALICE Collaboration at the LHC. Meanwhile, the strong interactions among $p\Xi^-$ [893], $p\Omega^-$ [894], $\Lambda\Lambda$ [274, 893], $\Xi^-\Xi^-$ [893] and antiproton-antiproton [275] pairs have been measured by the STAR Collaboration at RHIC. More recently, the femtoscopy technique has been used to understand the genuine three-body interaction for ppK^\pm [895], ppp [896], and $pp\Lambda$ [896]. In addition, it is worthwhile noting that the recent measurement of the pD^- , $\pi^\pm D^\pm$, and $K^\pm D^{(*)\pm}$ correlation functions demonstrated the potential to access the charm sector in experiments [897, 898].

On the other hand, the femtoscopy studies have also triggered a large number of related theoretical studies [626, 899–910] in the light quark (u, d, s) sector. The authors in Ref. [908] evaluated the $K\Sigma - K\Lambda - \eta N$ interactions in the chiral unitary approach. They demonstrated that the corresponding correlation

functions could illuminate the relation between the $N^*(1535)$ state and these coupled channels, emphasizing the need to analyze the data in terms of coupled channels to avoid misleading results. In Ref. [909], we conducted a model-independent analysis of the $\bar{K}^0 K^+$ correlation functions obtained from pp collisions at 13 TeV. The data imply the existence of the a_0 resonance, namely, $a_0(980)$. Detailed discussions of the correlation functions involving heavy charm and bottom quarks are given in the following subsections.

A. Experimental and theoretical basics of Femtoscopy

The critical observable in Femtoscopy is the momentum correlation function. It is defined as the ratio of the Lorentz-invariant two-particle spectrum to the product of single-particle inclusive momentum spectra [239, 876, 911–915],

$$C(\mathbf{p}_1, \mathbf{p}_2) = \frac{E_1 E_2 dN_{12}/(d^3p_1 d^3p_2)}{(E_1 dN_1/d^3p_1) \cdot (E_2 dN_2/d^3p_2)} = \frac{P(\mathbf{p}_1, \mathbf{p}_2)}{P(\mathbf{p}_1) \cdot P(\mathbf{p}_2)}, \quad (18)$$

where \mathbf{p}_i ($i = 1, 2$) is the momentum of each particle, and E_i ($i = 1, 2$) is the energy of particle i . The above definition can also be regarded as the ratio of the probability of simultaneously measuring two particles with momenta \mathbf{p}_1 and \mathbf{p}_2 to the product of the single-particle probabilities.

Experimentally, the correlation function can be obtained rather straightforwardly using the so-called mixed-event technique [279], which is computed as,

$$C(k) = \mathcal{N} \frac{N_{\text{same}}(k)}{N_{\text{mixed}}(k)}, \quad (19)$$

where the relative momentum of two particles $k = |\mathbf{p}_1 - \mathbf{p}_2|/2$, $N_{\text{same}}(k)$ and $N_{\text{mixed}}(k)$ represent the same event and different event k distributions, respectively. The normalization constant \mathcal{N} , which denotes the corrections of experimental effects, is usually evaluated in the high-momentum region (such as $k \in [500, 800]$ MeV/c), where the effect of final-state interactions is absent, and thus the correlation function approaches unity.

Theoretically, the two-particle momentum correlation function can be computed by the Koonin–Pratt (KP) formula [911, 916],

$$C(\mathbf{p}_1, \mathbf{p}_2) = \frac{\int d^4x_1 d^4x_2 S_1(x_1, \mathbf{p}_1) S_2(x_2, \mathbf{p}_2) |\Psi^{(-)}(\mathbf{r}, \mathbf{k})|^2}{\int d^4x_1 d^4x_2 S_1(x_1, \mathbf{p}_1) S_2(x_2, \mathbf{p}_2)} \quad (20a)$$

$$\simeq \int d\mathbf{r} S_{12}(r) |\Psi^{(-)}(\mathbf{r}, \mathbf{k})|^2, \quad (20b)$$

where $S_i(x_i, \mathbf{p}_i)$ ($i = 1, 2$) is the single-particle source function of particle i . $\Psi^{(-)}$ denotes the relative wave function with the relative coordinate \mathbf{r} and the relative momentum \mathbf{k} , in which the effects of final-state interactions are embedded. Eq. (20b) can be derived by integrating the c.m. coordinates from Eq. (20a)

neglecting the time difference of the particle emission and the momentum dependence of the source function, where $S_{12}(r)$ is the normalized source function of the pair and usually parametrized as a Gaussian normalized to unity $S_{12}(r) = \exp(-r^2/4R^2)/(2\sqrt{\pi}R)^3$. Due to the dominant role of S -wave interactions in the low-momentum region, only the S -wave final-state interactions are usually assumed to modify the relative wave function. For a non-identical two-particle system experiencing only strong interactions, the relative wave function in the two-body outgoing state can be written as,

$$\Psi_S^{(-)}(\mathbf{r}, \mathbf{k}) = e^{i\mathbf{k}\cdot\mathbf{r}} - j_0(kr) + \psi_0(r, k), \quad (21)$$

where the spherical Bessel function j_0 represents the $l = 0$ component of the non-interacting wave function, and ψ_0 denotes the $l = 0$ scattering wave function affected by the strong interaction. Substituting the relative wave function (21) into the KP formula, the correlation function then becomes

$$C(k) \simeq 1 + \int_0^\infty 4\pi r^2 dr S_{12}(r) [|\psi_0(r, k)|^2 - |j_0(kr)|^2]. \quad (22)$$

Before using exact scattering wave functions to evaluate correlation functions, it is useful to introduce an analytical model developed by Lednický and Lyuboshits (LL) [912]. It has been widely used to extract strong interactions from experimental data [279]. This model obtains correlation functions using the asymptotic wave function and the effective range correction. Then, correlation functions are given in terms of the scattering amplitude $f(k) = 1/(-1/a_0 + r_{\text{eff}}k^2/2 - ik)$ with the scattering length a_0 and the effective range r_{eff} ⁶,

$$C_{LL}(k) = 1 + \frac{|f(k)|^2}{2R^2} F_3\left(\frac{r_{\text{eff}}}{R}\right) + \frac{2\text{Re}f(k)}{\sqrt{\pi}R} F_1(2kR) - \frac{\text{Im}f(k)}{R} F_2(2kR), \quad (23)$$

where $F_1(2kR) = \int_0^{2kR} dx \exp[x^2 - (2kR)^2]/(2kR)$, $F_2(2kR) = (1 - \exp[-(2kR)^2])/(2kR)$, and $F_3(r_{\text{eff}}/R) = 1 - r_{\text{eff}}/(2\sqrt{\pi}R)$. The LL mode usually does not consider the Coulomb interaction and the coupled-channel effect.

In general, the exact scattering wave function can be obtained by solving the Schrödinger equation in coordinate space [903, 917] or the Lippmann-Schwinger (LS) equation in momentum space [280, 904]. For our purpose, it is convenient to first obtain the reaction amplitude T by solving the LS equation and then derive the scattering wave function using the relation $|\psi\rangle = |\varphi\rangle + G_0 T |\varphi\rangle$, where G_0 and $|\varphi\rangle$ represent the free propagator and the free wave function, respectively. More specifically, we use the following coupled-channel scattering equation to obtain the reaction amplitude,

$$T_{\nu'\nu}(k', k) = V_{\nu'\nu} \cdot f_{\Lambda_F}(k', k) + \sum_{\nu''} \int_0^\infty \frac{dk'' k''^2}{8\pi^2} \frac{V_{\nu'\nu''} \cdot f_{\Lambda_F}(k', k'') \cdot T_{\nu''\nu}(k'', k)}{E_{1,\nu''} E_{2,\nu''} (\sqrt{s} - E_{1,\nu''} - E_{2,\nu''} + i\epsilon)}, \quad (24)$$

⁶ Here a negative (positive) scattering length corresponds to a weakly attractive potential (repulsive potential or attractive potential capable of generating a bound state).

where $\sqrt{s} = E_{1,\nu}(k) + E_{2,\nu}(k)$, and $E_{1(2),\nu}(k) = \sqrt{k^2 + M_{1(2),\nu}^2}$. As shown in Eq. (24), to avoid ultraviolet divergence in numerical evaluations, we multiply the potential $V_{\nu'\nu''}$ with a Gaussian regulator $f_{\Lambda_F}(k, k') = \exp[-(k/\Lambda_F)^2 - (k'/\Lambda_F)^2]$ to suppress high-momentum contributions [280, 547], where Λ_F is a cutoff parameter to be determined. We can then compute the scattering wave function with the half-off-shell T -matrix in the following way,

$$\psi_{\nu'\nu}(r, k) = \delta_{\nu'\nu} j_0(kr) + \int_0^\infty \frac{dk' k'^2}{8\pi^2} \frac{T_{\nu'\nu}(k', k) \cdot j_0(k'r)}{E_{1,\nu'} E_{2,\nu'} (\sqrt{s} - E_{1,\nu'} - E_{2,\nu'} + i\epsilon)}, \quad (25)$$

where j_0 is the spherical Bessel function of angular momentum $l = 0$. The single-channel scattering wave function is called ψ_0 ($\nu' = \nu$). Using the above-obtained wave function, we can consider coupled-channel effects by replacing the modulus squared in Eq. (22) with

$$|\psi_0(r, k)|^2 \rightarrow \sum_{\nu'} \omega_{\nu'} |\psi_{\nu'\nu}(r, k)|^2, \quad (26)$$

where the sum runs over all possible coupled channels, and $\omega_{\nu'}$ is the weight for the individual components of the multi-channel wave function. In addition, the contribution from the Coulomb interaction has to be considered for systems of two charged particles, which is expected to play a significant role in the low-momentum region [907, 918]. One can treat the Coulomb force in momentum-space using the Vincent-Phatak method [919, 920].

It is worthwhile to note that in Ref. [286], a formalism was developed that allows one to factorize the scattering amplitudes outside the integrals in the formulae (see Eq. (24) and Eq. (25)). The integrals explicitly involve the range of the strong interaction. Following this approach, the T -matrix can be converted into an algebraic BS equation based on the on-shell approximation,

$$T = \frac{V}{1 - VG}, \quad (27)$$

for the single-channel case, where G is the loop function of the intermediate particles,

$$G(\sqrt{s}) = \int_0^{q_{\max}} \frac{d^3 k'}{(2\pi)^3} \frac{E_1(k') + E_2(k')}{2E_1(k')E_2(k')} \frac{1}{s - [E_1(k') + E_2(k')]^2 + i\epsilon}. \quad (28)$$

Eq. (27) in the cutoff regularization can be justified using dispersion relations [124], but can be equally obtained using a separable potential $V(k', k) = V \cdot \theta(q_{\max} - k') \cdot \theta(q_{\max} - k)$. Then, the scattering wave function can be expressed with the T -matrix by,

$$\Psi_S^{(-)}(\mathbf{r}, \mathbf{k}) = e^{i\mathbf{k}\cdot\mathbf{r}} + T(k, k) \cdot \theta(q_{\max} - k) \cdot \tilde{G}(r, \sqrt{s}), \quad (29)$$

where $\tilde{G}(r, \sqrt{s})$ function is given by,

$$\tilde{G}(r, \sqrt{s}) = \int_0^{q_{\max}} \frac{d^3 k'}{(2\pi)^3} \frac{E_1(k') + E_2(k')}{2E_1(k')E_2(k')} \frac{j_0(k'r)}{s - [E_1(k') + E_2(k')]^2 + i\epsilon}. \quad (30)$$

In practice, Eq. (27) can be easily generalized to coupled channels as $T = [1 - VG]^{-1}V$, where V is the transition potential V_{ij} between the channels i and j , and G is the diagonal loop function $G \equiv \text{diag}[G_i(\sqrt{s})]$, with $G_i(\sqrt{s})$ the loop function of each particular channel i . Finally, the coupled-channel correlation function can be written explicitly as,

$$C(k) = 1 + \theta(q_{\max} - k) \int_0^\infty 4\pi r^2 dr S_{12}(r) \times \left[|j_0(kr) + T_{ii} \cdot \tilde{G}_{(i)}(r, \sqrt{s})|^2 + \sum_{j \neq i} \omega_j |T_{ji} \cdot \tilde{G}_{(j)}(r, \sqrt{s})|^2 - |j_0(kr)|^2 \right]. \quad (31)$$

The factor $\theta(q_{\max} - k)$ is inoperative for relative momentum k of interest in correlation functions, with values of k smaller than q_{\max} .

B. Some general features of correlation functions

In this subsection, we review some general features of correlation functions concerning studies of hadronic molecules. A fundamental physical picture for femtoscopy is that relativistic heavy-ion collisions generate particle sources from which hadron-hadron pairs emerge with relative momentum k and can undergo final-state interactions before being detected. Consequently, k is reduced or increased via an attractive or repulsive interaction. In other words, the magnitude of the correlation function in the low-momentum region will be above unity for an attractive interaction, whereas between zero and unity for a repulsive interaction.

For transparency and without loss of generality, we work with the square-well model and study four potentials: repulsive, weakly attractive, moderately attractive, or strongly attractive. The scattering wave function is obtained analytically by solving the stationary Schrödinger equation $-\frac{\hbar^2}{2\mu} \nabla^2 \psi + V_0 \theta(d - r) \psi = E \psi$, where the reduced mass μ is chosen as 470 MeV, the range parameter d is set at 2.5 fm, and the depth parameter V_0 is set at 25, -10 , -25 , and -75 MeV for a repulsive potential, a weakly attractive potential not strong enough to generate a bound state, a moderately attractive potential capable of generating a shallow bound state, and a strongly attractive potential yielding a deep bound state, respectively ⁷.

In Fig. 31, panels (a1-d1) show the products of the relative distance r and the S -channel wave function ψ_0 for the relative momentum $k \simeq 3$ MeV/c. According to Eq. (22), the correlation function depends on two factors, namely, the difference between the free and scattering wave functions squared, i.e., $\Delta \equiv r^2(|\psi_{l=0}|^2 - |j_{l=0}|^2)$, and the source function S_{12} , shown as the blue solid line and colored regions in panels

⁷ Here we refer to a bound state as a shallow bound state if its binding energy can be described by the effective-range expansion up to q^2 , and otherwise as a deep bound state.

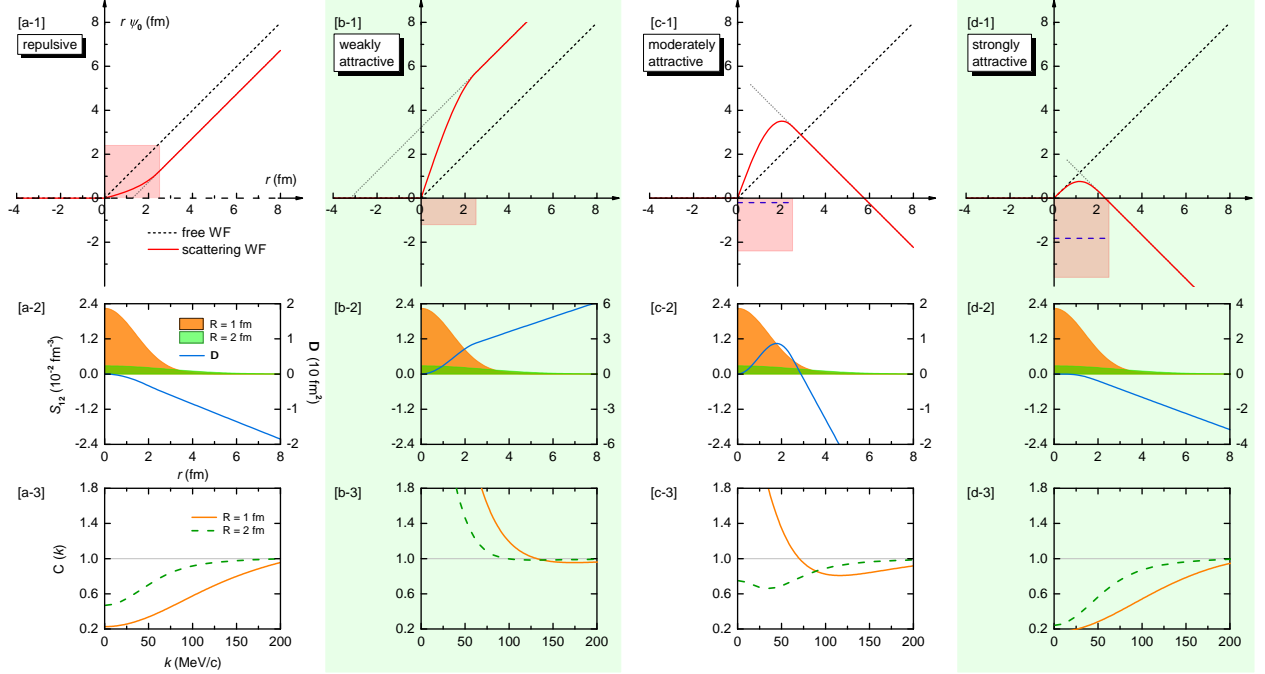


FIG. 31. Scattering wave functions, source functions, and correlation functions for the four different square-well potentials, namely, (a) a repulsive potential, (b) a weakly attractive potential, (c) a moderately attractive potential, and (d) a strongly attractive potential. Figures are taken from Ref. [280].

(a2-d2). The comparison between the free and scattering $r \cdot \psi_0$ can be captured by the sign of Δ , which is directly related to the properties of the correlation functions in the low-momentum region. As the source size R increases, the magnitude of the Gaussian source function decreases rapidly, and its tail becomes longer, reducing the corresponding correlation function. The final correlation functions are displayed in panels (a3-d3). One can conclude that (a) for a repulsive potential, the correlation functions are between zero and unity for different R ; (b) for a weakly attractive potential, they are above unity for different R ; (c) for a moderately attractive potential, the low-momentum correlation function is above unity for small R while below unity for large R ; and (d) for a strongly attractive potential, they are between zero and unity for different R [280]. The above observations based on the square-well model are consistent with the aforementioned physical picture and the analysis performed in the Lednicky-Lyuboshitz model [239], but more intuitive.

C. Correlation functions for $D_{s0}^*(2317)$, $D_0^*(2300)$, $D_1(2420)$, and $D_1(2430)$

The DK interaction in isospin zero is attractive to such an extent that a bound state can be generated [366, 368, 635], i.e., $D_{s0}^*(2317)$. It will be interesting to directly confirm the attractive nature of the

DK interaction. For such a purpose, we studied the DK correlation function for the first time, which, if measured, can be used to verify or refute the hadronic molecular picture of $D_{s0}^*(2317)$. We first evaluated the DK coupled-channel interaction in the leading order unitarized heavy-meson chiral perturbation theory and calculated the corresponding correlation function [280]. As shown in Fig. 32, the inelastic coupled-channel contribution, which is mainly from the $D^0 K^+ - D^+ K^0$ transition, can be sizable and lead to a cusp-like structure in the $D^0 K^+$ correlation function around the $D^+ K^0$ threshold. We found that the source size dependence of the DK correlation function is very different from that of moderately strong attractive interactions, which can be utilized to verify the nature of $D_{s0}^*(2317)$ as a deeply bound DK state. The above results are also confirmed in Ref. [281], where the interactions between a heavy pseudoscalar boson and a Nambu-Goldstone boson are derived from the next-to-leading-order unitarized heavy-meson chiral perturbation theory.

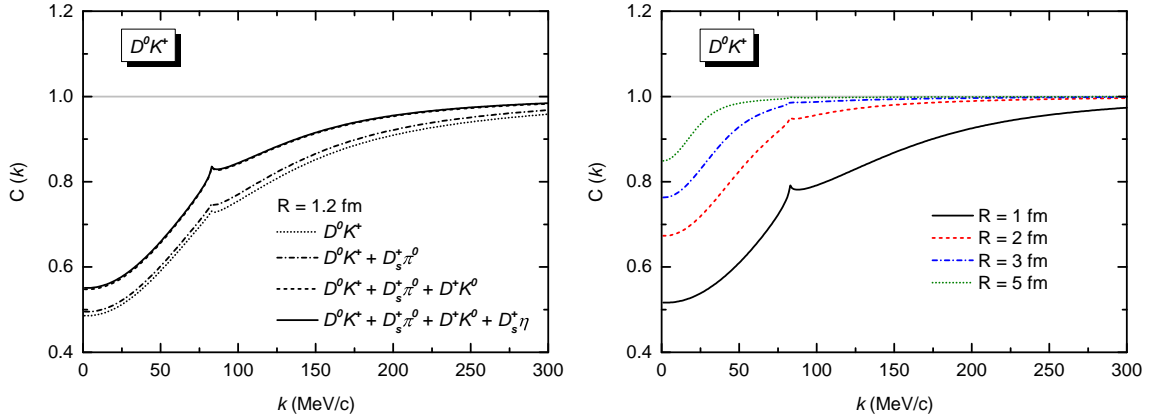


FIG. 32. (left panel) $D^0 K^+$ correlation function as a function of the relative momentum k . (right panel) Source size dependence of the $D^0 K^+$ correlation function. Figures are taken from Ref. [280].

Once experimental data are available, one can derive the corresponding strong interactions from those correlation functions, which is the so-called inverse problem in Femtoscopy studies [283, 287, 289, 921]. In Ref. [283], the authors deal with the inverse problem of extracting information from the $D^0 K^+$, $D^+ K^0$ and $D_s^+ \eta$ correlation functions in a model-independent way. In the absence of such data, they used the synthetic data extracted from an interaction model based on the local hidden gauge approach. Subsequently, they made no specific assumption on the potential V_{ij} except that the isospin symmetry and $V_{33}(3 \equiv D_s \eta) = 0$, the latter is quite general since the vertex $\eta\eta V$ vanishes in most models. Therefore, the interaction matrix

V gets a bit simplified to,

$$V = \begin{pmatrix} V_{11} & V_{12} & V_{13} \\ & V_{11} & V_{13} \\ & & 0 \end{pmatrix}. \quad (32)$$

where the indices $i = 1, 2, 3$ represent the $D^0 K^+$, $D^+ K^0$ and $D_s^+ \eta$ channels, respectively. To account for possible missing coupled channels and possible contribution of a non-molecular component, they introduced energy-dependent parts in the potential, such that,

$$V_{11} = V'_{11} + \frac{\alpha}{M_V^2}(s - \bar{s}), \quad (33a)$$

$$V_{12} = V'_{12} + \frac{\beta}{M_V^2}(s - \bar{s}), \quad (33b)$$

$$V_{13} = V'_{13} + \frac{\gamma}{M_V^2}(s - \bar{s}), \quad (33c)$$

where \bar{s} is the energy squared of the $D^0 K^+$ threshold. The T -matrix with the three coupled channels is evaluated through $T = [1 - VG]^{-1}V$. Using Eq. (31), there are eight parameters to describe the synthetic correlation functions, namely, V'_{11} , V'_{12} , V'_{13} , α , β , γ , q_{\max} and R . The question is whether one can determine these parameters from the three correlation functions. From the fits obtained with this set of free parameters, the authors of Ref. [283] found that the inverse problem can determine the existence of a bound state, its isospin nature, the compositeness, and the scattering length and effective range of all three channels. In other words, different magnitudes tied to the interaction of the channels can be evaluated from the correlation functions with reasonable accuracy.

For the system of lightest pseudoscalar open-charm mesons and Goldstone bosons with $(S, I) = (0, 1/2)$, Ref. [281] predicted the corresponding correlation functions and argued that the effect of the two-pole structure around 2300 MeV can be seen in the $D\pi$, $D\eta$, and $D_s \bar{K}$ correlation functions. As shown in Fig. 33, two distinct minima can be observed in the correlation functions $C_{D\pi}$ and $C_{D_s \bar{K}}$, especially for a small collision system, which are produced by the lower and higher $D_0^*(2300)$ poles, respectively.

Two lightest open-charm axial mesons exist, i.e., $D_1(2430)$ and $D_1(2420)$, whose masses are very similar, but the former has a larger width. In Ref. [282], the authors developed two models, which can produce compatible properties for the two lightest D_1 states but result in different scattering lengths: one in agreement with the findings of lattice QCD [922] (referred to as model A) and the other in agreement with the estimation obtained using the $D\pi$ results from the ALICE Collaboration [923–925] (referred to as model B). As shown in Fig. 34, they presented the correlation functions for both cases and found that $C_{D^* \pi}$ and $C_{D \rho}$ can be used to test both models and might encode sufficiently identifiable signatures of the

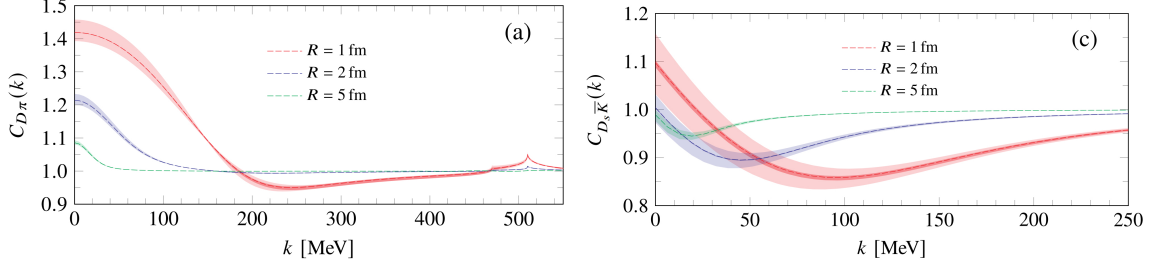


FIG. 33. Correlation functions for the $D\pi$ (left panel) and $D_s\bar{K}$ (right panel) channels with $I = I_z = 1/2$ as a function of their c.m. momentum k for different source sizes. Figures are taken from Ref. [281].

$D_1(2430)$ and $D_1(2420)$ states.

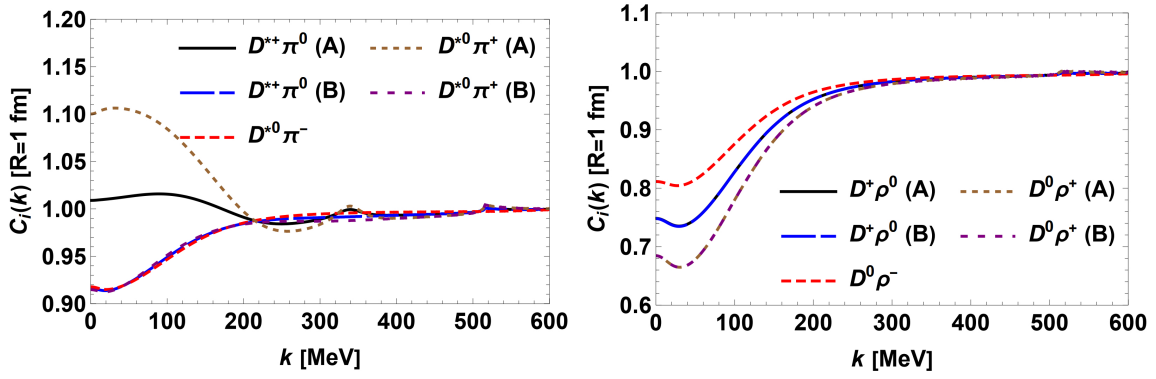


FIG. 34. Correlation functions for the physical $D^*\pi$ (left panel) and $D\rho$ (right panel) channels in models A and B, for $R = 1$ fm. Figures are taken from Ref. [282].

It is worthwhile to emphasize that except the pD^- correlation measured by the ALICE collaboration [897], results have been reported by the ALICE collaboration for $\pi^\pm D^{(*)\pm}$ and $K^\pm D^{(*)\pm}$ [898]. In Ref. [284], based on the next-to-leading order chiral potential, the authors calculated the correlation function of D mesons and light mesons using an off-shell T-matrix approach to access the two-meson wave function. They predicted the correlation functions involving charged D^+ , D^{*+} , D_s^+ and D_s^{*+} with π^\pm and K^\pm . Their results are similar to those of other theoretical models, which are comparable to experimental data. However, the predicted $D^+\pi^-$ correlation function significantly differs from the preliminary ALICE results. This puzzle must be solved by considering extra theoretical modifications or waiting for more definite experimental results.

D. Correlation functions for $T_{cc}(3875)$ and $X(3872)$

In this subsection, we discuss the potential of the femtoscopy study in understanding the nature of the $T_{cc}(3875)$ and $X(3872)$ states. Ref. [285] studied the correlation functions of the $D^0 D^{*+}$ ($D^+ D^{*0}$) and $D^0 \bar{D}^{*0}$ ($D^+ D^{*-}$) channels in connection with the $T_{cc}(3875)$ and $X(3872)$ states. They first constructed one-range Gaussian potentials for the DD^* and $D\bar{D}^*$ channels, which reproduce the empirical information, and then predicted the $D^0 D^{*+}$ ($D^+ D^{*0}$) and $D^0 \bar{D}^{*0}$ ($D^+ D^{*-}$) correlation functions, as shown in Fig. 35. The source size dependence is typical to the system with a shallow bound state for both correlation functions: enhancement in the small source case and suppression in the large source case.

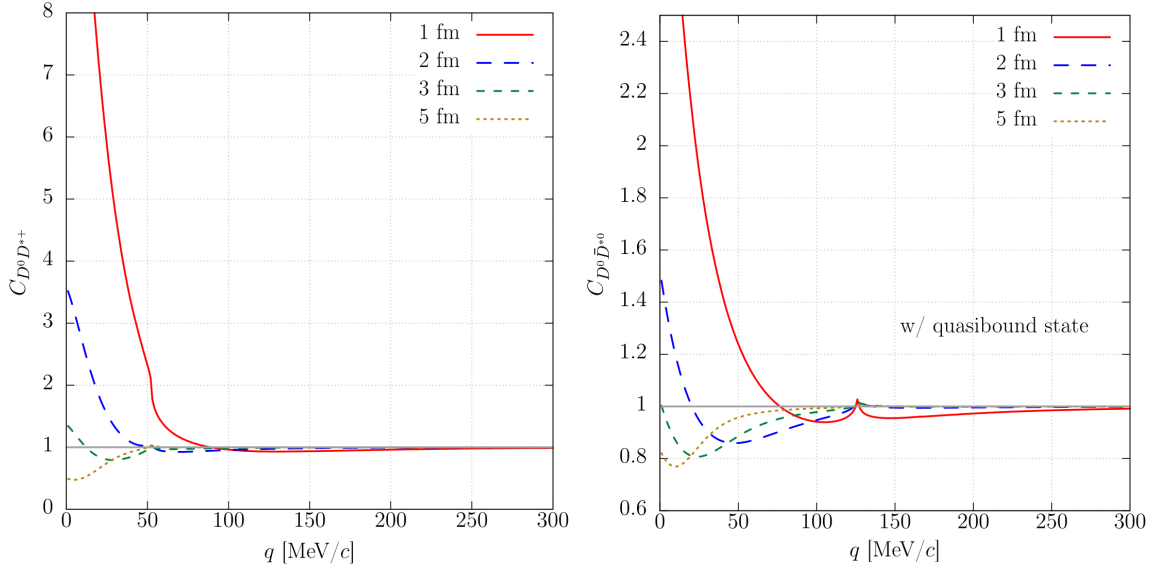


FIG. 35. Correlation functions of the $D^0 D^{*+}$ (left panel) and $D^0 \bar{D}^{*0}$ (right panel) pairs for source sizes $R = 1, 2, 3$, and 5 fm. Figures are taken from Ref. [285].

A different method formulated in momentum space, rather than in coordinate space, was used in Ref. [286] to obtain the $D^0 D^{*+}$ and $D^+ D^{*0}$ correlation functions, which are in qualitative agreement with Ref. [285]. In addition, the authors investigated the inverse problem of determining the $D^0 D^{*+}$ and $D^+ D^{*0}$ interactions from the pseudo correlation functions in Ref. [287]. With a coupled-channel unitary scheme, which has the freedom to accommodate missing channels relevant to the interaction and components of some genuine components of non-molecular nature, they demonstrated that from these synthetic data, one can extract the existence of the $T_{cc}(3875)$ bound state, the probabilities of each channel, and the scattering lengths and effective ranges for the coupled channels.

E. Correlation functions for $P_c(4312)$, $P_c(4440)$, and $P_c(4457)$

As mentioned above, the spins of the pentaquark states $P_c(4440)$ and $P_c(4457)$ play a decisive role in unraveling their nature but remain undetermined experimentally. There have been a large number of theoretical studies trying to distinguish their spins from various perspectives [174, 176, 177, 228, 231, 248, 545, 547–549, 555, 651, 653, 718, 721, 776, 777, 926–928]. Recently, we proposed to discriminate the spins of $P_c(4440)$ and $P_c(4457)$ with femtoscopic correlation functions [288].

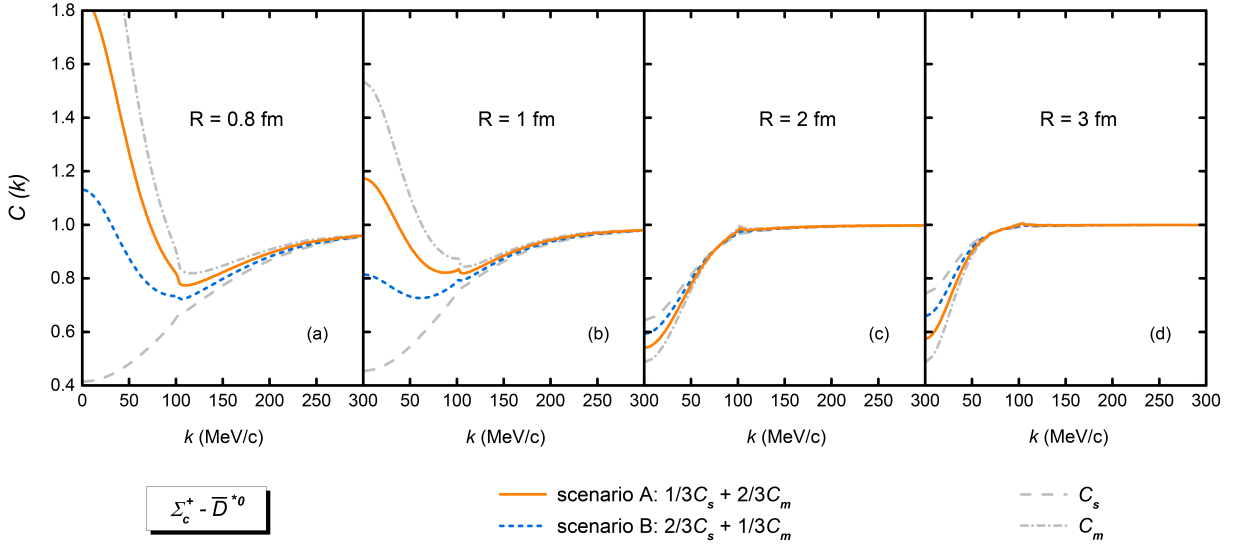


FIG. 36. Spin-averaged $\Sigma_c^+ \bar{D}^{*0}$ correlation function as a function of the relative momentum k for different source sizes $R = 0.8, 1, 2$ and 3 fm, respectively. The blue short-dashed lines represent the spin-averaged results in scenario A, where $P_c(4440)$ and $P_c(4457)$ have $J^P = (1/2)^-$ and $J^P = (3/2)^-$ respectively, while the orange solid lines represent the results in scenario B where $P_c(4440)$ and $P_c(4457)$ have $J^P = (3/2)^-$ and $J^P = (1/2)^-$. Figures are taken from Ref. [288].

In Ref. [288], assuming $P_c(4440)$ and $P_c(4457)$ are $\Sigma_c \bar{D}^*$ bound states, we first evaluated their interactions without specifying their spin by reproducing the masses of $P_c(4440)$ (strongly attractive) and $P_c(4457)$ (moderately attractive) in the resonance saturation model. Then, we calculated the corresponding $\Sigma_c^+ \bar{D}^{*0}$ correlation functions for the first time. In Fig. 36, the $\Sigma_c \bar{D}^*$ correlation functions C_s (C_m) calculated with the moderately (strongly) attractive interactions are shown as the dash-dotted (dashed) lines, which are in remarkable agreement with the aforementioned general features of correlation functions, namely, a moderately attractive interaction and a strongly attractive one may result in entirely different low-momentum behaviors. The spin-averaged $\Sigma_c \bar{D}^*$ correlation functions and their source size dependence are also shown in Fig. 36. We found that the low-momentum behaviors of the spin-averaged results are pretty different in

the two spin assignments, especially for a small collision system, which can be used to determine the spins of $P_c(4440)$ and $P_c(4457)$. In addition, to reduce the uncertainty of the source size, it is assumed that a common emitting source could characterize the $\Sigma_c^+ \bar{D}^{*0}$ and $\Sigma_c^+ \bar{D}^0$ systems. Similarly, we evaluated the $\Sigma_c^+ \bar{D}^0$ interaction by reproducing the $P_c(4440)$ mass and predicted the corresponding correlation function in Fig. 37, which exhibits an apparent and nonmonotonic source size dependence. It is worth noticing that the strategy proposed can be applied to decipher the nature of other hadronic molecules and thus deepen our understanding of the non-perturbative strong interaction.

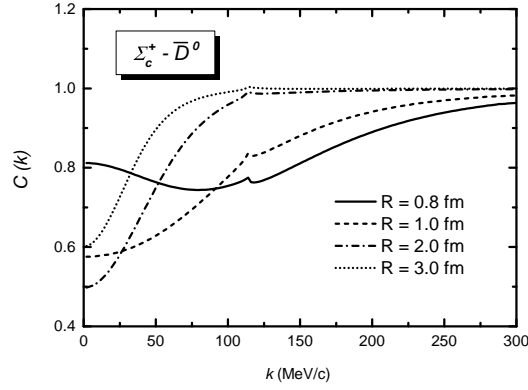


FIG. 37. Source size (R) dependence of the $\Sigma_c^+ \bar{D}^0$ correlation function. Figures are taken from Ref. [288].

F. Correlation functions for T_{bb}

Analogous to the $T_{cc}(3875)$ in the charm sector, a T_{bb} state in the bottom sector is expected to exist [258, 929–935]. In Ref. [258], the authors argued that the T_{bb} state could be built up from the $B^0 B^{*+}$ and $B^+ B^{*0}$ channels and is predicted to be a molecular state of these components with isospin $I = 0$, a binding energy of 21 MeV and a width of 14 eV in the local hidden gauge approach. More recently, the $B^0 B^{*+}$ and $B^+ B^{*0}$ correlation functions had been predicted with the input from the above local hidden gauge approach [289], where the interaction between the bottom mesons is generated by exchanging vector mesons.

Fig. 38 showed the $B^0 B^{*+}$ and $B^+ B^{*0}$ correlation functions for different source sizes R obtained in Ref. [289]. These correlation functions are all suppressed in a wide range of the relative momentum p for both small and large source sizes, which reflects the existence of the T_{bb} state. The magnitude of the correlation functions changes appreciably with R . Ref. [289] also addressed the inverse problem of determining the low-energy observables related to this interaction from the knowledge of correlation functions. For this, they parametrized the potential in a very general form, which explicitly considers the freedom of non-molecular nature. Using the parameters obtained by fitting to the synthetic data, the authors obtained a

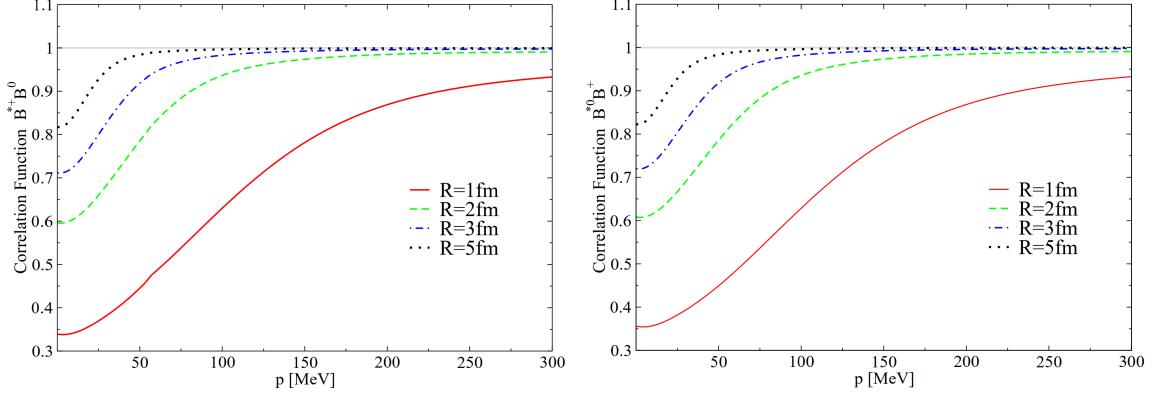


FIG. 38. $B^0 B^{*+}$ and $B^+ B^{*0}$ correlation functions for different source sizes. Figures are taken from Ref. [289].

bound state with a binding energy of 20.62 MeV, in excellent agreement with the known result of 21 MeV. These results show that it is promising for future experimental measurements of the $B^0 B^{*+}$ and $B^+ B^{*0}$ correlation functions to reveal the nature of the T_{bb} state.

More recently, Ref. [921] studied the $B^0 D^+$, $B^+ D^0$ correlation functions. The $B^0 D^+$ and $B^+ D^0$ system was shown to develop a BD bound state by about 40 MeV, using inputs consistent with the $T_{cc}(3875)$ state [286, 287]. The inverse problem was also studied, determining scattering observables from the correlation functions, including the existence of the bound state and its molecular nature. All correlation functions involving heavy charm and bottom quark studied are summarized in Table XLI.

VI. SUMMARY AND OUTLOOK

Since 2003, many states beyond the conventional $q\bar{q}$ mesons and qqq baryons have been discovered. These discoveries enrich hadron spectra and provide an invaluable opportunity to understand the non-perturbative strong interaction. These so-called exotic states have been proposed to be hadronic molecules, compact multiquark states, kinetic effects, or their mixtures. Among them, the hadronic molecular picture is one of the most prevailing interpretations since most exotic states are near the mass thresholds of pairs of conventional hadrons. Their mass spectrum, decay widths, and production rates have been thoroughly investigated within the molecular picture, most of which agree with existing limited data.

In this work, we first reviewed the experimental and theoretical status on several candidates for hadronic molecules containing heavy quarks. These include: $D_{s0}^*(2317)$, $D_{s1}(2460)$, $X(3872)$, $T_{cc}(3875)$, $Z_c(3900)$, $Z_c(4020)$, $Z_{cs}(3985)$, $P_c(4312)$, $P_c(4440)$, and $P_c(4312)$. These states are arguably the most studied among the exotic hadrons discovered. We provided a concise introduction to the experiments where they were observed and commented on the relevance of these experiments in deciphering their nature. We

TABLE XLI. Studies of correlation functions of heavy-flavor systems.

State	Mass MeV/c ²	Width MeV/c ²	S-wave threshold MeV/c ²	CF pair & Ref.
$D_{s0}^*(2317)$	2317.8 ± 0.5	< 3.8	$DK(+45.2)$ $D_s\eta(+198.4)$	D^0K^+/D^+K^0 [280, 281, 283] $D_s^+\eta$ [283]
$D_0^*(2300)$	2343 ± 10	229 ± 16	$D\pi(-336.9)$ $D\eta(+72.9)$ $D_s\bar{K}(+120.3)$	$D\pi$ ($I = 1/2$) [281] $D\eta$ ($I = 1/2$) [281] $D_s\bar{K}$ ($I = 1/2$) [281]
$D_1(2420)$	2422.1 ± 0.6	31.3 ± 1.9	$D\rho(+221.2)$	$D\rho$ ($I = 1/2$) [282]
$D_1(2430)$	2412 ± 9	314 ± 29	$D^*\pi(-264.8)$	$D^*\pi$ ($I = 1/2$) [282]
$T_{cc}(3875)$	3874.83 ± 0.11	0.41 ± 0.17	$DD^*(+2.3)$	D^0D^{*+}/D^+D^{*0} [285–287]
$X(3872)$	3871.65 ± 0.06	1.19 ± 0.21	$D\bar{D}^*(+5.5)$	$D^0\bar{D}^{*0}/D^+D^{*-}$ [285]
$P_c(4312)$	$4311.9^{+7.0}_{-0.9}$	10 ± 5	$\Sigma_c\bar{D}(+5.6)$	$\Sigma_c^+\bar{D}^0$ [288]
$P_c(4440)$	4440^{+4}_{-5}	21^{+10}_{-11}	$\Sigma_c\bar{D}^*(+19.2)$	$\Sigma_c^+\bar{D}^{*0}$ [288]
$P_c(4457)$	$4457.3^{+4.0}_{-1.8}$	$6.4^{+6.0}_{-2.8}$	$\Sigma_c\bar{D}^*(+2.2)$	$\Sigma_c^+\bar{D}^{*0}$ [288]
T_{bb} [predicted]	10583	1.4×10^{-5}	$BB^*(+21.2)$	B^0B^{*+}/B^+B^{*0} [289]
T_{bc} [predicted]	7110.41	—	$BD(7147.5)$	D^0B^+/D^+B^0 [921]

also summarized related theoretical studies on their properties, particularly those in the molecular picture. Here, we want to point out the connection between the unquenched quark model and the hadronic molecular picture. The unquenched quark model treats these states as mixtures of conventional $q\bar{q}/qqq$ hadrons and hadronic molecules [364, 430]. These studies supported the molecular picture. They only differ in the terminology. In the unquenched quark model, one explicitly treats the $q\bar{q}/qqq$ and MM/MB degrees of freedom. The (modified) $3P0$ model provides the couplings between the two components. On the other hand, in the hadronic molecular picture, only hadron-hadron interactions are explicitly considered. The existence of a $q\bar{q}$ or qqq core and the effects of missing coupled channels are hidden in the relevant parameters, such as those in the regulator function. The relative importance of these components can be quantified using the Weinberg compositeness. For this, there exist a large number of works; see Refs. [380, 936?–939] for example.

Now, the crucial question is to confirm or refute the molecular nature of these exotic states. This review discussed three novel approaches that can help confirm or deny the molecular picture.

First, one can derive from the molecular picture the underlying two-body hadron-hadron interactions. These interactions can be extended to other systems adopting heavy quark spin and flavor symmetry, SU(3)-flavor symmetry, and heavy antiquark diquark symmetry to predict multiplets of hadronic molecules. The discovery of these multiplets will provide a highly nontrivial verification of the hadronic molecular picture. Historically, this led to more confidence in the power of SU(3) flavor symmetry and the quark model's validity. Recent experimental discoveries of the three pentaquark states, $P_c(4312)$, $P_c(4440)$, $P_c(4457)$, the pentaquark and tetraquark states with strangeness, $P_{cs}(4459)$, $P_{cs}(4338)$, and $Z_{cs}(985)$, indeed hinted at the existence of multiplets of hadronic molecules. Much future work needs to be done regarding the predictions of multiplets. For instance, all the symmetries are broken at the level of a few tens percent. Such symmetry-breaking effects need to be studied in more detail because they can lead to the nonexistence of the predicted hadronic molecules. In addition, the discovery channels of these predicted states need to be identified, and whether they can be discovered at current or future experimental facilities should be examined. One more subtle issue is that compact quark models also predicted the existence of multiplets, see, e.g., Refs. [524, 940]. Therefore, even if they are discovered, a careful analysis of future experimental discoveries may be needed. It can well be that only by combining all three approaches summarized in the present review (and others not covered here) can one finally decipher the nature of the many exotic hadrons described in this review.

Second, assuming these exotic states are two-body hadronic molecules, one can derive their potential by reproducing their masses. With these potentials, one can study the existence of three-body hadronic molecules. The three-body hadronic molecules are made of three hadrons and thus have unique quantum numbers. They can form new kinds of matter in addition to nuclei and hypernuclei. If discovered, they can help verify the molecular nature of these exotic states. Therefore, we strongly encourage experimental searches for such three-body hadronic molecules. One notes that most previous studies focused on the heavy flavor sector. This is because, in the light flavor sector, the production/annihilation of light quark-antiquark pairs is easier from the energy perspective and, therefore, can occur more frequently. In addition, the kinematic effects of light hadrons are more significant, and therefore, relativistic effects need to be considered in many cases. As a result, light-quark sectors are more difficult to deal with. As discussed in this review, extensive studies on three-body hadronic molecules have been conducted, and significant progress has been made in the heavy flavor sector. Many three-body bound/resonant states, including their masses, intrinsic quantum numbers, and decay widths, have been predicted. These theoretical studies are valuable but still insufficient. More systematic and in-depth studies are needed. Most predictions of three-body hadronic molecules are based on assumptions about the existence of sub-two-body molecules, from which the underlying two-body hadron-hadron interactions are derived. We know that three-body forces

are important in nuclear physics and essential for precisely describing light nuclei (at least in nonrelativistic frameworks). Previous studies have neglected three-body forces. They need to be studied and their effects carefully evaluated in the future. The main difficulty lies in the lack of experimental constraints on three-body hadronic interactions. One also needs to figure out where to find the predicted three-body molecular states. Most previous studies mainly focused on their masses and decay widths. The ultimate way to verify all these theoretical studies is to discover them experimentally. One must study their production rates in various physical processes, inclusive or exclusive, in either hadron-hadron collisions or electron-positron colliders.

Third, we reviewed the application of the femtoscopy technique in providing direct experimental information on two-body hadron-hadron interactions. There were well-developed theoretical approaches to achieve such a purpose using the experimentally measured correlation functions. Using these interactions, one can, in principle, check whether they are strong enough to generate two-body bound states or resonances. Thus, one can check the hadronic molecular picture for the many discovered exotic states. In the past few years, we have seen increasing experimental and theoretical interests and the amount of work performed. Nevertheless, more work is still needed. For instance, although a spherical Gaussian source is often adopted in previous studies, there are still discussions on other choices, such as the Cauchy [941] or the lévy [942] distributions. Second, most previous studies rely on prior theoretical information to extract the underlying hadron-hadron interaction. It may be helpful to develop fully model-independent approaches to derive these interactions. The first experimental analyses have appeared, which require further theoretical investigation. Third, recent experimental and theoretical studies of three-hadron interaction using the femtoscopy technique have been reported [895, 896, 943]. This will provide an unprecedented opportunity for us to derive three-body interactions without complicated medium effects. This will also provide essential information for the studies of three-body hadronic molecules. Nevertheless, more theoretical studies are needed to exploit the experimental techniques fully.

To summarize, the experimental discoveries of the so-called exotic hadrons and the subsequent intensive theoretical studies have significantly enriched our understanding of the non-perturbative strong interaction. Nevertheless, a unified and complete picture of these hadrons is still missing, though the molecular picture seems to prevail. The three novel approaches reviewed in this work can help verify the molecular picture in a highly nontrivial way. We further point out future directions to advance the three approaches, our understanding of hadron spectra, and the underlying non-perturbative strong interaction.

VII. ACKNOWLEDGMENTS

We thank Eulogio Oset for carefully reading the draft and the many valuable comments on the first version of this manuscript. We are very grateful for our collaborators: Atsushi Hosaka, Xiang Liu, Manuel Pavon Valderrama, Ju-Jun Xie, Yin Huang, Si-Qiang Luo, Mario Sánchez Sánchez, Eulogio Oset, Xi-Zhe Ling, Fang-Zheng Peng, En Wang, Qi Wu, and Jia-Ming Xie. This work is partly supported by the National Key R&D Program of China under Grant No. 2023YFA1606703. Ming-Zhu Liu acknowledges support from the National Natural Science Foundation of China under Grant No.12105007. Zhi-Wei Liu acknowledges support from the National Natural Science Foundation of China under Grant No. 12347180, China Postdoctoral Science Foundation under Grants No. 2023M740189, and Postdoctoral Fellowship Program of CPSF under Grant No.GZC20233381.

Appendix A: Contact-range potentials

This section summarizes the contact-range potentials constrained by various symmetries. These serve as the basis for the predictions of multiplets of hadronic molecules.

1. $\bar{D}^{(*)}\Sigma_c^{(*)}$ heavy anti-meson and heavy baryon systems

In the EFTs, the leading-order interactions between pairs of hadrons include two terms: one-pion exchange and contact range, while the one-pion exchange can be treated perturbatively [160]. The following briefly explains how to construct the contact-range potentials for relevant systems constrained by the HQSS. For a pair of charmed mesons and baryons, the $\bar{D}^{(*)}\Sigma_c^{(*)}$ interaction results in seven states related by the HQSS [180, 547]. According to the HQSS, the spin wave function of the $\bar{D}^{(*)}\Sigma_c^{(*)}$ pairs can be written as follows, in terms of the spins of the heavy quarks s_{1H} and s_{2H} and those of the light quark(s) (often referred to as brown muck [944, 945]) s_{1L} and s_{2L} , where 1 and 2 denote $\bar{D}^{(*)}$ and $\Sigma_c^{(*)}$, respectively, via the following spin coupling formula,

$$|s_{1l}, s_{1h}, j_1; s_{2l}, s_{2h}, j_2; J\rangle = \sqrt{(2j_1 + 1)(2j_2 + 1)(2s_L + 1)(2s_H + 1)} \begin{pmatrix} s_{1l} & s_{2l} & s_L \\ s_{1h} & s_{2h} & s_H \\ j_1 & j_2 & J \end{pmatrix} |s_{1l}, s_{2l}, s_L; s_{1h}, s_{2h}, s_H; J\rangle. \quad (\text{A1})$$

More explicitly, for the seven $\bar{D}^{(*)}\Sigma_c^{(*)}$ states, the decomposition's read

$$\begin{aligned}
|\Sigma_c \bar{D}(1/2^-)\rangle &= \frac{1}{2}0_H \otimes 1/2_L + \frac{1}{2\sqrt{3}}1_H \otimes 1/2_L + \sqrt{\frac{2}{3}}1_H \otimes 3/2_L, \\
|\Sigma_c^* \bar{D}(3/2^-)\rangle &= -\frac{1}{2}0_H \otimes 3/2_L + \frac{1}{\sqrt{3}}1_H \otimes 1/2_L + \frac{\sqrt{\frac{5}{3}}}{2}1_H \otimes 3/2_L, \\
|\Sigma_c \bar{D}^*(1/2^-)\rangle &= \frac{1}{2\sqrt{3}}0_H \otimes 1/2_L + \frac{5}{6}1_H \otimes 1/2_L - \frac{\sqrt{2}}{3}1_H \otimes 3/2_L, \\
|\Sigma_c \bar{D}^*(3/2^-)\rangle &= \frac{1}{\sqrt{3}}0_H \otimes 3/2_L - \frac{1}{3}1_H \otimes 1/2_L + \frac{\sqrt{5}}{3}1_H \otimes 3/2_L, \\
|\Sigma_c^* \bar{D}^*(1/2^-)\rangle &= \sqrt{\frac{2}{3}}0_H \otimes 1/2_L - \frac{\sqrt{2}}{3}1_H \otimes 1/2_L - \frac{1}{3}1_H \otimes 3/2_L, \\
|\Sigma_c^* \bar{D}^*(3/2^-)\rangle &= \frac{\sqrt{\frac{5}{3}}}{2}0_H \otimes 3/2_L + \frac{\sqrt{5}}{3}1_H \otimes 1/2_L - \frac{1}{6}1_H \otimes 3/2_L, \\
|\Sigma_c^* \bar{D}^*(5/2^-)\rangle &= 1_H \otimes 3/2_L.
\end{aligned} \tag{A2}$$

In the heavy quark limit, the $\bar{D}^{(*)}\Sigma_c^{(*)}$ interactions are independent of the spin of the heavy quark. Therefore, the potentials can be parameterized by two coupling constants describing interactions between light quarks of spin 1/2 and 3/2, respectively, i.e., $F_{1/2} = \langle 1/2_L | V | 1/2_L \rangle$ and $F_{3/2} = \langle 3/2_L | V | 3/2_L \rangle$:

$$\begin{aligned}
V_{\Sigma_c \bar{D}(1/2^-)} &= \frac{1}{3}F_{1/2L} + \frac{2}{3}F_{3/2L}, \\
V_{\Sigma_c^* \bar{D}(3/2^-)} &= \frac{1}{3}F_{1/2L} + \frac{2}{3}F_{3/2L}, \\
V_{\Sigma_c \bar{D}^*(1/2^-)} &= \frac{7}{9}F_{1/2L} + \frac{2}{9}F_{3/2L}, \\
V_{\Sigma_c \bar{D}^*(3/2^-)} &= \frac{1}{9}F_{1/2L} + \frac{8}{9}F_{3/2L}, \\
V_{\Sigma_c^* \bar{D}^*(1/2^-)} &= \frac{8}{9}F_{1/2L} + \frac{1}{9}F_{3/2L}, \\
V_{\Sigma_c^* \bar{D}^*(3/2^-)} &= \frac{5}{9}F_{1/2L} + \frac{4}{9}F_{3/2L}, \\
V_{\Sigma_c^* \bar{D}^*(5/2^-)} &= F_{3/2L},
\end{aligned} \tag{A3}$$

which can be rewritten as a combination of C_a and C_b , i.e., $F_{1/2} = C_a - 2C_b$ and $F_{3/2} = C_a + C_b$ [547]. The potentials for the $\bar{D}^{(*)}\Sigma_c^{(*)}$ system are displayed in Table XLII. In terms of HADS, one can extend the $\bar{D}^{(*)}\Sigma_c^{(*)}$ system to the $\Xi_{cc}^{(*)}\Sigma_c^{(*)}$ and $\bar{D}^{(*)}T_{cc}^{(*)}$ systems, which indicate that the low energy constants of these systems are the same in the heavy quark limit [651, 682]. With a similar approach, we can easily derive the contact-range potentials for the $\Xi_{cc}^{(*)}\Sigma_c^{(*)}$ and $\bar{D}^{(*)}T_{cc}^{(*)}$ systems, which are tabulated in Table XLII.

If we apply the SU(3)-flavor symmetry to the $\bar{D}^{(*)}\Sigma_c^{(*)}$ system, it will result in another multiplet. For simplicity, we use the generic denotation $P^{(*)}$ for the heavy mesons and $\Sigma_Q^{(*)}$ for the heavy baryons. In addition, we use the notation $P_s^{(*)}$ for the heavy mesons with $S = -1$ and $\Xi_Q'^{(*)}$ ($\Omega_Q^{(*)}$) heavy baryons with

TABLE XLII. The lowest-order contact-range potentials for the heavy antimeson - heavy baryon, doubly heavy baryon - heavy baryon and compact doubly tetraquark states-heavy antimeson systems, which depend on two unknown coupling constants C_a and C_b .

state	J^P	V	state	J^P	V	state	J^P	V
$\bar{D}\Sigma_c$	$1/2^-$	C_a	$\Xi_{cc}\Sigma_c$	0^+	$C_a + \frac{2}{3}C_b$	$\bar{D}T_{\bar{c}\bar{c}}^0$	0^-	C_a
				1^+	$C_a - \frac{2}{9}C_b$	$\bar{D}^*T_{\bar{c}\bar{c}}^1$	0^-	$C_a - C_b$
$\bar{D}\Sigma_c^*$	$3/2^-$	C_a	$\Xi_{cc}\Sigma_c^*$	1^+	$C_a + \frac{5}{9}C_b$	$\bar{D}T_{\bar{c}\bar{c}}^1$	1^-	C_a
				2^+	$C_a - \frac{1}{3}C_b$	$\bar{D}^*T_{\bar{c}\bar{c}}^0$	1^-	C_a
$\bar{D}^*\Sigma_c$	$1/2^-$	$C_a - \frac{4}{3}C_b$	$\Xi_{cc}^*\Sigma_c$	1^+	$C_a - \frac{10}{9}C_b$	$\bar{D}^*T_{\bar{c}\bar{c}}^1$	1^-	$C_a - \frac{1}{2}C_b$
	$3/2^-$	$C_a + \frac{2}{3}C_b$		2^+	$C_a + \frac{2}{3}C_b$	$\bar{D}^*T_{\bar{c}\bar{c}}^2$	1^-	$C_a - \frac{3}{2}C_b$
	$1/2^-$	$C_a - \frac{5}{3}C_b$		0^+	$C_a - \frac{5}{3}C_b$	$\bar{D}T_{\bar{c}\bar{c}}^2$	2^-	C_a
$\bar{D}^*\Sigma_c^*$	$3/2^-$	$C_a - \frac{2}{3}C_b$	$\Xi_{cc}^*\Sigma_c^*$	1^+	$C_a - \frac{11}{9}C_b$	$\bar{D}^*T_{\bar{c}\bar{c}}^1$	2^-	$C_a + \frac{1}{2}C_b$
				2^+	$C_a - \frac{1}{3}C_b$	$\bar{D}^*T_{\bar{c}\bar{c}}^2$	2^-	$C_a - \frac{1}{2}C_b$
	$5/2^-$	$C_a + C_b$		3^+	$C_a + C_b$	$\bar{D}^*T_{\bar{c}\bar{c}}^2$	3^-	$C_a + C_b$

TABLE XLIII. SU(3)-flavor structure of the potentials for the heavy meson-baryon molecules, where the heavy meson belongs to a SU(3)-flavor triplet and the heavy baryon to a sextet.

Molecule	I	S	V	V_{eigen}
$\bar{P}\Sigma_Q$	$\frac{1}{2}$	0	V^O	—
$\bar{P}\Sigma_Q$	$\frac{3}{2}$	0	V^D	—
$\bar{P}\Xi'_Q$	0	-1	V^O	—
$\bar{P}\Xi'_Q - \bar{P}_s\Sigma_Q$	1	-1	$\begin{pmatrix} \frac{1}{3}V^O + \frac{2}{3}V^D & -\frac{\sqrt{2}}{3}(V^O - V^D) \\ -\frac{\sqrt{2}}{3}(V^O - V^D) & \frac{2}{3}V^O + \frac{1}{3}V^D \end{pmatrix}$	$\{V^O, V^D\}$
$\bar{P}\Omega_Q - \bar{P}_s\Xi'_Q$	$\frac{1}{2}$	-2	$\begin{pmatrix} \frac{1}{3}V^O + \frac{2}{3}V^D & -\frac{\sqrt{2}}{3}(V^O - V^D) \\ -\frac{\sqrt{2}}{3}(V^O - V^D) & \frac{2}{3}V^O + \frac{1}{3}V^D \end{pmatrix}$	$\{V^O, V^D\}$
$\bar{P}_s\Omega_Q$	0	-3	V^D	—

$S = -1$ ($S = -2$). In terms of SU(3)-flavor symmetry, the $(\bar{P}^{(*)}, \bar{P}_s^{(*)})$ heavy anti-mesons and $(\Sigma_Q^{(*)}, \Xi_Q'^{(*)}, \Omega_Q^{(*)})$ heavy baryons belong to the 3 and 6 representation of the SU(3)-flavor group. Such mesons and baryons can be decomposed into $3 \otimes 6 = 8 \oplus 10$, i.e., the octet and decuplet representations, where the SU(3) Clebsch-Gordan coefficients can be found in Ref. [666]. Their potentials can be decomposed into a

linear combination of an octet and decuplet contribution

$$V = \lambda_O V_O + \lambda_D V_D \quad (\text{A4})$$

with λ_O and λ_D numerical coefficients and V_O and V_D the octet and decuplet components. Table XLIII presents the heavy antimeson-baryon potentials decomposed into the octet and decuplet representations [667].

In addition, the heavy baryons belong to the “6” representation, the heavy baryons belong to the “3” representation (Λ_Q, Ξ_Q), and the heavy anti-meson would be decomposed into singlet and octet representations according to the SU(3)-flavor symmetry. According to the HQSS, the $\bar{P}^{(*)}B_3$ potentials are parameterised by one parameter [561]

$$V_{\bar{P}^{(*)}B_3} = C_a. \quad (\text{A5})$$

2. $\bar{D}^{(*)}D^{(*)}$ heavy anti-meson and heavy meson systems

The contact-range potentials of the $\bar{D}^{(*)}D^{(*)}$ system can also be derived using the same approach. Under HQSS, the $\bar{D}^{(*)}D^{(*)}$ system results in six states and are parameterized by two constants C_a and C_b [179]. With HADS, one can extend the $\bar{D}^{(*)}D^{(*)}$ system to the $\Xi_{cc}^{(*)}D^{(*)}$ and $\Xi_{cc}^{(*)}\Xi_{cc}^{(*)}$ systems, where the contact-range potentials C_a and C_b in these three systems are the same [684]. Table XLIV shows the potentials of these three systems.

If we apply the SU(3)-flavor symmetry to the $\bar{P}^{(*)}P^{(*)}$ system, we have a singlet and an octet irreducible group representation

$$3 \otimes \bar{3} = 1 \oplus 8. \quad (\text{A6})$$

The $\bar{P}^{(*)}P^{(*)}$ potential in terms of SU(3)-flavor symmetry are written as

$$V = \lambda_s V_s + \lambda_o V_o, \quad (\text{A7})$$

with V_s and V_o the singlet and octet components. For the potentials of the $D^{(*)}\bar{D}^{(*)}$ and $D_s^{(*)}\bar{D}_s^{(*)}$ in $I = 0$, it would be decomposed into

$$\begin{aligned} V(D^{(*)}\bar{D}^{(*)}(I=0)) &= \frac{1}{3}V_o + \frac{2}{3}V_s, \\ V(D_s^{(*)}\bar{D}_s^{(*)}(I=0)) &= \frac{2}{3}V_o + \frac{1}{3}V_s. \end{aligned} \quad (\text{A8})$$

Within HQSS, the S -wave heavy mesons form the doublet states (P, P^*). As the orbital angular momentum changes to $L = 1$, there will be two cases under HQSS. First, the orbital angular momentum $L = 1$

TABLE XLIV. Contact-range potentials for the heavy meson-heavy anti-meson, heavy meson-doubly heavy baryon, and doubly heavy baryon-doubly heavy anti-baryon systems depending on two unknown coupling constants, C_a and C_b . These coupling constants can be determined from the sum of C_a and C_b by reproducing the mass of $X(3872)$ and the ratio of C_a and C_b by the light-meson saturation approach.

state	J^{PC}	V	state	J^P	V	state	J^{PC}	V
$D\bar{D}$	0^{++}	C_a	$D\Xi_{cc}$	$\frac{1}{2}^-$	C_a	$\bar{\Xi}_{cc}\Xi_{cc}$	0^{-+}	$C_a - \frac{1}{3}C_b$
						$\bar{\Xi}_{cc}\Xi_{cc}$	1^{--}	$C_a + \frac{1}{9}C_b$
$D^*\bar{D}/D\bar{D}^*$	1^{++}	$C_a + C_b$	$D^*\Xi_{cc}$	$\frac{1}{2}^-$	$C_a + \frac{2}{3}C_b$		1^{-+}	$C_a + C_b$
	1^{+-}	$C_a - C_b$		$\frac{3}{2}^-$	$C_a - \frac{1}{3}C_b$	$\bar{\Xi}_{cc}^*\Xi_{cc}/\bar{\Xi}_{cc}\Xi_{cc}^*$	1^{--}	$C_a + \frac{1}{9}C_b$
							2^{-+}	$C_a + C_b$
							2^{--}	$C_a - \frac{5}{3}C_b$
			$D\Xi_{cc}^*$	$\frac{3}{2}^-$	C_a		0^{-+}	$C_a - \frac{5}{3}C_b$
	0^{++}	$C_a - 2C_b$		$\frac{1}{2}^-$	$C_a - \frac{5}{3}C_b$	$\bar{\Xi}_{cc}^*\Xi_{cc}^*$	1^{--}	$C_a - \frac{11}{9}C_b$
$D^*\bar{D}^*$	1^{+-}	$C_a - C_b$	$D^*\Xi_{cc}^*$	$\frac{3}{2}^-$	$C_a - \frac{2}{3}C_b$		2^{-+}	$C_a - \frac{1}{3}C_b$
	2^{++}	$C_a + C_b$		$\frac{5}{2}^-$	$C_a + C_b$		3^{--}	$C_a + C_b$

couples to the spin of the light quark, leading to total angular momenta $l = 1/2$ or $l = 3/2$, and then they couple to the spin of the heavy quark, finally resulting in two doublet states (D_0, D_1) and (D_1, D_2) . One should note that the widths of (D_0, D_1) are large, so they are not good candidates for hadronic molecules. However, the widths of (D_1, D_2) are rather narrow, which are good candidates for hadronic molecules. One example is the $Y(4260)$ which is proposed as a $\bar{D}D_1$ bound state [145, 477, 946]. Therefore, we also show the contact-range potentials of the $\bar{P}T$ system constrained by HQSS. In the heavy quark limit, their brown mucks are $s_{1l} = 1/2$ and $s_{2l} = 3/2$, which indicates that the $\bar{P}T$ potentials are only dependent on the two parameters F_1 and F_2 , i.e., $F_2 = \langle 2_L | V | 2_L \rangle$ and $F_1 = \langle 1_L | V | 1_L \rangle$. One should note that the $\bar{P}T$ system has direct and cross potentials. This work defines the direct potentials as D_a and D_b and the cross potentials as C_a and C_b . The cross potentials are related to their charge parity. Following ref. [484], the C-parity of the $\bar{P}T$ system is $C = \eta(-1)^{S-S_P-S_T}$ with $|\bar{P}T(\eta)\rangle = \frac{1}{\sqrt{2}}(|\bar{P}T\rangle + \eta|P\bar{T}\rangle)$, where S is the total spin of the $\bar{P}T$ system, S_P and S_T are the spins of meson P and T, and $\eta = \pm 1$. For $D\bar{D}_1$, the potential is $V_{D\bar{D}_1}^{J=1} = \frac{5}{8}F_2 + \frac{3}{8}F_1$, which is equal to D_a . In addition, in terms of $D^*D_2(J=3)$, we define $V_{D^*D_2}^{J=3} = F_2 = D_a + D_b$. With the above relationship, we obtain $F_1 = D_a - \frac{5}{3}D_b$ and $F_2 = D_a + D_b$. For the cross potential of $D\bar{D}_1$, we have $V = \frac{5}{8}F_2 + \frac{1}{8}F_1 = C_a$. From the $\bar{D}D_2^*$ potentials, we have $V = \frac{1}{8}F_2 - \frac{3}{8}F_1 = C_b$. We can obtain the cross potentials $F_1 = \frac{1}{2}C_a - \frac{5}{2}C_b$ and $F_2 = \frac{3}{2}C_a + \frac{1}{2}C_b$. Within

these relationships, the $\bar{P}H$ potentials are

$$\begin{aligned}
V_{\bar{D}D_1}(1^{-+}) &= \frac{5}{8}F_{2d} + \frac{3}{8}F_{1d} + \frac{5}{8}F_{2c} + \frac{1}{8}F_{1c} = D_a + C_a, \\
V_{\bar{D}D_1}(1^{--}) &= \frac{5}{8}F_{2d} + \frac{3}{8}F_{1d} - \frac{5}{8}F_{2c} - \frac{1}{8}F_{1c} = D_a - C_a, \\
V_{\bar{D}D_2^*}(2^{-+}) &= \frac{5}{8}F_{2d} + \frac{3}{8}F_{1d} + \frac{1}{8}F_{2c} - \frac{3}{8}F_{1c} = D_a + C_b, \\
V_{\bar{D}D_2^*}(2^{--}) &= \frac{5}{8}F_{2d} + \frac{3}{8}F_{1d} - \frac{1}{8}F_{2c} + \frac{3}{8}F_{1c} = D_a - C_b, \\
V_{\bar{D}^*D_1}(0^{-+}) &= F_{1d} - F_{1c} = D_a - \frac{5}{3}D_b - \frac{1}{2}C_a + \frac{5}{2}C_b, \\
V_{\bar{D}^*D_1}(0^{--}) &= F_{1d} + F_{1c} = D_a - \frac{5}{3}D_b + \frac{1}{2}C_a - \frac{5}{2}C_b, \\
V_{\bar{D}^*D_1}(1^{-+}) &= \frac{11}{16}F_{1d} + \frac{5}{16}F_{2d} + \frac{5}{16}F_{2c} - \frac{7}{16}F_{1c} = D_a - \frac{5}{6}D_b + \frac{1}{4}C_a + \frac{5}{4}C_b, \\
V_{\bar{D}^*D_1}(1^{--}) &= \frac{11}{16}F_{1d} + \frac{5}{16}F_{2d} - \frac{5}{16}F_{2c} + \frac{7}{16}F_{1c} = D_a - \frac{5}{6}D_b - \frac{1}{4}C_a - \frac{5}{4}C_b, \\
V_{\bar{D}^*D_1}(2^{-+}) &= \frac{1}{16}F_{1d} + \frac{15}{16}F_{2d} + \frac{3}{16}F_{2c} - \frac{1}{16}F_{1c} = D_a + \frac{5}{6}D_b + \frac{1}{4}C_a + \frac{1}{4}C_b, \\
V_{\bar{D}^*D_1}(2^{--}) &= \frac{1}{16}F_{1d} + \frac{15}{16}F_{2d} - \frac{3}{16}F_{2c} + \frac{1}{16}F_{1c} = D_a + \frac{5}{6}D_b - \frac{1}{4}C_a - \frac{1}{4}C_b, \\
V_{\bar{D}^*D_2^*}(1^{-+}) &= \frac{15}{16}F_{1d} + \frac{1}{16}F_{2d} + \frac{1}{16}F_{2c} + \frac{5}{16}F_{1c} = D_a - \frac{3}{2}D_b + \frac{1}{4}C_a - \frac{3}{4}C_b, \\
V_{\bar{D}^*D_2^*}(1^{--}) &= \frac{15}{16}F_{1d} + \frac{1}{16}F_{2d} - \frac{1}{16}F_{2c} - \frac{5}{16}F_{1c} = D_a - \frac{3}{2}D_b - \frac{1}{4}C_a + \frac{3}{4}C_b, \\
V_{\bar{D}^*D_2^*}(2^{-+}) &= \frac{9}{16}F_{1d} + \frac{7}{16}F_{2d} - \frac{5}{16}F_{2c} - \frac{9}{16}F_{1c} = D_a - \frac{1}{2}D_b - \frac{3}{4}C_a + \frac{5}{4}C_b, \\
V_{\bar{D}^*D_2^*}(2^{--}) &= \frac{9}{16}F_{1d} + \frac{7}{16}F_{2d} + \frac{5}{16}F_{2c} + \frac{9}{16}F_{1c} = D_a - \frac{1}{2}D_b + \frac{3}{4}C_a - \frac{5}{4}C_b, \\
V_{\bar{D}^*D_2^*}(3^{-+}) &= F_{2d} + F_{2c} = D_a + D_b + \frac{3}{2}C_a + \frac{1}{2}C_b, \\
V_{\bar{D}^*D_2^*}(3^{--}) &= F_{2d} - F_{2c} = D_a + D_b - \frac{3}{2}C_a - \frac{1}{2}C_b,
\end{aligned} \tag{A9}$$

which indicate that the $\bar{P}H$ potentials are dependent on four parameters. We should note that the potentials of Ref. [484] differ from ours by a factor of 2/3 due to the different conventions.

3. $\Sigma_Q \bar{\Sigma}_Q$ heavy baryon and heavy anti-baryon systems

Since the spin of the light quark of Σ_Q baryons is 1, the spin of the light quarks of $\Sigma_Q \bar{\Sigma}_Q$ can be 0, 1, or 2, which dictates that the $\Sigma_Q \bar{\Sigma}_Q$ potentials can be parameterized by three parameters denoted as C_0 , C_1 , and C_2 . In the following, we derive the $\Sigma_Q \bar{\Sigma}_Q$ contact-range potentials in detail. The C parity of the $\Sigma_Q \bar{\Sigma}_Q^*$ system is defined as $C = -\eta(-1)^{L+S}$ with the wave function $\frac{1}{\sqrt{2}}|\Sigma_Q \bar{\Sigma}_Q^* + \eta \bar{\Sigma}_Q \Sigma_Q^*\rangle$. Generally, the contact interactions of $\Sigma_Q^{(*)} \bar{\Sigma}_Q^{(*)}$ are expressed in three terms, i.e., $\mathcal{L} = C_0 + S_1 \cdot S_2 C_1 + Q_{ij} \cdot Q_{ij} C_2$, where C_1 is dependent on the spin-spin term, and $Q_{ij} \cdot Q_{ij}$ is related to the tensor-tensor interactions.

The three parameters C_1 , C_2 , and C_3 can be expressed by three parameters F_0 , F_1 , and F_2 . Assuming that $F_2 = C_0 + C_1 + C_2$, $\frac{2}{3}F_1 + \frac{1}{3}F_0 = C_0 - \frac{4}{3}C_1$, and $\frac{20}{27}F_2 + \frac{2}{9}F_1 + \frac{1}{27}F_0 = C_0 + \frac{4}{9}C_1$, we obtain $F_0 = C_0 - 2C_1 + 10C_2$, $F_1 = C_0 - C_1 - 5C_2$, and $F_2 = C_0 + C_1 + C_2$. As a result, one can parameterize the $\Sigma_Q^{(*)}\bar{\Sigma}_Q^{(*)}$ potentials by C_0 , C_1 , and C_2 as following:

$$\begin{aligned}
V_{\Sigma_Q\bar{\Sigma}_Q}(J^{PC} = 0^{-+}) &= \frac{2}{3}F_1 + \frac{1}{3}F_0 = C_0 - \frac{4}{3}C_1, \\
V_{\Sigma_Q\bar{\Sigma}_Q}(J^{PC} = 1^{--}) &= \frac{20}{27}F_2 + \frac{2}{9}F_1 + \frac{1}{27}F_0 = C_0 + \frac{4}{9}C_1, \\
V_{\bar{\Sigma}_Q^*\Sigma_Q}(J^{PC} = 1^{--}) &= \frac{5}{27}F_2 + \frac{2}{9}F_1 + \frac{16}{27}F_0 = C_0 - \frac{11}{9}C_1 + 5C_2, \\
V_{\bar{\Sigma}_Q^*\Sigma_Q}(J^{PC} = 1^{-+}) &= F_1 = C_0 - C_1 - 5C_2, \\
V_{\bar{\Sigma}_Q^*\Sigma_Q}(J^{PC} = 2^{-+}) &= \frac{2}{3}F_2 + \frac{1}{3}F_1 = C_0 + \frac{1}{3}C_1 - C_2, \\
V_{\bar{\Sigma}_Q^*\Sigma_Q}(J^{PC} = 2^{--}) &= F_2 = C_0 + C_1 + C_2, \\
V_{\Sigma_Q^*\bar{\Sigma}_Q^*}(J^{PC} = 0^{-+}) &= \frac{1}{3}F_1 + \frac{2}{3}F_0 = C_0 - \frac{5}{3}C_1 + 5C_2, \\
V_{\Sigma_Q^*\bar{\Sigma}_Q^*}(J^{PC} = 1^{--}) &= \frac{2}{27}F_2 + \frac{10}{27}F_0 + \frac{5}{9}F_1 = C_0 - \frac{11}{9}C_1 + C_2, \\
V_{\Sigma_Q^*\bar{\Sigma}_Q^*}(J^{PC} = 2^{-+}) &= \frac{1}{3}F_2 + \frac{2}{3}F_1 = C_0 - \frac{1}{3}C_1 - 3C_2, \\
V_{\Sigma_Q^*\bar{\Sigma}_Q^*}(J^{PC} = 3^{--}) &= F_2 = C_0 + C_1 + C_2.
\end{aligned} \tag{A10}$$

Appendix B: Light-meson saturation approach

The contact-range potentials of a given system are dependent on several couplings. The best approach to determine these couplings is to fit the experimental data. However, for the $\bar{D}^{(*)}D^{(*)}$ system there exists only one molecular candidate $X(3872)$, which can only determine the sum of C_a and C_b . We, therefore, resort to the light-meson saturation approach to estimate the ratio of C_a and C_b and determine the value of C_a and C_b [684]. The light meson saturation approach can only estimate the relative strength and the sign of these couplings from the hypothesis that they are saturated by the exchange of light mesons, in particular, the vector mesons ρ and ω , and scalar meson σ [164, 182]. The proportionality constant is unknown and depends on the details of the renormalization procedure.

The contact-range potentials of the $\bar{D}^{(*)}\Sigma_c^{(*)}$ system can be parameterized by two couplings C_a and C_b , which are saturated by the sigma and vector meson exchanges:

$$\begin{aligned}
C_a^{sat}(\Lambda \sim m_\sigma, m_V) &\propto C_a^S + C_a^V, \\
C_b^{sat}(\Lambda \sim m_\sigma, m_V) &\propto C_b^V,
\end{aligned} \tag{B1}$$

TABLE XLV. Couplings of the light mesons of the OBE model (π , σ , ρ , ω) to the heavy-meson and heavy-baryon fields. For the magnetic-type coupling of the ρ and ω vector mesons we have used the decomposition $f_V = \kappa_V g_V$, with $V = \rho, \omega$. M refers to the mass scale (in units of MeV) involved in the magnetic-type couplings [149].

Coupling Value for P/P^*		Coupling Value for		Coupling Value for Σ_Q/Σ_Q^*	
g_1	0.60	g_2	0.84	g_3	0.84
$g_{\sigma 1}$	3.4	$g_{\sigma 2}$	6.8	$g_{\sigma 3}$	3.4
$g_{\rho 1}$	2.6	$g_{\rho 2}$	5.8	$g_{\rho 2}$	5.8
$g_{\omega 1}$	2.6	$g_{\omega 2}$	5.8	$g_{\omega 2}$	5.8
$\kappa_{\rho 1}$	2.3	$\kappa_{\rho 2}$	1.7	$\kappa_{\rho 2}$	1.7
$\kappa_{\omega 1}$	2.3	$\kappa_{\omega 2}$	1.7	$\kappa_{\omega 2}$	1.7
M	940				

where the cutoff $\Lambda \sim m_\sigma, m_V$ implies that the saturation works at an EFT cutoff close to the masses of exchanged mesons, i.e., $0.6 \sim 0.8$ GeV. The values of saturated couplings are expected to be proportional to the potentials of light-meson exchanges in the OBE model once we have removed the spurious Dirac-delta potential [149].

Thus, C_a and C_b can be written as

$$\begin{aligned}
 C_a^{sat(\sigma)}(\Lambda \sim m_\sigma) &\propto -\frac{g_{\sigma 1} g_{\sigma 2}}{m_\sigma^2}, \\
 C_a^{sat(V)}(\Lambda \sim m_V) &\propto \frac{g_{v1} g_{v2}}{m_v^2} (1 + \vec{\tau}_1 \cdot \vec{T}_2), \\
 C_b^{sat(V)}(\Lambda \sim m_V) &\propto \frac{f_{v1} f_{v2}}{6M^2} (1 + \vec{\tau}_1 \cdot \vec{T}_2),
 \end{aligned} \tag{B2}$$

where g_{σ_i} denote the charm meson and charm baryon coupling to the sigma meson, g_{vi} and f_{vi} denote electric-type and magnetic-type couplings between charm mesons as well as charm baryons and light vector mesons, and M is a mass scale to render f_{vi} dimensionless, see, e.g., Table XLV. With the above preparations, we calculate the ratio of C_a^{sat} and C_b^{sat} as

$$\frac{C_b^{sat}}{C_a^{sat}} = 0.124. \tag{B3}$$

Generally, the couplings of C_a and C_b can be fully determined by reproducing the masses of $P_c(4440)$ and $P_c(4457)$. In scenario A, the $P_c(4440)$ and $P_c(4457)$ are assumed as the $\bar{D}^* \Sigma_c$ bound states with $J^P = 1/2^-$ and $J^P = 3/2^-$, while in scenario B they are assumed as $J^P = 3/2^-$ and $J^P = 1/2^-$. As the cutoff $\Lambda = 0.75$ GeV, we obtain the $C_a = -30.8 \text{ GeV}^{-2}$ and $C_b = 5.1 \text{ GeV}^{-2}$ for scenario A and $C_a = -34.2 \text{ GeV}^{-2}$ and $C_b = -5.1 \text{ GeV}^{-2}$ for scenario B. The ratio of C_a and C_b in scenario A and

scenario B can be estimated as

$$\begin{aligned}\left(\frac{C_b}{C_a}\right)^A &= -0.166, \\ \left(\frac{C_b}{C_a}\right)^B &= 0.149.\end{aligned}\tag{B4}$$

We can see that the ratio of C_a and C_b in scenario B coincides with the value of the light meson saturation approach, which shows that the OBE model supports the results of scenario B of the EFT, in agreement with our numerical calculation [547?]. In other words, we can see that the light meson saturation approach works well, which inspires us to apply the light meson saturation approach to other systems.

We estimate the couplings of C_a and C_b of the $\bar{D}^{(*)}D^{(*)}$ system by the sigma and vector meson exchange saturation. C_a and C_b can be written as

$$\begin{aligned}C_a^{sat(\sigma)}(\Lambda \sim m_\sigma) &\propto -\frac{g_{\sigma 1}^2}{m_\sigma^2}, \\ C_a^{sat(V)}(\Lambda \sim m_V) &\propto -\frac{g_{v1}^2}{m_v^2}(1 - \vec{\tau}_1 \cdot \vec{\tau}_2), \\ C_b^{sat(V)}(\Lambda \sim m_V) &\propto -\frac{f_{v1}^2}{6M^2}(1 - \vec{\tau}_1 \cdot \vec{\tau}_2).\end{aligned}\tag{B5}$$

Then we obtain the ratio of C_a and C_b

$$\frac{C_b^{sat}}{C_a^{sat}} = 0.347.\tag{B6}$$

Such a ratio is larger than that of the $\bar{D}^{(*)}\Sigma_c^{(*)}$ system, which indicates that the spin-spin term plays a more important role in the $\bar{D}^{(*)}D^{(*)}$ system. As for the $D^{(*)}D^{(*)}$ system, we obtain the ratio of C_a and C_b via the G-parity transformation

$$\frac{C_b^{sat}}{C_a^{sat}} = 0.246.\tag{B7}$$

For the $\bar{D}^{(*)}D_{1,2}$ system, the contact-range potentials are parameterized as four parameters, D_a , D_b , C_a and C_b , e.g.,

$$V = D_a + \sigma_1 \cdot S_2 D_b + \Sigma_1 \cdot \Sigma_2 C_a + Q_{1ij} \cdot Q_{2ji} C_b,\tag{B8}$$

where σ and S demote the operator of spin 1/2 and 1. Σ denotes the operator of spin 1 to 1/2 transition. The tensor operator Q is defined as $Q_{ij} = (\sigma_i \Sigma_j + \Sigma_j \sigma_i)/2$. Using the light meson saturation approach,

D_a , D_b , C_a , and C_b can be saturated by

$$\begin{aligned}
D_a^{sat(\sigma)}(\Lambda \sim m_\sigma) &\propto -\frac{g_{\sigma 1} g_{\sigma 3}}{m_\sigma^2}, \\
D_a^{sat(V)}(\Lambda \sim m_V) &\propto \frac{g_{v1} g_{v3}}{m_v^2} (\eta + \vec{\tau}_1 \cdot \vec{\tau}_2), \\
D_b^{sat(V)}(\Lambda \sim m_V) &\propto \frac{f_{v1} f_{v3}}{6M^2} (\eta + \vec{\tau}_1 \cdot \vec{\tau}_2), \\
C_a^{sat(V)}(\Lambda \sim m_V) &\propto -\frac{f_v'^2}{4M^2} \frac{\omega_v^2 + \frac{1}{3}\mu_V^2}{\mu_V^2} (\eta + \vec{\tau}_1 \cdot \vec{\tau}_2), \\
C_b^{sat(V)}(\Lambda \sim m_V) &\propto -\frac{h_v^2}{80M^4} \mu_V^2 (\eta + \vec{\tau}_1 \cdot \vec{\tau}_2),
\end{aligned} \tag{B9}$$

where f_v' and h_v' represent the electric dipole and magnetic quadrupole couplings of the vector meson. The couplings $\mu_v = \sqrt{m_V^2 - m_\omega^2}$ and $m_\omega = \sqrt{m_{D_1}^2 - m_D^2}$. The subscript of “3” denotes the couplings between D_1/D_2 and light mesons. The relevant couplings are $g_{\sigma 3} = 3.4$, $g_{v3} = 2.9$, $f_{v2} = 4.6 \cdot 2.9$, $f_v' = 3.1 \cdot 2.9$, and $h_v = 10.7 \cdot 2.9$ [484].

Appendix C: Effective Lagrangians

In this section, we numerate the effective Lagrangians relevant to the studies covered in this review. The Lagrangians describing the interactions between charmed mesons and σ , ρ , ω mesons read

$$\mathcal{L}_{HH\pi} = \frac{g_1}{\sqrt{2}f_\pi} \langle H^\dagger \vec{\sigma} \cdot \nabla (\vec{\tau} \cdot \vec{\pi}) H \rangle, \tag{C1}$$

$$\mathcal{L}_{HH\sigma} = g_{\sigma 1} \langle H^\dagger \sigma H \rangle, \tag{C2}$$

$$\mathcal{L}_{HH\rho} = g_{\rho 1} \langle H^\dagger \vec{\tau} \cdot \vec{\rho}_0 H \rangle - \frac{f_{\rho 1}}{4M_1} \langle \epsilon_{ijk} H^\dagger \sigma_k \vec{\tau} \cdot (\partial_i \vec{\rho}_j - \partial_j \vec{\rho}_i) H \rangle, \tag{C3}$$

$$\mathcal{L}_{HH\omega} = g_{\omega 1} \langle H^\dagger \omega_0 H \rangle - \frac{f_{\omega 1}}{4M_1} \langle \epsilon_{ijk} H^\dagger \sigma_k (\partial_i \omega_j - \partial_j \omega_i) H \rangle, \tag{C4}$$

where g_1 , $g_{\sigma 1}$, g_{v1} , and g_{v1} represent the couplings between a charmed meson and the light mesons, and H refers to the superfield, i.e., $H = D + D^* \cdot \sigma$, satisfying the HQSS.

The Lagrangians describing the interactions between charmed baryons and σ, ρ, ω mesons read

$$\mathcal{L}_{SS\pi} = \frac{g_2}{\sqrt{2}f_\pi} (\vec{S}^\dagger \times \vec{S}) \cdot \nabla(\vec{T} \cdot \vec{\pi}), \quad (\text{C5})$$

$$\mathcal{L}_{ST\pi} = \frac{g_3}{\sqrt{2}f_\pi} \vec{S}^\dagger \cdot \nabla \vec{\pi} T, \quad (\text{C6})$$

$$\mathcal{L}_{SS\sigma} = g_{\sigma 2} \vec{S}^\dagger \sigma \vec{S}, \quad (\text{C7})$$

$$\mathcal{L}_{SS\rho} = g_{\rho 2} \vec{S}^\dagger \vec{T} \cdot \vec{\rho}_0 \vec{S} - \frac{f_{\rho 2}}{4M_2} \epsilon_{ijk} (\vec{S}^\dagger \times \vec{S})_k \vec{T} \cdot (\partial_i \vec{\rho}_j - \partial_j \vec{\rho}_i), \quad (\text{C8})$$

$$\mathcal{L}_{SS\omega} = g_{\omega 2} \vec{S}^\dagger \omega_0 \vec{S} - \frac{f_{\omega 2}}{4M_2} \epsilon_{ijk} (\vec{S}^\dagger \times \vec{S})_k (\partial_i \omega_j - \partial_j \omega_i), \quad (\text{C9})$$

$$\mathcal{L}_{TT\omega} = g_{\omega 3} T^\dagger \omega_0 T, \quad (\text{C10})$$

$$\mathcal{L}_{ST\rho} = -\frac{f_{\rho 3}}{4M_3} \epsilon_{ijk} \vec{S}_k^\dagger (\partial_i \vec{\rho}_j - \partial_j \vec{\rho}_i) T, \quad (\text{C11})$$

where the superfield \vec{S} is $\vec{S} = \frac{1}{\sqrt{3}} \vec{\sigma} \vec{\Sigma}_c + \vec{\Sigma}_c^*$ in the heavy quark limit.

As for the excited charmed mesons, the superfield for D_1 and D_2 in the heavy quark limit is $G^i = D_2^{ij} \sigma^j + \sqrt{\frac{2}{3}} D_1^i + i \sqrt{\frac{1}{6}} \epsilon_{ijk} D_1^j \sigma^k$. The corresponding Lagrangians are written as

$$\mathcal{L}_{GG\pi} = \frac{g_3}{\sqrt{2}f_\pi} \langle G^{i\dagger} \vec{\sigma} \cdot \nabla(\vec{\tau} \cdot \vec{\pi}) G_i \rangle, \quad (\text{C12})$$

$$\mathcal{L}_{GH\pi} = \frac{g'_3}{\sqrt{2}f_\pi} \langle G^{i\dagger} \cdot \nabla_i \vec{\sigma} \cdot \nabla(\vec{\tau} \cdot \vec{\pi}) \rangle, \quad (\text{C13})$$

$$\mathcal{L}_{GG\sigma} = g_{\sigma 3} \langle G^{i\dagger} \sigma G_i \rangle, \quad (\text{C14})$$

$$\mathcal{L}_{GGv} = g_{v 3} \langle G^{i\dagger} \vec{\tau} \cdot \vec{\rho}_0 G_i \rangle - \frac{f_{v 3}}{4M_1} \langle \epsilon_{ijk} G^{\beta\dagger} \sigma_k \vec{\tau} \cdot (\partial_i \vec{\rho}_j - \partial_j \vec{\rho}_i) G_\beta \rangle, \quad (\text{C15})$$

$$\mathcal{L}_{GHv} = -\frac{f'_{v 3}}{4M_1} \langle G^{i\dagger} \sigma_j (\partial_i \omega_j - \partial_j \omega_i) H \rangle. \quad (\text{C16})$$

The coupling $g_{\sigma 3}$ is estimated to be $g_{\sigma 3} = \frac{1}{3} g_{\sigma NN}$, which equals the ground-state charmed meson couplings to the σ meson.

Appendix D: Lippmann-Schwinger equation

Hadronic molecules are bound states of $q\bar{q}$ mesons and qqq baryons. They manifest themselves as poles in the corresponding scattering amplitudes. As a result, it is necessary to study the scattering amplitudes T , defined by the S matrix, i.e., $S = 1 + 2i\rho T$. Since the S matrix conserves causality and the probability of current, it satisfies analyticity and unitarity. From the optical theorem $\text{Im } T = T^\dagger \rho T$ and the unitarity condition, one can obtain the imaginary part of the T matrix $\text{Im } T^{-1} = -\rho$ for $\sqrt{s} > m_1 + m_2$. One can obtain the T matrix by solving the Bethe-Salpeter (BS) equation or Lippmann-Schwinger (LS) equation with hadron-hadron potentials as inputs, i.e., $T = V + VGT$. As a result, the phase space is equal to $\rho = \text{Im } G$. The analytical continuation of the scattering amplitude T to the unphysical sheet has consequences

only in the loop functions. In terms of the Schwartz reflection theorem [947], an analytic function $f[z]$ in the complex plane obeys $f[z^*]^* = f[z]$. Applying this theorem to the loop function, one has $G(\sqrt{s} - i\varepsilon) = [G(\sqrt{s} + i\varepsilon)]^*$. With the relationship $[G(\sqrt{s} + i\varepsilon)]^* = G(\sqrt{s} + i\varepsilon) - i2\text{Im } G(\sqrt{s} + i\varepsilon)$, one can obtain $G(\sqrt{s} - i\varepsilon) = G(\sqrt{s} + i\varepsilon) - i2\text{Im } G(\sqrt{s} + i\varepsilon)$. Since the loop function at the end of the first Riemann sheet is equal to that at the beginning of the second Riemann sheet, i.e., $G_{II}(\sqrt{s} + i\varepsilon) = G_I(\sqrt{s} - i\varepsilon)$, the loop function in the second Riemann sheet is $G_{II}(\sqrt{s} + i\varepsilon) = G_I(\sqrt{s} + i\varepsilon) - i2\text{Im } G_I(\sqrt{s} + i\varepsilon)$. Therefore, the loop function in the second Riemann sheet is $G_{II}(\sqrt{s}) = G_I(\sqrt{s}) - 2i \text{Im } G_I(\sqrt{s})$. Moving from the first sheet to the second sheet, one needs to cross the unitarity cut and change the sign of the imaginary part of the loop function. The convention for the imaginary part is

$$\text{Sheet I } \text{Im}G > 0; \quad \text{Sheet II } \text{Im}G < 0; \quad (\text{D1})$$

As for the BS equation, it can be written as

$$T = V + VGT, \quad (\text{D2})$$

where V is the coupled-channel potential determined by the contact-range EFT approach described in the Appendix, and G is the two-body propagator. To avoid the ultraviolet divergence in evaluating the loop function G and keep the unitarity of the T matrix, we include a regulator of Gaussian form $F(q^2, k) = e^{-2q^2/\Lambda^2} / e^{-2k^2/\Lambda^2}$ in the integral as

$$G(\sqrt{s}) = 2m_1 \int \frac{d^3q}{(2\pi)^3} \frac{\omega_1 + \omega_2}{2\omega_1\omega_2} \frac{F(q^2, k)}{(\sqrt{s})^2 - (\omega_1 + \omega_2)^2 + i\varepsilon}, \quad (\text{D3})$$

where \sqrt{s} is the total energy in the center-of-mass (c.m.) frame of m_1 and m_2 , $\omega_i = \sqrt{m_i^2 + q^2}$ is the energy of the particle, Λ is the momentum cutoff, and the c.m. momentum k is ,

$$k = \frac{\sqrt{s - (m_1 + m_2)^2} \sqrt{s - (m_1 - m_2)^2}}{2\sqrt{s}}. \quad (\text{D4})$$

We denote the loop function in the physical and unphysical sheets as $G_I(\sqrt{s})$ and $G_{II}(\sqrt{s})$, which are related by $G_{II}(\sqrt{s}) = G_I(\sqrt{s}) - 2i\text{Im } G_I(\sqrt{s})$ [183, 947]. The imaginary part of Eq. (39) can be derived via the Plemelj-Sokhotski formula, i.e., $\text{Im } G(\sqrt{s}) = -\frac{2m_1}{8\pi} \frac{k}{\sqrt{s}}$, and then Eq. (39) in the unphysical sheet is written as

$$G_{II}(\sqrt{s}) = G_I(\sqrt{s}) + i\frac{2m_1}{4\pi} \frac{k}{\sqrt{s}}. \quad (\text{D5})$$

The loop function can also be regularized in other methods, such as the momentum cut-off scheme and the dimensional regularization scheme [123, 125, 127, 154, 948]. The loop function parameterized in the

dimensional regularization scheme is

$$\begin{aligned}
 G = & \frac{2M_l}{16\pi^2} \left\{ a(\mu) + \ln \frac{m^2}{\mu^2} + \frac{M^2 - m^2 + s}{2s} \ln \frac{M^2}{\mu^2} \right. \\
 & - \frac{p_{cm}(\sqrt{s})}{\sqrt{s}} [\ln(s - (M^2 - m^2) + 2\sqrt{s}p_{cm}(\sqrt{s})) \\
 & + \ln(s + (M^2 - m^2) + 2\sqrt{s}p_{cm}(\sqrt{s}))] \\
 & - \ln(-s - (M^2 - m^2) + 2\sqrt{s}p_{cm}(\sqrt{s}))] \\
 & \left. - \ln(-s + (M^2 - m^2) + 2\sqrt{s}p_{cm}(\sqrt{s})) \right\},
 \end{aligned} \tag{D6}$$

where $a(\mu)$ is the subtraction constant, μ is the regularisation scale, and p_{cm} is the c.m. momentum of a given system [949].

The loop function in the cut-off scheme is regularised as

$$(2\pi)^3 \frac{\omega_1 + \omega_2}{2\omega_1\omega_2} \frac{1}{(\sqrt{s})^2 - (\omega_1 + \omega_2)^2 + i\varepsilon}, \tag{D7}$$

where q_{max} is a cutoff momentum [123]. Generally speaking, these two approaches are equivalent [950].

The loop function in Eq.(39) is relativistic. Its non-relativistic form is

$$G(\sqrt{s}) = \int \frac{d^3q}{(2\pi)^3} \frac{F(q^2, k)}{\sqrt{s} - m_1 - m_2 - q^2/(2\mu_{12}) + i\varepsilon}, \tag{D8}$$

where the c.m. momentum is $k = \sqrt{2\mu_{12}(\sqrt{s} - m_1 - m_2)}$. As for the non-relativistic case, the amplitude is obtained by the LS equation. In the unphysical sheet, the non-relativistic loop function changes to

$$G_{II}(\sqrt{s}) = G_I(\sqrt{s}) + i \frac{\mu_{12}k}{\pi} F(k^2, k). \tag{D9}$$

The amplitudes T in the relativistic and non-relativistic cases are related via $T_r = 4m_1m_2T_{nor}$. In Fig. 1, we show the real part (left panel) and imaginary part (right panel) of the $\eta_c N$ loop function in both the relativistic (black) and non-relativistic (red) scenarios as a function of the c.m. energy. One can see that the difference between the real parts is more visible than that between the imaginary parts. One should be careful in dealing with coupled-channel problems, especially for hadrons containing light quarks.

Once the poles generated by the coupled-channel interactions are found, one determines the couplings between the molecular states and their constituents from the residues of the corresponding poles,

$$g_i g_j = \lim_{\sqrt{s} \rightarrow \sqrt{s_0}} (\sqrt{s} - \sqrt{s_0}) T_{ij}(\sqrt{s}), \tag{D10}$$

where g_i denotes the coupling of channel i to the dynamically generated state, and $\sqrt{s_0}$ is the pole position. The couplings reflect the strength of the molecule couplings to their constituents.

Recent studies have shown that elementary bare states can couple to hadronic molecules, resulting in the mixing of states composed of a bare state and a hadronic molecule. To estimate the proportion of each

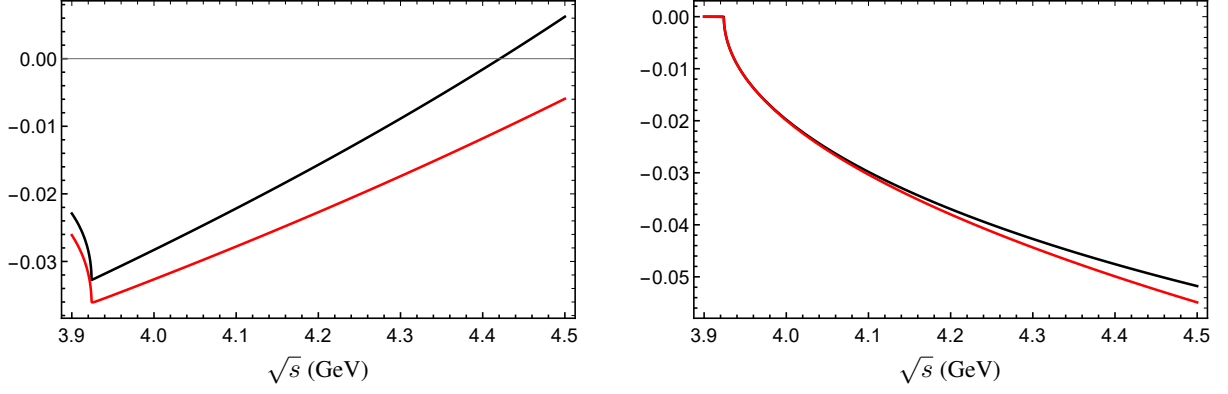


FIG. 39. Real (left) and imaginary (right) parts of the $\eta_c N$ loop function as a function of the c.m. energy \sqrt{s} . The black and red lines represent those of the relativistic and non-relativistic propagators.

component, one often turns to the Weinberg compositeness theorem, which is parameterized by a parameter Z [951]

$$Z = 1 - \int d\alpha |\langle \alpha | d \rangle|^2, \quad Z = \sum_n |\langle n | d \rangle|^2, \quad (\text{D11})$$

where $|\alpha\rangle$ and $|n\rangle$ represent the eigenstates of the continuum and discrete elementary particle state in a free Hamiltonian H_0 , and $|d\rangle$ represents the physical state in the total Hamiltonian H with the normalization of $\sum_n |n\rangle \langle n| + \int d\alpha |\alpha\rangle \langle \alpha| = 1$ and $\langle d | d \rangle = 1$. Z is the probability of finding an elementary component in the physical state corresponding to the field renormalization constant. Here, $Z = 0$ implies that the physical state is a pure hadronic molecule, and $0 < Z < 1$ indicates an elementary component inside the physical state. With the relationship $|d\rangle = [H - H_0]^{-1} V |d\rangle$, one can obtain

$$1 - Z = \text{Re} \left[\int d\alpha \frac{|\langle \alpha | V | d \rangle|^2}{(E_\alpha + B)^2} \right], \quad (\text{D12})$$

where $d\alpha = \frac{4\pi p^2 dp}{(2\pi)^3} = \frac{\mu^{3/2}}{\sqrt{2\pi^2}} E^{1/2} dE$. The coupling between $|d\rangle$ and $|\alpha\rangle$ can be characterised by an effective coupling constant g ,

$$g^2 = \frac{2\pi\sqrt{2\mu B}}{\mu^2} (1 - Z), \quad (\text{D13})$$

which encodes the structure information of the composite system. For a scattering process in the low energy approximation, the scattering length a and effective range r_0 are related

$$a = \frac{2(1 - Z)}{2 - Z} \frac{1}{\sqrt{2\mu B}}, \quad r_0 = -\frac{Z}{1 - Z} \frac{1}{\sqrt{2\mu B}}. \quad (\text{D14})$$

On the other hand, the applicability of the Weinberg compositeness rule can be extended by taking into account unstable hadrons, the CDD (Castillejo-Dalitz-Dyson) pole, and higher order corrections [374, 938, 952–958].

In general, hadron-hadron scattering amplitudes can be characterized by the scattering length a and effective range r_0 using the effective range expansion(ERE)

$$f(k) = \frac{1}{k \cot \delta - ik} \approx \frac{1}{-\frac{1}{a} + \frac{1}{2}r_0 k^2 - ik}, \quad (\text{D15})$$

where the typical momentum is defined as $k = \sqrt{2\mu E}$. Such a hadron-hadron scattering amplitude can also be described by the above T matrix, e.g., $T = (1 - VG)^{-1}V$. Based on the couplings g_i obtained above, one can further arrive at the probability of finding a state in a specific channel [959]

$$P_i = -g_i^2 \frac{\partial G_{ii}(\sqrt{s})}{\partial \sqrt{s}}, \quad (\text{D16})$$

and then obtain $Z = 1 - \sum_i P_i$, which can estimate the proportion of hadronic molecule components. In Ref. [380], the interaction range is considered to extend the applicability of the Weinberg compositeness rule originally obtained in the limit of small energy and a zero range interaction. Another extension of Weinberg's formula is proposed in Ref. [939].

In case of no poles (either bound, resonant, or virtual) around the mass threshold of m_1 and m_2 , one can study the corresponding scattering length, which is obtained from the above scattering amplitude $T(\sqrt{s})$

$$\begin{aligned} a_{\sqrt{s}=m_1+m_2} &= \frac{\mu}{2\pi} T_{non}(\sqrt{s}), \\ a_{\sqrt{s}=m_1+m_2} &= \frac{1}{8\pi\sqrt{s}} T_r(\sqrt{s}), \end{aligned} \quad (\text{D17})$$

where T_{non} and T_r represent the scattering amplitudes with nonrelativistic and relativistic propagators, respectively.

One should note that the above discussions only focused on separable potentials, e.g., contact-range potentials. Considering the potentials as a function of the momentum, one can not convert the L-S equation to a simple algebraic equation, which needs to be solved numerically [176, 177].

Appendix E: The Gaussian-Expansion Method

Many methods have been proposed to solve few-body systems, e.g., the Gaussian expansion method (GEM) [268, 960], the stochastic variational method (SVM) [961–963], the hyperspherical harmonic variational method (HH) [964], the Green function Monte Carlo (GFMC) [965], the diffusion Monte Carlo method (DMC) [588, 966–968], the no-core shell model (NCSM) [969–971], the resonating group method (RGM) [972], the Fadeev equation [973], the Fixed center approximation (FCA) [974, 975], Complex scaling (CS) [976, 977], the QCD sum rule (QSR) [978, 979], the Born-Oppenheimer (BO) approximation [980], etc. Kamimura proposed the GEM for the non-adiabatic three-body calculations of muonic

molecules and muon-atomic collisions in 1988 [960]. Due to its many advantages such as fast convergence and high precision [268, 981], the GEM has been widely applied to investigate few-body systems in nuclear physics [268] and hadron physics [270–273, 822, 829, 834, 982, 983]. Combining the GEM with the Complex scaling method, which Aguilar, Combes, and Balslev proposed in 1971 originally [984, 985], one can treat bound states, resonant states, and continuum states on an equal footing. For comprehensive benchmark studies of these few-body methods, one can refer to Refs [986, 987].

The Schrödinger equation of the three-body system reads

$$\hat{H}\Psi_{JM}^{total} = E\Psi_{JM}^{total}, \quad (E1)$$

with the corresponding Hamiltonian

$$\hat{H} = \sum_{i=1}^3 \frac{p_i^2}{2m_i} - T_{c.m.} + \sum_{1 \leq i < j}^3 V(r_{ij}), \quad (E2)$$

where $T_{c.m.}$ is the kinetic energy of the center of mass and $V(r_{ij})$ is the potential between particle i and particle j .

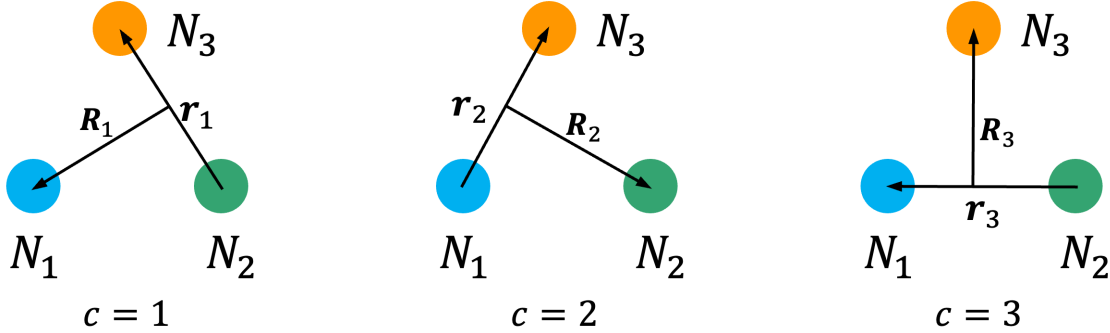


FIG. 40. Three permutations of the Jacobi coordinates for a three-body system

The three Jacobi coordinates for a three-body system are shown in Fig. 40. The total wave function is a sum of the amplitudes of the three rearrangements of the Jacobi coordinates, i.e., of the channels ($c = 1 - 3$) shown in Fig. 40

$$\Psi_{JM}^{total} = \sum_{c,\alpha} C_{c,\alpha} \Psi_{JM,\alpha}^c(\mathbf{r}_c, \mathbf{R}_c), \quad (E3)$$

where $\alpha = \{nl, NL, \Lambda, tT, s\Sigma\}$ and $C_{c,\alpha}$ are the expansion coefficients. Here l and L are the orbital angular momenta for the coordinates r and R , s and t are the spin and isospin of the two-body subsystem in each channel, Λ , T , and Σ are the total orbital angular momentum, isospin, and spin. n and N are the numbers of Gaussian basis functions corresponding to coordinates r and R , respectively.

The wave function of each channel has the following form

$$\Psi_{JM,\alpha}^c(\mathbf{r}_c, \mathbf{R}_c) = H_{t,T}^c \otimes [\chi_{s,\Sigma}^c \otimes \Phi_{lL,\Lambda}^c]_{JM}, \quad (\text{E4})$$

where $H_{t,T}^c$ is the isospin wave function, $\chi_{s,\Sigma}^c$ the spin wave function, and $\Phi_{lL,\Lambda}^c$ the orbital wave function.

The total isospin wave function reads

$$\begin{aligned} H_{t_1,T}^{c=1} &= [[\eta(N_2)\eta(N_3)]_{t_1}\eta(N_1)]_T, \\ H_{t_2,T}^{c=2} &= [[\eta(N_1)\eta(N_3)]_{t_2}\eta(N_2)]_T, \\ H_{t_3,T}^{c=3} &= [[\eta(N_2)\eta(N_1)]_{t_3}\eta(N_3)]_T, \end{aligned} \quad (\text{E5})$$

where η is the isospin wave function of each particle. The spin wave function can be obtained in a way similar to the isospin wave function. The orbital wave function $\Phi_{lL,\Lambda}^c$ is given in terms of the Gaussian basis functions

$$\Phi_{lL,\Lambda}^c(\mathbf{r}_c, \mathbf{R}_c) = [\phi_{n_c l_c}^G(\mathbf{r}_c) \psi_{N_c L_c}^G(\mathbf{R}_c)]_{\Lambda}, \quad (\text{E6})$$

with

$$\begin{aligned} \phi_{nlm}^G(\mathbf{r}_c) &= N_{nl} r_c^l e^{-\nu_n r_c^2} Y_{lm}(\hat{r}_c), \\ \psi_{NLM}^G(\mathbf{R}_c) &= N_{NL} R_c^L e^{-\lambda_n R_c^2} Y_{LM}(\hat{R}_c). \end{aligned} \quad (\text{E7})$$

Here $N_{nl}(N_{NL})$ are the normalization constants of the Gaussian basis, and the range parameters ν_n and λ_n are given by

$$\begin{aligned} \nu_n &= 1/r_n^2, \quad r_n = r_{min} a^{n-1} \quad (n = 1 - n_{max}), \\ \lambda_N &= 1/R_N^2, \quad R_N = R_{min} A^{N-1} \quad (N = 1 - N_{max}), \end{aligned} \quad (\text{E8})$$

in which $\{n_{max}, r_{min}, a \text{ or } r_{max}\}$ and $\{N_{max}, R_{min}, A \text{ or } R_{max}\}$ are Gaussian basis parameters.

With the basis expansion, the Schrödinger equation of this system is transformed into a generalized matrix eigenvalue problem:

$$[T_{\alpha\alpha'}^{ab} + V_{\alpha\alpha'}^{ab} - EN_{\alpha\alpha'}^{ab}] C_{b,\alpha'} = 0. \quad (\text{E9})$$

Here, $T_{\alpha\alpha'}^{ab}$ is the kinetic matrix element, $V_{\alpha\alpha'}^{ab}$ is the potential matrix element, and $N_{\alpha\alpha'}^{ab}$ is the normalization matrix element. a and b are Jacobi channels ranging from 1 to 3. The eigenenergy E and coefficients $C_{b,\alpha'}$ are determined by the Rayleigh-Ritz variational principle.

- [2] P. Hagler, Phys. Rept. **490**, 49 (2010), arXiv:0912.5483 [hep-lat].
- [3] C. A. Aidala, S. D. Bass, D. Hasch, and G. K. Mallot, Rev. Mod. Phys. **85**, 655 (2013), arXiv:1209.2803 [hep-ph].
- [4] M. Gell-Mann, Phys. Lett. **8**, 214 (1964).
- [5] S. Godfrey and N. Isgur, Phys. Rev. D **32**, 189 (1985).
- [6] S. Capstick and N. Isgur, Phys. Rev. D **34**, 2809 (1986).
- [7] T. Barnes, S. Godfrey, and E. S. Swanson, Phys. Rev. D **72**, 054026 (2005), arXiv:hep-ph/0505002.
- [8] B.-Q. Li and K.-T. Chao, Phys. Rev. **D79**, 094004 (2009), arXiv:0903.5506 [hep-ph].
- [9] S. Godfrey and K. Moats, Phys. Rev. D **92**, 054034 (2015), arXiv:1507.00024 [hep-ph].
- [10] S. K. Choi et al. (Belle), Phys. Rev. Lett. **91**, 262001 (2003), arXiv:hep-ex/0309032.
- [11] M. Ablikim et al. (BESIII), Phys. Rev. Lett. **129**, 192002 (2022), arXiv:2202.00621 [hep-ex].
- [12] M. Ablikim et al. (BESIII), Phys. Rev. Lett. **110**, 252001 (2013), arXiv:1303.5949 [hep-ex].
- [13] R. Aaij et al. (LHCb), (2021), arXiv:2109.01038 [hep-ex].
- [14] R. Aaij et al. (LHCb), Phys. Rev. Lett. **122**, 222001 (2019), arXiv:1904.03947 [hep-ex].
- [15] C. J. Morningstar and M. J. Peardon, Phys. Rev. D **56**, 4043 (1997), arXiv:hep-lat/9704011.
- [16] C. J. Morningstar and M. J. Peardon, Phys. Rev. D **60**, 034509 (1999), arXiv:hep-lat/9901004.
- [17] Y. Chen et al., Phys. Rev. D **73**, 014516 (2006), arXiv:hep-lat/0510074.
- [18] E. Klempt and A. Zaitsev, Phys. Rept. **454**, 1 (2007), arXiv:0708.4016 [hep-ph].
- [19] V. Mathieu, N. Kochelev, and V. Vento, Int. J. Mod. Phys. E **18**, 1 (2009), arXiv:0810.4453 [hep-ph].
- [20] E. Gregory, A. Irving, B. Lucini, C. McNeile, A. Rago, C. Richards, and E. Rinaldi, JHEP **10**, 170 (2012), arXiv:1208.1858 [hep-lat].
- [21] W. Ochs, J. Phys. G **40**, 043001 (2013), arXiv:1301.5183 [hep-ph].
- [22] N. Brambilla, A. Pineda, J. Soto, and A. Vairo, Rev. Mod. Phys. **77**, 1423 (2005), arXiv:hep-ph/0410047.
- [23] E. S. Swanson, Phys. Rept. **429**, 243 (2006), arXiv:hep-ph/0601110.
- [24] H.-X. Chen, W. Chen, X. Liu, and S.-L. Zhu, Phys. Rept. **639**, 1 (2016), arXiv:1601.02092 [hep-ph].
- [25] A. Hosaka, T. Hyodo, K. Sudoh, Y. Yamaguchi, and S. Yasui, Prog. Part. Nucl. Phys. **96**, 88 (2017), arXiv:1606.08685 [hep-ph].
- [26] R. F. Lebed, R. E. Mitchell, and E. S. Swanson, Prog. Part. Nucl. Phys. **93**, 143 (2017), arXiv:1610.04528 [hep-ph].
- [27] E. Oset et al., Int. J. Mod. Phys. E **25**, 1630001 (2016), arXiv:1601.03972 [hep-ph].
- [28] A. Esposito, A. Pilloni, and A. D. Polosa, Phys. Rept. **668**, 1 (2017), arXiv:1611.07920 [hep-ph].
- [29] H.-X. Chen, W. Chen, X. Liu, Y.-R. Liu, and S.-L. Zhu, Rept. Prog. Phys. **80**, 076201 (2017), arXiv:1609.08928 [hep-ph].
- [30] J.-M. Richard, Few Body Syst. **57**, 1185 (2016), arXiv:1606.08593 [hep-ph].
- [31] Y. Dong, A. Faessler, and V. E. Lyubovitskij, Prog. Part. Nucl. Phys. **94**, 282 (2017).
- [32] F.-K. Guo, C. Hanhart, U.-G. Meißner, Q. Wang, Q. Zhao, and B.-S. Zou, Rev. Mod. Phys. **90**, 015004 (2018), arXiv:1705.00141 [hep-ph].

- [33] S. L. Olsen, T. Skwarnicki, and D. Zieminska, *Rev. Mod. Phys.* **90**, 015003 (2018), arXiv:1708.04012 [hep-ph].
- [34] A. Ali, J. S. Lange, and S. Stone, *Prog. Part. Nucl. Phys.* **97**, 123 (2017), arXiv:1706.00610 [hep-ph].
- [35] M. Karliner, J. L. Rosner, and T. Skwarnicki, *Ann. Rev. Nucl. Part. Sci.* **68**, 17 (2018), arXiv:1711.10626 [hep-ph].
- [36] F.-K. Guo, X.-H. Liu, and S. Sakai, *Prog. Part. Nucl. Phys.* **112**, 103757 (2020), arXiv:1912.07030 [hep-ph].
- [37] N. Brambilla, S. Eidelman, C. Hanhart, A. Nefediev, C.-P. Shen, C. E. Thomas, A. Vairo, and C.-Z. Yuan, *Phys. Rept.* **873**, 1 (2020), arXiv:1907.07583 [hep-ex].
- [38] Y.-R. Liu, H.-X. Chen, W. Chen, X. Liu, and S.-L. Zhu, *Prog. Part. Nucl. Phys.* **107**, 237 (2019), arXiv:1903.11976 [hep-ph].
- [39] H.-X. Chen, W. Chen, X. Liu, Y.-R. Liu, and S.-L. Zhu, (2022), arXiv:2204.02649 [hep-ph].
- [40] L. Meng, B. Wang, G.-J. Wang, and S.-L. Zhu, (2022), arXiv:2204.08716 [hep-ph].
- [41] L. Micu, *Nucl. Phys. B* **10**, 521 (1969).
- [42] A. Le Yaouanc, L. Oliver, O. Pene, and J. C. Raynal, *Phys. Rev. D* **8**, 2223 (1973).
- [43] Z.-Y. Zhou and Z. Xiao, *Phys. Rev. D* **84**, 034023 (2011), arXiv:1105.6025 [hep-ph].
- [44] P. G. Ortega, J. Segovia, D. R. Entem, and F. Fernandez, *Phys. Rev. D* **94**, 074037 (2016), arXiv:1603.07000 [hep-ph].
- [45] S.-Q. Luo, B. Chen, Z.-W. Liu, and X. Liu, *Eur. Phys. J. C* **80**, 301 (2020), arXiv:1910.14545 [hep-ph].
- [46] Z. Yang, G.-J. Wang, J.-J. Wu, M. Oka, and S.-L. Zhu, (2021), arXiv:2107.04860 [hep-ph].
- [47] B.-Q. Li, C. Meng, and K.-T. Chao, *Phys. Rev. D* **80**, 014012 (2009), arXiv:0904.4068 [hep-ph].
- [48] B.-Q. Li and K.-T. Chao, *Commun. Theor. Phys.* **52**, 653 (2009), arXiv:0909.1369 [hep-ph].
- [49] Q.-T. Song, D.-Y. Chen, X. Liu, and T. Matsuki, *Phys. Rev. D* **91**, 054031 (2015), arXiv:1501.03575 [hep-ph].
- [50] Z. Yin and D. Jido, (2023), arXiv:2312.13582 [hep-ph].
- [51] R. L. Jaffe and F. Wilczek, *Phys. Rev. Lett.* **91**, 232003 (2003), arXiv:hep-ph/0307341.
- [52] H. Hogaasen and P. Sorba, *Mod. Phys. Lett. A* **19**, 2403 (2004), arXiv:hep-ph/0406078.
- [53] H. Hogaasen, J. M. Richard, and P. Sorba, *Phys. Rev. D* **73**, 054013 (2006), arXiv:hep-ph/0511039.
- [54] F. Buccella, H. Hogaasen, J.-M. Richard, and P. Sorba, *Eur. Phys. J. C* **49**, 743 (2007), arXiv:hep-ph/0608001.
- [55] J. Wu, Y.-R. Liu, K. Chen, X. Liu, and S.-L. Zhu, *Phys. Rev. D* **97**, 094015 (2018), arXiv:1605.01134 [hep-ph].
- [56] S.-Q. Luo, K. Chen, X. Liu, Y.-R. Liu, and S.-L. Zhu, *Eur. Phys. J. C* **77**, 709 (2017), arXiv:1707.01180 [hep-ph].
- [57] M. Karliner and J. L. Rosner, *Phys. Rev. D* **90**, 094007 (2014), arXiv:1408.5877 [hep-ph].
- [58] M. Karliner, S. Nussinov, and J. L. Rosner, *Phys. Rev. D* **95**, 034011 (2017), arXiv:1611.00348 [hep-ph].
- [59] M. Karliner and J. L. Rosner, *Phys. Rev. Lett.* **119**, 202001 (2017), arXiv:1707.07666 [hep-ph].
- [60] T. Mehen, *Phys. Rev. D* **96**, 094028 (2017), arXiv:1708.05020 [hep-ph].
- [61] J.-B. Cheng, S.-Y. Li, Y.-R. Liu, Z.-G. Si, and T. Yao, *Chin. Phys. C* **45**, 043102 (2021), arXiv:2008.00737 [hep-ph].
- [62] H.-T. An, Z.-W. Liu, F.-S. Yu, and X. Liu, *Phys. Rev. D* **106**, L111501 (2022), arXiv:2207.02813 [hep-ph].

- [63] Y. Kim, M. Oka, and K. Suzuki, Phys. Rev. D **105**, 074021 (2022), arXiv:2202.06520 [hep-ph].
- [64] T.-W. Wu and Y.-L. Ma, (2022), arXiv:2211.15094 [hep-ph].
- [65] G. Yang, J. Ping, and J. Segovia, Symmetry **12**, 1869 (2020), arXiv:2009.00238 [hep-ph].
- [66] J.-M. Richard, A. Valcarce, and J. Vijande, Phys. Rev. Lett. **124**, 212001 (2020), arXiv:2005.06894 [hep-ph].
- [67] Q. Meng, E. Hiyama, A. Hosaka, M. Oka, P. Gubler, K. U. Can, T. T. Takahashi, and H. S. Zong, Phys. Lett. B **814**, 136095 (2021), arXiv:2009.14493 [nucl-th].
- [68] T. A. DeGrand, R. L. Jaffe, K. Johnson, and J. E. Kiskis, Phys. Rev. D **12**, 2060 (1975).
- [69] R. L. Jaffe, Phys. Rev. D **15**, 267 (1977).
- [70] D. Strottman, Phys. Rev. D **20**, 748 (1979).
- [71] A. Bernotas and V. Simonis, Lith. J. Phys. **49**, 19 (2009), arXiv:0808.1220 [hep-ph].
- [72] A. Bernotas and V. Šimonis, Phys. Rev. D **87**, 074016 (2013), arXiv:1302.5918 [hep-ph].
- [73] W.-X. Zhang, H. Xu, and D. Jia, Phys. Rev. D **104**, 114011 (2021), arXiv:2109.07040 [hep-ph].
- [74] W.-X. Zhang, H.-T. An, and D. Jia, Eur. Phys. J. C **83**, 727 (2023), arXiv:2304.14876 [hep-ph].
- [75] S. H. Lee, A. Mihara, F. S. Navarra, and M. Nielsen, Phys. Lett. B **661**, 28 (2008), arXiv:0710.1029 [hep-ph].
- [76] Z.-G. Wang and T. Huang, Phys. Rev. D **89**, 054019 (2014), arXiv:1310.2422 [hep-ph].
- [77] J. M. Dias, F. S. Navarra, M. Nielsen, and C. M. Zanetti, Phys. Rev. D **88**, 016004 (2013), arXiv:1304.6433 [hep-ph].
- [78] C.-F. Qiao and L. Tang, Eur. Phys. J. C **74**, 2810 (2014), arXiv:1308.3439 [hep-ph].
- [79] H.-X. Chen, W. Chen, X. Liu, T. G. Steele, and S.-L. Zhu, Phys. Rev. Lett. **115**, 172001 (2015), arXiv:1507.03717 [hep-ph].
- [80] Z.-G. Wang, Eur. Phys. J. C **76**, 70 (2016), arXiv:1508.01468 [hep-ph].
- [81] H.-X. Chen, Q. Mao, W. Chen, A. Hosaka, X. Liu, and S.-L. Zhu, Phys. Rev. D **95**, 094008 (2017), arXiv:1703.07703 [hep-ph].
- [82] J. J. Dudek, R. G. Edwards, N. Mathur, and D. G. Richards, Phys. Rev. D **77**, 034501 (2008), arXiv:0707.4162 [hep-lat].
- [83] L. Liu, G. Moir, M. Peardon, S. M. Ryan, C. E. Thomas, P. Vilaseca, J. J. Dudek, R. G. Edwards, B. Joo, and D. G. Richards (Hadron Spectrum), JHEP **07**, 126 (2012), arXiv:1204.5425 [hep-ph].
- [84] J. J. Dudek, R. G. Edwards, P. Guo, and C. E. Thomas (Hadron Spectrum), Phys. Rev. D **88**, 094505 (2013), arXiv:1309.2608 [hep-lat].
- [85] G. Moir, M. Peardon, S. M. Ryan, C. E. Thomas, and L. Liu, JHEP **05**, 021 (2013), arXiv:1301.7670 [hep-ph].
- [86] S. Prelovsek, C. B. Lang, L. Leskovec, and D. Mohler, Phys. Rev. D **91**, 014504 (2015), arXiv:1405.7623 [hep-lat].
- [87] T. Inoue, N. Ishii, S. Aoki, T. Doi, T. Hatsuda, Y. Ikeda, K. Murano, H. Nemura, and K. Sasaki (HAL QCD), Phys. Rev. Lett. **106**, 162002 (2011), arXiv:1012.5928 [hep-lat].
- [88] D. Mohler, S. Prelovsek, and R. M. Woloshyn, Phys. Rev. D **87**, 034501 (2013), arXiv:1208.4059 [hep-lat].
- [89] D. Mohler, C. B. Lang, L. Leskovec, S. Prelovsek, and R. M. Woloshyn, Phys. Rev. Lett. **111**, 222001 (2013), arXiv:1308.3175 [hep-lat].

- [90] Y. Ikeda, B. Charron, S. Aoki, T. Doi, T. Hatsuda, T. Inoue, N. Ishii, K. Murano, H. Nemura, and K. Sasaki, *Phys. Lett. B* **729**, 85 (2014), arXiv:1311.6214 [hep-lat].
- [91] S. Prelovsek and L. Leskovec, *Phys. Rev. Lett.* **111**, 192001 (2013), arXiv:1307.5172 [hep-lat].
- [92] Y. Chen *et al.* (CLQCD), *Phys. Rev. D* **92**, 054507 (2015), arXiv:1503.02371 [hep-lat].
- [93] C. B. Lang, L. Leskovec, M. Padmanath, and S. Prelovsek, *Phys. Rev. D* **95**, 014510 (2017), arXiv:1610.01422 [hep-lat].
- [94] S. Gongyo *et al.*, *Phys. Rev. Lett.* **120**, 212001 (2018), arXiv:1709.00654 [hep-lat].
- [95] R. A. Briceno, J. J. Dudek, and R. D. Young, *Rev. Mod. Phys.* **90**, 025001 (2018), arXiv:1706.06223 [hep-lat].
- [96] S. Aoki and T. Doi, “Lattice QCD and Baryon-Baryon Interactions,” in *Handbook of Nuclear Physics*, edited by I. Tanihata, H. Toki, and T. Kajino (2023) pp. 1–31, arXiv:2402.11759 [hep-lat].
- [97] K. U. Can, G. Erkol, B. Isildak, M. Oka, and T. T. Takahashi, *Phys. Lett. B* **726**, 703 (2013), arXiv:1306.0731 [hep-lat].
- [98] K. U. Can, G. Erkol, B. Isildak, M. Oka, and T. T. Takahashi, *JHEP* **05**, 125 (2014), arXiv:1310.5915 [hep-lat].
- [99] H. Bahtiyar, K. U. Can, G. Erkol, and M. Oka, *Phys. Lett. B* **747**, 281 (2015), arXiv:1503.07361 [hep-lat].
- [100] K. U. Can, G. Erkol, M. Oka, and T. T. Takahashi, *Phys. Rev. D* **92**, 114515 (2015), arXiv:1508.03048 [hep-lat].
- [101] H. Bahtiyar, K. U. Can, G. Erkol, M. Oka, and T. T. Takahashi, *Phys. Lett. B* **772**, 121 (2017), arXiv:1612.05722 [hep-lat].
- [102] K. U. Can, *Int. J. Mod. Phys. A* **36**, 2130013 (2021), arXiv:2107.13159 [hep-lat].
- [103] E. Follana, C. Davies, G. Lepage, and J. Shigemitsu (HPQCD, UKQCD), *Phys. Rev. Lett.* **100**, 062002 (2008), arXiv:0706.1726 [hep-lat].
- [104] A. Bazavov *et al.* (Fermilab Lattice, MILC), *Phys. Rev. D* **85**, 114506 (2012), arXiv:1112.3051 [hep-lat].
- [105] H. Na, C. J. Monahan, C. T. H. Davies, R. Horgan, G. P. Lepage, and J. Shigemitsu, *Phys. Rev. D* **86**, 034506 (2012), arXiv:1202.4914 [hep-lat].
- [106] R. J. Dowdall, C. T. H. Davies, R. R. Horgan, C. J. Monahan, and J. Shigemitsu (HPQCD), *Phys. Rev. Lett.* **110**, 222003 (2013), arXiv:1302.2644 [hep-lat].
- [107] P. A. Boyle, L. Del Debbio, A. Jüttner, A. Khamseh, F. Sanfilippo, and J. T. Tsang, *JHEP* **12**, 008 (2017), arXiv:1701.02644 [hep-lat].
- [108] Y. Chen, W.-F. Chiu, M. Gong, Z. Liu, and Y. Ma (χ QCD), *Chin. Phys. C* **45**, 023109 (2021), arXiv:2008.05208 [hep-lat].
- [109] H. Na, C. T. H. Davies, E. Follana, G. P. Lepage, and J. Shigemitsu, *Phys. Rev. D* **82**, 114506 (2010), arXiv:1008.4562 [hep-lat].
- [110] C. M. Bouchard, G. P. Lepage, C. Monahan, H. Na, and J. Shigemitsu, *Phys. Rev. D* **90**, 054506 (2014), arXiv:1406.2279 [hep-lat].
- [111] S. Meinel, *Phys. Rev. Lett.* **118**, 082001 (2017), arXiv:1611.09696 [hep-lat].
- [112] L. J. Cooper, C. T. H. Davies, J. Harrison, J. Komijani, and M. Wingate (HPQCD), *Phys. Rev. D* **102**, 014513 (2020), [Erratum: *Phys.Rev.D* 103, 099901 (2021)], arXiv:2003.00914 [hep-lat].

- [113] W. G. Parrott, C. Bouchard, and C. T. H. Davies ((HPQCD collaboration)§, HPQCD), Phys. Rev. D **107**, 014510 (2023), arXiv:2207.12468 [hep-lat].
- [114] L. Liu, K. Orginos, F.-K. Guo, C. Hanhart, and U.-G. Meissner, Phys. Rev. **D87**, 014508 (2013), arXiv:1208.4535 [hep-lat].
- [115] A. Martínez Torres, E. Oset, S. Prelovsek, and A. Ramos, JHEP **05**, 153 (2015), arXiv:1412.1706 [hep-lat].
- [116] G. S. Bali, S. Collins, A. Cox, and A. Schäfer, Phys. Rev. D **96**, 074501 (2017), arXiv:1706.01247 [hep-lat].
- [117] G. K. C. Cheung, C. E. Thomas, D. J. Wilson, G. Moir, M. Peardon, and S. M. Ryan (Hadron Spectrum), JHEP **02**, 100 (2021), arXiv:2008.06432 [hep-lat].
- [118] J. Bulava et al. (Baryon Scattering (BaSc)), Phys. Rev. Lett. **132**, 051901 (2024), arXiv:2307.10413 [hep-lat].
- [119] J.-M. Xie, J.-X. Lu, L.-S. Geng, and B.-S. Zou, Phys. Rev. D **108**, L111502 (2023), arXiv:2307.11631 [hep-ph].
- [120] Y. Yamaguchi, A. Hosaka, S. Takeuchi, and M. Takizawa, J. Phys. G **47**, 053001 (2020), arXiv:1908.08790 [hep-ph].
- [121] N. Isgur and G. Karl, Phys. Rev. **D18**, 4187 (1978).
- [122] N. Kaiser, P. B. Siegel, and W. Weise, Nucl. Phys. A **594**, 325 (1995), arXiv:nucl-th/9505043.
- [123] E. Oset and A. Ramos, Nucl. Phys. **A635**, 99 (1998), arXiv:nucl-th/9711022 [nucl-th].
- [124] J. Oller and U. G. Meissner, Phys. Lett. B **500**, 263 (2001), arXiv:hep-ph/0011146.
- [125] D. Jido, J. A. Oller, E. Oset, A. Ramos, and U. G. Meissner, Nucl. Phys. **A725**, 181 (2003), arXiv:nucl-th/0303062 [nucl-th].
- [126] M. Lage, U.-G. Meissner, and A. Rusetsky, Phys. Lett. B **681**, 439 (2009), arXiv:0905.0069 [hep-lat].
- [127] T. Hyodo and D. Jido, Prog. Part. Nucl. Phys. **67**, 55 (2012), arXiv:1104.4474 [nucl-th].
- [128] Z.-H. Guo and J. A. Oller, Phys. Rev. C **87**, 035202 (2013), arXiv:1210.3485 [hep-ph].
- [129] J.-X. Lu, L.-S. Geng, M. Doering, and M. Mai, (2022), arXiv:2209.02471 [hep-ph].
- [130] J. K. Ahn (LEPS), Nucl. Phys. A **721**, 715 (2003).
- [131] G. Agakishiev et al. (HADES), Phys. Rev. C **87**, 025201 (2013), arXiv:1208.0205 [nucl-ex].
- [132] K. Moriya et al. (CLAS), Phys. Rev. C **87**, 035206 (2013), arXiv:1301.5000 [nucl-ex].
- [133] S. Ajimura et al. (J-PARC E15), Phys. Lett. B **789**, 620 (2019), arXiv:1805.12275 [nucl-ex].
- [134] A. V. Anisovich, A. V. Sarantsev, V. A. Nikonov, V. Burkert, R. A. Schumacher, U. Thoma, and E. Klempt, Eur. Phys. J. A **56**, 139 (2020).
- [135] A. De Rujula, H. Georgi, and S. L. Glashow, Phys. Rev. Lett. **38**, 317 (1977).
- [136] M. B. Voloshin and L. B. Okun, JETP Lett. **23**, 333 (1976).
- [137] A. V. Manohar and M. B. Wise, Nucl. Phys. B **399**, 17 (1993), arXiv:hep-ph/9212236.
- [138] T. E. O. Ericson and G. Karl, Phys. Lett. B **309**, 426 (1993).
- [139] D. Gamermann and E. Oset, Phys. Rev. **D80**, 014003 (2009), arXiv:0905.0402 [hep-ph].
- [140] N. Li and S.-L. Zhu, Phys. Rev. D **86**, 074022 (2012), arXiv:1207.3954 [hep-ph].
- [141] Q. Wu, D.-Y. Chen, and T. Matsuki, Eur. Phys. J. C **81**, 193 (2021), arXiv:2102.08637 [hep-ph].
- [142] N. A. Tornqvist, Phys. Rev. Lett. **67**, 556 (1991).

- [143] N. A. Tornqvist, Z. Phys. **C61**, 525 (1994), arXiv:hep-ph/9310247 [hep-ph].
- [144] E. S. Swanson, Phys. Lett. B **588**, 189 (2004), arXiv:hep-ph/0311229.
- [145] G.-J. Ding, Phys. Rev. D **79**, 014001 (2009), arXiv:0809.4818 [hep-ph].
- [146] Y.-R. Liu, X. Liu, W.-Z. Deng, and S.-L. Zhu, Eur. Phys. J. **C56**, 63 (2008), arXiv:0801.3540 [hep-ph].
- [147] X. Liu, Z.-G. Luo, Y.-R. Liu, and S.-L. Zhu, Eur. Phys. J. C **61**, 411 (2009), arXiv:0808.0073 [hep-ph].
- [148] Z.-C. Yang, Z.-F. Sun, J. He, X. Liu, and S.-L. Zhu, Chin. Phys. **C36**, 6 (2012), arXiv:1105.2901 [hep-ph].
- [149] M.-Z. Liu, T.-W. Wu, M. Sánchez Sánchez, M. P. Valderrama, L.-S. Geng, and J.-J. Xie, Phys. Rev. D **103**, 054004 (2021), arXiv:1907.06093 [hep-ph].
- [150] D. P. Rathaud and A. K. Rai, (2017), arXiv:1706.09323 [hep-ph].
- [151] T. Iritani et al. (HAL QCD), Phys. Lett. B **792**, 284 (2019), arXiv:1810.03416 [hep-lat].
- [152] Y. Lyu, H. Tong, T. Sugiura, S. Aoki, T. Doi, T. Hatsuda, J. Meng, and T. Miyamoto, Phys. Rev. Lett. **127**, 072003 (2021), arXiv:2102.00181 [hep-lat].
- [153] J. He and D.-Y. Chen, Eur. Phys. J. C **78**, 94 (2018), arXiv:1712.05653 [hep-ph].
- [154] J.-J. Wu, R. Molina, E. Oset, and B. S. Zou, Phys. Rev. Lett. **105**, 232001 (2010), arXiv:1007.0573 [nucl-th].
- [155] C. W. Xiao, J. Nieves, and E. Oset, Phys. Rev. **D88**, 056012 (2013), arXiv:1304.5368 [hep-ph].
- [156] L. Roca, J. Nieves, and E. Oset, Phys. Rev. D **92**, 094003 (2015), arXiv:1507.04249 [hep-ph].
- [157] Y. Yamaguchi, Y. Abe, K. Fukukawa, and A. Hosaka, EPJ Web Conf. **204**, 01007 (2019).
- [158] L. S. Geng and E. Oset, Phys. Rev. **D79**, 074009 (2009), arXiv:0812.1199 [hep-ph].
- [159] R. Molina and E. Oset, Phys. Rev. D **80**, 114013 (2009), arXiv:0907.3043 [hep-ph].
- [160] J.-X. Lu, L.-S. Geng, and M. P. Valderrama, Phys. Rev. **D99**, 074026 (2019), arXiv:1706.02588 [hep-ph].
- [161] X.-K. Dong, F.-K. Guo, and B.-S. Zou, Progr. Phys. **41**, 65 (2021), arXiv:2101.01021 [hep-ph].
- [162] X.-K. Dong, F.-K. Guo, and B.-S. Zou, Commun. Theor. Phys. **73**, 125201 (2021), arXiv:2108.02673 [hep-ph].
- [163] K. Chen, R. Chen, L. Meng, B. Wang, and S.-L. Zhu, (2021), arXiv:2109.13057 [hep-ph].
- [164] F.-Z. Peng, M. Sánchez Sánchez, M.-J. Yan, and M. Pavon Valderrama, Phys. Rev. D **105**, 034028 (2022), arXiv:2101.07213 [hep-ph].
- [165] J. Gasser and H. Leutwyler, Annals Phys. **158**, 142 (1984).
- [166] J. Gasser and H. Leutwyler, Nucl. Phys. B **250**, 465 (1985).
- [167] J. Gasser, M. E. Sainio, and A. Svarc, Nucl. Phys. B **307**, 779 (1988).
- [168] S. Weinberg, Phys. Lett. B **251**, 288 (1990).
- [169] S. Weinberg, Nucl. Phys. B **363**, 3 (1991).
- [170] E. Epelbaum, H.-W. Hammer, and U.-G. Meissner, Rev. Mod. Phys. **81**, 1773 (2009), arXiv:0811.1338 [nucl-th].
- [171] R. Machleidt and D. R. Entem, Phys. Rept. **503**, 1 (2011), arXiv:1105.2919 [nucl-th].
- [172] J.-X. Lu, C.-X. Wang, Y. Xiao, L.-S. Geng, J. Meng, and P. Ring, Phys. Rev. Lett. **128**, 142002 (2022), arXiv:2111.07766 [nucl-th].
- [173] D.-L. Yao, L.-Y. Dai, H.-Q. Zheng, and Z.-Y. Zhou, Rept. Prog. Phys. **84**, 076201 (2021), arXiv:2009.13495 [hep-ph].

- [174] M.-L. Du, V. Baru, F.-K. Guo, C. Hanhart, U.-G. Meißner, J. A. Oller, and Q. Wang, JHEP **08**, 157 (2021), arXiv:2102.07159 [hep-ph].
- [175] M.-J. Yan and M. P. Valderrama, Phys. Rev. D **105**, 014007 (2022), arXiv:2108.04785 [hep-ph].
- [176] M. Pavon Valderrama, Phys. Rev. D **100**, 094028 (2019), arXiv:1907.05294 [hep-ph].
- [177] M.-L. Du, V. Baru, F.-K. Guo, C. Hanhart, U.-G. Meißner, J. A. Oller, and Q. Wang, Phys. Rev. Lett. **124**, 072001 (2020), arXiv:1910.11846 [hep-ph].
- [178] M.-L. Du, V. Baru, X.-K. Dong, A. Filin, F.-K. Guo, C. Hanhart, A. Nefediev, J. Nieves, and Q. Wang, Phys. Rev. D **105**, 014024 (2022), arXiv:2110.13765 [hep-ph].
- [179] F.-K. Guo, C. Hidalgo-Duque, J. Nieves, and M. P. Valderrama, Phys. Rev. **D88**, 054007 (2013), arXiv:1303.6608 [hep-ph].
- [180] M.-Z. Liu, F.-Z. Peng, M. Sánchez Sánchez, and M. P. Valderrama, Phys. Rev. **D98**, 114030 (2018), arXiv:1811.03992 [hep-ph].
- [181] Z. Yang, X. Cao, F.-K. Guo, J. Nieves, and M. P. Valderrama, Phys. Rev. D **103**, 074029 (2021), arXiv:2011.08725 [hep-ph].
- [182] F.-Z. Peng, M.-Z. Liu, M. Sánchez Sánchez, and M. Pavon Valderrama, Phys. Rev. D **102**, 114020 (2020), arXiv:2004.05658 [hep-ph].
- [183] J. A. Oller and E. Oset, Nucl. Phys. **A620**, 438 (1997), [Erratum: Nucl. Phys.A652,407(1999)], arXiv:hep-ph/9702314 [hep-ph].
- [184] R. Molina, T. Branz, and E. Oset, Phys. Rev. D **82**, 014010 (2010), arXiv:1005.0335 [hep-ph].
- [185] H.-X. Chen, L.-S. Geng, W.-H. Liang, E. Oset, E. Wang, and J.-J. Xie, Phys. Rev. C **93**, 065203 (2016), arXiv:1510.01803 [hep-ph].
- [186] C. W. Xiao, J. Nieves, and E. Oset, Phys. Rev. **D100**, 014021 (2019), arXiv:1904.01296 [hep-ph].
- [187] R. Aaij *et al.* (LHCb), Sci. Bull. **65**, 1983 (2020), arXiv:2006.16957 [hep-ex].
- [188] J. L. Rosner, Phys. Rev. D **74**, 076006 (2006), arXiv:hep-ph/0608102.
- [189] M. Mikhasenko, B. Ketzer, and A. Sarantsev, Phys. Rev. D **91**, 094015 (2015), arXiv:1501.07023 [hep-ph].
- [190] F. Aceti, L. R. Dai, and E. Oset, Phys. Rev. D **94**, 096015 (2016), arXiv:1606.06893 [hep-ph].
- [191] X.-K. Dong, F.-K. Guo, and B.-S. Zou, Phys. Rev. Lett. **126**, 152001 (2021), arXiv:2011.14517 [hep-ph].
- [192] G. D. Alexeev *et al.* (COMPASS), Phys. Rev. Lett. **127**, 082501 (2021), arXiv:2006.05342 [hep-ph].
- [193] X.-K. Dong, V. Baru, F.-K. Guo, C. Hanhart, and A. Nefediev, Phys. Rev. Lett. **126**, 132001 (2021), [Erratum: Phys.Rev.Lett. 127, 119901 (2021)], arXiv:2009.07795 [hep-ph].
- [194] J.-J. Wu, X.-H. Liu, Q. Zhao, and B.-S. Zou, Phys. Rev. Lett. **108**, 081803 (2012), arXiv:1108.3772 [hep-ph].
- [195] E. Wang, J.-J. Xie, W.-H. Liang, F.-K. Guo, and E. Oset, Phys. Rev. C **95**, 015205 (2017), arXiv:1610.07117 [hep-ph].
- [196] S. Sakai, E. Oset, and A. Ramos, Eur. Phys. J. A **54**, 10 (2018), arXiv:1705.03694 [hep-ph].
- [197] M. Bayar, F. Aceti, F.-K. Guo, and E. Oset, Phys. Rev. D **94**, 074039 (2016), arXiv:1609.04133 [hep-ph].
- [198] C. Adolph *et al.* (COMPASS), Phys. Rev. Lett. **115**, 082001 (2015), arXiv:1501.05732 [hep-ex].
- [199] F.-K. Guo, Phys. Rev. Lett. **122**, 202002 (2019), arXiv:1902.11221 [hep-ph].

- [200] U.-G. Meissner, Nucl. Phys. A **629**, 72C (1998), arXiv:hep-ph/9706367.
- [201] N. Cabibbo, Phys. Rev. Lett. **93**, 121801 (2004), arXiv:hep-ph/0405001.
- [202] N. Cabibbo and G. Isidori, JHEP **03**, 021 (2005), arXiv:hep-ph/0502130.
- [203] G. Colangelo, J. Gasser, B. Kubis, and A. Rusetsky, Phys. Lett. B **638**, 187 (2006), arXiv:hep-ph/0604084.
- [204] M. Bissegger, A. Fuhrer, J. Gasser, B. Kubis, and A. Rusetsky, Phys. Lett. B **659**, 576 (2008), arXiv:0710.4456 [hep-ph].
- [205] J. R. Batley et al., Eur. Phys. J. C **64**, 589 (2009), arXiv:0912.2165 [hep-ex].
- [206] X.-H. Liu, F.-K. Guo, and E. Epelbaum, Eur. Phys. J. C **73**, 2284 (2013), arXiv:1212.4066 [hep-ph].
- [207] E. Braaten, M. Kusunoki, and S. Nussinov, Phys. Rev. Lett. **93**, 162001 (2004), arXiv:hep-ph/0404161.
- [208] E. Braaten and M. Kusunoki, Phys. Rev. D **72**, 014012 (2005), arXiv:hep-ph/0506087.
- [209] M. Zito, Phys. Lett. B **586**, 314 (2004), arXiv:hep-ph/0401014.
- [210] C.-H. Chen, H.-Y. Cheng, C. Q. Geng, and Y. K. Hsiao, Phys. Rev. D **78**, 054016 (2008), arXiv:0806.1108 [hep-ph].
- [211] Z. Yang, Q. Wang, and U.-G. Meißner, Phys. Lett. B **775**, 50 (2017), arXiv:1706.00960 [hep-ph].
- [212] C. Q. Geng, Y. K. Hsiao, C.-W. Liu, and T.-H. Tsai, Phys. Rev. D **99**, 073003 (2019), arXiv:1810.01079 [hep-ph].
- [213] C.-K. Chua, W.-S. Hou, and S.-Y. Tsai, Phys. Rev. D **65**, 034003 (2002), arXiv:hep-ph/0107110.
- [214] C.-K. Chua, W.-S. Hou, and S.-Y. Tsai, Phys. Rev. D **66**, 054004 (2002), arXiv:hep-ph/0204185.
- [215] C.-K. Chua and W.-S. Hou, Eur. Phys. J. C **29**, 27 (2003), arXiv:hep-ph/0211240.
- [216] C. Q. Geng and Y. K. Hsiao, Phys. Rev. D **72**, 037901 (2005).
- [217] C. Q. Geng and Y. K. Hsiao, Phys. Rev. D **74**, 094023 (2006), arXiv:hep-ph/0606141.
- [218] C. Q. Geng, Y. K. Hsiao, and J. N. Ng, Phys. Rev. Lett. **98**, 011801 (2007), arXiv:hep-ph/0608328.
- [219] H.-Y. Cheng, C. Q. Geng, and Y. K. Hsiao, Phys. Rev. D **89**, 034005 (2014), arXiv:1205.0117 [hep-ph].
- [220] H.-Y. Cheng and K.-C. Yang, Phys. Rev. D **66**, 014020 (2002), arXiv:hep-ph/0112245.
- [221] H.-Y. Cheng and K.-C. Yang, Phys. Rev. D **66**, 094009 (2002), arXiv:hep-ph/0208185.
- [222] H.-Y. Cheng and K.-C. Yang, Phys. Lett. B **633**, 533 (2006), arXiv:hep-ph/0511305.
- [223] H.-Y. Cheng, Int. J. Mod. Phys. A **21**, 4209 (2006), arXiv:hep-ph/0603003.
- [224] W.-F. Wang and H.-n. Li, Phys. Lett. B **763**, 29 (2016), arXiv:1609.04614 [hep-ph].
- [225] Z. Rui, Y. Li, and W.-F. Wang, Eur. Phys. J. C **77**, 199 (2017), arXiv:1701.02941 [hep-ph].
- [226] Z.-T. Zou, Y. Li, Q.-X. Li, and X. Liu, Eur. Phys. J. C **80**, 394 (2020), arXiv:2003.03754 [hep-ph].
- [227] W.-S. Fang, Z.-T. Zou, and Y. Li, Phys. Rev. D **108**, 113007 (2023), arXiv:2311.17678 [hep-ph].
- [228] Q. Wu and D.-Y. Chen, Phys. Rev. D **100**, 114002 (2019), arXiv:1906.02480 [hep-ph].
- [229] Y.-K. Hsiao, Y. Yu, and B.-C. Ke, Eur. Phys. J. C **80**, 895 (2020), arXiv:1909.07327 [hep-ph].
- [230] X.-Z. Ling, M.-Z. Liu, J.-X. Lu, L.-S. Geng, and J.-J. Xie, Phys. Rev. D **103**, 116016 (2021), arXiv:2102.05349 [hep-ph].
- [231] T. J. Burns and E. S. Swanson, Phys. Rev. D **106**, 054029 (2022), arXiv:2207.00511 [hep-ph].
- [232] Y.-W. Pan, M.-Z. Liu, and L.-S. Geng, Phys. Rev. D **108**, 114022 (2023), arXiv:2309.12050 [hep-ph].

- [233] L.-L. Chau, Phys. Rept. **95**, 1 (1983).
- [234] L.-L. Chau and H.-Y. Cheng, Phys. Rev. D **36**, 137 (1987), [Addendum: Phys.Rev.D 39, 2788–2791 (1989)].
- [235] A. Andronic, P. Braun-Munzinger, and J. Stachel, Nucl. Phys. A **772**, 167 (2006), arXiv:nucl-th/0511071.
- [236] A. Andronic, P. Braun-Munzinger, and J. Stachel, Phys. Lett. B **673**, 142 (2009), [Erratum: Phys.Lett.B 678, 516 (2009)], arXiv:0812.1186 [nucl-th].
- [237] A. Andronic, P. Braun-Munzinger, J. Stachel, and H. Stocker, Phys. Lett. B **697**, 203 (2011), arXiv:1010.2995 [nucl-th].
- [238] S. Cho et al. (ExHIC), Phys. Rev. Lett. **106**, 212001 (2011), arXiv:1011.0852 [nucl-th].
- [239] S. Cho et al. (ExHIC), Prog. Part. Nucl. Phys. **95**, 279 (2017), arXiv:1702.00486 [nucl-th].
- [240] K.-J. Sun and L.-W. Chen, Phys. Rev. C **95**, 044905 (2017), arXiv:1701.01935 [nucl-th].
- [241] K.-J. Sun, C. M. Ko, and B. Dönigus, Phys. Lett. B **792**, 132 (2019), arXiv:1812.05175 [nucl-th].
- [242] H. Yun, D. Park, S. Noh, A. Park, W. Park, S. Cho, J. Hong, Y. Kim, S. Lim, and S. H. Lee, Phys. Rev. C **107**, 014906 (2023), arXiv:2208.06960 [hep-ph].
- [243] H. Zhang, J. Liao, E. Wang, Q. Wang, and H. Xing, Phys. Rev. Lett. **126**, 012301 (2021), arXiv:2004.00024 [hep-ph].
- [244] H.-g. Xu, Z.-L. She, D.-M. Zhou, L. Zheng, X.-L. Kang, G. Chen, and B.-H. Sa, Eur. Phys. J. C **81**, 784 (2021), arXiv:2105.06261 [hep-ph].
- [245] T.-C. Wu and L.-S. Geng, Phys. Rev. D **108**, 014015 (2023), arXiv:2211.01846 [hep-ph].
- [246] Q. Wang, X.-H. Liu, and Q. Zhao, Phys. Rev. D **92**, 034022 (2015), arXiv:1508.00339 [hep-ph].
- [247] A. N. Hiller Blin, C. Fernández-Ramírez, A. Jackura, V. Mathieu, V. I. Mokeev, A. Pilloni, and A. P. Szczepaniak, Phys. Rev. D **94**, 034002 (2016), arXiv:1606.08912 [hep-ph].
- [248] X.-Y. Wang, X.-R. Chen, and J. He, Phys. Rev. **D99**, 114007 (2019), arXiv:1904.11706 [hep-ph].
- [249] A. Ali et al. (GlueX), Phys. Rev. Lett. **123**, 072001 (2019), arXiv:1905.10811 [nucl-ex].
- [250] S. Chen, Y. Li, W. Qian, Z. Shen, Y. Xie, Z. Yang, L. Zhang, and Y. Zhang, Front. Phys. **18**, 44601 (2023), arXiv:2111.14360 [hep-ex].
- [251] Z. Liu and R. E. Mitchell, Sci. Bull. **68**, 2148 (2023), arXiv:2310.09465 [hep-ex].
- [252] S. Jia, W. Xiong, and C. Shen, Chin. Phys. Lett. **40**, 121301 (2023), arXiv:2312.00403 [hep-ex].
- [253] J. Nieves and M. P. Valderrama, Phys. Rev. D **84**, 056015 (2011), arXiv:1106.0600 [hep-ph].
- [254] Z.-F. Sun, J. He, X. Liu, Z.-G. Luo, and S.-L. Zhu, Phys. Rev. **D84**, 054002 (2011), arXiv:1106.2968 [hep-ph].
- [255] J. Nieves and M. P. Valderrama, Phys. Rev. **D86**, 056004 (2012), arXiv:1204.2790 [hep-ph].
- [256] V. Baru, E. Epelbaum, A. A. Filin, C. Hanhart, U.-G. Meißner, and A. V. Nefediev, Phys. Lett. B **763**, 20 (2016), arXiv:1605.09649 [hep-ph].
- [257] M.-Z. Liu, T.-W. Wu, M. Pavon Valderrama, J.-J. Xie, and L.-S. Geng, Phys. Rev. **D99**, 094018 (2019), arXiv:1902.03044 [hep-ph].
- [258] L. R. Dai, E. Oset, A. Feijoo, R. Molina, L. Roca, A. M. Torres, and K. P. Khemchandani, Phys. Rev. D **105**, 074017 (2022), [Erratum: Phys.Rev.D 106, 099904 (2022)], arXiv:2201.04840 [hep-ph].
- [259] S. Chatrchyan et al. (CMS), Phys. Lett. B **727**, 57 (2013), arXiv:1309.0250 [hep-ex].

- [260] X. H. He et al. (Belle), Phys. Rev. Lett. **113**, 142001 (2014), arXiv:1408.0504 [hep-ex].
- [261] A. Ekström, G. R. Jansen, K. A. Wendt, G. Hagen, T. Papenbrock, B. D. Carlsson, C. Forssén, M. Hjorth-Jensen, P. Navrátil, and W. Nazarewicz, Phys. Rev. C **91**, 051301 (2015), arXiv:1502.04682 [nucl-th].
- [262] V. Somà, P. Navrátil, F. Raimondi, C. Barbieri, and T. Duguet, Phys. Rev. C **101**, 014318 (2020), arXiv:1907.09790 [nucl-th].
- [263] H. W. Hammer, S. König, and U. van Kolck, Rev. Mod. Phys. **92**, 025004 (2020), arXiv:1906.12122 [nucl-th].
- [264] H. Hergert, Front. in Phys. **8**, 379 (2020), arXiv:2008.05061 [nucl-th].
- [265] S. Elhatisari et al., (2022), arXiv:2210.17488 [nucl-th].
- [266] R. Machleidt, Few Body Syst. **64**, 77 (2023), arXiv:2307.06416 [nucl-th].
- [267] R. Machleidt and F. Sammarruca, (2024), arXiv:2402.14032 [nucl-th].
- [268] E. Hiyama, Y. Kino, and M. Kamimura, Prog. Part. Nucl. Phys. **51**, 223 (2003).
- [269] E. Hiyama and K. Nakazawa, Ann. Rev. Nucl. Part. Sci. **68**, 131 (2018).
- [270] T.-W. Wu, M.-Z. Liu, and L.-S. Geng, Few Body Syst. **62**, 38 (2021), arXiv:2105.09017 [hep-ph].
- [271] T.-W. Wu, Y.-W. Pan, M.-Z. Liu, and L.-S. Geng, Sci. Bull. **67**, 1735 (2022), arXiv:2208.00882 [hep-ph].
- [272] Y.-W. Pan, M.-Z. Liu, J.-X. Lu, and L.-S. Geng, (2023), arXiv:2312.13801 [hep-ph].
- [273] T.-W. Wu, M.-Z. Liu, L.-S. Geng, E. Hiyama, and M. P. Valderrama, Phys. Rev. D **100**, 034029 (2019), arXiv:1906.11995 [hep-ph].
- [274] L. Adamczyk et al. (STAR), Phys. Rev. Lett. **114**, 022301 (2015), arXiv:1408.4360 [nucl-ex].
- [275] L. Adamczyk et al. (STAR), Nature **527**, 345 (2015), arXiv:1507.07158 [nucl-ex].
- [276] S. Acharya et al. (ALICE), Phys. Rev. Lett. **123**, 112002 (2019), arXiv:1904.12198 [nucl-ex].
- [277] A. Collaboration et al. (ALICE), Nature **588**, 232 (2020), [Erratum: Nature 590, E13 (2021)], arXiv:2005.11495 [nucl-ex].
- [278] S. Acharya et al. (ALICE), Phys. Rev. Lett. **127**, 172301 (2021), arXiv:2105.05578 [nucl-ex].
- [279] L. Fabbietti, V. Mantovani Sarti, and O. Vazquez Doce, Ann. Rev. Nucl. Part. Sci. **71**, 377 (2021), arXiv:2012.09806 [nucl-ex].
- [280] Z.-W. Liu, J.-X. Lu, and L.-S. Geng, Phys. Rev. D **107**, 074019 (2023), arXiv:2302.01046 [hep-ph].
- [281] M. Albaladejo, J. Nieves, and E. Ruiz-Arriola, Phys. Rev. D **108**, 014020 (2023), arXiv:2304.03107 [hep-ph].
- [282] K. P. Khemchandani, L. M. Abreu, A. Martinez Torres, and F. S. Navarra, (2023), arXiv:2312.11811 [hep-ph].
- [283] N. Ikeno, G. Toledo, and E. Oset, Phys. Lett. B **847**, 138281 (2023), arXiv:2305.16431 [hep-ph].
- [284] J. M. Torres-Rincon, A. Ramos, and L. Tolos, Phys. Rev. D **108**, 096008 (2023), arXiv:2307.02102 [hep-ph].
- [285] Y. Kamiya, T. Hyodo, and A. Ohnishi, Eur. Phys. J. A **58**, 131 (2022), arXiv:2203.13814 [hep-ph].
- [286] I. Vidana, A. Feijoo, M. Albaladejo, J. Nieves, and E. Oset, Phys. Lett. B **846**, 138201 (2023), arXiv:2303.06079 [hep-ph].
- [287] M. Albaladejo, A. Feijoo, I. Vidaña, J. Nieves, and E. Oset, (2023), arXiv:2307.09873 [hep-ph].
- [288] Z.-W. Liu, J.-X. Lu, M.-Z. Liu, and L.-S. Geng, Phys. Rev. D **108**, L031503 (2023), arXiv:2305.19048 [hep-ph].
- [289] A. Feijoo, L. R. Dai, L. M. Abreu, and E. Oset, (2023), arXiv:2309.00444 [hep-ph].

- [290] N. Brambilla et al., Eur. Phys. J. C **71**, 1534 (2011), arXiv:1010.5827 [hep-ph].
- [291] D. Johnson, I. Polyakov, T. Skwarnicki, and M. Wang, (2024), 10.1146/annurev-nucl-102422-040628, arXiv:2403.04051 [hep-ex].
- [292] B. Aubert et al. (BaBar), Phys. Rev. Lett. **90**, 242001 (2003), arXiv:hep-ex/0304021.
- [293] D. Besson et al. (CLEO), Phys. Rev. D **68**, 032002 (2003), [Erratum: Phys.Rev.D 75, 119908 (2007)], arXiv:hep-ex/0305100.
- [294] Y. Mikami et al. (Belle), Phys. Rev. Lett. **92**, 012002 (2004), arXiv:hep-ex/0307052.
- [295] M. Ablikim et al. (BESIII), Phys. Rev. D **97**, 051103 (2018), arXiv:1711.08293 [hep-ex].
- [296] P. Krokovny et al. (Belle), Phys. Rev. Lett. **91**, 262002 (2003), arXiv:hep-ex/0308019.
- [297] B. Aubert et al. (BaBar), Phys. Rev. Lett. **93**, 181801 (2004), arXiv:hep-ex/0408041.
- [298] S. K. Choi et al. (Belle), Phys. Rev. D **91**, 092011 (2015), [Addendum: Phys.Rev.D 92, 039905 (2015)], arXiv:1504.02637 [hep-ex].
- [299] B. Aubert et al. (BaBar), Phys. Rev. D **74**, 031103 (2006), arXiv:hep-ex/0605036.
- [300] B. Aubert et al. (BaBar), Phys. Rev. D **69**, 031101 (2004), arXiv:hep-ex/0310050.
- [301] B. Aubert et al. (BaBar), Phys. Rev. D **74**, 032007 (2006), arXiv:hep-ex/0604030.
- [302] D. Acosta et al. (CDF), Phys. Rev. Lett. **93**, 072001 (2004), arXiv:hep-ex/0312021.
- [303] V. M. Abazov et al. (D0), Phys. Rev. Lett. **93**, 162002 (2004), arXiv:hep-ex/0405004.
- [304] A. Abulencia et al. (CDF), Phys. Rev. Lett. **96**, 102002 (2006), arXiv:hep-ex/0512074.
- [305] A. Abulencia et al. (CDF), Phys. Rev. Lett. **98**, 132002 (2007), arXiv:hep-ex/0612053.
- [306] T. Aaltonen et al. (CDF), Phys. Rev. Lett. **103**, 152001 (2009), arXiv:0906.5218 [hep-ex].
- [307] B. Aubert et al. (BaBar), Phys. Rev. D **71**, 071103 (2005), arXiv:hep-ex/0406022.
- [308] B. Aubert et al. (BaBar), Phys. Rev. Lett. **96**, 052002 (2006), arXiv:hep-ex/0510070.
- [309] B. Aubert et al. (BaBar), Phys. Rev. D **77**, 111101 (2008), arXiv:0803.2838 [hep-ex].
- [310] R. Aaij et al. (LHCb), Phys. Rev. Lett. **110**, 222001 (2013), arXiv:1302.6269 [hep-ex].
- [311] R. Aaij et al. (LHCb), JHEP **08**, 123 (2020), arXiv:2005.13422 [hep-ex].
- [312] R. Aaij et al. (LHCb), Eur. Phys. J. C **72**, 1972 (2012), arXiv:1112.5310 [hep-ex].
- [313] S. Chatrchyan et al. (CMS), JHEP **04**, 154 (2013), arXiv:1302.3968 [hep-ex].
- [314] B. Aubert et al. (BaBar), Phys. Rev. D **74**, 071101 (2006), arXiv:hep-ex/0607050.
- [315] B. Aubert et al. (BaBar), Phys. Rev. Lett. **102**, 132001 (2009), arXiv:0809.0042 [hep-ex].
- [316] V. Bhardwaj et al. (Belle), Phys. Rev. Lett. **107**, 091803 (2011), arXiv:1105.0177 [hep-ex].
- [317] R. Aaij et al. (LHCb), Nucl. Phys. B **886**, 665 (2014), arXiv:1404.0275 [hep-ex].
- [318] M. Ablikim et al. (BESIII), Phys. Rev. Lett. **122**, 202001 (2019), arXiv:1901.03992 [hep-ex].
- [319] R. Aaij et al. (LHCb), JHEP **09**, 028 (2019), arXiv:1907.00954 [hep-ex].
- [320] M. Ablikim et al. (BESIII), Phys. Rev. Lett. **122**, 232002 (2019), arXiv:1903.04695 [hep-ex].
- [321] R. Aaij et al. (LHCb), Phys. Rev. D **92**, 011102 (2015), arXiv:1504.06339 [hep-ex].
- [322] M. Ablikim et al. (BESIII), Phys. Rev. Lett. **124**, 242001 (2020), arXiv:2001.01156 [hep-ex].
- [323] R. Aaij et al. (LHCb), JHEP **02**, 024 (2021), [Erratum: JHEP 04, 170 (2021)], arXiv:2011.01867 [hep-ex].

- [324] A. M. Sirunyan et al. (CMS), Phys. Rev. Lett. **125**, 152001 (2020), arXiv:2005.04764 [hep-ex].
- [325] M. Ablikim et al. (BESIII), Phys. Rev. Lett. **112**, 092001 (2014), arXiv:1310.4101 [hep-ex].
- [326] B. Aubert et al. (BaBar), Phys. Rev. Lett. **93**, 041801 (2004), arXiv:hep-ex/0402025.
- [327] B. Aubert et al. (BaBar), Phys. Rev. D **77**, 011102 (2008), arXiv:0708.1565 [hep-ex].
- [328] T. Aushev et al. (Belle), Phys. Rev. D **81**, 031103 (2010), arXiv:0810.0358 [hep-ex].
- [329] P. del Amo Sanchez et al. (BaBar), Phys. Rev. D **82**, 011101 (2010), arXiv:1005.5190 [hep-ex].
- [330] G. Gokhroo et al. (Belle), Phys. Rev. Lett. **97**, 162002 (2006), arXiv:hep-ex/0606055.
- [331] R. Aaij et al. (LHCb), JHEP **07**, 084 (2023), arXiv:2302.10629 [hep-ex].
- [332] X. L. Wang et al. (Belle), Phys. Rev. D **105**, 112011 (2022), arXiv:2105.06605 [hep-ex].
- [333] M. Ablikim et al. (BESIII), Phys. Rev. Lett. **118**, 092001 (2017), arXiv:1611.01317 [hep-ex].
- [334] M. Ablikim et al. (BESIII), Phys. Rev. Lett. **118**, 092002 (2017), arXiv:1610.07044 [hep-ex].
- [335] M. Ablikim et al. (BESIII), Phys. Rev. D **96**, 032004 (2017), [Erratum: Phys.Rev.D 99, 019903 (2019)], arXiv:1703.08787 [hep-ex].
- [336] M. Ablikim et al. (BESIII), Phys. Rev. D **104**, 052012 (2021), arXiv:2107.09210 [hep-ex].
- [337] M. Ablikim et al. (BESIII), Phys. Rev. Lett. **114**, 092003 (2015), arXiv:1410.6538 [hep-ex].
- [338] M. Ablikim et al. (BESIII), Phys. Rev. D **99**, 091103 (2019), arXiv:1903.02359 [hep-ex].
- [339] M. Ablikim et al. ((BESIII),, BESIII), Chin. Phys. C **46**, 111002 (2022), arXiv:2204.07800 [hep-ex].
- [340] M. Ablikim et al. (BESIII), Phys. Rev. Lett. **122**, 102002 (2019), arXiv:1808.02847 [hep-ex].
- [341] M. Ablikim et al. (BESIII), Phys. Rev. Lett. **130**, 121901 (2023), arXiv:2301.07321 [hep-ex].
- [342] M. Ablikim et al. (BESIII), Phys. Rev. D **107**, 092005 (2023), arXiv:2211.08561 [hep-ex].
- [343] M. Ablikim et al. (BESIII), Phys. Rev. D **102**, 031101 (2020), arXiv:2003.03705 [hep-ex].
- [344] M. Ablikim et al. (BESIII), (2023), arXiv:2310.03361 [hep-ex].
- [345] B. Aubert et al. (BaBar), Phys. Rev. Lett. **98**, 212001 (2007), arXiv:hep-ex/0610057.
- [346] X. L. Wang et al. (Belle), Phys. Rev. Lett. **99**, 142002 (2007), arXiv:0707.3699 [hep-ex].
- [347] J. P. Lees et al. (BaBar), Phys. Rev. D **89**, 111103 (2014), arXiv:1211.6271 [hep-ex].
- [348] X. L. Wang et al. (Belle), Phys. Rev. D **91**, 112007 (2015), arXiv:1410.7641 [hep-ex].
- [349] M. Ablikim et al. (BESIII), Phys. Rev. D **106**, 052012 (2022), arXiv:2208.00099 [hep-ex].
- [350] M. Ablikim et al. (BESIII), Phys. Rev. D **104**, 092001 (2021), arXiv:2107.03604 [hep-ex].
- [351] B. Aubert et al. (BaBar), in 32nd International Conference on High Energy Physics (2004) arXiv:hep-ex/0408067.
- [352] A. Drutskey et al. (Belle), Phys. Rev. Lett. **94**, 061802 (2005), arXiv:hep-ex/0409026.
- [353] Y. S. Kalashnikova, Phys. Rev. D **72**, 034010 (2005), arXiv:hep-ph/0506270.
- [354] M. Suzuki, Phys. Rev. D **72**, 114013 (2005), arXiv:hep-ph/0508258 [hep-ph].
- [355] T. Barnes and E. S. Swanson, Phys. Rev. C **77**, 055206 (2008), arXiv:0711.2080 [hep-ph].
- [356] P. G. Ortega, J. Segovia, D. R. Entem, and F. Fernandez, Phys. Rev. D **81**, 054023 (2010), arXiv:0907.3997 [hep-ph].
- [357] I. V. Danilkin and Y. A. Simonov, Phys. Rev. Lett. **105**, 102002 (2010), arXiv:1006.0211 [hep-ph].

- [358] J. Ferretti, G. Galatà, and E. Santopinto, Phys. Rev. C **88**, 015207 (2013), arXiv:1302.6857 [hep-ph].
- [359] J. Ferretti and E. Santopinto, Phys. Rev. D **90**, 094022 (2014), arXiv:1306.2874 [hep-ph].
- [360] M. Albaladejo, P. Fernandez-Soler, J. Nieves, and P. G. Ortega, Eur. Phys. J. C **78**, 722 (2018), arXiv:1805.07104 [hep-ph].
- [361] S.-Q. Luo, B. Chen, X. Liu, and T. Matsuki, Phys. Rev. D **103**, 074027 (2021), arXiv:2102.00679 [hep-ph].
- [362] W. Hao, Y. Lu, and B.-S. Zou, Phys. Rev. D **106**, 074014 (2022), arXiv:2208.10915 [hep-ph].
- [363] J.-J. Yang, W. Hao, X. Wang, D.-M. Li, Y.-X. Li, and E. Wang, Eur. Phys. J. C **83**, 1098 (2023), arXiv:2303.11815 [hep-ph].
- [364] R.-H. Ni, J.-J. Wu, and X.-H. Zhong, (2023), arXiv:2312.04765 [hep-ph].
- [365] T. Barnes, F. E. Close, and H. J. Lipkin, Phys. Rev. D **68**, 054006 (2003), arXiv:hep-ph/0305025.
- [366] D. Gamermann, E. Oset, D. Strottman, and M. J. Vicente Vacas, Phys. Rev. **D76**, 074016 (2007), arXiv:hep-ph/0612179 [hep-ph].
- [367] D. Gamermann and E. Oset, Eur. Phys. J. A **33**, 119 (2007), arXiv:0704.2314 [hep-ph].
- [368] F.-K. Guo, P.-N. Shen, H.-C. Chiang, R.-G. Ping, and B.-S. Zou, Phys. Lett. **B641**, 278 (2006), arXiv:hep-ph/0603072 [hep-ph].
- [369] Z.-X. Xie, G.-Q. Feng, and X.-H. Guo, Phys. Rev. D **81**, 036014 (2010).
- [370] M. Cleven, F.-K. Guo, C. Hanhart, and U.-G. Meissner, Eur. Phys. J. A **47**, 19 (2011), arXiv:1009.3804 [hep-ph].
- [371] Z.-H. Guo, U.-G. Meißner, and D.-L. Yao, Phys. Rev. D **92**, 094008 (2015), arXiv:1507.03123 [hep-ph].
- [372] C. B. Lang, L. Leskovec, D. Mohler, S. Prelovsek, and R. M. Woloshyn, Phys. Rev. D **90**, 034510 (2014), arXiv:1403.8103 [hep-lat].
- [373] C. Alexandrou, J. Berlin, J. Finkenrath, T. Leontiou, and M. Wagner, Phys. Rev. D **101**, 034502 (2020), arXiv:1911.08435 [hep-lat].
- [374] T. Hyodo, D. Jido, and A. Hosaka, Phys. Rev. C **85**, 015201 (2012), arXiv:1108.5524 [nucl-th].
- [375] Y. Yamaguchi, H. García-Tecocoatzi, A. Giachino, A. Hosaka, E. Santopinto, S. Takeuchi, and M. Takizawa, Phys. Rev. D **101**, 091502 (2020), arXiv:1907.04684 [hep-ph].
- [376] T. Kinugawa and T. Hyodo, (2023), arXiv:2303.07038 [hep-ph].
- [377] I. Terashima and T. Hyodo, Phys. Rev. C **108**, 035204 (2023), arXiv:2305.10689 [hep-ph].
- [378] S. Weinberg, Phys. Rev. **137**, B672 (1965).
- [379] M. Albaladejo, D. Jido, J. Nieves, and E. Oset, Eur. Phys. J. C **76**, 300 (2016), arXiv:1604.01193 [hep-ph].
- [380] J. Song, L. R. Dai, and E. Oset, Eur. Phys. J. A **58**, 133 (2022), arXiv:2201.04414 [hep-ph].
- [381] Fayyazuddin and Riazuddin, Phys. Rev. D **69**, 114008 (2004), arXiv:hep-ph/0309283.
- [382] S. Ishida, M. Ishida, T. Komada, T. Maeda, M. Oda, K. Yamada, and I. Yamauchi, AIP Conf. Proc. **717**, 716 (2004), arXiv:hep-ph/0310061.
- [383] W. Wei, P.-Z. Huang, and S.-L. Zhu, Phys. Rev. D **73**, 034004 (2006), arXiv:hep-ph/0510039.
- [384] M. Nielsen, Phys. Lett. B **634**, 35 (2006), arXiv:hep-ph/0510277.
- [385] A. Faessler, T. Gutsche, V. E. Lyubovitskij, and Y.-L. Ma, Phys. Rev. D **76**, 014005 (2007), arXiv:0705.0254

- [hep-ph].
- [386] A. Faessler, T. Gutsche, V. E. Lyubovitskij, and Y.-L. Ma, Phys. Rev. **D76**, 114008 (2007), arXiv:0709.3946 [hep-ph].
- [387] H.-L. Fu, H. W. Griebhammer, F.-K. Guo, C. Hanhart, and U.-G. Meißner, Eur. Phys. J. A **58**, 70 (2022), arXiv:2111.09481 [hep-ph].
- [388] A. Faessler, T. Gutsche, S. Kovalenko, and V. E. Lyubovitskij, Phys. Rev. D **76**, 014003 (2007), arXiv:0705.0892 [hep-ph].
- [389] P. Colangelo, G. Nardulli, A. A. Ovchinnikov, and N. Paver, Phys. Lett. B **269**, 201 (1991).
- [390] S. Veseli and I. Dunietz, Phys. Rev. D **54**, 6803 (1996), arXiv:hep-ph/9607293.
- [391] H.-Y. Cheng, C.-K. Chua, and C.-W. Hwang, Phys. Rev. D **69**, 074025 (2004), arXiv:hep-ph/0310359.
- [392] P. Colangelo, F. De Fazio, and A. Ozpineci, Phys. Rev. D **72**, 074004 (2005), arXiv:hep-ph/0505195.
- [393] H.-Y. Cheng and C.-K. Chua, Phys. Rev. D **74**, 034020 (2006), arXiv:hep-ph/0605073.
- [394] J. Segovia, C. Albertus, E. Hernandez, F. Fernandez, and D. R. Entem, Phys. Rev. D **86**, 014010 (2012), arXiv:1203.4362 [hep-ph].
- [395] A. Datta, H. J. Lipkin, and P. J. O'Donnell, Phys. Rev. D **69**, 094002 (2004), arXiv:hep-ph/0312160.
- [396] M.-Z. Liu, X.-Z. Ling, and L.-S. Geng, Phys. Rev. D **109**, 056014 (2024).
- [397] K. Abe et al. (Belle), in 22nd International Symposium on Lepton-Photon Interactions at High Energy (LP 2005) (2005) arXiv:hep-ex/0505037.
- [398] V. Bhardwaj et al. (Belle), Phys. Rev. D **99**, 111101 (2019), arXiv:1904.07015 [hep-ex].
- [399] J. P. Lees et al. (BaBar), Phys. Rev. Lett. **124**, 152001 (2020), arXiv:1911.11740 [hep-ex].
- [400] A. M. Sirunyan et al. (CMS), Phys. Rev. Lett. **128**, 032001 (2022), arXiv:2102.13048 [hep-ex].
- [401] P. A. Zyla et al. (Particle Data Group), PTEP **2020**, 083C01 (2020).
- [402] R. Aaij et al. (LHCb), Phys. Rev. D **108**, L011103 (2023), arXiv:2204.12597 [hep-ex].
- [403] I. Adachi et al. (Belle), in 34th International Conference on High Energy Physics (2008) arXiv:0809.1224 [hep-ex].
- [404] S. K. Choi et al. (Belle), Phys. Rev. D **84**, 052004 (2011), arXiv:1107.0163 [hep-ex].
- [405] V. Bhardwaj et al. (Belle), Phys. Rev. Lett. **111**, 032001 (2013), arXiv:1304.3975 [hep-ex].
- [406] M. Ablikim et al. (BESIII), (2023), arXiv:2309.01502 [hep-ex].
- [407] R. Aaij et al. (LHCb), Phys. Rev. D **102**, 092005 (2020), arXiv:2005.13419 [hep-ex].
- [408] H. Hirata et al. (Belle), Phys. Rev. D **107**, 112011 (2023), arXiv:2302.02127 [hep-ex].
- [409] K. Abe et al. (Belle), Phys. Rev. Lett. **94**, 182002 (2005), arXiv:hep-ex/0408126.
- [410] B. Aubert et al. (BaBar), Phys. Rev. Lett. **101**, 082001 (2008), arXiv:0711.2047 [hep-ex].
- [411] S. Uehara et al. (Belle), Phys. Rev. Lett. **104**, 092001 (2010), arXiv:0912.4451 [hep-ex].
- [412] J. P. Lees et al. (BaBar), Phys. Rev. D **86**, 072002 (2012), arXiv:1207.2651 [hep-ex].
- [413] R. Aaij et al. (LHCb), Phys. Rev. D **102**, 112003 (2020), arXiv:2009.00026 [hep-ex].
- [414] R. Aaij et al. (LHCb), Phys. Rev. Lett. **125**, 242001 (2020), arXiv:2009.00025 [hep-ex].
- [415] M.-X. Duan, S.-Q. Luo, X. Liu, and T. Matsuki, Phys. Rev. D **101**, 054029 (2020), arXiv:2002.03311 [hep-ph].

- [416] M.-X. Duan, J.-Z. Wang, Y.-S. Li, and X. Liu, Phys. Rev. D **104**, 034035 (2021), arXiv:2104.09132 [hep-ph].
- [417] (2022), arXiv:2210.15153 [hep-ex].
- [418] (2022), arXiv:2211.05034 [hep-ex].
- [419] S. Uehara *et al.* (Belle), Phys. Rev. Lett. **96**, 082003 (2006), arXiv:hep-ex/0512035.
- [420] B. Aubert *et al.* (BaBar), Phys. Rev. D **81**, 092003 (2010), arXiv:1002.0281 [hep-ex].
- [421] R. Aaij *et al.* (LHCb), JHEP **07**, 035 (2019), arXiv:1903.12240 [hep-ex].
- [422] T. Aaltonen *et al.* (CDF), Phys. Rev. Lett. **102**, 242002 (2009), arXiv:0903.2229 [hep-ex].
- [423] T. Aaltonen *et al.* (CDF), Mod. Phys. Lett. A **32**, 1750139 (2017), arXiv:1101.6058 [hep-ex].
- [424] S. Chatrchyan *et al.* (CMS), Phys. Lett. B **734**, 261 (2014), arXiv:1309.6920 [hep-ex].
- [425] V. M. Abazov *et al.* (D0), Phys. Rev. D **89**, 012004 (2014), arXiv:1309.6580 [hep-ex].
- [426] V. M. Abazov *et al.* (D0), Phys. Rev. Lett. **115**, 232001 (2015), arXiv:1508.07846 [hep-ex].
- [427] R. Aaij *et al.* (LHCb), Phys. Rev. Lett. **118**, 022003 (2017), arXiv:1606.07895 [hep-ex].
- [428] R. Aaij *et al.* (LHCb), Phys. Rev. Lett. **127**, 082001 (2021), arXiv:2103.01803 [hep-ex].
- [429] M.-X. Duan and X. Liu, Phys. Rev. D **104**, 074010 (2021), arXiv:2107.14438 [hep-ph].
- [430] Q. Deng, R.-H. Ni, Q. Li, and X.-H. Zhong, (2023), arXiv:2312.10296 [hep-ph].
- [431] J. Song, L. R. Dai, and E. Oset, Phys. Rev. D **108**, 114017 (2023), arXiv:2307.02382 [hep-ph].
- [432] M. B. Voloshin, Phys. Lett. B **579**, 316 (2004), arXiv:hep-ph/0309307.
- [433] M. T. AlFiky, F. Gabbiani, and A. A. Petrov, Phys. Lett. B **640**, 238 (2006), arXiv:hep-ph/0506141.
- [434] M. Karliner and J. L. Rosner, Phys. Rev. Lett. **115**, 122001 (2015), arXiv:1506.06386 [hep-ph].
- [435] C. Li and C.-Z. Yuan, Phys. Rev. D **100**, 094003 (2019), arXiv:1907.09149 [hep-ex].
- [436] E. Braaten and M. Kusunoki, Phys. Rev. D **72**, 054022 (2005), arXiv:hep-ph/0507163.
- [437] C. Hanhart, Y. S. Kalashnikova, A. E. Kudryavtsev, and A. V. Nefediev, Phys. Rev. D **85**, 011501 (2012), arXiv:1111.6241 [hep-ph].
- [438] S. Takeuchi, K. Shimizu, and M. Takizawa, PTEP **2014**, 123D01 (2014), [Erratum: PTEP 2015, 079203 (2015)], arXiv:1408.0973 [hep-ph].
- [439] Z.-Y. Zhou and Z. Xiao, Phys. Rev. D **97**, 034011 (2018), arXiv:1711.01930 [hep-ph].
- [440] Y. Dong, A. Faessler, T. Gutsche, and V. E. Lyubovitskij, J. Phys. G **38**, 015001 (2011), arXiv:0909.0380 [hep-ph].
- [441] T. A. Lahde, Nucl. Phys. A **714**, 183 (2003), arXiv:hep-ph/0208110.
- [442] T. Barnes and S. Godfrey, Phys. Rev. D **69**, 054008 (2004), arXiv:hep-ph/0311162.
- [443] A. M. Badalian, V. D. Orlovsky, Yu. A. Simonov, and B. L. G. Bakker, Phys. Rev. **D85**, 114002 (2012), arXiv:1202.4882 [hep-ph].
- [444] E. S. Swanson, Phys. Lett. B **598**, 197 (2004), arXiv:hep-ph/0406080.
- [445] Q. Wu, M.-Z. Liu, and L.-S. Geng, (2023), arXiv:2304.05269 [hep-ph].
- [446] C. Meng, Y.-J. Gao, and K.-T. Chao, Phys. Rev. D **87**, 074035 (2013), arXiv:hep-ph/0506222.
- [447] W.-H. Liang, T. Ban, and E. Oset, (2023), arXiv:2310.04087 [hep-ph].
- [448] F.-K. Guo, C. Hanhart, U.-G. Meißner, Q. Wang, and Q. Zhao, Phys. Lett. B **725**, 127 (2013), arXiv:1306.3096

- [hep-ph].
- [449] M. Ablikim *et al.* (BESIII), Phys. Rev. Lett. **130**, 151904 (2023), arXiv:2212.07291 [hep-ex].
- [450] R.-Q. Qian and X. Liu, Phys. Rev. D **108**, 094046 (2023), arXiv:2308.14072 [hep-ph].
- [451] A. Cisek, W. Schäfer, and A. Szczurek, Eur. Phys. J. C **82**, 1062 (2022), arXiv:2203.07827 [hep-ph].
- [452] P. G. Ortega, J. Segovia, D. R. Entem, and F. Fernández, Phys. Lett. B **778**, 1 (2018), arXiv:1706.02639 [hep-ph].
- [453] T. Ji, X.-K. Dong, M. Albaladejo, M.-L. Du, F.-K. Guo, and J. Nieves, Phys. Rev. D **106**, 094002 (2022), arXiv:2207.08563 [hep-ph].
- [454] X. Liu, Z.-G. Luo, and Z.-F. Sun, Phys. Rev. Lett. **104**, 122001 (2010), arXiv:0911.3694 [hep-ph].
- [455] T. Wang, G.-L. Wang, H.-F. Fu, and W.-L. Ju, JHEP **07**, 120 (2013), arXiv:1305.1067 [hep-ph].
- [456] S. Prelovsek, S. Collins, D. Mohler, M. Padmanath, and S. Piemonte, JHEP **06**, 035 (2021), arXiv:2011.02542 [hep-lat].
- [457] M. Bayar, A. Feijoo, and E. Oset, Phys. Rev. D **107**, 034007 (2023), arXiv:2207.08490 [hep-ph].
- [458] Y. Chen, H. Chen, C. Meng, H.-R. Qi, and H.-Q. Zheng, Eur. Phys. J. C **83**, 381 (2023), arXiv:2302.06278 [hep-ph].
- [459] S. S. Agaev, K. Azizi, and H. Sundu, Phys. Rev. D **107**, 054017 (2023), arXiv:2211.14129 [hep-ph].
- [460] D.-Y. Chen, Eur. Phys. J. C **76**, 671 (2016), arXiv:1611.00109 [hep-ph].
- [461] W. Hao, G.-Y. Wang, E. Wang, G.-N. Li, and D.-M. Li, Eur. Phys. J. C **80**, 626 (2020), arXiv:1909.13099 [hep-ph].
- [462] Q.-F. Lü and Y.-B. Dong, Phys. Rev. D **94**, 074007 (2016), arXiv:1607.05570 [hep-ph].
- [463] J. Ferretti, E. Santopinto, M. N. Anwar, and Y. Lu, Eur. Phys. J. C **80**, 464 (2020), arXiv:2002.09401 [hep-ph].
- [464] J. J. Aubert *et al.* (E598), Phys. Rev. Lett. **33**, 1404 (1974).
- [465] J. E. Augustin *et al.* (SLAC-SP-017), Phys. Rev. Lett. **33**, 1406 (1974).
- [466] B. Aubert *et al.* (BaBar), Phys. Rev. Lett. **95**, 142001 (2005), arXiv:hep-ex/0506081.
- [467] T. E. Coan *et al.* (CLEO), Phys. Rev. Lett. **96**, 162003 (2006), arXiv:hep-ex/0602034.
- [468] C. Z. Yuan *et al.* (Belle), Phys. Rev. Lett. **99**, 182004 (2007), arXiv:0707.2541 [hep-ex].
- [469] B. Aubert *et al.* (BaBar), Phys. Rev. D **73**, 011101 (2006), arXiv:hep-ex/0507090.
- [470] R. Garg *et al.* (Belle), Phys. Rev. D **99**, 071102 (2019), arXiv:1901.06470 [hep-ex].
- [471] G. Pakhlova *et al.* (Belle), Phys. Rev. Lett. **101**, 172001 (2008), arXiv:0807.4458 [hep-ex].
- [472] M. Ablikim *et al.* (BESIII), Phys. Rev. Lett. **131**, 211902 (2023), arXiv:2308.15362 [hep-ex].
- [473] M. Ablikim *et al.* (BES), eConf **C070805**, 02 (2007), arXiv:0705.4500 [hep-ex].
- [474] J.-Z. Wang, D.-Y. Chen, X. Liu, and T. Matsuki, Phys. Rev. D **99**, 114003 (2019), arXiv:1903.07115 [hep-ph].
- [475] X.-H. Liu and G. Li, Phys. Rev. D **88**, 014013 (2013), arXiv:1306.1384 [hep-ph].
- [476] M. Cleven, Q. Wang, F.-K. Guo, C. Hanhart, U.-G. Meißner, and Q. Zhao, Phys. Rev. D **90**, 074039 (2014), arXiv:1310.2190 [hep-ph].
- [477] Q. Wang, C. Hanhart, and Q. Zhao, Phys. Rev. Lett. **111**, 132003 (2013), arXiv:1303.6355 [hep-ph].
- [478] Y. Dong, A. Faessler, T. Gutsche, and V. E. Lyubovitskij, Phys. Rev. D **90**, 074032 (2014), arXiv:1404.6161

- [hep-ph].
- [479] W. Qin, S.-R. Xue, and Q. Zhao, Phys. Rev. D **94**, 054035 (2016), arXiv:1605.02407 [hep-ph].
 - [480] X.-K. Dong, Y.-H. Lin, and B.-S. Zou, Phys. Rev. D **101**, 076003 (2020), arXiv:1910.14455 [hep-ph].
 - [481] A. Martinez Torres, K. P. Khemchandani, D. Gamermann, and E. Oset, Phys. Rev. D **80**, 094012 (2009), arXiv:0906.5333 [nucl-th].
 - [482] A. Martinez Torres, K. P. Khemchandani, L. S. Geng, M. Napsuciale, and E. Oset, Phys. Rev. D **78**, 074031 (2008), arXiv:0801.3635 [nucl-th].
 - [483] T. Ji, X.-K. Dong, F.-K. Guo, and B.-S. Zou, Phys. Rev. Lett. **129**, 102002 (2022), arXiv:2205.10994 [hep-ph].
 - [484] F.-Z. Peng, M.-J. Yan, M. Sánchez Sánchez, and M. Pavon Valderrama, (2022), arXiv:2205.13590 [hep-ph].
 - [485] Z.-P. Wang, F.-L. Wang, G.-J. Wang, and X. Liu, (2023), arXiv:2312.03512 [hep-ph].
 - [486] Z. Q. Liu et al. (Belle), Phys. Rev. Lett. **110**, 252002 (2013), [Erratum: Phys.Rev.Lett. 111, 019901 (2013)], arXiv:1304.0121 [hep-ex].
 - [487] M. Ablikim et al. (BESIII), Phys. Rev. Lett. **112**, 022001 (2014), arXiv:1310.1163 [hep-ex].
 - [488] T. Xiao, S. Dobbs, A. Tomaradze, and K. K. Seth, Phys. Lett. **B727**, 366 (2013), arXiv:1304.3036 [hep-ex].
 - [489] M. Ablikim et al. (BESIII), Phys. Rev. Lett. **111**, 242001 (2013), arXiv:1309.1896 [hep-ex].
 - [490] M. Ablikim et al. (BESIII), Phys. Rev. Lett. **112**, 132001 (2014), arXiv:1308.2760 [hep-ex].
 - [491] K. Chilikin et al. (Belle), Phys. Rev. D **90**, 112009 (2014), arXiv:1408.6457 [hep-ex].
 - [492] R. Aaij et al. (LHCb), Phys. Rev. D **90**, 012003 (2014), arXiv:1404.5673 [hep-ex].
 - [493] A. Vinokurova et al. (Belle), JHEP **06**, 132 (2015), [Erratum: JHEP 02, 088 (2017)], arXiv:1501.06351 [hep-ex].
 - [494] V. M. Abazov et al. (D0), Phys. Rev. D **98**, 052010 (2018), arXiv:1807.00183 [hep-ex].
 - [495] M. Ablikim et al. (BESIII), Phys. Rev. Lett. **126**, 102001 (2021), arXiv:2011.07855 [hep-ex].
 - [496] L. Meng, B. Wang, G.-J. Wang, and S.-L. Zhu, Sci. Bull. **66**, 2065 (2021), arXiv:2104.08469 [hep-ph].
 - [497] S. Han and L.-Y. Xiao, Phys. Rev. D **105**, 054008 (2022).
 - [498] Y.-H. Wang, J. Wei, C.-S. An, and C.-R. Deng, Chin. Phys. Lett. **40**, 021201 (2023).
 - [499] Y. Yu, Z. Xiong, H. Zhang, B.-C. Ke, J.-W. Zhang, D.-Z. He, and R.-Y. Zhou, Phys. Lett. B **848**, 138363 (2024), arXiv:2305.01352 [hep-ph].
 - [500] R.-H. Wua, C.-Y. Wang, C. Meng, Y.-Q. Ma, and K.-T. Chao, (2023), arXiv:2312.14224 [hep-ph].
 - [501] S. K. Choi et al. (Belle), Phys. Rev. Lett. **100**, 142001 (2008), arXiv:0708.1790 [hep-ex].
 - [502] B. Aubert et al. (BaBar), Phys. Rev. D **79**, 112001 (2009), arXiv:0811.0564 [hep-ex].
 - [503] R. Aaij et al. (LHCb), Phys. Rev. Lett. **112**, 222002 (2014), arXiv:1404.1903 [hep-ex].
 - [504] R. Mizuk et al. (Belle), Phys. Rev. D **78**, 072004 (2008), arXiv:0806.4098 [hep-ex].
 - [505] J. P. Lees et al. (BaBar), Phys. Rev. D **85**, 052003 (2012), arXiv:1111.5919 [hep-ex].
 - [506] R. Aaij et al. (LHCb), Eur. Phys. J. C **78**, 1019 (2018), arXiv:1809.07416 [hep-ex].
 - [507] A. Bondar et al. (Belle), Phys. Rev. Lett. **108**, 122001 (2012), arXiv:1110.2251 [hep-ex].
 - [508] J.-R. Zhang, Phys. Rev. D **87**, 116004 (2013), arXiv:1304.5748 [hep-ph].
 - [509] C.-Y. Cui, Y.-L. Liu, W.-B. Chen, and M.-Q. Huang, J. Phys. G **41**, 075003 (2014), arXiv:1304.1850 [hep-ph].

- [510] M. Albaladejo, F.-K. Guo, C. Hidalgo-Duque, and J. Nieves, *Phys. Lett. B* **755**, 337 (2016), arXiv:1512.03638 [hep-ph].
- [511] Y.-H. Chen, M.-L. Du, and F.-K. Guo, (2023), arXiv:2310.15965 [hep-ph].
- [512] Y. Chen *et al.*, *Phys. Rev. D* **89**, 094506 (2014), arXiv:1403.1318 [hep-lat].
- [513] B. Wang, L. Meng, and S.-L. Zhu, *Phys. Rev. D* **102**, 114019 (2020), arXiv:2009.01980 [hep-ph].
- [514] L. Meng, B. Wang, and S.-L. Zhu, *Phys. Rev. D* **102**, 111502 (2020), arXiv:2011.08656 [hep-ph].
- [515] B. Wang, L. Meng, and S.-L. Zhu, *Phys. Rev. D* **103**, L021501 (2021), arXiv:2011.10922 [hep-ph].
- [516] M.-L. Du, M. Albaladejo, F.-K. Guo, and J. Nieves, *Phys. Rev. D* **105**, 074018 (2022), arXiv:2201.08253 [hep-ph].
- [517] M. Cleven, Q. Wang, F.-K. Guo, C. Hanhart, U.-G. Meissner, and Q. Zhao, *Phys. Rev. D* **87**, 074006 (2013), arXiv:1301.6461 [hep-ph].
- [518] Y. Dong, A. Faessler, T. Gutsche, and V. E. Lyubovitskij, *J. Phys. G* **40**, 015002 (2013), arXiv:1203.1894 [hep-ph].
- [519] W. Chen, T. G. Steele, H.-X. Chen, and S.-L. Zhu, *Phys. Rev. D* **92**, 054002 (2015), arXiv:1505.05619 [hep-ph].
- [520] Z.-G. Wang, *Chin. Phys. C* **44**, 063105 (2020), arXiv:1901.10741 [hep-ph].
- [521] C. Deng, J. Ping, and F. Wang, *Phys. Rev. D* **90**, 054009 (2014), arXiv:1402.0777 [hep-ph].
- [522] M. N. Anwar, J. Ferretti, and E. Santopinto, *Phys. Rev. D* **98**, 094015 (2018), arXiv:1805.06276 [hep-ph].
- [523] Z.-G. Wang, *Chin. Phys. C* **45**, 073107 (2021), arXiv:2011.10959 [hep-ph].
- [524] J. Ferretti and E. Santopinto, *Sci. Bull.* **67**, 1209 (2022), arXiv:2111.08650 [hep-ph].
- [525] D.-Y. Chen, X. Liu, and T. Matsuki, *Phys. Rev. D* **88**, 036008 (2013), arXiv:1304.5845 [hep-ph].
- [526] F. Aceti, M. Bayar, E. Oset, A. Martinez Torres, K. P. Khemchandani, J. M. Dias, F. S. Navarra, and M. Nielsen, *Phys. Rev. D* **90**, 016003 (2014), arXiv:1401.8216 [hep-ph].
- [527] Y. Ikeda, S. Aoki, T. Doi, S. Gongyo, T. Hatsuda, T. Inoue, T. Iritani, N. Ishii, K. Murano, and K. Sasaki (HAL QCD), *Phys. Rev. Lett.* **117**, 242001 (2016), arXiv:1602.03465 [hep-lat].
- [528] Y.-H. Ge, X.-H. Liu, and H.-W. Ke, *Eur. Phys. J. C* **81**, 854 (2021), arXiv:2103.05282 [hep-ph].
- [529] N. Ikeno, R. Molina, and E. Oset, *Phys. Lett. B* **814**, 136120 (2021), arXiv:2011.13425 [hep-ph].
- [530] M. Ablikim *et al.* (BESIII), *Phys. Rev. Lett.* **115**, 112003 (2015), arXiv:1506.06018 [hep-ex].
- [531] M. Ablikim *et al.* (BESIII), *Phys. Rev. D* **92**, 092006 (2015), arXiv:1509.01398 [hep-ex].
- [532] M. Ablikim *et al.* (BESIII), *Phys. Rev. Lett.* **115**, 222002 (2015), arXiv:1509.05620 [hep-ex].
- [533] M. Ablikim *et al.* (BESIII), *Phys. Rev. D* **102**, 012009 (2020), arXiv:2004.13788 [hep-ex].
- [534] M. Ablikim *et al.* (BESIII), *Phys. Rev. D* **100**, 111102 (2019), arXiv:1906.00831 [hep-ex].
- [535] M. Ablikim *et al.* (BESIII), *Phys. Rev. Lett.* **113**, 212002 (2014), arXiv:1409.6577 [hep-ex].
- [536] M. Ablikim *et al.* (BESIII), *Phys. Rev. Lett.* **115**, 182002 (2015), arXiv:1507.02404 [hep-ex].
- [537] M. Ablikim *et al.* (BESIII), *Phys. Rev. Lett.* **129**, 112003 (2022), arXiv:2204.13703 [hep-ex].
- [538] R. Aaij *et al.* (LHCb), *Phys. Rev. Lett.* **115**, 072001 (2015), arXiv:1507.03414 [hep-ex].
- [539] R. Aaij *et al.* (LHCb), *Phys. Rev. Lett.* **131**, 031901 (2023), arXiv:2210.10346 [hep-ex].

- [540] R. Aaij *et al.* (LHCb), Sci. Bull. **66**, 1278 (2021), arXiv:2012.10380 [hep-ex].
- [541] R. Aaij *et al.* (LHCb), Phys. Rev. Lett. **117**, 082003 (2016), [Addendum: Phys.Rev.Lett. 117, 109902 (2016), Addendum: Phys.Rev.Lett. 118, 119901 (2017)], arXiv:1606.06999 [hep-ex].
- [542] R. Aaij *et al.* (LHCb), Phys. Rev. D **102**, 112012 (2020), arXiv:2007.11292 [hep-ex].
- [543] R. Aaij *et al.* (LHCb), Phys. Rev. Lett. **128**, 062001 (2022), arXiv:2108.04720 [hep-ex].
- [544] L. Collaboration (LHCb), (2022), arXiv:2210.10346 [hep-ex].
- [545] Y.-H. Lin and B.-S. Zou, Phys. Rev. **D100**, 056005 (2019), arXiv:1908.05309 [hep-ph].
- [546] S. Sakai, H.-J. Jing, and F.-K. Guo, Phys. Rev. **D100**, 074007 (2019), arXiv:1907.03414 [hep-ph].
- [547] M.-Z. Liu, Y.-W. Pan, F.-Z. Peng, M. Sánchez Sánchez, L.-S. Geng, A. Hosaka, and M. Pavon Valderrama, Phys. Rev. Lett. **122**, 242001 (2019), arXiv:1903.11560 [hep-ph].
- [548] C.-J. Xiao, Y. Huang, Y.-B. Dong, L.-S. Geng, and D.-Y. Chen, Phys. Rev. D **100**, 014022 (2019), arXiv:1904.00872 [hep-ph].
- [549] J.-M. Xie, X.-Z. Ling, M.-Z. Liu, and L.-S. Geng, Eur. Phys. J. C **82**, 1061 (2022), arXiv:2204.12356 [hep-ph].
- [550] M. I. Eides, V. Y. Petrov, and M. V. Polyakov, Mod. Phys. Lett. A **35**, 2050151 (2020), arXiv:1904.11616 [hep-ph].
- [551] A. Ali and A. Ya. Parkhomenko, Phys. Lett. **B793**, 365 (2019), arXiv:1904.00446 [hep-ph].
- [552] Z.-G. Wang, Int. J. Mod. Phys. **A35**, 2050003 (2020), arXiv:1905.02892 [hep-ph].
- [553] J.-B. Cheng and Y.-R. Liu, Phys. Rev. **D100**, 054002 (2019), arXiv:1905.08605 [hep-ph].
- [554] X.-Z. Weng, X.-L. Chen, W.-Z. Deng, and S.-L. Zhu, Phys. Rev. **D100**, 016014 (2019), arXiv:1904.09891 [hep-ph].
- [555] R. Zhu, X. Liu, H. Huang, and C.-F. Qiao, Phys. Lett. **B797**, 134869 (2019), arXiv:1904.10285 [hep-ph].
- [556] A. Pimikov, H.-J. Lee, and P. Zhang, Phys. Rev. **D101**, 014002 (2020), arXiv:1908.04459 [hep-ph].
- [557] W. Ruangyoo, K. Phumphan, C.-C. Chen, A. Limphirat, and Y. Yan, (2021), arXiv:2105.14249 [hep-ph].
- [558] C. Fernández-Ramírez, A. Pilloni, M. Albaladejo, A. Jackura, V. Mathieu, M. Mikhasenko, J. A. Silva-Castro, and A. P. Szczepaniak (JPAC), Phys. Rev. Lett. **123**, 092001 (2019), arXiv:1904.10021 [hep-ph].
- [559] S. X. Nakamura, Phys. Rev. D **103**, 111503 (2021), arXiv:2103.06817 [hep-ph].
- [560] C. Xiao, J. Nieves, and E. Oset, Phys. Lett. B **799**, 135051 (2019), arXiv:1906.09010 [hep-ph].
- [561] M.-Z. Liu, Y.-W. Pan, and L.-S. Geng, Phys. Rev. D **103**, 034003 (2021), arXiv:2011.07935 [hep-ph].
- [562] C. W. Xiao, J. J. Wu, and B. S. Zou, Phys. Rev. D **103**, 054016 (2021), arXiv:2102.02607 [hep-ph].
- [563] F.-L. Wang and X. Liu, Phys. Lett. B **835**, 137583 (2022), arXiv:2207.10493 [hep-ph].
- [564] A. Feijoo, W.-F. Wang, C.-W. Xiao, J.-J. Wu, E. Oset, J. Nieves, and B.-S. Zou, Phys. Lett. B **839**, 137760 (2023), arXiv:2212.12223 [hep-ph].
- [565] R. Aaij *et al.* (LHCb), Phys. Rev. Lett. **119**, 112001 (2017), arXiv:1707.01621 [hep-ex].
- [566] R. Aaij *et al.* (LHCb), (2021), arXiv:2109.01056 [hep-ex].
- [567] M. Padmanath and S. Prelovsek, Phys. Rev. Lett. **129**, 032002 (2022), arXiv:2202.10110 [hep-lat].
- [568] S. Chen, C. Shi, Y. Chen, M. Gong, Z. Liu, W. Sun, and R. Zhang, Phys. Lett. B **833**, 137391 (2022), arXiv:2206.06185 [hep-lat].

- [569] Y. Lyu, S. Aoki, T. Doi, T. Hatsuda, Y. Ikeda, and J. Meng, Phys. Rev. Lett. **131**, 161901 (2023), arXiv:2302.04505 [hep-lat].
- [570] F.-Z. Peng, M.-J. Yan, and M. Pavon Valderrama, Phys. Rev. D **108**, 114001 (2023), arXiv:2304.13515 [hep-ph].
- [571] X.-Z. Ling, M.-Z. Liu, L.-S. Geng, E. Wang, and J.-J. Xie, Phys. Lett. B **826**, 136897 (2022), arXiv:2108.00947 [hep-ph].
- [572] L. Meng, G.-J. Wang, B. Wang, and S.-L. Zhu, Phys. Rev. D **104**, 051502 (2021), arXiv:2107.14784 [hep-ph].
- [573] A. Feijoo, W. H. Liang, and E. Oset, Phys. Rev. D **104**, 114015 (2021), arXiv:2108.02730 [hep-ph].
- [574] R. Chen, Q. Huang, X. Liu, and S.-L. Zhu, Phys. Rev. D **104**, 114042 (2021), arXiv:2108.01911 [hep-ph].
- [575] Q.-Y. Zhai, M.-Z. Liu, J.-X. Lu, and L.-S. Geng, (2023), arXiv:2311.06569 [hep-ph].
- [576] L. Dai, S. Fleming, R. Hodges, and T. Mehen, Phys. Rev. D **107**, 076001 (2023), arXiv:2301.11950 [hep-ph].
- [577] B. Wang and L. Meng, Phys. Rev. D **107**, 094002 (2023), arXiv:2212.08447 [hep-ph].
- [578] M.-L. Du, A. Filin, V. Baru, X.-K. Dong, E. Epelbaum, F.-K. Guo, C. Hanhart, A. Nefediev, J. Nieves, and Q. Wang, Phys. Rev. Lett. **131**, 131903 (2023), arXiv:2303.09441 [hep-ph].
- [579] J.-Z. Wang, Z.-Y. Lin, and S.-L. Zhu, (2023), arXiv:2309.09861 [hep-ph].
- [580] L. Meng, V. Baru, E. Epelbaum, A. A. Filin, and A. M. Gasparyan, (2023), arXiv:2312.01930 [hep-lat].
- [581] M. Albaladejo, (2021), arXiv:2110.02944 [hep-ph].
- [582] G.-J. Wang, Z. Yang, J.-J. Wu, M. Oka, and S.-L. Zhu, (2023), arXiv:2306.12406 [hep-ph].
- [583] L. R. Dai, J. Song, and E. Oset, Phys. Lett. B **846**, 138200 (2023), arXiv:2306.01607 [hep-ph].
- [584] L. R. Dai, L. M. Abreu, A. Feijoo, and E. Oset, Eur. Phys. J. C **83**, 983 (2023), arXiv:2304.01870 [hep-ph].
- [585] X.-Z. Weng, W.-Z. Deng, and S.-L. Zhu, Chin. Phys. C **46**, 013102 (2022), arXiv:2108.07242 [hep-ph].
- [586] Y. Song and D. Jia, Commun. Theor. Phys. **75**, 055201 (2023), arXiv:2301.00376 [hep-ph].
- [587] S.-Y. Li, Y.-R. Liu, Z.-L. Man, Z.-G. Si, and J. Wu, (2023), arXiv:2401.00115 [hep-ph].
- [588] Y. Ma, L. Meng, Y.-K. Chen, and S.-L. Zhu, (2023), arXiv:2309.17068 [hep-ph].
- [589] V. E. Barnes et al., Phys. Rev. Lett. **12**, 204 (1964).
- [590] U. G. Meissner, Rept. Prog. Phys. **56**, 903 (1993), arXiv:hep-ph/9302247.
- [591] E. E. Jenkins and A. V. Manohar, Phys. Lett. B **255**, 558 (1991).
- [592] V. Bernard, N. Kaiser, J. Kambor, and U. G. Meissner, Nucl. Phys. B **388**, 315 (1992).
- [593] T. Fuchs, J. Gegelia, G. Japaridze, and S. Scherer, Phys. Rev. D **68**, 056005 (2003), arXiv:hep-ph/0302117.
- [594] L. Geng, Front. Phys. (Beijing) **8**, 328 (2013), arXiv:1301.6815 [nucl-th].
- [595] N. Isgur and M. B. Wise, Phys. Lett. B **232**, 113 (1989).
- [596] N. Isgur and M. B. Wise, Phys. Lett. B **237**, 527 (1990).
- [597] T.-M. Yan, H.-Y. Cheng, C.-Y. Cheung, G.-L. Lin, Y. C. Lin, and H.-L. Yu, Phys. Rev. D **46**, 1148 (1992), [Erratum: Phys.Rev.D 55, 5851 (1997)].
- [598] M. B. Wise, Phys. Rev. D **45**, R2188 (1992).
- [599] R. Casalbuoni, A. Deandrea, N. Di Bartolomeo, R. Gatto, F. Feruglio, and G. Nardulli, Phys. Rept. **281**, 145 (1997), arXiv:hep-ph/9605342.

- [600] I. Caprini, L. Lellouch, and M. Neubert, Nucl. Phys. B **530**, 153 (1998), arXiv:hep-ph/9712417.
- [601] R. Casalbuoni, A. Deandrea, N. Di Bartolomeo, R. Gatto, F. Feruglio, and G. Nardulli, Phys. Lett. **B299**, 139 (1993), arXiv:hep-ph/9211248 [hep-ph].
- [602] H.-Y. Cheng, C.-Y. Cheung, and C.-W. Hwang, Phys. Rev. D **55**, 1559 (1997), arXiv:hep-ph/9607332.
- [603] N. Brambilla, A. Vairo, and T. Rosch, Phys. Rev. D **72**, 034021 (2005), arXiv:hep-ph/0506065.
- [604] J. Hu and T. Mehen, Phys. Rev. **D73**, 054003 (2006), arXiv:hep-ph/0511321 [hep-ph].
- [605] M. J. Savage and M. B. Wise, Phys. Lett. **B248**, 177 (1990).
- [606] M.-Z. Liu, Y. Xiao, and L.-S. Geng, Phys. Rev. **D98**, 014040 (2018), arXiv:1807.00912 [hep-ph].
- [607] M.-Z. Liu, T.-W. Wu, J.-J. Xie, M. Pavon Valderrama, and L.-S. Geng, Phys. Rev. **D98**, 014014 (2018), arXiv:1805.08384 [hep-ph].
- [608] S. Aoki et al. (Flavour Lattice Averaging Group), Eur. Phys. J. C **80**, 113 (2020), arXiv:1902.08191 [hep-lat].
- [609] C.-D. Lü, W. Wang, and F.-S. Yu, Phys. Rev. D **93**, 056008 (2016), arXiv:1601.04241 [hep-ph].
- [610] C. Q. Geng, Y. K. Hsiao, C.-W. Liu, and T.-H. Tsai, JHEP **11**, 147 (2017), arXiv:1709.00808 [hep-ph].
- [611] X.-G. He, Y.-J. Shi, and W. Wang, Eur. Phys. J. C **80**, 359 (2020), arXiv:1811.03480 [hep-ph].
- [612] C. Q. Geng, Y. K. Hsiao, C.-W. Liu, and T.-H. Tsai, Phys. Rev. D **97**, 073006 (2018), arXiv:1801.03276 [hep-ph].
- [613] C.-P. Jia, D. Wang, and F.-S. Yu, Nucl. Phys. B **956**, 115048 (2020), arXiv:1910.00876 [hep-ph].
- [614] C.-Q. Geng, C.-W. Liu, T.-H. Tsai, and Y. Yu, Phys. Rev. D **99**, 114022 (2019), arXiv:1904.11271 [hep-ph].
- [615] C.-Q. Geng, X.-G. He, X.-N. Jin, C.-W. Liu, and C. Yang, (2023), arXiv:2310.05491 [hep-ph].
- [616] F. Huang, Y. Xing, and J. Xu, Eur. Phys. J. C **82**, 1075 (2022), arXiv:2209.01716 [hep-ph].
- [617] Q. Qin, J.-L. Qiu, and F.-S. Yu, Eur. Phys. J. C **83**, 227 (2023), arXiv:2212.03590 [hep-ph].
- [618] N. Li, Y. Xing, and X.-H. Hu, Eur. Phys. J. C **83**, 1013 (2023), arXiv:2303.08008 [hep-ph].
- [619] W.-H. Han, J. Xu, and Y. Xing, (2023), arXiv:2310.17125 [hep-ph].
- [620] S. Aoki (Sinya AOKI for HAL QCD), Prog. Part. Nucl. Phys. **66**, 687 (2011), arXiv:1107.1284 [hep-lat].
- [621] K.-W. Li, X.-L. Ren, L.-S. Geng, and B. Long, Phys. Rev. D **94**, 014029 (2016), arXiv:1603.07802 [hep-ph].
- [622] X.-L. Ren, K.-W. Li, L.-S. Geng, B.-W. Long, P. Ring, and J. Meng, Chin. Phys. **C42**, 014103 (2018), arXiv:1611.08475 [nucl-th].
- [623] J. Song, K.-W. Li, and L.-S. Geng, Phys. Rev. C **97**, 065201 (2018), arXiv:1802.04433 [nucl-th].
- [624] Y. Yamaguchi and T. Hyodo, Phys. Rev. C **94**, 065207 (2016), arXiv:1607.04053 [hep-ph].
- [625] K.-W. Li, T. Hyodo, and L.-S. Geng, Phys. Rev. C **98**, 065203 (2018), arXiv:1809.03199 [nucl-th].
- [626] Y. Kamiya, K. Sasaki, T. Fukui, T. Hyodo, K. Morita, K. Ogata, A. Ohnishi, and T. Hatsuda, Phys. Rev. C **105**, 014915 (2022), arXiv:2108.09644 [hep-ph].
- [627] J. R. Green, A. D. Hanlon, P. M. Junnarkar, and H. Wittig, Phys. Rev. Lett. **127**, 242003 (2021), arXiv:2103.01054 [hep-lat].
- [628] R. Chen, J. He, and X. Liu, Chin. Phys. C **41**, 103105 (2017), arXiv:1609.03235 [hep-ph].
- [629] B. Wang, L. Meng, and S.-L. Zhu, Phys. Rev. D **101**, 034018 (2020), arXiv:1912.12592 [hep-ph].
- [630] F.-Z. Peng, M.-J. Yan, M. Sánchez Sánchez, and M. P. Valderrama, (2020), arXiv:2011.01915 [hep-ph].

- [631] J.-T. Zhu, L.-Q. Song, and J. He, Phys. Rev. D **103**, 074007 (2021), arXiv:2101.12441 [hep-ph].
- [632] M.-J. Yan, F.-Z. Peng, M. Sánchez Sánchez, and M. Pavon Valderrama, Phys. Rev. D **104**, 114025 (2021), arXiv:2102.13058 [hep-ph].
- [633] M.-L. Du, Z.-H. Guo, and J. A. Oller, Phys. Rev. D **104**, 114034 (2021), arXiv:2109.14237 [hep-ph].
- [634] M.-Z. Liu, J.-J. Xie, and L.-S. Geng, Phys. Rev. D **102**, 091502 (2020), arXiv:2008.07389 [hep-ph].
- [635] M. Altenbuchinger, L. S. Geng, and W. Weise, Phys. Rev. D **89**, 014026 (2014), arXiv:1309.4743 [hep-ph].
- [636] M.-W. Hu, X.-Y. Lao, P. Ling, and Q. Wang, Chin. Phys. C **45**, 021003 (2021), arXiv:2008.06894 [hep-ph].
- [637] S.-Y. Kong, J.-T. Zhu, D. Song, and J. He, Phys. Rev. D **104**, 094012 (2021), arXiv:2106.07272 [hep-ph].
- [638] M.-Z. Liu, X.-Z. Ling, and L.-S. Geng, (2023), arXiv:2312.01433 [hep-ph].
- [639] R. Aaij *et al.* (LHCb), Phys. Rev. Lett. **131**, 041902 (2023), arXiv:2212.02716 [hep-ex].
- [640] H.-X. Chen, W. Chen, R.-R. Dong, and N. Su, (2020), arXiv:2008.07516 [hep-ph].
- [641] Y. Huang, J.-X. Lu, J.-J. Xie, and L.-S. Geng, (2020), arXiv:2008.07959 [hep-ph].
- [642] C.-J. Xiao, D.-Y. Chen, Y.-B. Dong, and G.-W. Meng, Phys. Rev. D **103**, 034004 (2021), arXiv:2009.14538 [hep-ph].
- [643] R. Molina and E. Oset, Phys. Lett. B **811**, 135870 (2020), arXiv:2008.11171 [hep-ph].
- [644] B. Wang, K. Chen, L. Meng, and S.-L. Zhu, (2023), arXiv:2309.02191 [hep-ph].
- [645] M.-J. Yan, X.-H. Liu, S. González-Solís, F.-K. Guo, C. Hanhart, U.-G. Meißner, and B.-S. Zou, Phys. Rev. D **98**, 091502 (2018), arXiv:1805.10972 [hep-ph].
- [646] L. Meng and S.-L. Zhu, Phys. Rev. D **100**, 014006 (2019), arXiv:1811.07320 [hep-ph].
- [647] T.-W. Wu, M.-Z. Liu, L.-S. Geng, E. Hiyama, M. P. Valderrama, and W.-L. Wang, Eur. Phys. J. C **80**, 901 (2020), arXiv:2004.09779 [hep-ph].
- [648] W.-F. Wang, A. Feijoo, J. Song, and E. Oset, Phys. Rev. D **106**, 116004 (2022), arXiv:2208.14858 [hep-ph].
- [649] A. Faessler, T. Gutsche, V. E. Lyubovitskij, and Y.-L. Ma, Phys. Rev. D **77**, 114013 (2008), arXiv:0801.2232 [hep-ph].
- [650] C. B. Lang, D. Mohler, S. Prelovsek, and R. M. Woloshyn, Phys. Lett. B **750**, 17 (2015), arXiv:1501.01646 [hep-lat].
- [651] Y.-W. Pan, M.-Z. Liu, F.-Z. Peng, M. Sánchez Sánchez, L.-S. Geng, and M. Pavon Valderrama, Phys. Rev. D **102**, 011504 (2020), arXiv:1907.11220 [hep-ph].
- [652] M. Pavon Valderrama, Phys. Rev. D **100**, 094028 (2019), arXiv:1907.05294 [hep-ph].
- [653] L. Meng, B. Wang, G.-J. Wang, and S.-L. Zhu, Phys. Rev. D **100**, 014031 (2019), arXiv:1905.04113 [hep-ph].
- [654] N. Yalikun, Y.-H. Lin, F.-K. Guo, Y. Kamiya, and B.-S. Zou, Phys. Rev. D **104**, 094039 (2021), arXiv:2109.03504 [hep-ph].
- [655] T. J. Burns and E. S. Swanson, Phys. Rev. D **100**, 114033 (2019), arXiv:1908.03528 [hep-ph].
- [656] F.-Z. Peng, J.-X. Lu, M. Sánchez Sánchez, M.-J. Yan, and M. Pavon Valderrama, Phys. Rev. D **103**, 014023 (2021), arXiv:2007.01198 [hep-ph].
- [657] R. Chen, N. Li, Z.-F. Sun, X. Liu, and S.-L. Zhu, Phys. Lett. B **822**, 136693 (2021), arXiv:2108.12730 [hep-ph].

- [658] C.-W. Shen, Y.-h. Lin, and U.-G. Meißner, *Eur. Phys. J. C* **83**, 70 (2023), arXiv:2208.10865 [hep-ph].
- [659] X. Liu, Y. Tan, X. Chen, D. Chen, H. Huang, and J. Ping, (2023), arXiv:2312.04390 [hep-ph].
- [660] K. Chen, B. Wang, and S.-L. Zhu, *Phys. Rev. D* **105**, 096004 (2022), arXiv:2112.13203 [hep-ph].
- [661] B. Wang, K. Chen, L. Meng, and S.-L. Zhu, (2023), arXiv:2312.13591 [hep-ph].
- [662] R. Chen and X. Liu, *Phys. Rev. D* **105**, 014029 (2022), arXiv:2201.07603 [hep-ph].
- [663] M. Karliner and J. L. Rosner, *Phys. Rev. D* **106**, 036024 (2022), arXiv:2207.07581 [hep-ph].
- [664] A. Giachino, A. Hosaka, E. Santopinto, S. Takeuchi, M. Takizawa, and Y. Yamaguchi, (2022), arXiv:2209.10413 [hep-ph].
- [665] K. Chen, Z.-Y. Lin, and S.-L. Zhu, *Phys. Rev. D* **106**, 116017 (2022), arXiv:2211.05558 [hep-ph].
- [666] T. A. Kaeding, *Atom. Data Nucl. Data Tabl.* **61**, 233 (1995), arXiv:nucl-th/9502037.
- [667] F.-Z. Peng, M.-Z. Liu, Y.-W. Pan, M. Sánchez Sánchez, and M. Pavon Valderrama, (2019), arXiv:1907.05322 [hep-ph].
- [668] C.-W. Shen and U.-G. Meißner, *Phys. Lett. B* **831**, 137197 (2022), arXiv:2203.09804 [hep-ph].
- [669] J. A. Marsé-Valera, V. K. Magas, and A. Ramos, *Phys. Rev. Lett.* **130**, 091903 (2023), arXiv:2210.02792 [hep-ph].
- [670] F.-L. Wang, R. Chen, and X. Liu, *Phys. Rev. D* **103**, 034014 (2021), arXiv:2011.14296 [hep-ph].
- [671] M.-J. Yan, F.-Z. Peng, M. Sánchez Sánchez, and M. Pavon Valderrama, *Eur. Phys. J. C* **82**, 574 (2022), arXiv:2108.05306 [hep-ph].
- [672] M.-J. Yan, F.-Z. Peng, M. Sánchez Sánchez, and M. Pavon Valderrama, (2022), arXiv:2207.11144 [hep-ph].
- [673] Z.-Y. Yang, F.-Z. Peng, M.-J. Yan, M. Sánchez Sánchez, and M. Pavon Valderrama, (2022), arXiv:2211.08211 [hep-ph].
- [674] M. Padmanath, R. G. Edwards, N. Mathur, and M. Peardon, *Phys. Rev. D* **91**, 094502 (2015), arXiv:1502.01845 [hep-lat].
- [675] Y.-C. Chen and T.-W. Chiu (TWQCD), *Phys. Lett. B* **767**, 193 (2017), arXiv:1701.02581 [hep-lat].
- [676] C. Alexandrou and C. Kallidonis, *Phys. Rev. D* **96**, 034511 (2017), arXiv:1704.02647 [hep-lat].
- [677] N. Mathur and M. Padmanath, *Phys. Rev. D* **99**, 031501 (2019), arXiv:1807.00174 [hep-lat].
- [678] Y.-W. Pan, M.-Z. Liu, and L.-S. Geng, *Phys. Rev. D* **102**, 054025 (2020), arXiv:2004.07467 [hep-ph].
- [679] P. Junnarkar and N. Mathur, *Phys. Rev. Lett.* **123**, 162003 (2019), arXiv:1906.06054 [hep-lat].
- [680] Z.-G. Wang, (2019), arXiv:1912.07230 [hep-ph].
- [681] R. Chen, F.-L. Wang, A. Hosaka, and X. Liu, *Phys. Rev. D* **97**, 114011 (2018), arXiv:1804.02961 [hep-ph].
- [682] Y.-W. Pan, T.-W. Wu, M.-Z. Liu, and L.-S. Geng, *Eur. Phys. J. C* **82**, 908 (2022), arXiv:2208.05385 [hep-ph].
- [683] D. Gamermann, J. Nieves, E. Oset, and E. Ruiz Arriola, *Phys. Rev. D* **81**, 014029 (2010), arXiv:0911.4407 [hep-ph].
- [684] M.-Z. Liu and L.-S. Geng, *Eur. Phys. J. C* **81**, 179 (2021), arXiv:2012.05096 [hep-ph].
- [685] A. Ozpineci, C. W. Xiao, and E. Oset, *Phys. Rev. D* **88**, 034018 (2013), arXiv:1306.3154 [hep-ph].
- [686] C. Hidalgo-Duque, J. Nieves, and M. P. Valderrama, *Phys. Rev. D* **87**, 076006 (2013), arXiv:1210.5431 [hep-ph].

- [687] L. Meng, B. Wang, and S.-L. Zhu, *Sci. Bull.* **66**, 1288 (2021), arXiv:2012.09813 [hep-ph].
- [688] T. Ji, X.-K. Dong, M. Albaladejo, M.-L. Du, F.-K. Guo, J. Nieves, and B.-S. Zou, (2022), 10.1016/j.scib.2023.02.034, arXiv:2212.00631 [hep-ph].
- [689] M.-Z. Liu, D.-J. Jia, and D.-Y. Chen, *Chin. Phys.* **C41**, 053105 (2017), arXiv:1702.04440 [hep-ph].
- [690] F.-K. Guo, C. Hidalgo-Duque, J. Nieves, and M. P. Valderrama, *Phys. Rev.* **D88**, 054014 (2013), arXiv:1305.4052 [hep-ph].
- [691] R. Chen, A. Hosaka, and X. Liu, *Phys. Rev.* **D96**, 114030 (2017), arXiv:1711.09579 [hep-ph].
- [692] J.-M. Xie, M.-Z. Liu, and L.-S. Geng, (2022), arXiv:2207.12178 [hep-ph].
- [693] L. R. Dai, R. Molina, and E. Oset, *Phys. Rev. D* **105**, 016029 (2022), [Erratum: *Phys.Rev.D* 106, 099902 (2022)], arXiv:2110.15270 [hep-ph].
- [694] R. Chen and Q. Huang, *Phys. Rev. D* **103**, 034008 (2021), arXiv:2011.09156 [hep-ph].
- [695] E. J. Eichten and C. Quigg, *Phys. Rev. Lett.* **119**, 202002 (2017), arXiv:1707.09575 [hep-ph].
- [696] Q. Meng, M. Harada, E. Hiyama, A. Hosaka, and M. Oka, *Phys. Lett. B* **824**, 136800 (2022), arXiv:2106.11868 [hep-ph].
- [697] J. Z. Bai *et al.* (BES), *Phys. Rev. Lett.* **88**, 101802 (2002), arXiv:hep-ex/0102003.
- [698] M. Sanchez Sanchez, L.-S. Geng, J.-X. Lu, T. Hyodo, and M. P. Valderrama, *Phys. Rev.* **D98**, 054001 (2018), arXiv:1707.03802 [hep-ph].
- [699] J. He, Y. Liu, J.-T. Zhu, and D.-Y. Chen, *Eur. Phys. J. C* **80**, 246 (2020), arXiv:1912.08420 [hep-ph].
- [700] X.-D. Yang, F.-L. Wang, Z.-W. Liu, and X. Liu, *Eur. Phys. J. C* **81**, 807 (2021), arXiv:2103.03127 [hep-ph].
- [701] X.-Z. Ling, M.-Z. Liu, and L.-S. Geng, *Eur. Phys. J. C* **81**, 1090 (2021), arXiv:2110.13792 [hep-ph].
- [702] N. Lee, Z.-G. Luo, X.-L. Chen, and S.-L. Zhu, *Phys. Rev. D* **84**, 014031 (2011), arXiv:1104.4257 [hep-ph].
- [703] Z.-S. Jia, M.-J. Yan, Z.-H. Zhang, P.-P. Shi, G. Li, and F.-K. Guo, *Phys. Rev. D* **107**, 074029 (2023), arXiv:2211.02479 [hep-ph].
- [704] Z.-S. Jia, Z.-H. Zhang, G. Li, and F.-K. Guo, *Phys. Rev. D* **108**, 094038 (2023), arXiv:2307.11047 [hep-ph].
- [705] L. Meng, G.-J. Wang, B. Wang, and S.-L. Zhu, *Phys. Rev. D* **104**, 094003 (2021), arXiv:2109.01333 [hep-ph].
- [706] F. K. Guo, C. Hidalgo-Duque, J. Nieves, A. Ozpineci, and M. P. Valderrama, *Eur. Phys. J. C* **74**, 2885 (2014), arXiv:1404.1776 [hep-ph].
- [707] Z.-G. Wang, (2023), arXiv:2309.01337 [hep-ph].
- [708] R. Molina, D. Nicmorus, and E. Oset, *Phys. Rev. D* **78**, 114018 (2008), arXiv:0809.2233 [hep-ph].
- [709] J. He and D.-Y. Chen, *Eur. Phys. J.* **C79**, 887 (2019), arXiv:1909.05681 [hep-ph].
- [710] Y.-b. Dong, A. Faessler, T. Gutsche, and V. E. Lyubovitskij, *Phys. Rev. D* **77**, 094013 (2008), arXiv:0802.3610 [hep-ph].
- [711] Y. Dong, A. Faessler, T. Gutsche, and V. E. Lyubovitskij, *Phys. Rev. D* **88**, 014030 (2013), arXiv:1306.0824 [hep-ph].
- [712] C.-W. Shen, F.-K. Guo, J.-J. Xie, and B.-S. Zou, *Nucl. Phys. A* **954**, 393 (2016), arXiv:1603.04672 [hep-ph].
- [713] K. Azizi, Y. Sarac, and H. Sundu, *Phys. Rev. D* **103**, 094033 (2021), arXiv:2101.07850 [hep-ph].
- [714] H.-X. Chen, Y.-X. Yan, and W. Chen, *Phys. Rev. D* **106**, 094019 (2022), arXiv:2207.08593 [hep-ph].

- [715] Z.-G. Wang, Phys. Rev. D **109**, 014017 (2024), arXiv:2310.02030 [hep-ph].
- [716] U. Skerbis and S. Prelovsek, Phys. Rev. **D99**, 094505 (2019), arXiv:1811.02285 [hep-lat].
- [717] T. J. Burns and E. S. Swanson, Eur. Phys. J. A **58**, 68 (2022), arXiv:2112.11527 [hep-ph].
- [718] Z. Zhang, J. Liu, J. Hu, Q. Wang, and U.-G. Meißner, Sci. Bull. **68**, 981 (2023), arXiv:2301.05364 [hep-ph].
- [719] R. Aaij et al. (LHCb), Phys. Rev. Lett. **122**, 222001 (2019), arXiv:1904.03947 [hep-ex].
- [720] F. Guo and H.-S. Li, (2023), arXiv:2304.10981 [hep-ph].
- [721] M.-W. Li, Z.-W. Liu, Z.-F. Sun, and R. Chen, Phys. Rev. D **104**, 054016 (2021), arXiv:2106.15053 [hep-ph].
- [722] Y. Dong, A. Faessler, T. Gutsche, S. Kovalenko, and V. E. Lyubovitskij, Phys. Rev. D **79**, 094013 (2009), arXiv:0903.5416 [hep-ph].
- [723] Y. Wang, Q. Wu, G. Li, W.-H. Qin, X.-H. Liu, C.-S. An, and J.-J. Xie, Phys. Rev. D **106**, 074015 (2022), arXiv:2209.12206 [hep-ph].
- [724] M. Albaladejo, F. K. Guo, C. Hidalgo-Duque, J. Nieves, and M. P. Valderrama, Eur. Phys. J. **C75**, 547 (2015), arXiv:1504.00861 [hep-ph].
- [725] P.-P. Shi, J. M. Dias, and F.-K. Guo, (2023), arXiv:2302.13017 [hep-ph].
- [726] T. Branz, R. Molina, and E. Oset, Phys. Rev. D **83**, 114015 (2011), arXiv:1010.0587 [hep-ph].
- [727] G. Li, Eur. Phys. J. C **73**, 2621 (2013), arXiv:1304.4458 [hep-ph].
- [728] C.-J. Xiao, D.-Y. Chen, Y.-B. Dong, W. Zuo, and T. Matsuki, Phys. Rev. D **99**, 074003 (2019), arXiv:1811.04688 [hep-ph].
- [729] X.-Y. Qi, Q. Wu, and D.-Y. Chen, Eur. Phys. J. C **83**, 1006 (2023), arXiv:2302.10050 [hep-ph].
- [730] D.-Y. Chen and Y.-B. Dong, Phys. Rev. D **93**, 014003 (2016), arXiv:1510.00829 [hep-ph].
- [731] X.-Y. Wang, G. Li, C.-S. An, and J.-J. Xie, Phys. Rev. D **106**, 074026 (2022), arXiv:2210.06783 [hep-ph].
- [732] Q. Wu and D.-Y. Chen, Phys. Rev. D **104**, 074011 (2021), arXiv:2108.06700 [hep-ph].
- [733] M. Cleven, H. W. Griebhammer, F.-K. Guo, C. Hanhart, and U.-G. Meißner, Eur. Phys. J. **A50**, 149 (2014), arXiv:1405.2242 [hep-ph].
- [734] c.-J. Xiao, D.-Y. Chen, and Y.-L. Ma, Phys. Rev. **D93**, 094011 (2016), arXiv:1601.06399 [hep-ph].
- [735] Y. S. Amhis et al. (HFLAV), Phys. Rev. D **107**, 052008 (2023), arXiv:2206.07501 [hep-ex].
- [736] H.-Y. Cheng and C.-W. Chiang, Phys. Rev. D **81**, 074021 (2010), arXiv:1001.0987 [hep-ph].
- [737] H.-n. Li, C.-D. Lu, and F.-S. Yu, Phys. Rev. D **86**, 036012 (2012), arXiv:1203.3120 [hep-ph].
- [738] Q. Qin, H.-n. Li, C.-D. Lü, and F.-S. Yu, Phys. Rev. D **89**, 054006 (2014), arXiv:1305.7021 [hep-ph].
- [739] J.-J. Han, H.-Y. Jiang, W. Liu, Z.-J. Xiao, and F.-S. Yu, Chin. Phys. C **45**, 053105 (2021), arXiv:2101.12019 [hep-ph].
- [740] Y. Cao, Y. Cheng, and Q. Zhao, (2023), arXiv:2303.00535 [hep-ph].
- [741] F.-S. Yu, H.-Y. Jiang, R.-H. Li, C.-D. Lü, W. Wang, and Z.-X. Zhao, Chin. Phys. **C42**, 051001 (2018), arXiv:1703.09086 [hep-ph].
- [742] M.-Z. Liu, X.-Z. Ling, L.-S. Geng, En-Wang, and J.-J. Xie, Phys. Rev. D **106**, 114011 (2022), arXiv:2209.01103 [hep-ph].
- [743] M. Bauer, B. Stech, and M. Wirbel, Z. Phys. C **34**, 103 (1987).

- [744] M. Beneke, G. Buchalla, M. Neubert, and C. T. Sachrajda, Nucl. Phys. B **591**, 313 (2000), arXiv:hep-ph/0006124.
- [745] M. Beneke, G. Buchalla, M. Neubert, and C. T. Sachrajda, Nucl. Phys. B **606**, 245 (2001), arXiv:hep-ph/0104110.
- [746] M. Beneke and M. Neubert, Nucl. Phys. B **675**, 333 (2003), arXiv:hep-ph/0308039.
- [747] A. Ali, G. Kramer, and C.-D. Lu, Phys. Rev. D **58**, 094009 (1998), arXiv:hep-ph/9804363.
- [748] Z.-G. Wang, Eur. Phys. J. C **75**, 427 (2015), arXiv:1506.01993 [hep-ph].
- [749] G.-L. Wang, Phys. Lett. B **650**, 15 (2007), arXiv:0705.2621 [hep-ph].
- [750] R. C. Verma, J. Phys. G **39**, 025005 (2012), arXiv:1103.2973 [hep-ph].
- [751] R. Aaij et al. (LHCb), Eur. Phys. J. C **72**, 1972 (2012), arXiv:1112.5310 [hep-ex].
- [752] F.-K. Guo, U.-G. Meißner, and Z. Yang, Phys. Lett. B **740**, 42 (2015), arXiv:1410.4674 [hep-ph].
- [753] E. Braaten, L.-P. He, and K. Ingles, Phys. Rev. D **100**, 031501 (2019), arXiv:1904.12915 [hep-ph].
- [754] E. Braaten, L.-P. He, and K. Ingles, Phys. Rev. D **101**, 014021 (2020), arXiv:1909.03901 [hep-ph].
- [755] E. Braaten and M. Kusunoki, Phys. Rev. D **71**, 074005 (2005), arXiv:hep-ph/0412268.
- [756] E. Braaten, L.-P. He, and K. Ingles, Phys. Rev. D **100**, 074028 (2019), arXiv:1902.03259 [hep-ph].
- [757] S. Sakai, E. Oset, and F.-K. Guo, Phys. Rev. D **101**, 054030 (2020), arXiv:2002.03160 [hep-ph].
- [758] M.-J. Yan, Y.-H. Ge, and X.-H. Liu, Phys. Rev. D **106**, 114002 (2022), arXiv:2208.03943 [hep-ph].
- [759] H.-N. Wang, L.-S. Geng, Q. Wang, and J.-J. Xie, Chin. Phys. Lett. **40**, 021301 (2023), arXiv:2211.14994 [hep-ph].
- [760] G.-Y. Chen, W.-S. Huo, and Q. Zhao, Chin. Phys. C **39**, 093101 (2015), arXiv:1309.2859 [hep-ph].
- [761] W. Wang and Q. Zhao, Phys. Lett. B **755**, 261 (2016), arXiv:1512.03123 [hep-ph].
- [762] S. Cho et al. (ExHIC), Phys. Rev. C **84**, 064910 (2011), arXiv:1107.1302 [nucl-th].
- [763] B. Chen, L. Jiang, X.-H. Liu, Y. Liu, and J. Zhao, Phys. Rev. C **105**, 054901 (2022), arXiv:2107.00969 [hep-ph].
- [764] Q. Wu, D.-Y. Chen, X.-J. Fan, and G. Li, Eur. Phys. J. C **79**, 265 (2019), arXiv:1902.05737 [hep-ph].
- [765] R. Molina, J.-J. Xie, W.-H. Liang, L.-S. Geng, and E. Oset, Phys. Lett. B **803**, 135279 (2020), arXiv:1908.11557 [hep-ph].
- [766] R. L. Workman et al. (Particle Data Group), PTEP **2022**, 083C01 (2022).
- [767] Q. Zhao, Nucl. Phys. Rev. **37**, 260 (2020).
- [768] A. F. Falk and M. Neubert, Phys. Rev. D **47**, 2982 (1993), arXiv:hep-ph/9209269.
- [769] T. Gutsche, M. A. Ivanov, J. G. Körner, and V. E. Lyubovitskij, Phys. Rev. D **98**, 074011 (2018), arXiv:1806.11549 [hep-ph].
- [770] C. W. Xiao, J. X. Lu, J. J. Wu, and L. S. Geng, Phys. Rev. D **102**, 056018 (2020), arXiv:2007.12106 [hep-ph].
- [771] M. Karliner and J. L. Rosner, Phys. Lett. B **752**, 329 (2016), arXiv:1508.01496 [hep-ph].
- [772] J.-J. Wu, T. S. H. Lee, and B.-S. Zou, Phys. Rev. C **100**, 035206 (2019), arXiv:1906.05375 [nucl-th].
- [773] S.-Y. Li, Y.-R. Liu, Y.-N. Liu, Z.-G. Si, and X.-F. Zhang, Commun. Theor. Phys. **69**, 291 (2018), arXiv:1706.04765 [hep-ph].

- [774] M. B. Voloshin, Phys. Rev. D **99**, 093003 (2019), arXiv:1903.04422 [hep-ph].
- [775] C.-h. Chen, Y.-L. Xie, H.-g. Xu, Z. Zhang, D.-M. Zhou, Z.-L. She, and G. Chen, Phys. Rev. D **105**, 054013 (2022), arXiv:2111.03241 [hep-ph].
- [776] P. Ling, X.-H. Dai, M.-L. Du, and Q. Wang, Eur. Phys. J. C **81**, 819 (2021), arXiv:2104.11133 [hep-ph].
- [777] P.-P. Shi, F.-K. Guo, and Z. Yang, Phys. Rev. D **106**, 114026 (2022), arXiv:2208.02639 [hep-ph].
- [778] R. B. Wiringa, Phys. Rev. C **43**, 1585 (1991).
- [779] J. Carlson and R. Schiavilla, Rev. Mod. Phys. **70**, 743 (1998).
- [780] B. S. Pudliner, V. R. Pandharipande, J. Carlson, S. C. Pieper, and R. B. Wiringa, Phys. Rev. C **56**, 1720 (1997), arXiv:nucl-th/9705009.
- [781] H. Bando, T. Motoba, and J. Zofka, Int. J. Mod. Phys. A **5**, 4021 (1990).
- [782] O. Hashimoto and H. Tamura, Prog. Part. Nucl. Phys. **57**, 564 (2006).
- [783] E. Hiyama and T. Yamada, Prog. Part. Nucl. Phys. **63**, 339 (2009).
- [784] H. Garcilazo, F. Fernandez, A. Valcarce, and R. D. Mota, Phys. Rev. C **56**, 84 (1997).
- [785] H. Garcilazo, A. Valcarce, and F. Fernández, Phys. Rev. C **60**, 044002 (1999).
- [786] R. D. Mota, H. Garcilazo, A. Valcarce, and F. Fernandez, Phys. Rev. C **59**, 46 (1999).
- [787] A. Valcarce, H. Garcilazo, R. D. Mota, and F. Fernandez, J. Phys. G **27**, L1 (2001).
- [788] R. D. Mota, A. Valcarce, F. Fernandez, D. R. Entem, and H. Garcilazo, Phys. Rev. C **65**, 034006 (2002), arXiv:nucl-th/0112059.
- [789] H. Garcilazo, T. Fernandez-Carames, and A. Valcarce, Phys. Rev. C **75**, 034002 (2007), arXiv:hep-ph/0701275.
- [790] T. Fernandez-Carames, A. Valcarce, H. Garcilazo, and P. Gonzalez, Phys. Rev. C **73**, 034004 (2006), arXiv:hep-ph/0601252.
- [791] H. Garcilazo and A. Valcarce, Symmetry **14**, 2381 (2022), arXiv:2211.13970 [nucl-th].
- [792] H. Garcilazo and A. Valcarce, Phys. Rev. C **92**, 014004 (2015), arXiv:1507.03733 [hep-ph].
- [793] H. Garcilazo, Phys. Rev. C **93**, 024001 (2016).
- [794] H. Garcilazo and A. Valcarce, Phys. Rev. C **93**, 034001 (2016), arXiv:1605.04108 [hep-ph].
- [795] H. Garcilazo and A. Valcarce, Chin. Phys. C **44**, 104104 (2020), arXiv:2006.16567 [nucl-th].
- [796] H. Garcilazo, A. Valcarce, and J. Vijande, Phys. Rev. C **94**, 024002 (2016), arXiv:1608.05192 [nucl-th].
- [797] H. Garcilazo and A. Valcarce, Phys. Rev. C **99**, 014001 (2019), arXiv:1901.05678 [hep-ph].
- [798] L. Zhang, S. Zhang, and Y.-G. Ma, Eur. Phys. J. C **82**, 416 (2022), arXiv:2112.02766 [hep-ph].
- [799] T. Suzuki et al., Phys. Lett. B **597**, 263 (2004).
- [800] Y. Maezawa, T. Hatsuda, and S. Sasaki, Prog. Theor. Phys. **114**, 317 (2005), arXiv:hep-ph/0412025.
- [801] M. Sato (KEK-PS E471/E549), AIP Conf. Proc. **842**, 480 (2006).
- [802] M. Sato et al., Phys. Lett. B **659**, 107 (2008), arXiv:0708.2968 [nucl-ex].
- [803] M. Sato et al. (KEK-PS E549), Int. J. Mod. Phys. A **24**, 442 (2009).
- [804] H. Yim et al., Phys. Lett. B **688**, 43 (2010).
- [805] A. Dote, T. Hyodo, and W. Weise, Int. J. Mod. Phys. E **19**, 2618 (2010).

- [806] A. Dote, T. Hyodo, and W. Weise, *Hyperfine Interact.* **193**, 245 (2009), arXiv:0811.0869 [nucl-th].
- [807] N. Barnea, A. Gal, and E. Z. Liverts, *Phys. Lett. B* **712**, 132 (2012), arXiv:1203.5234 [nucl-th].
- [808] Y. Ikeda, H. Kamano, and T. Sato, *Prog. Theor. Phys.* **124**, 533 (2010), arXiv:1004.4877 [nucl-th].
- [809] J. Révai and N. V. Shevchenko, *Phys. Rev. C* **90**, 034004 (2014), arXiv:1403.0757 [nucl-th].
- [810] S. Wycech and A. M. Green, *Few Body Syst.* **45**, 95 (2009).
- [811] N. V. Shevchenko, A. Gal, J. Mares, and J. Revai, *Phys. Rev. C* **76**, 044004 (2007), arXiv:0706.4393 [nucl-th].
- [812] Y. Kanada-En'yo and D. Jido, *Phys. Rev. C* **78**, 025212 (2008), arXiv:0804.3124 [nucl-th].
- [813] T. Hyodo and W. Weise, “Theory of Kaon-Nuclear Systems,” in *Handbook of Nuclear Physics*, edited by I. Tanihata, H. Toki, and T. Kajino (2022) pp. 1–34, arXiv:2202.06181 [nucl-th].
- [814] R. Y. Kezerashvili, S. M. Tsiklauri, and N. Z. Takibayev, *Prog. Part. Nucl. Phys.* **121**, 103909 (2021).
- [815] R. H. Dalitz and S. F. Tuan, *Phys. Rev. Lett.* **2**, 425 (1959).
- [816] R. H. Dalitz and S. F. Tuan, *Annals Phys.* **10**, 307 (1960).
- [817] J.-J. Xie, A. Martinez Torres, and E. Oset, *Phys. Rev. C* **83**, 065207 (2011), arXiv:1010.6164 [nucl-th].
- [818] D. Jido and Y. Kanada-En'yo, *Phys. Rev. C* **78**, 035203 (2008), arXiv:0806.3601 [nucl-th].
- [819] A. Martinez Torres, K. P. Khemchandani, and L.-S. Geng, *Phys. Rev. D* **99**, 076017 (2019), arXiv:1809.01059 [hep-ph].
- [820] J.-Y. Pang, J.-J. Wu, and L.-S. Geng, *Phys. Rev. D* **102**, 114515 (2020), arXiv:2008.13014 [hep-lat].
- [821] V. R. Debastiani, J. M. Dias, and E. Oset, *Phys. Rev. D* **96**, 016014 (2017), arXiv:1705.09257 [hep-ph].
- [822] T.-W. Wu, M.-Z. Liu, and L.-S. Geng, *Phys. Rev. D* **103**, L031501 (2021), arXiv:2012.01134 [hep-ph].
- [823] L. Ma, Q. Wang, and U.-G. Meißner, *Chin. Phys. C* **43**, 014102 (2019), arXiv:1711.06143 [hep-ph].
- [824] X.-L. Ren, B. B. Malabarba, L.-S. Geng, K. P. Khemchandani, and A. Martínez Torres, *Phys. Lett. B* **785**, 112 (2018), arXiv:1805.08330 [hep-ph].
- [825] X. Wei, Q.-H. Shen, and J.-J. Xie, *Eur. Phys. J. C* **82**, 718 (2022), arXiv:2205.12526 [hep-ph].
- [826] Y. Huang, M.-Z. Liu, Y.-W. Pan, L.-S. Geng, A. Martínez Torres, and K. P. Khemchandani, *Phys. Rev. D* **101**, 014022 (2020), arXiv:1909.09021 [hep-ph].
- [827] Y. Li *et al.* (Belle), *Phys. Rev. D* **102**, 112001 (2020), arXiv:2008.13341 [hep-ex].
- [828] Y. Li, Y.-B. He, X.-H. Liu, B. Chen, and H.-W. Ke, (2023), arXiv:2302.02518 [hep-ph].
- [829] Y.-W. Pan, T.-W. Wu, M.-Z. Liu, and L.-S. Geng, *Phys. Rev. D* **105**, 114048 (2022), arXiv:2204.02295 [hep-ph].
- [830] S. S. Agaev, K. Azizi, and H. Sundu, *Nucl. Phys. B* **975**, 115650 (2022), arXiv:2108.00188 [hep-ph].
- [831] H. Ren, F. Wu, and R. Zhu, *Adv. High Energy Phys.* **2022**, 9103031 (2022), arXiv:2109.02531 [hep-ph].
- [832] S. Fleming, R. Hodges, and T. Mehen, *Phys. Rev. D* **104**, 116010 (2021), arXiv:2109.02188 [hep-ph].
- [833] T.-W. Wu, Y.-W. Pan, M.-Z. Liu, S.-Q. Luo, X. Liu, and L.-S. Geng, (2021), arXiv:2108.00923 [hep-ph].
- [834] S.-Q. Luo, T.-W. Wu, M.-Z. Liu, L.-S. Geng, and X. Liu, (2021), arXiv:2111.15079 [hep-ph].
- [835] M. Bayar, A. Martinez Torres, K. P. Khemchandani, R. Molina, and E. Oset, *Eur. Phys. J. C* **83**, 46 (2023), arXiv:2211.09294 [hep-ph].
- [836] M. Bayar, C. W. Xiao, T. Hyodo, A. Dote, M. Oka, and E. Oset, *Phys. Rev. C* **86**, 044004 (2012),

- arXiv:1205.2275 [hep-ph].
- [837] C. W. Xiao, M. Bayar, and E. Oset, Phys. Rev. D **84**, 034037 (2011), arXiv:1106.0459 [hep-ph].
 - [838] S.-Q. Luo, L.-S. Geng, and X. Liu, Phys. Rev. D **106**, 014017 (2022), arXiv:2206.04586 [hep-ph].
 - [839] A. Martinez Torres, K. P. Khemchandani, M. Nielsen, and F. S. Navarra, Phys. Rev. D **87**, 034025 (2013), arXiv:1209.5992 [hep-ph].
 - [840] T.-W. Wu, Y.-W. Pan, M.-Z. Liu, J.-X. Lu, L.-S. Geng, and X.-H. Liu, (2021), arXiv:2106.11450 [hep-ph].
 - [841] C. W. Xiao, M. Bayar, and E. Oset, Phys. Rev. D **86**, 094019 (2012), arXiv:1207.4030 [hep-ph].
 - [842] C. W. Xiao, Eur. Phys. J. A **53**, 176 (2017), arXiv:1611.00543 [hep-ph].
 - [843] B. Durkaya and M. Bayar, Phys. Rev. D **92**, 036006 (2015).
 - [844] X.-L. Ren, B. B. Malabarba, K. P. Khemchandani, and A. Martinez Torres, JHEP **05**, 103 (2019), arXiv:1904.06768 [hep-ph].
 - [845] N. Ikeno, M. Bayar, and E. Oset, Phys. Rev. D **107**, 034006 (2023), arXiv:2208.03698 [hep-ph].
 - [846] M. P. Valderrama, Phys. Rev. D **98**, 034017 (2018), arXiv:1805.10584 [hep-ph].
 - [847] T.-W. Wu, S.-Q. Luo, M.-Z. Liu, L.-S. Geng, and X. Liu, Phys. Rev. D **108**, L091506 (2023), arXiv:2301.00630 [hep-ph].
 - [848] T.-W. Wu and L.-S. Geng, Few Body Syst. **62**, 89 (2021), arXiv:2105.09703 [hep-ph].
 - [849] J. M. Dias, V. R. Debastiani, L. Roca, S. Sakai, and E. Oset, Phys. Rev. D **96**, 094007 (2017), arXiv:1709.01372 [hep-ph].
 - [850] J. M. Dias, L. Roca, and S. Sakai, Phys. Rev. D **97**, 056019 (2018), arXiv:1801.03504 [hep-ph].
 - [851] L. Ma, Q. Wang, and U.-G. Meißner, Phys. Rev. D **100**, 014028 (2019), arXiv:1812.09750 [hep-ph].
 - [852] H. Garcilazo and A. Valcarce, Phys. Lett. B **784**, 169 (2018), arXiv:1808.00226 [hep-ph].
 - [853] M. Bayar, P. Fernandez-Soler, Z.-F. Sun, and E. Oset, Eur. Phys. J. A **52**, 106 (2016), arXiv:1510.06570 [hep-ph].
 - [854] X.-L. Ren and Z.-F. Sun, Phys. Rev. D **99**, 094041 (2019), arXiv:1812.09931 [hep-ph].
 - [855] M. Bayar, N. Ikeno, and L. Roca, Phys. Rev. D **107**, 054042 (2023), arXiv:2301.07436 [hep-ph].
 - [856] M. P. Valderrama, Phys. Rev. D **98**, 014022 (2018), arXiv:1805.05100 [hep-ph].
 - [857] S. Sakai, L. Roca, and E. Oset, Phys. Rev. D **96**, 054023 (2017), arXiv:1704.02196 [hep-ph].
 - [858] Z. T. Draper, A. D. Hanlon, B. Hörz, C. Morningstar, F. Romero-López, and S. R. Sharpe, JHEP **05**, 137 (2023), arXiv:2302.13587 [hep-lat].
 - [859] T. D. Blanton and S. R. Sharpe, Phys. Rev. D **104**, 034509 (2021), arXiv:2105.12094 [hep-lat].
 - [860] F. Romero-López, Rev. Mex. Fis. Suppl. **3**, 0308003 (2022), arXiv:2112.05170 [hep-lat].
 - [861] F. Romero-López, PoS LATTICE2022, 235 (2023), arXiv:2212.13793 [hep-lat].
 - [862] B. Hörz, PoS LATTICE2021, 006 (2022).
 - [863] M. Mai and M. Doring, Phys. Rev. Lett. **122**, 062503 (2019), arXiv:1807.04746 [hep-lat].
 - [864] M. Mai, A. Alexandru, R. Brett, C. Culver, M. Döring, F. X. Lee, and D. Sadasivan (GWQCD), Phys. Rev. Lett. **127**, 222001 (2021), arXiv:2107.03973 [hep-lat].
 - [865] T. D. Blanton, A. D. Hanlon, B. Hörz, C. Morningstar, F. Romero-López, and S. R. Sharpe, JHEP **10**, 023

- (2021), arXiv:2106.05590 [hep-lat].
- [866] A. Alexandru, R. Brett, C. Culver, M. Döring, D. Guo, F. X. Lee, and M. Mai, Phys. Rev. D **102**, 114523 (2020), arXiv:2009.12358 [hep-lat].
- [867] M. Mai, M. Döring, and A. Rusetsky, Eur. Phys. J. ST **230**, 1623 (2021), arXiv:2103.00577 [hep-lat].
- [868] J. Bulava *et al.*, in *Snowmass 2021* (2022) arXiv:2203.03230 [hep-lat].
- [869] Z. T. Draper, M. T. Hansen, F. Romero-López, and S. R. Sharpe, JHEP **07**, 226 (2023), arXiv:2303.10219 [hep-lat].
- [870] M. T. Hansen and S. R. Sharpe, Ann. Rev. Nucl. Part. Sci. **69**, 65 (2019), arXiv:1901.00483 [hep-lat].
- [871] R. Hanbury Brown and R. Q. Twiss, Nature **178**, 1046 (1956).
- [872] G. Goldhaber, S. Goldhaber, W.-Y. Lee, and A. Pais, Phys. Rev. **120**, 300 (1960).
- [873] M. Gyulassy, S. K. Kauffmann, and L. W. Wilson, Phys. Rev. C **20**, 2267 (1979).
- [874] W. A. Zajc *et al.*, Phys. Rev. C **29**, 2173 (1984).
- [875] S. Y. Fung, W. Gorn, G. P. Kiernan, J. J. Lu, Y. T. Oh, and R. T. Poe, Phys. Rev. Lett. **41**, 1592 (1978).
- [876] U. A. Wiedemann and U. W. Heinz, Phys. Rept. **319**, 145 (1999), arXiv:nucl-th/9901094.
- [877] S. Acharya *et al.* (ALICE), Phys. Lett. B **813**, 136030 (2021), arXiv:2007.08315 [nucl-ex].
- [878] S. Acharya *et al.* (ALICE), (2023), arXiv:2312.12830 [hep-ex].
- [879] S. Acharya *et al.* (ALICE), Phys. Lett. B **833**, 137335 (2022), arXiv:2111.06611 [nucl-ex].
- [880] S. Acharya *et al.* (ALICE), Phys. Lett. B **774**, 64 (2017), arXiv:1705.04929 [nucl-ex].
- [881] S. Acharya *et al.* (ALICE), Phys. Lett. B **790**, 22 (2019), arXiv:1809.07899 [nucl-ex].
- [882] S. Acharya *et al.* (ALICE), Phys. Rev. Lett. **124**, 092301 (2020), arXiv:1905.13470 [nucl-ex].
- [883] S. Acharya *et al.* (ALICE), Eur. Phys. J. C **83**, 340 (2023), arXiv:2205.15176 [nucl-ex].
- [884] S. Acharya *et al.* (ALICE), Phys. Rev. C **103**, 055201 (2021), arXiv:2005.11124 [nucl-ex].
- [885] S. Acharya *et al.* (ALICE), Phys. Lett. B **845**, 138145 (2023), arXiv:2305.19093 [nucl-ex].
- [886] S. Acharya *et al.* (ALICE), Phys. Rev. C **99**, 024001 (2019), arXiv:1805.12455 [nucl-ex].
- [887] S. Acharya *et al.* (ALICE), Phys. Lett. B **833**, 137272 (2022), arXiv:2104.04427 [nucl-ex].
- [888] S. Acharya *et al.* (ALICE), Phys. Lett. B **805**, 135419 (2020), arXiv:1910.14407 [nucl-ex].
- [889] S. Acharya *et al.* (ALICE), Phys. Lett. B **797**, 134822 (2019), arXiv:1905.07209 [nucl-ex].
- [890] S. Acharya *et al.* (ALICE), Phys. Lett. B **844**, 137223 (2023), arXiv:2204.10258 [nucl-ex].
- [891] S. Acharya *et al.* (ALICE), Phys. Lett. B **802**, 135223 (2020), arXiv:1903.06149 [nucl-ex].
- [892] S. Acharya *et al.* (ALICE), Phys. Lett. B **829**, 137060 (2022), arXiv:2105.05190 [nucl-ex].
- [893] M. Isshiki (STAR), EPJ Web Conf. **259**, 11015 (2022), arXiv:2109.10953 [nucl-ex].
- [894] J. Adam *et al.* (STAR), Phys. Lett. B **790**, 490 (2019), arXiv:1808.02511 [hep-ex].
- [895] S. Acharya *et al.* (ALICE), Eur. Phys. J. A **59**, 298 (2023), arXiv:2303.13448 [nucl-ex].
- [896] S. Acharya *et al.* (ALICE), Eur. Phys. J. A **59**, 145 (2023), arXiv:2206.03344 [nucl-ex].
- [897] S. Acharya *et al.* (ALICE), Phys. Rev. D **106**, 052010 (2022), arXiv:2201.05352 [nucl-ex].
- [898] S. Acharya *et al.* (ALICE), (2024), arXiv:2401.13541 [nucl-ex].
- [899] K. Morita, T. Furumoto, and A. Ohnishi, Phys. Rev. C **91**, 024916 (2015), arXiv:1408.6682 [nucl-th].

- [900] K. Morita, A. Ohnishi, F. Etminan, and T. Hatsuda, Phys. Rev. C **94**, 031901 (2016), [Erratum: Phys.Rev.C 100, 069902 (2019)], arXiv:1605.06765 [hep-ph].
- [901] A. Ohnishi, K. Morita, K. Miyahara, and T. Hyodo, Nucl. Phys. A **954**, 294 (2016), arXiv:1603.05761 [nucl-th].
- [902] K. Morita, S. Gongyo, T. Hatsuda, T. Hyodo, Y. Kamiya, and A. Ohnishi, Phys. Rev. C **101**, 015201 (2020), arXiv:1908.05414 [nucl-th].
- [903] Y. Kamiya, T. Hyodo, K. Morita, A. Ohnishi, and W. Weise, Phys. Rev. Lett. **124**, 132501 (2020), arXiv:1911.01041 [nucl-th].
- [904] J. Haidenbauer, Nucl. Phys. A **981**, 1 (2019), arXiv:1808.05049 [hep-ph].
- [905] K. Ogata, T. Fukui, Y. Kamiya, and A. Ohnishi, Phys. Rev. C **103**, 065205 (2021), arXiv:2103.00100 [nucl-th].
- [906] J. Haidenbauer and U.-G. Meißner, Phys. Lett. B **829**, 137074 (2022), arXiv:2109.11794 [nucl-th].
- [907] Z.-W. Liu, K.-W. Li, and L.-S. Geng, Chin. Phys. C **47**, 024108 (2023), arXiv:2201.04997 [hep-ph].
- [908] R. Molina, C.-W. Xiao, W.-H. Liang, and E. Oset, (2023), arXiv:2310.12593 [hep-ph].
- [909] R. Molina, Z.-W. Liu, L.-S. Geng, and E. Oset, (2023), arXiv:2312.11993 [hep-ph].
- [910] V. M. Sarti, A. Feijoo, I. Vidaña, A. Ramos, F. Giacosa, T. Hyodo, and Y. Kamiya, (2023), arXiv:2309.08756 [hep-ph].
- [911] S. E. Koonin, Phys. Lett. B **70**, 43 (1977).
- [912] R. Lednicky and V. L. Lyuboshits, Yad. Fiz. **35**, 1316 (1981).
- [913] W. Bauer, C. K. Gelbke, and S. Pratt, Ann. Rev. Nucl. Part. Sci. **42**, 77 (1992).
- [914] U. W. Heinz and B. V. Jacak, Ann. Rev. Nucl. Part. Sci. **49**, 529 (1999), arXiv:nucl-th/9902020.
- [915] M. A. Lisa, S. Pratt, R. Soltz, and U. Wiedemann, Ann. Rev. Nucl. Part. Sci. **55**, 357 (2005), arXiv:nucl-ex/0505014.
- [916] S. Pratt, T. Csorgo, and J. Zimanyi, Phys. Rev. C **42**, 2646 (1990).
- [917] D. L. Mihaylov, V. Mantovani Sarti, O. W. Arnold, L. Fabbietti, B. Hohlweger, and A. M. Mathis, Eur. Phys. J. C **78**, 394 (2018), arXiv:1802.08481 [hep-ph].
- [918] J. Haidenbauer, G. Krein, and T. C. Peixoto, Eur. Phys. J. A **56**, 184 (2020), arXiv:2004.08136 [nucl-th].
- [919] C. M. Vincent and S. C. Phatak, Phys. Rev. C **10**, 391 (1974).
- [920] B. Holzenkamp, K. Holinde, and J. Speth, Nucl. Phys. A **500**, 485 (1989).
- [921] H. P. Li, J. Y. Yi, C. W. Xiao, D. L. Yao, W. H. Liang, and E. Oset, (2024), arXiv:2401.14302 [hep-ph].
- [922] N. Lang and D. J. Wilson (Hadron Spectrum), Phys. Rev. Lett. **129**, 252001 (2022), arXiv:2205.05026 [hep-ph].
- [923] F. Grosa, ALICE determines the scattering parameters of D mesons with light-flavor hadrons, Tech. Rep. (ALICE Collaboration, 2022).
- [924] L. Fabbietti, D meson scattering parameters with light-flavor hadrons, Tech. Rep. (ALICE Collaboration, 2022).
- [925] D. Battistini, Measurement of scattering parameters governing the residual strong interaction between charm and light hadrons, Tech. Rep. (ALICE Collaboration, 2023).

- [926] Y.-P. Xie, X. Cao, Y.-T. Liang, and X. Chen, (2020), arXiv:2003.11729 [hep-ph].
- [927] X.-Z. Ling, J.-X. Lu, M.-Z. Liu, and L.-S. Geng, Phys. Rev. D **104**, 074022 (2021), arXiv:2106.12250 [hep-ph].
- [928] U. Özdem, Eur. Phys. J. C **81**, 277 (2021), arXiv:2102.01996 [hep-ph].
- [929] S. Ohkoda, Y. Yamaguchi, S. Yasui, K. Sudoh, and A. Hosaka, Phys. Rev. D **86**, 034019 (2012), arXiv:1202.0760 [hep-ph].
- [930] N. Li, Z.-F. Sun, X. Liu, and S.-L. Zhu, Phys. Rev. D **88**, 114008 (2013), arXiv:1211.5007 [hep-ph].
- [931] P. Bicudo and M. Wagner (European Twisted Mass), Phys. Rev. D **87**, 114511 (2013), arXiv:1209.6274 [hep-ph].
- [932] P. Bicudo, K. Cichy, A. Peters, and M. Wagner, Phys. Rev. D **93**, 034501 (2016), arXiv:1510.03441 [hep-lat].
- [933] B. Wang, Z.-W. Liu, and X. Liu, Phys. Rev. D **99**, 036007 (2019), arXiv:1812.04457 [hep-ph].
- [934] M.-T. Yu, Z.-Y. Zhou, D.-Y. Chen, and Z. Xiao, Phys. Rev. D **101**, 074027 (2020), arXiv:1912.07348 [hep-ph].
- [935] M.-J. Zhao, Z.-Y. Wang, C. Wang, and X.-H. Guo, Phys. Rev. D **105**, 096016 (2022), arXiv:2112.12633 [hep-ph].
- [936] T. Hyodo, Int. J. Mod. Phys. A **28**, 1330045 (2013), arXiv:1310.1176 [hep-ph].
- [937] F. Aceti, L. R. Dai, L. S. Geng, E. Oset, and Y. Zhang, Eur. Phys. J. A **50**, 57 (2014), arXiv:1301.2554 [hep-ph].
- [938] T. Sekihara, T. Hyodo, and D. Jido, PTEP **2015**, 063D04 (2015), arXiv:1411.2308 [hep-ph].
- [939] Y. Li, F.-K. Guo, J.-Y. Pang, and J.-J. Wu, Phys. Rev. D **105**, L071502 (2022), arXiv:2110.02766 [hep-ph].
- [940] L. Maiani, A. D. Polosa, and V. Riquer, Sci. Bull. **66**, 1616 (2021), arXiv:2103.08331 [hep-ph].
- [941] A. Oliver Werner, Study of the hyperon-nucleon interaction via femtoscopy in elementary systems with HADES and ALICE, Dissertation, Technische Universität München, München (2017).
- [942] M. Csanád and D. Kincses, in 52nd International Symposium on Multiparticle Dynamics (2024) arXiv:2401.01249 [hep-ph].
- [943] S. Acharya et al. (ALICE), (2023), arXiv:2308.16120 [nucl-ex].
- [944] N. Isgur and M. B. Wise, Adv. Ser. Direct. High Energy Phys. **10**, 234 (1992).
- [945] J. M. Flynn and N. Isgur, J. Phys. G **18**, 1627 (1992), arXiv:hep-ph/9207223.
- [946] G. Li and X.-H. Liu, Phys. Rev. D **88**, 094008 (2013), arXiv:1307.2622 [hep-ph].
- [947] L. Roca, E. Oset, and J. Singh, Phys. Rev. D **72**, 014002 (2005), arXiv:hep-ph/0503273.
- [948] V. R. Debastiani, J. M. Dias, W. H. Liang, and E. Oset, Phys. Rev. D **97**, 094035 (2018), arXiv:1710.04231 [hep-ph].
- [949] J. A. Oller and E. Oset, Phys. Rev. D **60**, 074023 (1999), arXiv:hep-ph/9809337.
- [950] J. A. Oller, E. Oset, and J. R. Pelaez, Phys. Rev. D **59**, 074001 (1999), [Erratum: Phys.Rev.D 60, 099906 (1999), Erratum: Phys.Rev.D 75, 099903 (2007)], arXiv:hep-ph/9804209.
- [951] S. Weinberg, Phys. Rev. **130**, 776 (1963).
- [952] T. Hyodo, Phys. Rev. Lett. **111**, 132002 (2013), arXiv:1305.1999 [hep-ph].
- [953] Z.-H. Guo and J. A. Oller, Phys. Rev. D **93**, 096001 (2016), arXiv:1508.06400 [hep-ph].
- [954] Y. Kamiya and T. Hyodo, Phys. Rev. C **93**, 035203 (2016), arXiv:1509.00146 [hep-ph].

- [955] Y. Kamiya and T. Hyodo, PTEP **2017**, 023D02 (2017), arXiv:1607.01899 [hep-ph].
- [956] T. Sekihara, Phys. Rev. C **95**, 025206 (2017), arXiv:1609.09496 [quant-ph].
- [957] T. Kinugawa and T. Hyodo, Phys. Rev. C **106**, 015205 (2022), arXiv:2205.08470 [hep-ph].
- [958] M. Albaladejo and J. Nieves, Eur. Phys. J. C **82**, 724 (2022), arXiv:2203.04864 [hep-ph].
- [959] F. Aceti and E. Oset, Phys. Rev. D **86**, 014012 (2012), arXiv:1202.4607 [hep-ph].
- [960] M. Kamimura, Phys. Rev. A **38**, 621 (1988).
- [961] K. Varga and Y. Suzuki, Phys. Rev. C **52**, 2885 (1995), arXiv:nucl-th/9508023.
- [962] K. Varga, Y. Ohbayasi, and Y. Suzuki, Phys. Lett. B **396**, 1 (1997), arXiv:nucl-th/9612014.
- [963] J. Usukura, K. Varga, and Y. Suzuki, Phys. Rev. A **58**, 1918 (1998), arXiv:physics/9804023.
- [964] M. Viviani, A. Kievsky, and S. Rosati, Few Body Syst. **18**, 25 (1995).
- [965] B. L. G. Bakker, M. I. Polikarpov, and A. I. Veselov, Few Body Syst. **25**, 101 (1998), arXiv:quant-ph/9511009.
- [966] M. C. Gordillo, F. De Soto, and J. Segovia, Phys. Rev. D **102**, 114007 (2020), arXiv:2009.11889 [hep-ph].
- [967] M. C. Gordillo, F. De Soto, and J. Segovia, Phys. Rev. D **104**, 054036 (2021), arXiv:2105.11976 [hep-ph].
- [968] Y. Ma, L. Meng, Y.-K. Chen, and S.-L. Zhu, Phys. Rev. D **107**, 054035 (2023), arXiv:2211.09021 [hep-ph].
- [969] P. Navratil and B. R. Barrett, Phys. Rev. C **59**, 1906 (1999), arXiv:nucl-th/9812062.
- [970] P. Navratil, G. P. Kamuntavicius, and B. R. Barrett, Phys. Rev. C **61**, 044001 (2000), arXiv:nucl-th/9907054.
- [971] P. Navratil, J. P. Vary, and B. R. Barrett, Phys. Rev. Lett. **84**, 5728 (2000), arXiv:nucl-th/0004058.
- [972] D. R. Entem, F. Fernandez, and A. Valcarce, Phys. Rev. C **62**, 034002 (2000).
- [973] H. Garcilazo, A. Valcarce, and T. F. Caramés, Phys. Rev. D **96**, 074009 (2017).
- [974] A. Deloff, Phys. Rev. C **61**, 024004 (2000).
- [975] L. Roca and E. Oset, Phys. Rev. D **82**, 054013 (2010), arXiv:1005.0283 [hep-ph].
- [976] N. Moiseyev, Phys. Rept. **302**, 212 (1998).
- [977] T. Myo, Y. Kikuchi, H. Masui, and K. Katō, Prog. Part. Nucl. Phys. **79**, 1 (2014), arXiv:1410.4356 [nucl-th].
- [978] M. A. Shifman, A. I. Vainshtein, and V. I. Zakharov, Nucl. Phys. B **147**, 385 (1979).
- [979] P. Colangelo and A. Khodjamirian, , 1495 (2000), arXiv:hep-ph/0010175.
- [980] M. Born and R. Oppenheimer, Annalen Phys. **389**, 457 (1927).
- [981] E. Hiyama and M. Kamimura, Front. Phys. (Beijing) **13**, 132106 (2018), arXiv:1809.02619 [nucl-th].
- [982] E. Hiyama, M. Kamimura, A. Hosaka, H. Toki, and M. Yahiro, Phys. Lett. B **633**, 237 (2006), arXiv:hep-ph/0507105.
- [983] T. Yoshida, E. Hiyama, A. Hosaka, M. Oka, and K. Sadato, Phys. Rev. D **92**, 114029 (2015), arXiv:1510.01067 [hep-ph].
- [984] J. Aguilar and J. M. Combes, Commun. Math. Phys. **22**, 269 (1971).
- [985] E. Balslev and J. M. Combes, Commun. Math. Phys. **22**, 280 (1971).
- [986] H. Kamada et al., Phys. Rev. C **64**, 044001 (2001), arXiv:nucl-th/0104057.
- [987] L. Meng, Y.-K. Chen, Y. Ma, and S.-L. Zhu, Phys. Rev. D **108**, 114016 (2023), arXiv:2310.13354 [hep-ph].